WERNER COMPLEXES: SYNTHESIS, STRUCTURE AND ENCLATHRATION PROPERTIES

by

LUCIE MEVOE OBIANG

Thesis submitted in the fulfilment of the requirements for the degree

Master of science in Chemistry

In the faculty of Applied Sciences at

CAPE PENINSULA UNIVERSITY OF TECHNOLOGY

Supervisor: Professor Merrill M. Wicht

Co-supervisor: Professor Luigi R. Nassimbeni

Cape Town

December 2020

DECLARATION

I, Lucie Mevoe Obiang, declare that the contents of this thesis represent my own unaided work, and that the thesis has not previously been submitted for academic examination towards any qualification. Furthermore, it represents my own opinions and not necessarily those of the Cape Peninsula University of Technology.

11 December 2020

....

Signature   **Date**

ABSTRACT

Crystal engineering methods were used to combine Werner complexes with one or more components in a single solid form, with well-defined stoichiometry in order to create Werner clathrates and investigate their selectivity towards similar xylene isomers. Two families of six hosts, zinc tetrahedral $ZnCl_2L_2$ [H1 (L=nicotinamide), H2 (L=isonicotinamide) and H3 (L=mixed ligands, nicotinamide and isonicotinamide)] and cobalt octahedral $Co(NCS)_2L_4$ [H4 (L=nicotinamide), H5 (L=isonicotinamide) and H6 (L=mixed ligands nicotinamide and isonicotinamide)], were designed and synthesised. They were used in the formation of three types of complexes upon the crystallisation process with guests and/or solvents. These are Werner clathrate and mixed ligand complexes. Three types of complexes were prepared in the same process of crystallisation with different solvents, giving ten crystal structures. These produced thereof two complexes made from the zinc tetrahedral complex $H2_c$ and $H3_c$, six Werner clathrates H1•nic, H4•propOH, H4•nic•H_2O, H5•2isonic, H5•2isonic•propOH and H6•H_2O from both zinc and cobalt complexes and two mixed ligand cobalt complexes H7 and H8. In four crystal structures, nicotinamide or isonicotinamide self-included as guests to form Werner clathrate complexes which contained one or two independent enclathrated nicotinamide or isonicotinamide molecules. This occurred serendipitously, although this process has previously been reported.

Werner clathrates and complexes were linked into a three-dimensional network via intermolecular interactions such as N-H•••O, O-H•••S and N-H•••Cl. However, an intramolecular interaction was observed in H4•propOH via N-H•••O which affected the flexibility in the torsion angles of H4•propOH complexes. The Werner clathrate complexes synthesised from H4 and H5 presented similar arrangement and channels in their packing diagrams, although they were not isostructural. H7 and H8 crystal structures resulted from the substitution of two nicotinamide ligands by two solvent DMSO and methanol molecules respectively. This exchange of ligands in H4 and H6 complexes occurred during the evaporation procedure and was facilitated by the stronger pKa value and dipole moment of the DMSO or methanol ligands, compared with those of nicotinamide.

All structures were elucidated via single crystal X-ray diffraction (SCXRD), thermogravimetric analysis (TGA) and differential scanning calorimetry (DSC). Powder X-ray diffraction (PXRD) scrutiny was used to compare differences between hosts, starting material and crystal structures.

The study of the zinc complexes (H1•nic, $H2_c$ and $H3_c$) indicated the importance of the halide interactions revealed in the molecular structure and the importance of stabilising frameworks of the structure. Similarly, the thiocyanato sulfur provided interactions between N-H•••S and O-H•••S in H4, H5 and H6 which also provided a stabilising effect on the framework of these crystal structures.

Although all six host Werner complexes were exposed to the xylene isomers, H6 differentiated towards ortho-xylene from a 50:50 ortho/meta-xylene mixture. The selectivity of ortho-xylene was confirmed by single crystal X-ray analysis and the complex properties were shown by TG, Hirshfeld surface and fingerprint analysis.

ACKNOWLEDGEMENTS

I wish to thanks,

- GOD for his presence and love.

- My Supervisor, Professor Merrill Wicht for her patience, total assistance, advice, understanding and encouragement throughout the entire project. She was more than a Supervisor for me.

- Prof L. Nassimbeni for all his support and all the Professor and Doctors who contributed.

- The National Research Foundation (NRF) and Cape Peninsula University of Technology and University of Cape Town for all the support.

- Family and friend and anyone who contributed for the accomplishment of this thesis.

CONFERENCES

Parts of this thesis have been presented at the following conference:

- The 4th International symposium on halogen bonding, 2 – 5 November 2020 held in South Africa.

  Title: Chloride and sulfur form stabilising hydrogen bonds in metal centred complexes

STRUCTURE cif FILES

Crystal structures of the eleven crystalline solids which were elucidated by single crystal X-ray diffraction are included in the following cif files, followed by CCDC deposition numbers assigned to each structure:

Cif file name	CCDC deposition number
H1nic.cif	2049534
H2c.cif	2049535
H3c.cif	2049536
H4propoh.cif	2059714
H42h2o2nic.cif	2059715
H52isonic.cif	2059716
H52isonicpropoh.cif	2059717
H6h2o.cif	2059718
H7.cif	2059719
H8.cif	2059720
H9ox.cif	2059721

DEDICATION

I dedicated my thesis to my Mom Marcelle Betto Minko and my siblings Mida, Martine, Yolande and Michel.

TABLE OF CONTENTS

CHAPTER I: INTRODUCTION

CHAPTER II: EXPERIMENTAL METHODS AND MATERIALS

CHAPTER III: TETRAHEDRAL ZINC COMPLEXES

CHAPTER IV: OCTAHEDRAL COBALT COMPLEXES WITH HYDROGEN BONDING FUNCTIONALITIES

CHAPTER V: SUBSTITUTION OF LIGANDS IN WERNER CLATHRATE COMPLEXES: MIXED ORGANIC LIGAND COMPLEXES

CHAPTER VI: SEPARATION OF ISOMERS BY ENCLATHRATION

CHAPTER VII: SYMMARY AND CONCLUSION

LIST OF FIGURES

CHAPTER I: INTRODUCTION

Figure 1.6 Schematic illustration of molecular and lattice inclusion, a) Inclusion of guest molecule in the cavity of the host molecule resulting in the conversion of a cavitand into a cavitate; b) Inclusion of

CHAPTER II: EXPERIMENTAL AND MATERIALS

CHAPTER III: TETRAHEDRAL ZINC COMPLEXES

CHAPTER VI: OCTAHEDRAL COBALT COMPLEXES WITH HYDROGEN BONDING FUNCTIONALITIES

CHAPTER V: SUBSTITUTION OF LIGANDS IN WERNER CLATHRTATE COMPLEXES: MIXED ORGANIC LIGANDS COMPLEXES

CHAPTER VI: SEPARTION OF ISOMERS BY ENCLATHRATION

CHAPTER VII: SUMMARY AND CONCLUSION

LIST OF TABLES

CHAPTER I: INTRODUCTION

CHAPTER II: EXPERIMENTAL AND MATERIALS

CHAPTER III: TETRAHEDRAL ZINC COMPLEXES

CHAPTER IV: OCTAHEDRAL COBALT COMPLEXES WITH HYDROGEN BONDING FUNCTIONALITIES

CHAPTER V: SUBSTITUTION OF LIGANDS IN WERNER CLATHRTATE COMPLEXES: MIXED ORGANIC LIGANDS COMPLEXES

CHAPTER VI: SEPARTION OF ISOMERS BY ENCLATHRATION

CHAPTER VII: SUMMARY AND CONCLUSION

LIST OF CHARTS

CHAPTER I: INTRODUCTION

GLOSSARY

Terms/Acronyms/Abbreviations	Definitions/Explanation
%	Percentage
˚C	Degree
a, b, c	Unit cell axes
α	Angle between b and c unit cell axes
β	Angle between a and c unit cell axes
γ	Angle between a and b unit cell axes
E_a	Activation energy
G	Guest
K	Kelvin
L	Ligand
T	Temperature
V	Unit cell volume
Z	Number of formula units per cell
W	Water
Hr	Hour
H	Host
bp	Boiling point
HSM	Hot stage microscope
Isonic	Isonicotinamide
CSD	Cambridge structure data
DTG	Differential thermogravimetric ratio
DSC	Differential scanning calorimetry
DMSO	Dimethyl sulfoxide
min	Minutes
mx	meta-xylene
mp	Melting point
nic	Nicotinamide
px	para-xylene
ox	ortho-xylene
PXRD	Powder X-ray diffraction
SCXRD	Single crystal X-ray diffraction
T	Temperature
TGA	Thermogravimetry analysis
T_{on}	Onset temperature
T_{peak}	Peak temperature

ATOM COLOURS

Carbon

Chlorine

Cobalt

Hydrogen

Nitrogen

Oxygen

Sulfur

Zinc

CHAPTER I

INTRODUCTION

This work interrogates the design and synthesis of host materials in order to obtain more structural information on selected complexes and/or clathrates, and on the nature of host-guest and guest-guest interactions. This study describes ways to combine a Werner complex with one or more components, with well-defined stoichiometry in order to create Werner clathrates.

One of the functions of Werner complexes is to include guest/s. Hence the study has broadened the Werner complexes by altering the combination of metal ions and ligands to produce complexes with different properties and enclathration abilities.

1.1.   Supramolecular chemistry

The aim of supramolecular chemistry is to develop large, highly complex chemical systems formed from the molecules interacting through intermolecular contacts (Lehn, 2004). The study of supramolecular chemistry can be traced way back to1894 with Emil Fischer's (Fischer, 1894) work on the functioning of enzymes also called 'the lock and key principle' [(the enzyme (lock) needs a small molecule (key) to enable it to work (open the lock)], and this concept was the origin of molecular recognition (Behr, 1994). Molecular recognition is the linking of a guest to a complementary host molecule forming a host-guest complex (Figure 1.1).

<div align="center">**Lock-key model**   **Host-gest interaction**</div>
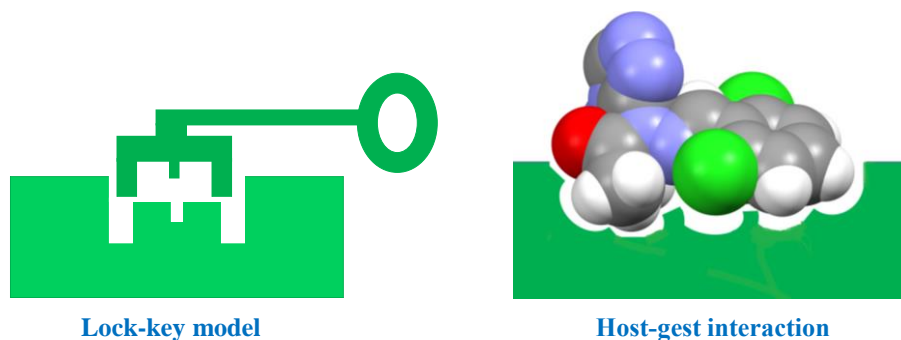
Figure 1.1 Schematic representation of lock and key interaction in enzymology and host-guest chemistry (adapted from (Bag, 2012).

In 1978, Jean-Marie Lehn introduced an updated version of supramolecular chemistry through his work in the area. It was described as 'chemistry of molecular assemblies and of the intermolecular bond', and it was a major step in establishing supramolecular chemistry as a field of study (Lehn, 1995). Supramolecular chemistry is also defined as "the chemistry beyond the molecule" or "the chemistry of intermolecular bonds" and it is based on the mutual recognition of molecules as is shown in Figure 1.1. The main difference between traditional chemistry and supramolecular chemistry is the interaction between molecules. Traditional chemistry focuses on the covalent bond while supramolecular chemistry relies on the use of non-covalent interactions between molecules such as hydrogen bonding, hydrophobic effects, van der Waals interactions, dipole interactions and dispersive forces. Figure 1.2

illustrates the evolution from molecular chemistry to supramolecular chemistry; molecular chemistry relies on the molecular information saved in covalent bonds of assembly components, whereas the supramolecular form is reliant on non-covalent interactions. These non-covalent interactions formed between hosts and guests include a number of repulsive and attractive forces. However, most common interactions are hydrogen bonding, CH$\cdots\pi$, dipole-dipole interactions, van der Waals forces, $\pi\cdots\pi$ interactions and halogen bonding (Nagendrappa, 2011).
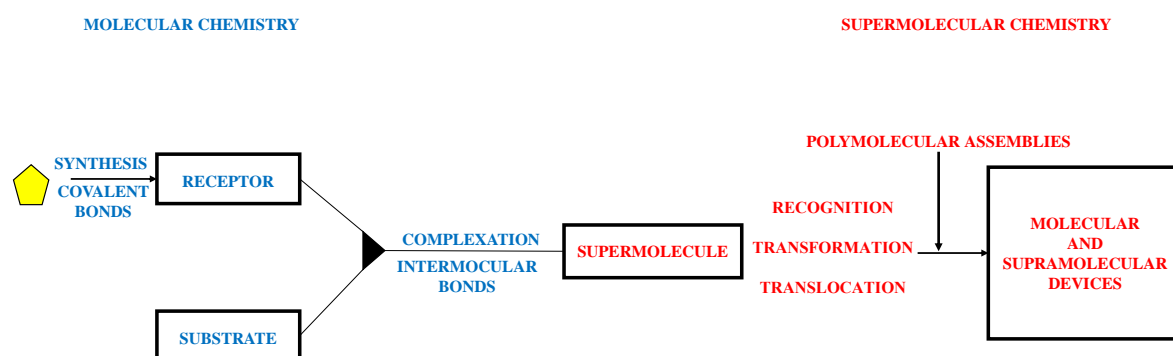
Figure 1.2 *Schematic representations of the evolution from molecular chemistry to supermolecular chemistry.*

As a discipline supramolecular chemistry is divided in two main subsets, host-guest chemistry and self-assembly. The difference between the two is due to the size and shape of the molecules involved. In self-assembly there is no significant difference in the size of the interacting species; two or more species are held together by non-covalent bonds. In the case of host-guest chemistry a small molecule called the guest becomes enveloped by a larger molecule which is called the host in a binding region.
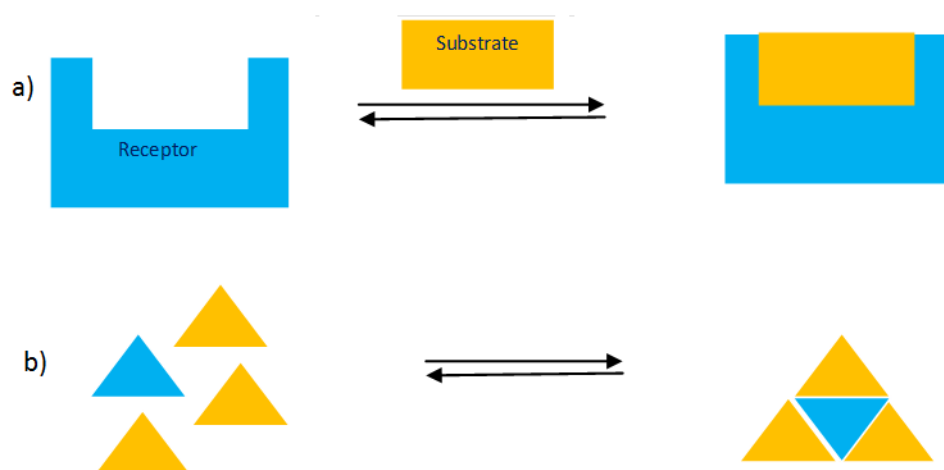
Figure 1.3 *Supramolecular chemistry, a) host-guest recognition and b) self-assembly (adapted from* (Evans & Akien, 2018).

Host-guest chemistry is one of the main points of discussion in this research; it consists of host matrices with large voids in the form of cages, channels or interlayer space where the guest may be enclathrated.

The design of these compounds is the main interest in the understanding of guest-host interactions, and the dynamics of the guest molecule in the lattice structures could lead to the possibility of separating stereoisomers.

1.2. Crystal Engineering

Crystal engineering is a field emerging from supramolecular chemistry and was described by Behr in the enzyme-substrate interaction using key-lock analogy which anticipated the principles for molecular recognition and host-guest chemistry (Behr, 1994). However, the concept of crystal engineering was first addressed by both Pepinsky in 1955 and Von Hippel in 1962 (von Hippel, 1962), (Pepinsky, 1955). It is the understanding of intermolecular interaction and molecular architecture in the context of crystal packing to design new solids with desirable physical and chemical properties (Wolff et al., 2010) . In simple words the new molecules are generated by the formation of covalent bonds which incorporate coordinate bonds for metal-organic chemistry. This methodology is a combination of two subjects, chemistry and crystallography. The relation between the two is the interplay between the structure and properties of molecules on one hand and those of extended assemblies of molecules on the other (Gautam R Desiraju, 1989). Bragg showed that certain structural units such as a benzene ring has definite size and form that might be retained with hardly any change when going from one crystal structure to another (Bragg, 1921). He therefore showed the correlation between the molecular and crystal forms. However, recent crystallographic studies of hexamethylbenzene have shown that deviation from planarity may occur. In the case of aromatic compounds these may be due to electronic, steric, and/or intermolecular factors resulting in deviations from expected results. Although ring internal angles should be close to the ideal value of 120°, angular distortions may occur in the plane of the ring. Structure validation involves checking for internal consistency. X-ray crystallography is a self-checking technique that allows for accurate structure determination (Clegg, 2021).

Crystal engineering consists of three main operations which are interrelated. The first is determination of the crystal structure which is the way the molecules are packed. The second is to understand the nature of intermolecular interactions which determines how the molecules are packed in the crystalline phase. Lastly, exploitation of the knowledge behind crystal engineering is to construct designer materials to meet the desired application. Thus, to achieve the required crystal engineering, a method was proposed by Desiraju and co-workers in which the strategy of using synthons was described. This method uses the concept of a synthon to represent the identification of molecular precursors in the analysis of a target crystal network (Desiraju, 1997).

1.3. Coordination chemistry

Coordination chemistry is the study of compounds that use their nature to become a crystal engineering subject based on Alfred Werner's coordination compounds. In 1913 he received the Nobel Prize in Chemistry for his theory on coordination chemistry. Thus in 1883, Alfred Werner developed the idea of coordination chemistry which was focused on compounds of organic amines bonded to metal centres. His study allowed him to define a stable complex formed between cobalt (II) as a central metal ion and six bound ammonia molecules surrounding the metal ion with an arrangement as far apart as possible at six corners of an octahedron. Coordination compounds or complexes are the linking of poly-coordinate metal ions with polydentate ligands. They consist of central metal ions bonded to a surrounding array of anions or ligands, while a coordination polymer is an infinite array of coordination complexes in which metal ions are bridged by multidentate ligands. Werner's discovery of coordination was based on the colour of the complexes, in which the cobalt cation occurs in a cis:trans dichloro pair. X-ray diffraction, not discovered during Werner's time, now shows that the presence of a third salt of the same elemental composition powerfully boosts his theoretical discovery of two stereochemically distinct forms (Bernal & Lalancette, 2020).

1.4. Inclusion compounds

Inclusion compounds are representative of a class of chemistry called supramolecular chemistry (which is well defined by Lehn as chemistry of molecular assemblies and of the intermolecular bond). It may be defined as a complex which is formed when one component, the host, interacts with a second component, the guest. The host can form a cavity or, in the case of a crystal it consists of crystal lattices containing spaces such as voids, channels or layers in which the molecular entities of the second chemical species called the guest molecule are located. There is no covalent bonding between the guest and the host, and the interaction is mainly attributed to the van der Waals forces. The essential criteria are simply that the enclosed guest be of a suitable size and shape to fit into a cavity within the solid structure formed by the host molecules. Secondly, the stereochemistry and possibly the polarity of both the host and the guest molecules determine whether inclusion can occur. The close fit of the two components produces a combination of significant strength. If the spaces in the host lattices are enclosed from all sides so that the guest molecule species is trapped inside the cage the compounds are called clathrates or cage compounds. Powell suggested that the word clathrate indicates the situation where the molecule is completely enclosed by the host and cannot escape from its surroundings (Palin & Powell, 1948).

The scientist named Mylius observed the first inclusion compound in 1886 as an unusual complexation occurring between hydroquinone and several volatile compounds. He proposed that the two components were interacting without chemical bonding and suggested that one molecule was enclosed within the

other. A few years later these observations were confirmed by X-ray analysis and it was determined that one molecule of gas or liquid formed an insoluble inclusion compound with three molecules of hydroquinone (Palin & Powell, 1947). The general title for the class of complexes was given as "Einshluβverbindung" which is a German name for inclusion compounds. It was first used by Schlenk (Schlenk, 1949), and seems to be suitable for all inclusion type systems. Other terms were also used to describe these complexes as occlusion compounds, adducts, host-guest complexes, addition compounds, supramolecular assemblies and clathrates.

The formation of an inclusion compound is driven by thermodynamics, with a reaction between solid host (H) and gaseous guest (G):

$$\mathbf{H_{solid} + G_{gas} = [HG]_{solid}}$$
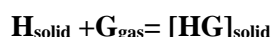
Inclusion compounds were classified into many broad categories depending on the concept used to classify them.

For example the scientist Barrer divided the inclusion compounds into three categories based on the very context of the host crystals (Barrer, 1986).

- Those that are stable in the presence and in the absence of the guest molecule alike;
- Compounds which have a critical concentration of guest molecules, below which that host structure becomes metastable and recrystallizes;
- Those in which the host framework continuously readjusts itself as the content of guest molecules fluctuates.

Inclusion compounds are classified according the topology of cavity space of the host framework (Dyadin, Y.A. and Terekhova, 2004), and Figure 1.4 illustrates some examples.

- Cryptoclathrates: also called cage-type inclusion compounds, wherein the guest molecules are included within closed cavities formed by the host molecules;
- Tubulatoclathrates: channel-type inclusion compounds in which the host forms non-intersecting channels or tunnels which include the guest molecules;
- Intercalatoclathrates: there are layered-type inclusion compounds and guest molecules are sandwiched between sheets of the host matrix.
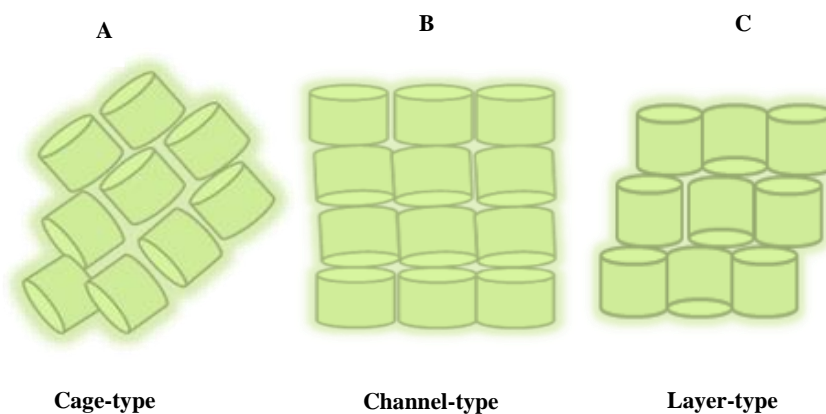
Figure 1.4 *Representation of three types of inclusion compounds, a) cage-type inclusion compounds, b) channel-type inclusion compounds and c) layered-type inclusion compounds (adapted from* (Shigemitsu & Kida, 2018).

These three types of inclusion compounds are also called cryptates, tubulates and intercalates. The following classification of inclusion compounds is based on their structure and properties (Frank, 1975):

- Polymolecular inclusion compounds: these possess channel-like spaces and cage-like spaces

The polymolecular inclusion compounds are composed of a host structure composed of several molecules oriented in a loosely arranged lattice. The individual members of the host lattice interact with each other through hydrogen bonds and other non-covalent interactions to form a channel-like space or a cage-like space structure by enclosing the guest molecule.

Clathrates are one class of polymolecular inclusion compounds which are one of the earliest documented inclusion complexes. It has been used to describe the term cage-like structure of hydroquinone inclusion compounds;

- Monomolecular inclusion compounds

These compounds have only one molecule of the guest and one molecule of the host. This monomolecular inclusion compound constitutes the second major class of inclusion compounds;

- Product of the blue-iodine reaction

Polymerization of iodine within unique channels formed by starch, cyclodextrins, cellulose and barbaturic acid gives blue addition compounds (Schoch & Williams, 1944);

- Macromolecular inclusion compounds

Macromolecular inclusion compounds or molecular sieves (zeolites) are very big molecules. The zeolites are the most common in this category although modified dextrin, silicate gel, agro gel and other substances are also included under this category.

Inclusion compound of host organic molecules are among a wide variety including zeolites, Hoffman and Werner complexes, cyclodextrins and metal organic framework (MOF's).

Zeolites are robust tetrahedral crystalline frameworks of aluminium-oxygen or silicon-oxygen which form a three dimensional array with many cavities and interconnecting channels (Grosse-Kunstleve, *et al*., 1999). They have large vacant space in their structures that allow ions or small molecules to enter and be enclosed within the network. Some of them have their vacant spaces connected so that they form channels which allow the guest molecules easy entrance and exit.

Hoffman inclusion compounds are polymeric or molecular crystalline solids where crystal lattice voids result from the assembly of metal complexes, with general formula $M(NH_3)_2M(CN)_42G$, where M is an octahedrally coordinated metal cation such as Mn(II), Zn(II) or Cd(II), M is a square-planar coordinated metal cation such as Ni(II), Pd(II) or Pt(II), and G is a small aromatic molecule (Hoffman and Küspert, 1897).

Cyclodextrins are host molecules used for the construction of small molecule enzyme mimics.

1.5.   The chemistry of clathrates

Clathrates are defined as inclusion compounds with a 3-D frame (Kovnir & Shevelkov, 2004). It is a lattice formed by several of one type of molecule which traps and contains a second type of molecule. For instance, clathrate hydrates are clathrates formed by water which may enclose a molecule which is not normally attracted. The history of clathrates can be traced back to 1810 and 1811, when the scientist Humphry Davy led (experimented by putting) chlorine gas under high pressure through water cooled to 275-276 K. He discovered the formation of solid structures with unidentified nominal composition and at this time it was poorly understood. However, in 1823, Faraday revised the data, and determined its stoichiometry to be $Cl_2(H_2O)_{10}$ and called it a clathrate hydrate (Faraday, 1823). Many authors reported other observations and variable compositions for their syntheses, which today are recognised as significant in the field of inclusion compounds. These include the preparation of β-quinol with H_2S and SO_2 in 1849, the Hoffman inclusion compound, and nickel cyanide ammonia inclusion compounds in 1859 (Wöhler, 1859). The exact composition and crystal structure of this chlorine hydrate was determined in 1948 (Palin & Powell, 1948). Additionally, their publication in 1948 revealed the structure of the β-quinol complex with sulfur dioxide and proposed to call it a clathrate compound (Powell, 1948). Powell defined this as a kind of inclusion compound in which two or more compounds are enclosed as a set of molecules in a suitable structure. His work was inspired from the suggestion made by Mylius 60 years earlier in the complex compounds formed by hydroquinone with certain volatile substances. He suggested that the molecule of one component was able to lock the molecules of the second component into position, but without chemical bonding.

Clathrate is the chemical definition for "cage" or "enclosed" and it is derived from the Latin word *clathratus* which means enclosed by cross bars or lattice grating. A clathrate is a chemical substance consisting of a lattice that traps or contains molecules. The trapped molecule is called the guest while the other molecule is called the host, which provides the structure and space for the formation of a complex. This inclusion compound is able to include another molecule without affecting the bonding systems of both components. So, clathrates are host-guest complexes where the guest molecule is in a suitable cage structure formed by the host molecule or a lattice of host molecules. The cage is held together by very weak forces like hydrogen bonding, ion pairing, dipole interaction and van der Waals attraction (Vaidya, 2008). Such caged host-guest complexes are often referred to as extra molecular assemblies, supramolecular assemblies, inclusion compounds and occlusion compounds. Molecular recognition describes this kind of inclusion compound and hence the process of inclusion compound synthesis may be described by the following equation:

$$\mathbf{H}_{\alpha\text{-phase(s)}} + n\mathbf{G}_{(I)/(g)} \rightarrow \mathbf{H} \cdot n\mathbf{G}_{\beta\text{-phase(s)}}$$
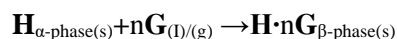
l=liquid phase, s=solid phase, g=gas phase
α = nonporous phase of the pure host H or apohost
β = the phase of the host-guest compound
n = host: guest ratio

where the non-porous α-phase of the host **H** or apohost is a solid that dissolves in a liquid guest **G** yielding a β-phase of host-guest complex **H·G** controlled by guest-host ratio **n**, and written **H·nG.**

The host complex may adopt three different modification phases depending on the structural features, the alpha-, beta-, and gamma-γ-phases. The α-phase is the non-clathrating modification or the empty phase where the molecular packing of the host molecules is unable to form any suitable voids in the crystal lattice due to reasons such as steric or electronic interactions (Papanicolaou, 1983). The β-phase is the clathrating modification where the energies in the system are favorable. Last, the γ-phase is where the cavities formed are of the layer-type (Papanicolaou, 1983).

The general formation and decomposition of an inclusion compound may be summarised in five steps as illustrated in Figure 1.5.

- Step 1 the apohost is dissolved in the liquid guest: $\mathbf{H}_{\alpha\text{-phase(s)}} + n\mathbf{G}_{(I)/(g)}$;
- Step 2 the solution is allowed to concentrate until the host-guest complex is formed as β-phase crystals: $\mathbf{H} \cdot \mathbf{G}_{\mathbf{n}\beta\text{-phase(S)}}$;
- Step 3 the reformation of the α-phase: $\mathbf{H} \cdot \mathbf{G}_{\mathbf{n}\beta\text{-phase(S)}} \rightarrow \mathbf{H}_{\alpha\text{-phase(s)}} + \mathbf{-nG}_{(I)/(g)}\uparrow$;
- Step 4 the introduction of a new γ-phase: $\mathbf{H} \cdot \mathbf{G}_{\mathbf{m}\beta\text{-phase(S)}} \rightarrow \mathbf{H} \cdot \mathbf{G}_{(\mathbf{n}\text{-m})\gamma\text{-phase(s)}} + \mathbf{mG}_{(g)}$;
- Step 5 formation of the β_0 phase or empty clathrate, $\mathbf{H} \cdot \mathbf{G}_{\mathbf{n}\beta\text{-phase(S)}} \rightarrow \mathbf{H} \cdot \mathbf{G}_{\mathbf{n}\beta_\circ\text{-phase(S)}}$.
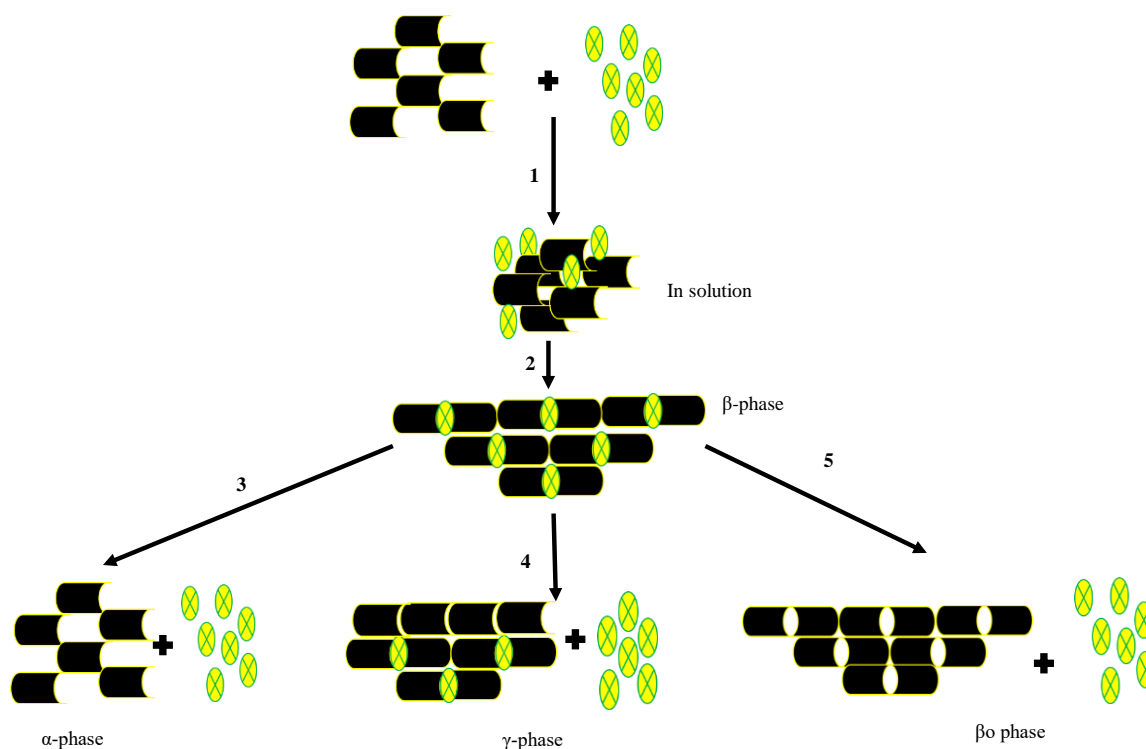
Figure 1.5 *General scheme of formation and decomposition of an inclusion compound.*

Host-guest compounds can be divided into two distinct groups depending on the type of the host compound and the topological relationship between the host and guest which are clathrands and cavitands (Groom et al., 2016).

As illustrated in the Figure 1.6 below, a cavitand is a single large molecule containing a central hole and forms a cavitate host and guest aggregate referred to as molecular inclusion. Examples include cyclophanes and cryptands (Desiraju, 2013).

Clathrands are large compounds which pack in such a way as to form a clathrate, referred to as a crystal lattice inclusion. Examples are urea and Macnicol's hexa-host (Steed & Atwood, 2009).
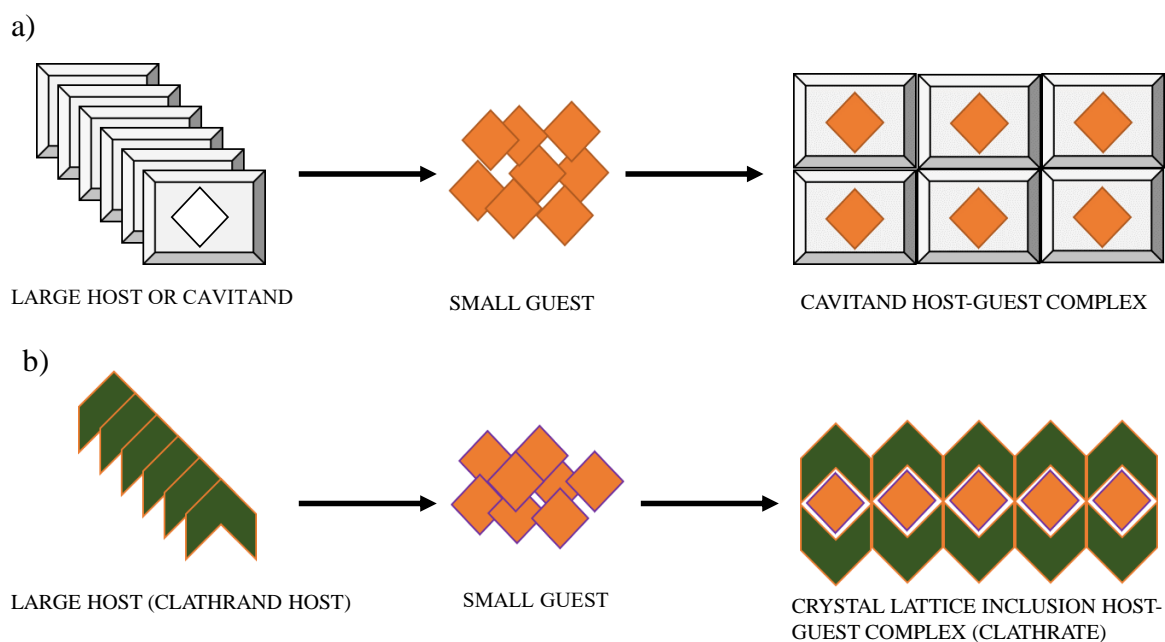
a)

LARGE HOST OR CAVITAND   SMALL GUEST   CAVITAND HOST-GUEST COMPLEX

b)

LARGE HOST (CLATHRAND HOST)   SMALL GUEST   CRYSTAL LATTICE INCLUSION HOST-GUEST COMPLEX (CLATHRATE)

Figure 1.6 Schematic illustration of molecular and lattice inclusion, a) Inclusion of guest molecule in the cavity of the host molecule resulting in the conversion of a cavitand into a cavitate and b) inclusion of the guest in the lattice formed between the host molecules which results in the conversion of a clathrand into a clathrate.

The use of clathrate chemistry or technique involves selective removal of a specific component from a mixture by the formation of a molecular compound or clathrate between a complex and the component. The clathrate is separated from the reaction mixture and the clathrate compound is recovered. This process of separation or selection can occur by melting, sublimation or dissolution. Since the interaction between host and guest is weak, the molecular structure and properties of the separated material are not affected throughout this process of separation. Among different classes of host molecules, Werner complexes are the type of hosts which present remarkable clathrating ability (Williams, 1957). They are used for separating compounds and particularly isomers, which are difficult to separate by conventional methods such as fractional distillation and fractional crystallization. For instance, many investigators have worked on Werner complexes for separating aromatic hydrocarbon isomers of substituted benzenes and they have been successful. The use of Werner clathrates to separate isomer compounds were proved by many articles and this has been successfully achieved. The selectivity of four xylene aromatic compounds was successfully demonstrated using Werner inclusion compounds as a host to separate a mixture of isomers (Wicht et al., 2016; Wicht et al., 2015).

1.6. Werner complexes

Werner complexes were discovered by Schaeffer in 1957. Werner clathrates are coordination complexes which are able to absorb organic compounds in a reversible manner (Schaeffer et al., 1957a). The

complex consists of a host and guest species with general formula $MX_2A_4 \cdot nG$, where M is a divalent transition metal cation such as Mn^{2+}, Fe^{2+}, Co^{2+}, Cu^{2+}, Zn^{2+}, Ni^{2+}, Hg^{2+}, Cr^{2+} or Cd^{2+}; X is the anionic component such as NCS^-, NCO^-, CN^-, NO_3^-, Br, Cl$^-$, or I$^-$; A represents a neutral amine donor ligand usually a pyridine or its derivative thereof and G is the guest compound with n giving the ratio of guest: host. Thus, by varying the host constituents or using different guests we can end up with thousands of Werner clathrates. In general, the formula, MX_2A_4 stands for the Werner host complex which has enclathrating ability of a small or large guest molecule. A good example to illustrate and describe Werner clathrates are the most common structures called the organic zeolites, with a formula of $[Ni(NCS)_2(4-RPy)_4]$ host and 4-Mepy guest, where R is an aryl or alkyl group, Me for methyl and Py is a pyridyl group (Moore et al., 1987; Soldatov, 2004). Organic zeolites have remarkable physicochemical behaviour. They are solids that are able to reversibly and selectively absorb large amounts of organic species while showing poor tendency toward sorption of inorganic compounds.

Indeed, the adaptability of a Werner host structure to the size of the guest molecule is remarkable, as demonstrated in 1984 by Lipkowski with the tetrakis (4-methyl pyridine) nickel (II) thiocyanate(TMPNT) Werner complex, one of the most versatile complexes which has been studied and that can form clathrate inclusion compounds with a variety of guest species (Starzewski et al., 1984). This is due to the rotational freedom of the pyridine rings about their Ni-N bonds and so the complex is able to adjust its molecular shape and capture guest molecules of different size, shape and polarity (Bond et al., 1983). Furthermore, apart from this ability to enclathate a wide variety of guest species, Werner complexes have another major advantage in that their synthesis is usually simple. In the case of the TMPNT preparation for example, an addition of an SCN$^-$ salt to a nickel hydrate followed by addition of pyridine is all that is required to precipitate a host powder (Papanicolaou, 1983).

However, two conditions are required for Werner complexes synthesis:

- The central ion is a transition d-series element;
- The ligand prevents close packing of the complex molecules due to steric hindrance in the crystal lattice (Karunakaran et al., 2000).

Most reported Werner clathrate syntheses were prepared by dissolving the host material in a suitable solvent and adding the guest, which could then be enclathrated upon crystallization. However, the choice of components available for the construction of systems is limited by the solubility of the host and the guest (Friščić et al., 2006). Hence, the TMPNT complex has been investigated to study the unusual properties of the Werner clathrates leading to a certain number of general rules regarding guest inclusion into a host lattice (Papanicolaou, 1983).

For guest molecules:

- Aromatic guests with electronegative groups must be avoided, since the aromatic nucleus of the amine of the Werner complex is an acceptor of π-electron density from the aromatic nucleus of the guest;

- Only compounds containing at least one aromatic ring are clathrated;

- Accumulation of polar group diminishes clathrating ability;

- Very polar or reactive substituents on the ring must be avoided;

- Accumulation of bulky groups makes the compound less easily clathrated.

Barbour reported the use of a simple, economic and environmentally friendly method of synthesis to obtain two Werner complexes and their solid solution with mechano-chemical synthesis (Barbour et al., 2012). This synthesis was used for Werner clathrates that could not be obtained by conventional solution chemistry. Mechano-chemistry is defined as the process in which solids undergo a chemical reaction by the application of mechanical energy (Fernández-Bertran, 1999). This process can be achieved by ball milling or manual grinding with a mortar and pestle.

The structure of most Werner complexes presents a cis or trans-octahedral coordination with the two anionic ligands in a *trans*-position. Further recent research discovered a new type with the cobalt cation having both cis:trans-octahedral geometry (example: cis:trans dichloro pair) (Bernal & Lalancette, 2020). There are two general configurations of the ligands which are 'centrosymmetric' and 'four-blade propeller' structures as illustrated in Figure 1.7. The 'four-blade propeller' structure presents an arrangement of ligands around the central cation which minimizes the energy of non-bonded interactions in the molecule, while the centrosymmetric structure has an arrangement with higher repulsive inter-ligand interactions due to the close proximity of the anions and two of the four pyridine rings. The most common structure is a four-blade propeller, because the co-planar arrangement is not suitable for the pyridine ligands due to the steric hindrance between them and the anions. Nevertheless, the centrosymmetric structures could be likely if the metal ion was larger and/ or the anion smaller such as in the Cd^{+2} and ONO^- complexes.
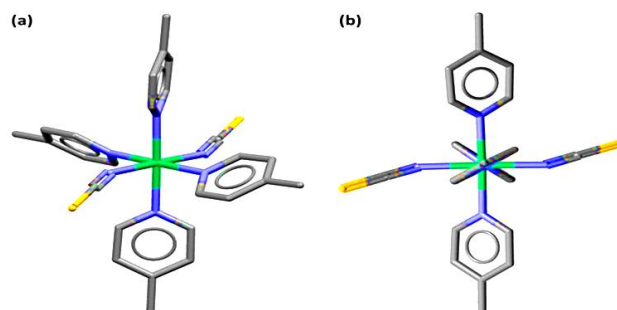
Figure 1.7 *A common conformation of the Werner complex Ni(NCS)$_2$(4-methylpyridine)$_4$, the four-blade propeller conformation shown in a) and b) showing how the ligand forms a four-blade propeller (adapted from* (Starzewski et al., 1984).

The structure of Werner clathrates presents in general three basic structural types of inclusion compounds: the true clathrate, the channel compound or zeolite-type compounds and layered structures.

The true clathrates or the cage-type clathrates are structures in which the host forms cavities available for the inclusion of the guest molecules separated from one another. They are trigonal with a 1:2/3 host to guest ratio.

Organic zeolites or the β-phases are the channel-type clathrates in which cavities are interconnected to give a three-dimensional network of cages. They are tetragonal with a 1:1 host-guest ratio.

The layered-structure or the γ-phases are layer-type clathrates which are monoclinic or triclinic with a 1:2 host-guest ratio.

The study of the host [Ni(NCS)$_2$(4-methylpyridine)$_4$] by Soldatov revealed that the complex exists in either of two polymorphic modifications: a microporous β-form or a dense α-form (Soldatov, 2004). This complex can form two kinds of inclusion compounds with benzene (C$_6$H$_6$), a β-type phase clathrate and γ-type phase clathrate from its pure α-type phase as illustrated in Figure 1.8 and as previously shown in Figure 1.5.
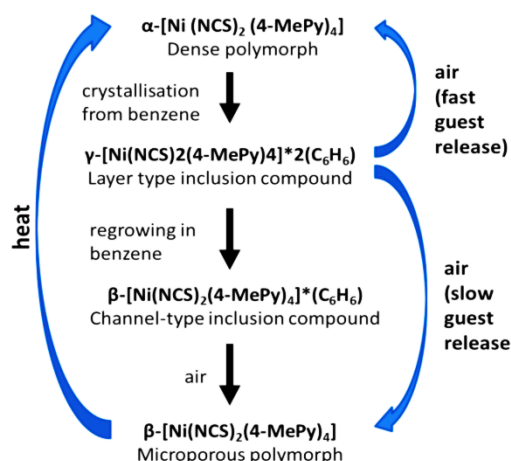
Figure 1.8 *Scheme representation of the α, γ and β phases of the Werner host Ni(NCS)$_2$(4-methylpyridine)$_4$ (adapted from* Soldatov et al., 2004).

An important point to underline in the study of Werner inclusion compounds is the selective sorption or inclusion within the host material for a given guest. This involves the selection of suitable hosts which, when exposed to a mixture of guests, enclathrates selectively a particular guest to form a crystalline inclusion compound. This interest was stimulated by Schaeffer and Dorsey, who announced a new method of separating mixtures of aromatic compounds and isomers from petroleum fractions. This process was called "Union Oil's New Clathration Process". Examples of isomers that were separated are cymenes, xylenes and methylnaphthalenes. The mechanism of selectivity is driven by the process of

molecular recognition and in the solution can be quantitatively evaluated by measuring the equilibrium constant of the reaction (Pivovar et al., 2001).

Taking into account the many observations described above, in 1996, Lipkowski created a stepwise procedure for the host-guest recognition process which takes place upon the clathrate formation.

- The host may choose a given guest from a mixture of guests present in the solution with which to cocrystallize;
- The host and guest may choose the most appropriate, thermodynamically favoured structure type for the clathrate to form;
- In solid clathrate formation, the molecular structure of the host may adapt its shape and form in order to attain the best possible steric fit with the guest species present.

1.7. Intermolecular interactions
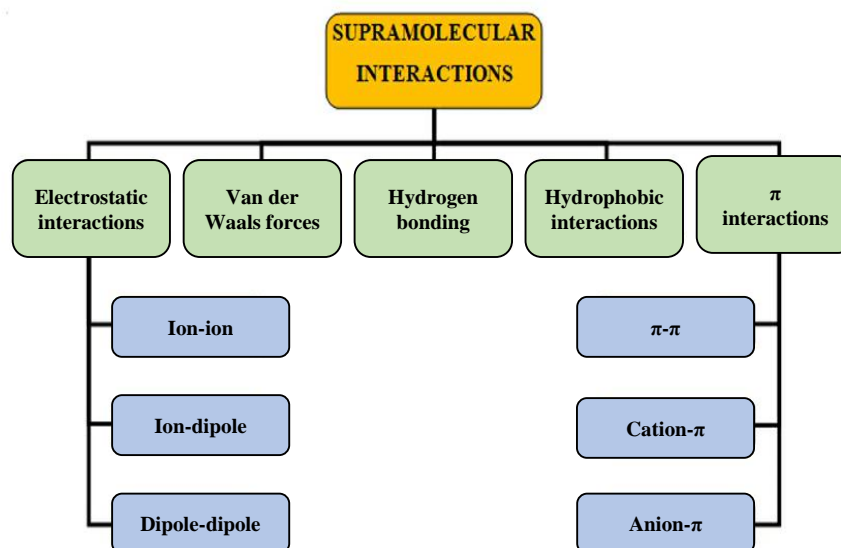
Flow chart 1.1 Different types of interactions.

Desiraju defines crystal engineering as the understanding of intermolecular interactions in the context of crystal packing and then exploits this knowledge to construct designer materials. Therefore, the proper understanding of intermolecular interactions lies at the heart of controlling the crystal structure (Desiraju, 1989). By definition, intermolecular interactions or non-covalent interactions are driving forces with electrostatic origin found between molecules. They can be divided in two types: isotropic

medium range forces (non-directional) and anisotropic long-range forces (directional forces). Isotropic forces (C···C, C···H, H···H interaction) are repulsive forces and define the shape, size and close packing, whereas anisotropic forces (O-H···N, N-H···O, C-H···O, C-H···N, O-H···π, X···X, and X···N), known as dispersive forces, are electrostatic and include hydrogen bond and heteroatom interactions.

Table 1.1 Different intermolecular interactions of hydrogen bonds and examples (adapted from Nangia, 2002).

Interaction type	Examples
Very strong hydrogen bonds	O—H···O⁻, F—H···F⁻
Coordinative bonds	M—N, M—O
Strong hydrogen bonds	O—H···O, N—H···O
Weak hydrogen bonds	C—H···O, O—H···π
van der Waals interactions	CH_3···CH_3, CH_3···Ph
Heteroatom interaction	N···Cl, I···I, Br···Br
π-stacking	Ph···Ph, nucleobases

However, the main common interactions formed between host and guest molecules are hydrogen bonding, CH···π interactions, dipole-dipole interactions, van der Waals forces, π···π interactions and halogen bonding. Intermolecular interactions play an important role in supramolecular chemistry which is associated with the formation of new compounds caused by the bonding of molecules using supramolecular synthons. In the table below are details of the different types of interactions that relate the host and guest to their surroundings.

Table 1.2 Summary of intermolecular interactions from the strongest to the weakest strength (adapted from Atwood & Steed, 2004).

Interactions	Strength(kJ/mol)	Examples
Ion-ion	200-300	Sodium chloride
Ion-dipole	50-200	15-Crown-5-sodium complex
Dipole-dipole	5-50	Acetone
Hydrogen bonding	4-120	DNA
Cation-π	5-80	(K^+ with in benzene ring)
π-π stacking	0-50	Benzene and graphite
van der Waals	<5 (variable depending on the surface area)	Argon, packing in molecular crystals
Hydrophobic	Related to solvent-solvent interaction energy	Cyclodextrin inclusion compounds

1.7.1 Ion-ion interactions

The strength is comparable to covalent bonding, 100-350 kJ/mol and these kinds of attractions refer to the forces existing between two ions (as illustrated in Figure 1.9) in ionic crystals (Clugston et al., 2002; Kotz et al., 2009).

Some characteristics:

- can be a very strong bond
- can be an attractive or repulsive force
- long range (1/r)
- non-directional
- highly dependent on the dielectric constant of the medium.
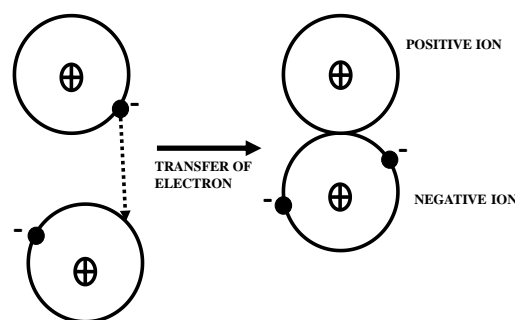
Figure 1.9 *Ion-ion interaction.*

1.7.2 Ion-dipole interactions

When ions bond with polar molecules, forces of attraction are generated between them and this leads to an ion-dipole interaction with strength between 50–200 kJ/mol (Clugston et al., 2002). These interactions are observed in both solid state and solution, e.g. cation-binding hosts and metal complexes or the bonding of ions with polar molecules such as water. Some characteristics can also be described:

- these are directional forces
- can be attractive or repulsive
- medium range ($1/r^2$) with r= distance from charge to centre of dipole
- significantly weaker than ion-ion interaction.
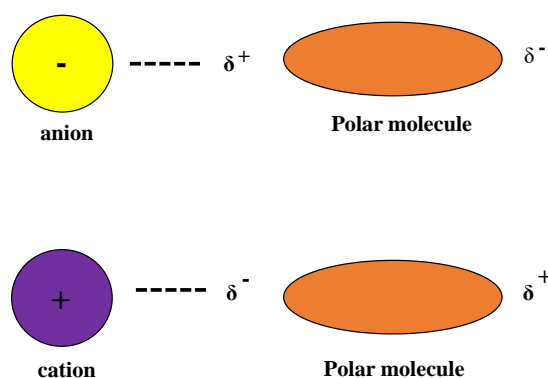
Figure 1.10 *Ion-dipole interaction.*

1.7.3 Dipole-dipole interactions

These interactions occur when two interaction dipoles are oriented relative to each other, such as the interaction of dipoles located on adjacent molecules or the opposing alignment of one dipole with the other (Steed *et al.*, 2000). So, it depends on a specific orientation of both components.

- Relatively weak (5-50 kJ/mol)
- Useful for bringing species into alignment, as the interaction requires a specific orientation of both entities.
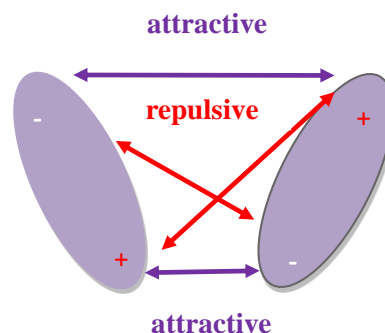
Figure 1.11 Dipole-dipole interaction.

1.7.4 Hydrogen bonding

Hydrogen bonding is forming a hydrogen bond between atoms, molecules or ions in the gas, liquid, solid or supercritical phases (Aakeröy & Seddon, 1993). It is a special type of dipole-dipole attraction when a hydrogen atom covalently bonded to a strongly electronegative atom such as N, O or F exists in the vicinity of another electronegative atom with a lone pair of electrons. In supramolecular chemistry, the hydrogen bond is able to control and direct the structures of molecular assemblies because it is sufficiently strong and directional (Desiraju & Steiner, 1999).

The hydrogen bond is represented as D-H⋯A where D is a donor and A the acceptor. There are three common types of hydrogen bonding geometries because D-H can be bonded to more than one acceptor, simple (involving only one donor and one acceptor), bifurcated (three-centre which means two acceptors) and trifurcated (four-centre, which means three acceptors) as shown in Figure 1.12.
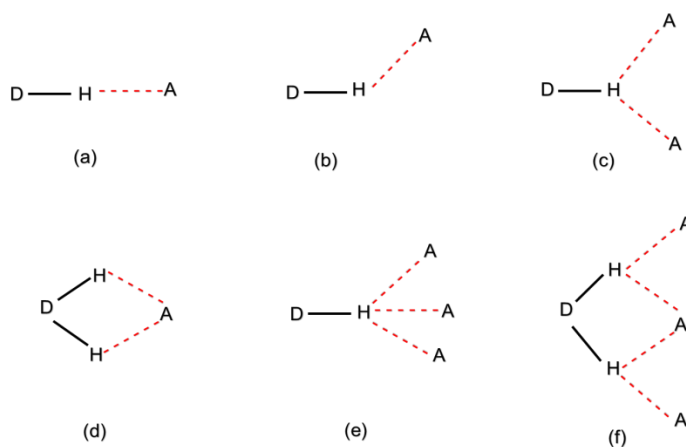
Figure 1.12 Hydrogen bond arrangements, a) linear, b) bent, (c) donating bifurcated; d) accepting bifurcated, e) trifurcated and f) three-centre bifurcated (adapted from Aakeröy & Seddon, 1993).

The properties of the donor and acceptor in hydrogen bonding determine the hydrogen bond length d(D-H) or d(H···A) (Taylor & Kennard, 1984). Depending on the number of acceptors involved in the hydrogen bond, the distance d will vary. So, the larger the number of acceptors, the shorter the d distances. The strength of hydrogen bonds is extremely variable (Pimentel & McClellan, 1971). For a neutral molecule the bond strength lies in the range of 10-65 kJ/mol, whereas, when one component of the hydrogen bond is ionic, the strength lies in the range of 40-190 kJ/mol. According to Jeffrey, the strength of the hydrogen bond is classified into three categories: very strong, strong and weak hydrogen bonds as illustrated in Table 1.3 below (Jeffrey, 1997).

Table 1.3 The properties of hydrogen bond interactions (adapted from Desiraju et al., 2011).

Strength	examples	D···A/Å	H···A/Å	D-H···A/(°)
Very strong	[F-H-F]⁻	2.2-2.5	1.2-1.5	175-180
Strong	O-H···O-H	2.6-3.0	1.6-2.2	145-180
	O-H···N-H	2.6-3.0	1.7-2.3	140-180
	N-H···O=C	2.8-3.0	1.8-2.3	150-180
	N-H···O-H	2.7-3.1	1.9-2.3	150-180
	N-H···N-H	2.8-3.1	2.0-2.5	135-180
Weak	C-H···O	3.0-4.0	2.0-3.0	110-180

Very strong hydrogen bonds mean hydrogen bonds that can control crystal and supramolecular structure. They are formed by unusually activated donors and acceptors. They are also formed between an acid and its conjugate base, X—H···X⁻ or between a base and its conjugate acid X⁺—H···X.

Strong hydrogen bonds are formed between neutral donor and neutral acceptor groups via dipole attraction.

Weak hydrogen bonds mean hydrogen bonds whose influence on crystal structure and packing is variable, and Table 1.4 shows details of the differences between the three types of hydrogen bonds.

Table 1.4 Some properties of strong, moderate and weak hydrogen bonds. (adapted from Desiraju & Steiner, 1999).

	Very strong	Strong	Weak
Bond energy (Kcal/mol)	15-40	4-15	<4
Bond lengths	H—A≈ X—H	H···A > X—H	H···A >> X —H
Lengthening of X-H (Å)	0.05-0.2	0.01-0.05	≤0.01
D(X···A) range (Å)	2.2-2.5	2.5-3.2	3.0-4.0
d(H···A) range (Å)	1.2-1.5	1.5-2.2	2.0-3.0
θ(X-H···A) range (°)	175-180	130-180	90-180
Bonds shorter than vdW	100%	Almost 100%	30-80%
at room temperature	>25	7-25	<7
Effect on crystal packing	Strong	Distinctive	Variable
Covalency	Pronounced	Weak	Vanishing
Electrostatics	Significant	Dominant	Moderate

Supramolecular synthons

The concept of supramolecular synthons was elaborated by Desiraju for the profound examination of structural effects of crystal packing. He defined it as "*structural units within supramolecules that can be formed and/or assembled by known or conceivable synthetic processes involving intermolecular interactions*" (Desiraju, 1995). It is useful not only for characterization but also in the understanding of the biological recognition or drug-enzyme binding. Supramolecular synthon recognition is termed the Graph Set theory developed by Etter and Bernstein, which consists of identifying different types of H-bonds and ranking them by chemical priority and empirical rules for hydrogen bonding (Etter, 1991) (Bernstein et al., 1995). The Graph Sets or motifs are described by:

$$G^a_d (n)$$

where G is the pattern of hydrogen bonding which can be represented by four different designators:

C – an infinite chain

R – a ring

D – a noncyclic dimer

S – an intramolecular ring

The other terms in the graph set refer to:

n – the total number of atoms in the repeat unit

a – the number of acceptors and

d – the number of donors.

Supramolecular synthons were classified by Zaworotko into two (Flow chart 1.2), heterosynthons which form between different but complementary functional groups and supramolecular homosynthons which form between the same complementary functional groups (Almarsson & Zaworotko, 2004).
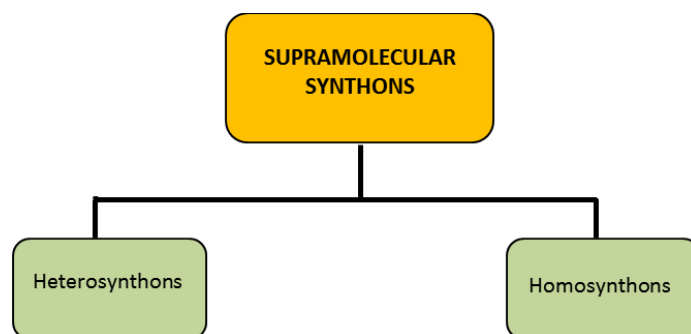
Flow chart 1.2 Different types of synthons

1.7.5 Cation-π interactions

These types of interactions occur between an adjacent cation and an electron rich π-system. Example would be when a cation such as potassium ions interacts with benzene to form a complex with a similar energy to the K^+-OH_2 interaction (Ma & Dougherty, 1997).

1.7.6 π-π stacking/interactions

These types of interactions are weak electrostatic interactions and are often called donor-acceptor interactions because they occur between one aromatic ring that is electron-rich or the donor and another aromatic ring that is electron-deficient or the acceptor. Two major types of π···π interactions are usually observed: the face-to-face and the edge-to-face interactions as illustrated in Figure 1.13.

a)   b)
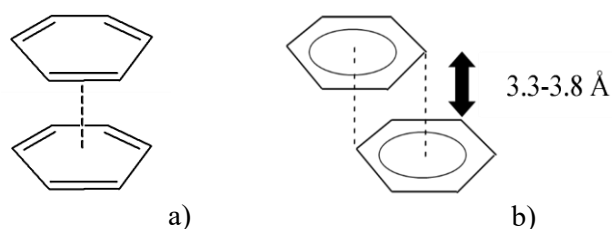
Figure 1.13 *The two pi-pi interactions, a) face-to-face interaction b) edge-to-face interaction (adapted from* Steed et al., 2007).

The face-to-face interactions occur when two faces of aromatic rings interact with one another. The edge-to-face interactions are observed when a weak hydrogen bond is formed between the slightly electron deficient-hydrogen atom and the electron-rich π-cloud of aromatic compounds (Steed & Atwood, 2000). π-π interactions display a wide variety of geometric arrangements or orientations which are parallel face-centred, parallel offset, perpendicular t-shaped, perpendicular y-shaped and parallel offset for toluene, (McGaughey et al., 1998; Martinez & Iverson, 2012).

1.7.7   van der Waals forces

These arise from fluctuations of the electron distribution between species that are in close proximity to one another.

- Weak interaction forces (2–20 kJ/mol)
- Mutually induced dipoles
- Dispersive effects: London interaction and the exchange and repulsion interaction
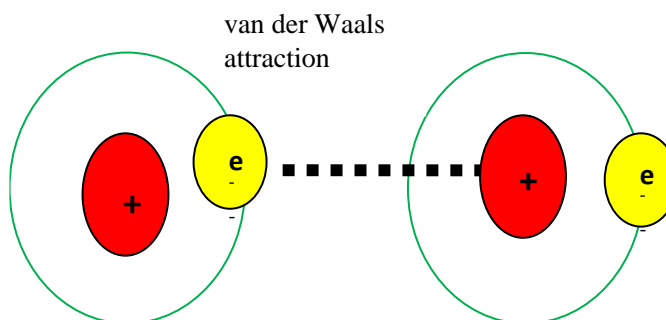
Figure 1.14 Schematic diagram of van der Waals force attractive force.

1.7.8 Hydrophobic interactions

Hydrophobic effects arise from the exclusion of non-polar groups or molecules from aqueous solute.

1.8.   Separation by selective inclusion

The interaction between the host and the guest can be very selective and seems to give a simple but promising strategy for the separation of mixtures which are otherwise difficult to separate. If the host compound has a preference for a particular guest in a mixture of two or more guests, it is said to show a degree of selectivity towards that guest. The selectivity can be defined as the ability of a host exposed to a mixture of guests to separate and combine with a particular guest to form a crystalline inclusion compound. The separation protocols are based on selective inclusion which requires that the host exhibit some preference for inclusion of one particular guest over another (Pivovar et al., 2001).
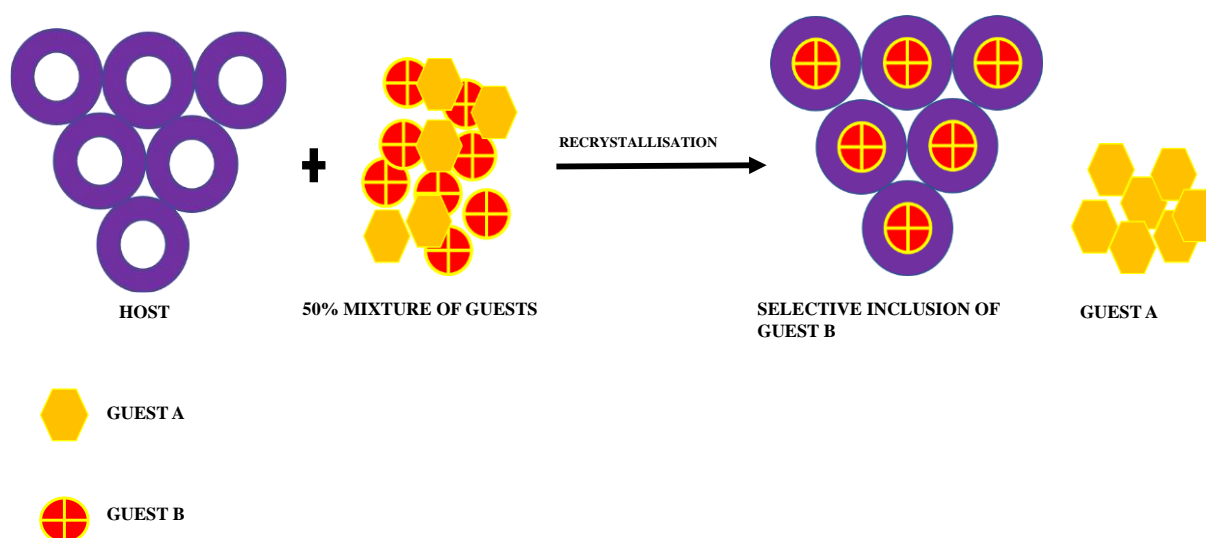
Figure 1.15 Scheme showing selective inclusion (adapted from Bouanga Boudiombo et al., 2018).

Crystals of the corresponding inclusion compound, grown from a solution containing a mixture of guests, would thus be enriched in one of the guests. There are many factors that influence the selectivity, such as co-operativity of the binding groups, pre-organisation of the host conformation and complementarity of the host and guest binding sites (Steed et al., 2007). There are two types of selectivity, namely thermodynamic and kinetic selectivity.

Kinetic selectivity is the rate at which competing substrates are transformed, with the enzyme being selective for the fastest-reacting substrate (Jacobs et al., 2008).

Thermodynamic selectivity can be defined as a ratio of the equilibrium constant when the host is exposed to two or more guests. The reaction may be formulated as:

$$\mathbf{H_{(s)} + nG_{(g,I)} \rightarrow H \bullet_n G = host:guest\ ratio}$$
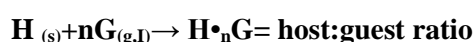
The concept of a selectivity coefficient, $\mathbf{K_{B:A}}$ is defined as (Jacobs, A. et al. 2008):

$$\mathbf{K_{B:A} + (K_{B:A})^{-1} = Z_A/Z_B{}^* X_B/X_A} \qquad \mathbf{(X_A + X_B) = 1}$$

A and **B** represent the two guests

$\mathbf{X_A}$ and $\mathbf{X_B}$ = mole fractions of each of the guests in the liquid mixture

$\mathbf{Z_A}$ and $\mathbf{Z_B}$ = mole fractions of the guest in crystal.

1.9   Mixed ligand complexes

The advent of the use of a set of mixed ligands in a Werner complex is an area relating to new complexes which may form new architectures in the crystal frameworks. This has been shown by enhanced selectivity of a nickel (II) thiocyanato complex by Wicht et al. (Wicht et al., 2016). In this case isoquinoline and 4-phenylpyridine were the two ligands which promoted discrimination towards ortho-xylene in equimolar mixtures of the three xylene isomers. Mixed ligand coordination complexes of transition metal cations containing coumarilate and N,N'-diethylnicotinamide were synthesized by Dağli et al. (Dağlı et al., 2017). In these octahedral complexes the structures formed network lattice structures via hydrogen bonding. Some of these complexes offered antimicrobial effects towards pathogenic microorganisms in varying proportions. In a similar manner, Dağli and co-workers studied mixed ligand complexes of Co(II), Ni(II), Cu(II) and Zn(II) with coumarilic acid and 1,10-phenanthroline which gave similar results to the previously mentioned paper (Dağlı et al., 2019).

1.10   Host and guest under study

A host:guest complex is a mixture of host molecules that non-covalently bond (by hydrogen bonding, ion pairing, metal-to-ligand binding, van der Waals forces, solvent reorganizing and partially made and broken covalent bonds) to a guest molecule. This then forms the complex.

1.10.1 Host compounds under study

This study reveals the synthesis and characterisation of six coordination compounds. These compounds have been named Werner complexes, and were synthesised by the Schaeffer method, with a general formula of $MX_2A_4 \cdot nG$. In this research, the six complexes were divided in two groups (A and B) according to the metal centre shown in Figure 1.16. The design of group A was made of one zinc (II) cation, two chloride anions and two nicotinamides H1, two isonicotinamides H2 or both ligands H3. The asymmetric units of group B consist of one cobalt (II) cation, two thiocyanate anions and four ligands such as nicotinamides H4, isonicotinamides H5 or both ligands H6.

The study of these complexes reveals that the main structural features of the Werner complexes in the case of Zn is that it has a symmetry of three two-fold axes which are parallel to the unit cell axes. The metal central atom has two nicotinamide ligands coordinated to it in the equatorial plane. The ligands have a symbiotic arrangement with respect to the equatorial plane. The chloride ligand groups coordinated axially lie on the complex axis. Thus the Zn complexes are all tetrahedral.

a)   b)

Host 1   Host 4
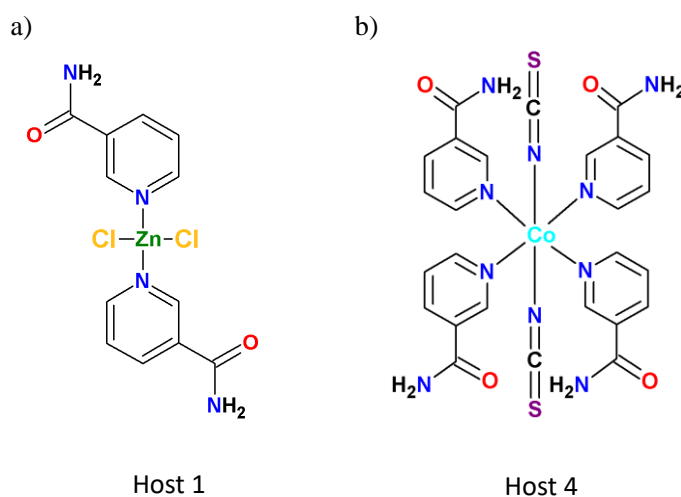
Figure 1.16 *Structure of two Werner complexes representing a wireframe configuration, a) host 1 (zinc) and b) host 4 (cobalt).*

Cobalt and zinc are elements of the d-block in the periodic table where cobalt is a d^7 element and zinc d^{10}. Generally, the d-block elements are used because they have rich and interesting chemical properties such as a variety of oxidation states, an extensive ability to form complexes, can ne involved in biochemical processes, can form organometallic compounds and useful solid compounds, and they have the ability to participate in catalysis. Zinc (four, five and six coordinate complexes) and cobalt (four and

six coordinate complexes) play an important role in the biological function of the metal in metallo-enzymes such as carbonic anhydrase. In both d^7 and d^{10} elements, the absence of any important ligand-field preference for a particular coordination number or geometry is reflected in the facile interconversion between coordination types. Zinc has no useful magnetic or spectroscopic properties whereas cobalt is a d^7 element with associate para-magnetism and 'd-d' spectra. It provides the highest magneto-crystalline properties and slow relaxation of the magnetization. One of the interesting structural aspects of working with cobalt in contrast to some other metals is the range of geometries, octahedral, tetrahedral, square-pyramidal, trigonal-bipyramidal and square-planar that are stable (Griffith, 1964).

The cobalt (Co^{II}) complexes formed are six-fold coordinated by two terminal N-bonding thiocyanate anions and N atoms of four nicotinamide ligands, forming octahedral complexes. Furthermore, cobalt can have a wide range of colours which makes it easy, in many cases, to identify different geometries (Lever, 1984). Many colours were observed in this research when using different guests, for example, pink when mixed with alcohols such as hexanol, ethanol and methanol, purple, orange or light pink with trimethoxybenzene isomers, orange when H5 was mixed with xylene isomers and green, yellow, brown and the unusual colourless on mixing H6 with xylenes.

Zinc, on the other hand, did not present a variety of colours; most of the crystals were colourless. Zinc is one of the most abundant transition metals with functions such as forming active sites of hydrophobic enzymes; it is a hard-donor coordinator of nitrogen and oxygen (Lipscomb & Sträter, 1996). According to Vallee and Auld, zinc has long been recognised as a Lewis acid catalyst that can readily adopt four, five or six-coordinations (Vallee & Auld, 1993).

1.10.2 Guest compounds under study

Guests used to study the behaviour of the two types of hosts include:

1. Alcohols
2. Trimethoxybenzene (TMB) isomers
3. Xylene isomers
4. Methyl benzyl alcohols (MBA)
5. Ketones
6. Benzoic acids (BA)

Table 1.5 Guest compounds and properties

	Names	Formula	Molar mass g/mol	Boiling point (°C)	Melting point (°C)	Abbreviation
Alcohols	Methanol	CH_2OH	32.04	64.7	-97.6	meOH
	1-Propanol	C_3H_7OH	60.09	97	-126	propOH
	2-Propanol	C_3H_7OH	60.09	82.3	-87.9	2-propOH
	3-Pentanol	$C_5H_{12}OH$	88.45	116	-63.68	3-pentOH
	Hexanol	$C_6H\ OH$	102.16	157	-45	hexOH
	Ethanol	C_2H_5OH	46.07	78.37	-114.1	ethOH
Benzoic acid and derivatives	Benzoic acid	$C_7H_6O_2$	122.13	249.2	122.4	BA
	meta-Amino BA			352.5	172-180	m-ABA
	para-Amino BA	$C_7H_7NO_2$	137.134	339.9	188.5	p-ABA
	4-Iodobenzoic acid	$C_7H_5\ IO_2$	248.02	318.5	270-273	4-IBA
	4-Bromoobenzoic acid	$C_7H_5\ BrO_2$	201.17	-	252-254	4-BrBA
	4-Chlorobenzoic acid	$C_7H_5\ ClO_2$	156.57	275	243	4-ClBA
Trimethoxybenzene isomers	1,2,3-TMB	$C_9H_{12}O_3$	168.16	241	43-47	1,2,3-TMB
	1,3,5-TMB			255	50-53	1,3,5-TMB
	1,2,4-TMB			247	19-21	1,2,4-TMB
Methyl benzyl alcohols	2-MBA	$C_8H_{10}O$	122.16	224	33-38	2-MBA
	3-MBA			215.5	-20	3-MBA
	4-MBA			217	61.5	4-MBA
Water	Water	H_2O	18.01	100	0	H_2O
#Ligands	Nicotinamide	$C_6H_6N_2O$	122.12	334	128-131	nic
	Isonicotinamide			334	155-157	isonic
DMSO	Dimethyl sulfoxide	C_2H_6OS	84.166	189	18.5	dmso
Ketones	2-Butanone	C_4H_8O	72.107	80	-86.67	2-butO
	Pentanone	$C_5H_{10}O$	86.13	102	-78	2-PentO
	2-Hexanone	$C_6H_{12}O$	100.15	127.8	-55.5	2-HexO
Xylene isomers	meta-Xylene	C_8H_{10}	106.17	139.1	-47.85	mx
	para-Xylene			138.3	13.3	px
	ortho-Xylene			144.5	-25.16	ox

 # both ligands self-included in some crystal structures

1.11 Objectives

- To synthesise Werner host complexes whose structures produce different physical and chemical properties.

- To prepare novel Werner clathrates with these hosts and a selection of guest compounds.

- To fully characterize compounds through powder X-ray diffraction, thermal analysis techniques as well as single crystal analysis should suitable crystals be synthesised.

- To enhance the selectivity of the host towards one guest from a mixture of guests and to analyse the resulting complex.

- To explore functional groups with the promotion of hydrogen bonding and to characterize the framework pattern formed in the crystal packing.

- To develop mixed ligand structures as a means of forming better inclusion compounds.

- To show the importance of ligand binding facilities such as electronegativity, dipole moment and basicity of the ligands in substitution reactions.

REFERENCES

Aakeröy, C.B. & Seddon, K.R. 1993. The hydrogen bond and crystal engineering. *Chemical Society Reviews*, 22(6): 397–407.

Almarsson, Ö. & Zaworotko, M.J. 2004. Crystal engineering of the composition of pharmaceutical phases. Do pharmaceutical co-crystals represent a new path to improved medicines? *Chemical Communications*, (17): 1889–1896.

Atwood, J. & Steed, J. 2004. *Encyclopedia of supramolecular chemistry*.

Bag, S.S. 2012. NPTEL- Module 1: Introduction to bio-organic Chemistry (WEB). *Syllabus*.

Barbour, L., Jacobs, T., Batisai, E. & Lusi, M. 2012. A mechanochemically synthesised solid solution enables engineering of the sorption properties of a Werner clathrate. *Chemical Communications*, 2: 2–4.

Barrer, R.M. 1986. Natural zeolites. *Zeolites*, 6(1): 72.

Behr, J.P. 1994. The Lock and Key Principle: The State of the Art-100 Years on. , 1: 173–318.

Bernal, I. & Lalancette, R.A. 2020. Serendipity: Werner's argument that the 'two-only forms' (green and violet) of [CoCl2(en)2]+ salts demanded his octahedral model was correct. True? *Acta Crystallographica Section C: Structural Chemistry*, 76(3): 298–301. http://scripts.iucr.org/cgi-bin/paper?dg3005 23 January 2021.

Bernstein, J., Davis, R.E., Shimoni, L. & Chang, N. -L. 1995. Patterns in Hydrogen Bonding: Functionality and Graph Set Analysis in Crystals. *Angewandte Chemie International Edition in English*, 34(15): 1555–1573.

Bond, D.R., Jackson, G.E. & Nassimbeni, L.R. 1983. Studies in Werner clathrates: part 1: structures of bis (isothiocyanato) bis (4-methylpyridine) bis-(4-phenylpyridine) nickel (II). methyl cellosolve and bis. *J. Chem. Soc.*, 1: 36.

Bouanga Boudiombo, J.S., Su, H., Bourne, S.A. & Nassimbeni, L.R. 2018. Separation of Trimethoxybenzene Isomers by Bile Acids. *Crystal Growth and Design*, 18(1): 424–430.

Bragg, S.W.H. 1921. The Structure of Organic Crystals. *Proceedings of the Physical Society of London*, 34(1): 33–50.

Clegg, W. 2021. Distortions, deviations and alternative facts: reliability in crystallography. *IUCrJ*, 8(1): 4–11.

Clugston, M.J., Flemming, R. & Vogt, D. 2002. *Chemistry : an introduction for southern African students*. Oxford: Oxford University Press.

Dağlı, Ö., Köse, D.A., Avcı, G.A. & Şahin, O. 2017. Novel mixed-ligand complexes of coumarilate/N,N′-diethylnicotinamide with some transition metals: Synthesis and structural characterization. *Journal of Thermal Analysis and Calorimetry*, 129(3): 1389–1402.

Dağlı, Ö., Köse, D.A., İçten, O., Avcı, G.A. & Şahin, O. 2019. The mixed ligand complexes of Co(II), Ni(II), Cu(II) and Zn(II) with coumarilic acid/1,10-phenanthroline: Synthesis, crystal characterization and biological applications. *Journal of Thermal Analysis and Calorimetry*, 136(4): 1467–1480.

Desiraju, Gautam R. 1989. *Crystal engineering : the design of organic solids*. Elsevier.

Desiraju, G.R. 2013. Crystal engineering: From molecule to crystal. *Journal of the American Chemical Society*, 135(27): 9952–9967.

Desiraju, Gautam R. 1989. Crystal Engineering the design of organic solids, materials science monographs. *ELSRIVER*, 54: 312.

Desiraju, G.R. 1997. Desihner Crystals/ Intermolecular Interactions, Network structures and Supramolecular Synthons. *Chem. Commun.*, 16: 1475–1482.

Desiraju, G.R. 1995. Supramolecular Synthons in Crystal Engineering—A New Organic Synthesis. *Angewandte Chemie International Edition in English*, 34(21): 2311–2327.

Desiraju, G.R. (Gautam R.. & Steiner, T. 1999. *The weak hydrogen bond : in structural chemistry and biology*. Oxford University Press.

Desiraju, G.R., Vittal, J.J. & Ramanan, A. 2011. *Crystal Engineering*. Co-Published with Indian Institute of Science (IISc), Bangalore, India.

Dyadin, Y.A. and Terekhova, I.. 2004. Classical Description of Inclusion Compounds. , 1: 253–260.

Etter, M.C. 1991. Hydrogen bonds as design elements in organic chemistry. *Journal of Physical Chemistry*, 95(12): 4601–4610.

Evans, N.H. & Akien, G.R. 2018. Rapid and simultaneous synthesis of a hydrogen bond templated [3]rotaxane and its related [2]rotaxane molecular shuttle. *Supramolecular Chemistry*, 30(9): 758–764.

Faraday. 1823. LXXXVI. On fluid chlorine . *The Philosophical Magazine*, 62(308): 413–416.

Fernández-Bertran, J.F. 1999. Mechanochemistry: an overview. *Pure and Applied Chemistry*, 71(4): 581–586.

Fischer, E. 1894. Einfluss der Configuration auf die Wirkung der Enzyme. *Berichte der deutschen chemischen Gesellschaft*, 27(3): 2985–2993.

Frank, S.G. 1975. Inclusion Compounds. *Journal of Pharmaceutical Sciences*, 64(10): 1585–1604.

Friščić, T., Trask, A. V., Jones, W. & Motherwell, W.D.S. 2006. Screening for Inclusion Compounds and Systematic Construction of Three-Component Solids by Liquid-Assisted Grinding. *Angewandte Chemie International Edition*, 45(45): 7546–7550.

Gg. *Supramolecular Chemistry*. https://homepage.univie.ac.at/jeanluc.mieusset/Supramolecular Chemistry 1 - Concepts.pdf 2 May 2019.

Griffith, J.S. (John S. 1964. *The theory of transition-metal ions.* Print book. Cambridge University Press.

Groom, C.R., Bruno, I.J., Lightfoot, M.P. & Ward, S.C. 2016. The Cambridge Structural Database. *Acta Crystallographica Section B Structural Science, Crystal Engineering and Materials*, 72(2): 171–179.

Grosse-Kunstleve, R., Section, A.B.-A.C. & 1999, undefined. A highly automated heavy-atom search procedure for macromolecular structures. *scripts.iucr.org*.

von Hippel, A.R. 1962. Molecular Designing of Materials: Science, guided by molecular understanding, takes up the challenge to create materials for the future. *Science*, 138(3537): 91–108.

Hofmann, K.A. & Küspert, F. 1897. Verbindungen von Kohlenwasserstoffen mit Metallsalzen. *Zeitschrift für anorganische Chemie*, 15(1): 204–207.

Jacobs, A., Nassimbeni, L.R., Nohako, K.L., Su, H. & Taljaard, J.H. 2008. Inclusion with mixed guests: Structure and selectivity. *Crystal Growth and Design*, 8(4): 1301–1305.

Jeffrey, G.A. 1997. *An introduction to hydrogen bonding*.

Karunakaran, C., Thomas, K.R.J., Shunmugasundaram, A. & Murugesan, R. 2000. Synthesis , X-ray crystal structure and spectroscopy of a Werner-type host Co (II) complex , trans -bisisothiocyanatotetrakis (trans -4-styrylpyridine) cobalt (II). , 523: 213–221.

Kotz, J.C., Treichel, P.M. & Townsend, J. 2009. *Chemistry & Chemical Reactivity, 7th Edition*. 7th ed. Cengage Learning.

Kovnir, K.A. & Shevelkov, A. V. 2004. Semiconducting clathrates: Synthesis, structure, and properties. *Uspekhi Khimii*, 73(9): 999–1015.

Lehn, J.-M. (Jean-M. 1995. *Supramolecular chemistry : concepts and perspectives : a personal account built*

upon the George Fisher Baker lectures in chemistry at Cornell University [and] Lezioni Lincee, Accademia nazionale dei Lincei, Roma. VCH.

Lehn, J.. 2004. Supramolecular chemistry: from molecular information towards self-organization and complex matter. *Rep. Prog. Phys.*, 67(3): 249–265.

Lever, A.B.P. (Alfred B.P. 1984. *Inorganic electronic spectroscopy*. 2nd ed. Amsterdam: Elsevier.

Lipscomb, W.N. & Sträter, N. 1996. Recent Advances in Zinc Enzymology. *Chemical reviews*, 96(7): 2375–2434.

Ma, J.C. & Dougherty, D.A. 1997. The cation-π interaction. *Chemical Reviews*, 97(5): 1303–1324.

Martinez, C.R. & Iverson, B.L. 2012. Rethinking the term "pi-stacking". *Chemical Science*, 3(7): 2191.

McGaughey, G.B., Gagné, M. & Rappé, A.K. 1998. pi-Stacking interactions. Alive and well in proteins. *The Journal of biological chemistry*, 273(25): 15458–63.

Moore, M.H., Nassimbeni, L.R. & Niven, M.L. 1987. Studies in Werner clathrates. Part 4. Structures of tetrakis(4-ethylpyridine)di-isothiocyanatonickel(II) and its clathrates with p-, m-, and o-xylene, carbon disulphide, and carbon tetrachloride. *Journal of the Chemical Society, Dalton Transactions*, 0(9): 2125.

Nagendrappa, G. 2011. Hermann Emil Fischer: Life and achievements. *Resonance*, 16(7): 606–618.

Nangia, A. 2002. Database research in crystal engineering. *CrystEngComm*, 4(17): 93–101.

Palin, D.E. & Powell, H.M. 1948. 163. The structure of molecular compounds. Part VI. The β-type clathrate compounds of quinol. *J. Chem. Soc.*, 0(0): 815–821.

Palin, D.E. & Powell, H.M. 1947. 50. The structure of molecular compounds. Part III. Crystal structure of addition complexes of quinol with certain volatile compounds. *Journal of the Chemical Society (Resumed)*, 0(0): 208.

Papanicolaou, S. 1983. *STRUCTURES OF WERNER CLATHRATES ACKNOWLEDGEMENTS*. Cape Town: University of Cape Town.

Pepinsky, R. 1955. Crystal engineering new concept in crytstallography. *Physical Review*, 100: 971.

Pimentel, G.C. & Mcclellan, A.L. 1971. *HYDROGEN BONDING*. www.annualreviews.org 7 April 2020.

Pivovar, A.M., Holman, K.T. & Ward, M.D. 2001. Shape-selective separation of molecular isomers with tunable hydrogen-bonded host frameworks. *Chemistry of Materials*, 13(9): 3018–3031.

Powell, H.M. 1948. 15. The structure of molecular compounds. Part IV. Clathrate compounds. *Journal of the Chemical Society (Resumed)*, 0(0): 61.

Schaeffer, W.D., Dorsey, W.S., Skinner, D.A. & Christian, C.G. 1957. Separation of Xylenes, Cymenes, Methylnaphthalenes and Other Isomers by Clathration with Inorganic Complexes. *Journal of the American Chemical Society*, 79(22): 5870–5876.

Schlenk, W. 1949. Die Harnstoff-Addition der aliphatischen Verbindungen. *Justus Liebigs Annalen der Chemie*, 565(2): 204–240.

Schoch, T.J. & Williams, C.B. 1944. ADSORPTION OF FATTY ACID BY THE LINEAR COMPONENT OF CORN STARCH. *Journal of the American Chemical Society*, 66(7): 1232–1233.

Shigemitsu, H. & Kida, T. 2018. Preparation of nano- and microstructures through molecular assembly of cyclic oligosaccharides. *Polymer Journal*, 50(8): 541–550.

Soldatov, D. V, Enright, G.D. & Ripmeester, J.A. 2004. Polymorphism and Pseudopolymorphism of the Compound that Led to the Concept of " Organic 2004. *Growth (Lakeland)*, 4.

Soldatov, D.V. 2004. Soft Supramolecular Materials. *Journal of Inclusion Phenomena*, 48(1/2): 3–9.

Starzewski, P., Zielenkiewicz, W. & Lipkowski, J. 1984. A thermokinetic study of the clathration of isomeric xylenes by the Ni(NCS)2 (4-methylpyridine)4 host. *Journal of Inclusion Phenomena*, 1(3): 223–232.

Steed, J.W. & Atwood, J.L. 2009. *Supramolecular chemistry*.

Steed, J.W., Turner, D.R. & Wallace, K.J. 2007. *Core concepts in supramolecular chemistry and nanochemistry*. John Wiley.

Taylor, R. & Kennard, O. 1984. Hydrogen-bond geometry in organic crystals. *Accounts of Chemical Research*, 17(9): 320–326.

Vaidya, S. 2008. Clathrates — An exploration of the chemistry of caged compounds. *Resonance*, 9(7): 18–31.

Vallee, B.L. & Auld, D.S. 1993. Zinc: Biological Functions and Coordination Motifs. *Accounts of Chemical Research*, 26(10): 543–551.

Wicht, M.M., Báthori, N.B. & Nassimbeni, L.R. 2016. Enhanced selectivity towards xylene isomers of a mixed ligand Ni(II) thiocyanato complex. *Polyhedron*, 119.

Wicht, M.M., Báthori, N.B. & Nassimbeni, L.R. 2015. Isoquinoline-based Werner clathrates with xylene isomers: Aromatic interactions vs. molecular flexibility. *Dalton Transactions*, 44(15): 6863–6870.

Williams, F. V. 1957. Clathrate Compounds of Werner Complexes with p-Disubstituted Benzene Derivatives. *Journal of the American Chemical Society*, 79(22): 5876–5877.

Wöhler, F. 1859. Ueber die Bestandtheile des Meteorsteines vom Capland. *Justus Liebigs Annalen der Chemie*, 110(3): 369–374.

Wolff, S.K., Grimwood, D.J., Mckinnon, J.J., Jayatilka, D. & Spackman, M.A. 2010. Crystal Explorer 2.1. *University of western Australia, Perth.*

CHAPTER II

EXPERIMENTAL METHODS AND MATERIALS

2.1 HOST AND GUEST

2.1.1 Host compounds

This research was based on the synthesis of Werner complexes of two transition metals, cobalt and zinc. The complexes were used as hosts in the formation and analysis of inclusion compounds called Werner clathrates. The hosts were prepared using a specific procedure established by Nassimbeni and co-workers (Lavelle & Nassimbeni, 1993), which is a revised method of Schaeffer (Schaeffer et al., 1957). Six hosts were synthesised in this study, three with zinc ion as the host centre and the other three using cobalt ion as a host centre of the Werner complexes.

Preparation of the powdered Werner complexes (hosts), $[ZnX_2A_2]$ and $[CoX_2A_4]$, where X= NCS/ Cl$^-$ and A= nicotinamide or isonicotinamide

The host compound H1, bis(chloride)bis(nicotinamide) zinc(II), was obtained by adding the ligand nicotinamide (6.0×10^{-3} mol plus 10% excess) to $ZnCl_2$ (1.5×10^{-3} mol) in ethanol. In the case of H2, bis(chloride)bis(isonicotinamide) zinc (II), the same amount of ligand isonicotinamide was added, and for H3, bis(chloride) (nicotinamide) (isonicotinamide) zinc (II), both nicotinamide and isonicotinamide were added in an equal ratio. Despite the addition of the ligand as four times the amount of metal, the resulting compound did not meet this requirement.

In the case of host metal cobalt, $Co(NCS)_2$ was prepared by adding NH_4NCS (3×10^{-3} mol) to $CoCl_2.H_2O$ (1.5×10^{-3} mol) and dissolving in 20 mL of ethanol. The solution was filtered to remove any NH_4Cl. The Werner complexes were synthesised with a slow addition of ligand (6×10^{-3} mol plus a 10% excess) in an ethanolic solution to the $Co(NCS)_2$ previously prepared. With constant stirring for 30 min to ensure complete reaction, the compound precipitated, was filtered and allowed to air dry for 48 h. The three complexes were H4, bis(isothiocyanato)tetrakisnicotinamide cobalt(II), H5, bis(isothiocyanato) tetrakisisonicotinamide cobalt(II) and H6 bis(isothiocyanato)bisnicotinamidebisisonicotinamide cobalt(II).

Table 2.1 Zinc and cobalt Werner complex properties.

Host		Formula [AX$_2$B$_4$]	Powder colour	Molecular mass (g/mol)
Zinc	H1	Zn(Cl)$_2$(C$_6$H$_6$N$_2$O)$_2$	White	380.53
	H2	Zn(Cl)$_2$(C$_6$H$_6$N$_2$O)$_2$	White	
	H3	Zn(Cl)$_2$(C$_6$H$_6$N$_2$O)(C$_6$H$_6$N$_2$O)	White	
Cobalt	H4	Co(NCS)$_2$(C$_6$H$_6$N$_2$O)$_4$	Light blue	663.41
	H5	Co(NCS)$_2$(C$_6$H$_6$N$_2$O)$_4$	Light pink	
	H6	Co(NCS)$_2$(C$_6$H$_6$N$_2$O)$_2$(C$_6$H$_6$N$_2$O)$_2$.	Light pink	
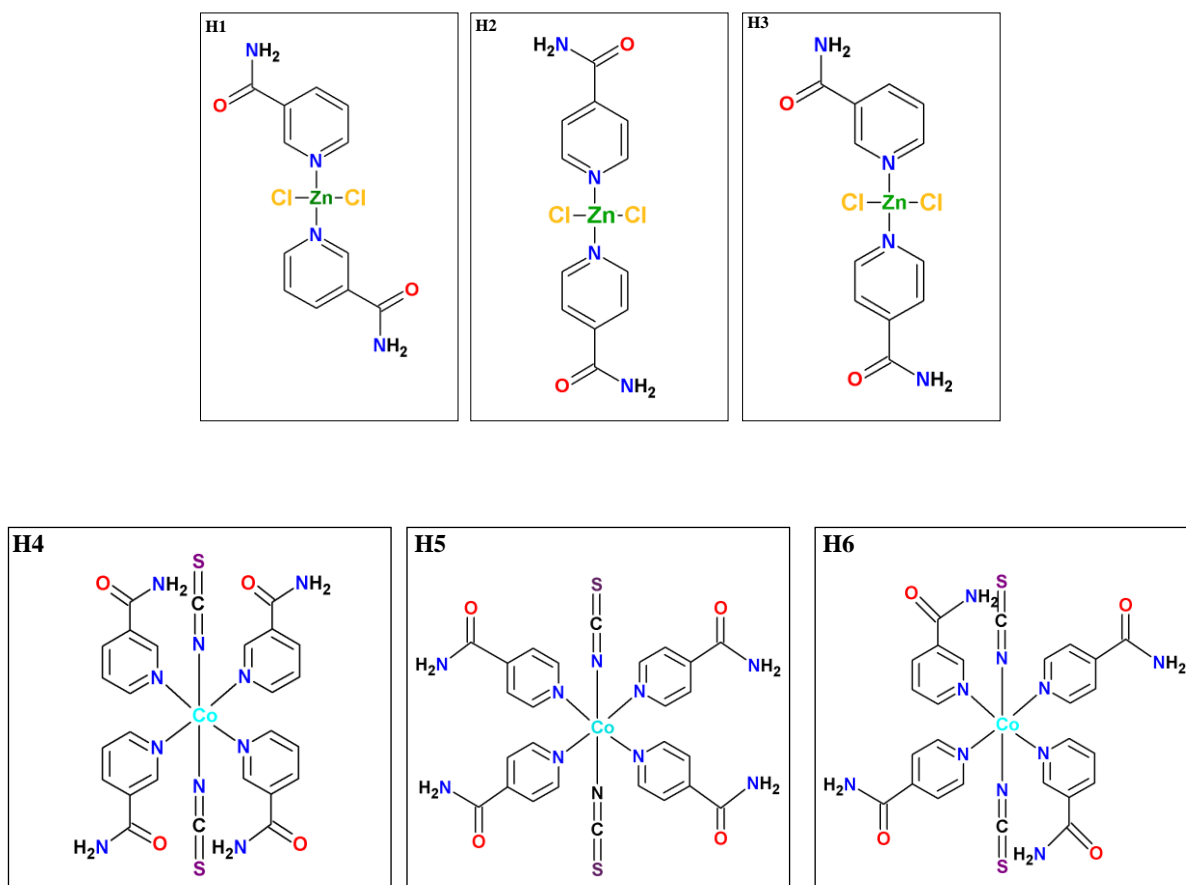
Figure 2.1: Structures of zinc host compounds from H1 to H3 and cobalt host compounds from H4 to H6.

The purity of each host was determined and confirmed by using thermogravimetric analysis (TGA). Thus, after the analysis, the percentage yields were calculated for each complex to determine the purity. Zinc and cobalt Werner complex TG curves showing theoretical values of the components in each host versus the experimental values confirm the composition of each. The percentage loss found for each ligand is indicated by the % loss by TG analysis.
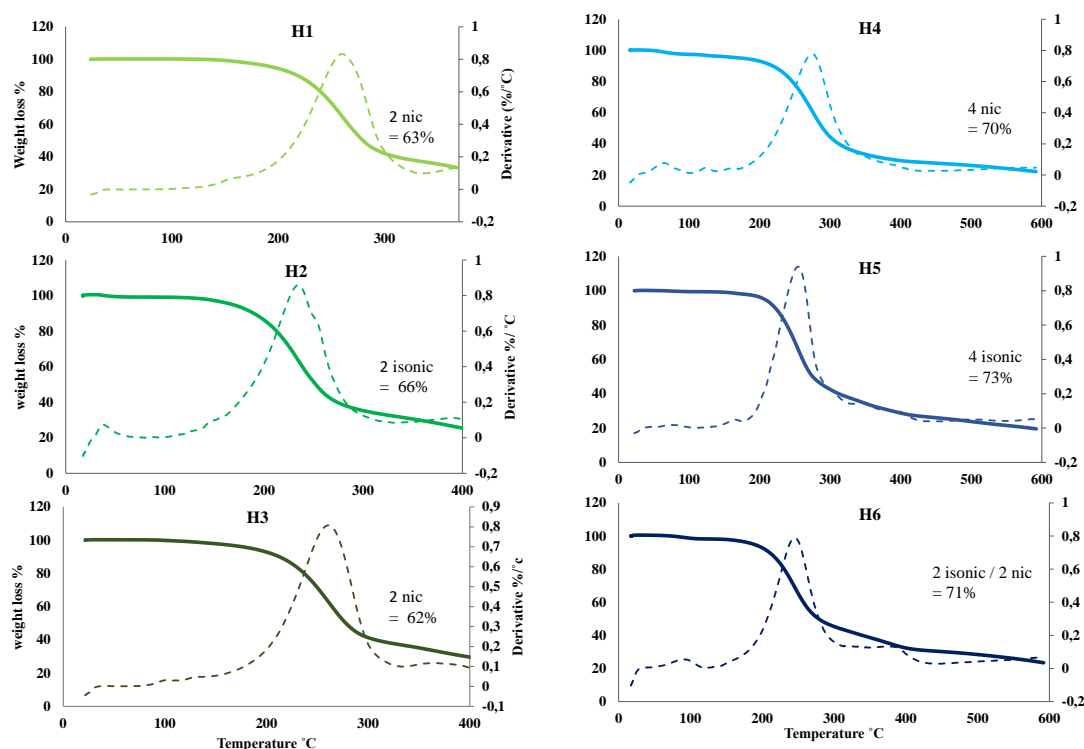
Figure 2.2: *TGA traces for Werner complex H1 to H6, showing the percentage loss.*

2.1.2 Solubility studies

The solubility was tested with over 15 solvents, but unfortunately only a few solvents were suitable such as DMF, DMSO, ethanol and methanol; the complexes were insoluble even in other solvents when heated to boiling. This factor implies the use of co-solvent. So DMF, DMSO, and methanol were used as either solvent or co-solvent with the possibility of being included in the clathrate. The solubility here could be defined as the amount of substance dissolved in a given amount of solvent. We also noticed that some solvents were not suitable for all hosts. Each host reacted slightly differently depending on the solvent used. Thus, in Table 2.2, the measure of the solubility of each solvent toward H1 to H6 is shown.

Table 2.2 Qualitative solubility observations.

solvents	H1	H2	H3	H4	H5	H6
DMF	vS	vS	vS	vS	vS	vS
DMSO	vS	vS	vS	vS	vs	vS
THF	vS	vS	vS	vS	vS	vS
Methanol	pS	pS	pS	S	Sh	Sh
Ethanol	pS	pS	pS	Sh	Sh	Sh
1-Propanol	I	I	I	I	I	I
2-Propanol	I	I	I	I	I	I
2-Pentanol	pS	pS	pS	Sh	Sh	Sh
3-Pentanol	pS	pS	pS	pS	pS	pS
1-Hexanol	I	I	I	I	I	I
2-Butanone	pS	I	I	I	I	I
3-Methylcyclohexanone	pS	I	I	I	I	I
4-Methylcyclohexanone	I	I	I	I	I	I
Isoamyl alcohol	I	I	I	I	I	I
Isobutyl ketone	I	I	I	I	I	I

where the solubility is expressed as

vS = very soluble

S   = soluble

Sh = soluble only with heat

pS = partially soluble

I   = insoluble

2.1.3 Guest compounds

The guests chosen are listed in Table 2.3, with their formulas and physical properties.

Table 2.3 *Guest compounds' physical properties and structures.*

Guests	Molecular formula	Molecular mass (g/mol)	Melting point (°C)	Boiling point (°C)	Density g/mL
Methanol	CH_3OH	32.04	-98.0	64.7	0.791
Ethanol	C_2H_5OH	46.07	-114	78.2	0.800
1-propanol	C_3H_7OH	60.09	-126	97.2	0.083
Propan-2-ol	C_3H_7OH	60.10	-89.0	82.5	0.785
1-butanol	C_4H_9OH	74.12	-90.0	117	0.810
2-butanol	C_4H_9OH	74.12	-115	100	0.808
1-pentanol	$C_5H_{11}OH$	88.15	-78.0	139	0.811
2-pentanol	$C_5H_{11}OH$	88.15	-73.0	119	0.812
3-pentanol	$C_5H_{11}OH$	88.15	-63.7	115	0.815
1-Hexanol	$C_6H_{13}OH$	102.2	-45.0	157	0.820
2-butanone	C_4H_8O	102.2	-86.0	79.6	0.805
Butanone	C_4H_8O	72.11	-86.7	79.6	0.805
3-MCH	$C_7H_{12}O$	112.2	104	170	0.914
4-MCH	$C_7H_{12}O$	112.2	-125	169	0.914
2-MCH	$C_7H_{12}O$	112.2	-14.0	163	0.924
2-MBA	$C_8H_8O_2$	136.2	104	259	1.060
3-MBA	$C_8H_8O_2$	136.2	111	263	1.050
4-MBA	$C_8H_8O_2$	136.2	180	274	1.060
BA	$C_7H_6O_2$	122.1	122	249	1.270
m-ABA	$C_7H_7NO_2$	137.1	178	-	1.510
p-ABA	C_7H_8NO2	137.1	187	340	1.370

ABA= amino benzoic acid - MCH= methyl cyclohexanone – MBA= methylbenzoic acid.

In some complex structures, nicotinamide and isonicotinamide ligands self-included as guests, and this happened serendipitously without any extra ligand being added to the mixture. After crystallisation, one or two nicotinamides/isonicotinamides were self-enclathrated forming a Werner clathrate complex. This was unexpected, but these results happened in other studies published by Tristan Neumann et al. (Neumann et al., 2016). In this publication two isonicotinamides were self-included after the crystallisation process to form a cobalt complex the same as H5. Two isonicotinamides and (solvent) were included in the crystal structure. Aakeröy and co-worker included one isonicotinamide after the slow evaporation process to form tetra aquabis (pyridine-4-carboxamide-N) zinc(II) 1,5-naphthalenedisulfonate-isonicotinamide-water (1:2:4) (Aakeröy & Beatty, 2004). These structures will be discussed in Chapters 3 and 4.

2.2 CRYSTALLISATION

2.2.1 Crystal growth

Crystallisation is the solidification of a multitude of atoms or molecules into a highly structured form called a crystal. It is also a solid-liquid separation technique in which mass transfer from liquid solution to a pure solid crystalline phase occurs. The main processes of crystallisation are nucleation and crystal growth. Nucleation is the step where the solute starts to gather into clusters. These molecular aggregates must be stable; in the case of unstable aggregates they redissolve. In crystal growth, nucleation and growth continue to occur simultaneously while supersaturation exists. The supersaturation is the driving force of the crystallisation.

Three different methods of crystallisation growth can be used, namely slow evaporation, crystal growth at low temperatures and slow cooling.

Slow evaporation: the inclusion compound is formed by dissolving the host compound in excess guest(s) in the presence of a solvent. The solution is heated to 40-50 °C with stirring for 30 minutes and allowed to cool before filtering through 0.45 µm nylon syringe membranes. The solvent is allowed to evaporate slowly at room temperature with the vials left open or covered with pierced parafilm.

Slow cooling: the crystal solutions were prepared as described in the slow evaporation technique. Once the solution was prepared, the vials were sealed and placed in the thermo-flask containing hot water and left to cool overnight.

Crystal growth at low temperatures: the crystal solutions were prepared as described in the slow evaporation technique, sealed and were placed in the refrigerator at a temperature of 4° C.

2.3 THERMAL ANALYSIS (TA)

Thermal analyses are techniques used to evaluate the physical properties of the compounds. The change of the weight of the sample as a function of the temperature or time was determined using thermogravimetric analysis (TGA) (Haines, 1995). The change in heat flow rate between sample and reference as a function of time or temperature was determined using differential scanning calorimetry (DSC). Both TG and DSC used Universal Analysis 2000 software (V4.5A, TA Instrument Water LLC) and were operated under a nitrogen purge gas flow rate of 30 mL.min^{-1} with a constant scanning rate of 10° C.min^{-1}. The temperature range was selected according to the nature of the host molecule in the crystalline compound. In our case the TG temperature run started at 30 °C ending at 400 °C for the Zn complexes and 600 °C for Co complexes. For DSC, the run ended at 350 °C and the sample size was varied between 2 to 10 mg. Both TG and DSC results are influenced by the sample size, particle size, flow rate and heating of the N_2 gas (Coats & Redfern, 1963).

2.3.1 Thermogravimetry analysis (TGA)

Thermogravimetric analysis was performed using a TA instrument Q-500 thermogravimetric analyser with 50 ml.min^{-1} dry nitrogen gas flow rate. This instrument measures the change in the mass of the sample over a range of temperatures. It shows the mass loss of a sample as a result of volatile guest loss and decomposition of the host complex. It uses a thermo-balance which measures accurate mass changes of the sample as a function of temperature. The temperature is monitored via a thermocouple. For the analysis the crystal was removed from the mother liquor, dried using filter paper to remove any surface solvent and crushed. The mass of the sample powder between 2 to 5 mg was placed in an open platinum pan for the experiment (Haines, 1995). A TG curve is plotted as percentage of mass loss as a function of temperature and can be used to calculate the stoichiometry of the inclusion compound being analysed.

2.3.2   Differential scanning calorimetry (DSC)

The thermoanalytical technique of differential scanning calorimetry (DSC) was used to measure changes of various physical quantities with changing temperature. A DSC experiment results in a curve of heat flow versus temperature. This can be used to calculated enthalpies of transitions. The main applications of DSC include phase transition, melting point determination, glass transition, determination of crystallinity and kinetic studies. The sample to be analysed can undergo an endothermic or exothermic process, where the endothermic peaks are plotted upwards and the exothermic peaks downwards. The instrument used was a TA Instrument Q-500 differential scanning calorimeter (in some cases a Perkin-Elmer Pyris® instrument was also used). For the analysis the crystal was removed from the mother liquor, dried using filter paper to remove any surface solvent and crushed. The sample powder was weighed on the balance. The mass of the powder varied between 1 and 3 mg. The sample was analysed in a crimped and vended aluminium closed pans, against a similarly treated empty aluminium pan. The temperature of both pans was increased at a constant rate (Brown, 1989).

2.4 X-RAY DIFFRACTION TECHNIQUES (XRD)

In 1912, Max Von Laue discovered that crystalline substances are acting as three-dimensional diffraction gratings for X-ray wavelengths similar to the spacing of used the planes in a crystal lattice. The exact nature of X-rays was established, and now X-ray diffraction is a common technique for the study of crystal structures and atomic spacing. They are used to determine the arrangement of atoms of a crystalline solid in three-dimensional space. The technique relies on obtaining and analysing the X-ray diffraction pattern from a crystalline solid and the identification of inclusion compounds. The

specimen may be in the form of a powder or a single crystal. This technique takes advantage of the interatomic spacing of most crystalline solids by employing them as a diffraction gradient for X-ray light, which has wavelengths in the order of 1 Angstrom (10^{-8} cm) (Caira & Nassimbeni, 1996).

The diffraction is based on Bragg's law

$$n\lambda = 2d\sin\theta$$

which relates the wavelength of electromagnetic radiation to the diffraction angle and the lattice spacing in a crystalline sample, where:

d= the distance between atomic layers in a crystal

θ= angle of incidence

n= an integer

λ= the wavelength of the incident X-ray beam.

2.4.1 Powder X-ray diffraction (PXRD)

Powder X-ray diffraction is used for a qualitative identification of the crystalline material and can provide information on unit cell dimensions. All the analyses were performed using a Bruker® D2 (2010) Phaser Advance diffractometer equipped with a Lynxeye detector using a graphite-monochromated CuK$_\alpha$ radiation (λ=1.5406 Å) at room temperature (Rissanen, 2014). This instrumentation consists of three basic elements which are an X-ray tube, an X-ray detector and a sample holder.

The samples were ground into a fine powder and placed on a zero-background silicon sample holder. This was loaded onto a reflection transmission spinner. The calculated powder X-ray diffraction patterns were generated by LAZY PULVERIX from single crystal X-ray data (Yvon et al., 1977).

2.4.2 Single crystal X-ray diffraction (SCXRD)

SCXRD is one of the most defined techniques used to determine the atomic and molecular structure of a crystal. It determines the packing and configuration of molecules and the intermolecular interactions within a crystal. In general, it is a non-destructive technique that uses the diffraction of X-rays from a suitable single crystal providing accurate data of cell parameters and diffraction intensities. The instrument used was a Bruker® DUO APEX II diffractometer (2005, version 1.0-27) using MoK$_\alpha$ (λ=0.71069 Å) at 173 K using an Oxford Cryo stream 700. The cell refinement and data reduction were

performed using SAINT-PLUS intensities and pre-determined cell parameters as inputs to program XPREP (Version, 5.1, 1997). Structures were solved using X-Seed, by direct methods using SHELXS (Sheldrick, 2008) and refined using full-matrix least squares/difference Fourier technique using SHELXL version 2014/7 (Sheldrick, 2015a) and SHELXT version 2014/5 (Sheldrick, 2015b). Diagrams and publication material were generated using PLATON (Spek, 2009) and X-Seed (Barbour, 2001). All the crystal packing diagrams were generated with POV-Ray version 3.6. The crystals were immediately covered in Paratone oil to prevent loss of included solvent. A suitable single crystal was then selected under a microscope and attached on a nylon loop connected to a rigid mounting on the goniometer head under a cold stream of nitrogen gas.

Shelxs-97

This is software that involves minimising the value of the function $\Sigma w(F_o^2 - kF_c^2)^2$ by employing the full matrix least number of squares method. The agreement between the observed (F_o) and calculated (F_c) intensities of reflections is expressed by the residual indices R_1 and wR_2 – equations (1) and (2) based on the structure factor F and F^2, respectively. The collective residual index R is an indirect measure of the structural accuracy and is used to monitor the refinement by achieving the lowest possible value giving a satisfactory model.

$$R_1 = \frac{\sum \|F_o| - |F_c\|}{\sum |F_o|} \tag{1}$$

$$wR_2 = \sqrt{\frac{\sum w(F_o^2 - F_c^2)^2}{\sum w(F_o^2)^2}} \tag{2}$$

The default weighting scheme employed including parameters a and b was refined for each structure and is shown in equation (3) where P is defined in equation (4).

$$w = \frac{1}{\sigma^2 F_o^2 + (aP)^2 + bP} \tag{3}$$

$$P = \frac{\max(0, F_o^2) + F_c^2}{3} \tag{4}$$

For each structure the Goodness of Fit (S) was quoted and is based on F^2.

$$S = \left(\frac{\sum w(F_o^2 - F_c^2)^2}{n - p}\right)^{\frac{1}{2}} \tag{5}$$

where n is the number of reflections and p is the total number of parameters refined.

2.5 FOURIER TRANSFORM INFRA-RED SPECTROSCOPY (FTIR)

Fourier Transform Infrared Spectroscopy (FTIR) is one of the techniques that is used for measuring the intensity of infrared radiation as a function of frequency or wavelength (Mimoza, 2016). The range of the infrared region between 12800 to 10 cm^{-1} can be divided into three regions, near-infrared region (12800-4000 cm^{-1}), mid-infrared region (4000-600 cm^{-1}), and far-infrared region (1000-50 cm^{-1}), where the common region for infrared absorption spectroscopy is the mid infrared region. This instrument was used to characterise the new solid forms. When sample molecules are exposed to infrared radiation, the sample absorbs radiation of specific wavelengths which causes the change of dipole moment of sample molecules. Different functional groups have different vibration modes that correspond to absorption at characteristic wavelengths and produce bond absorptions at different locations and intensities in the IR spectrum. Recognizing where the absorptions generated by the common functional groups occur will help to interpret and confirm the results of the new solids synthesised. Spectra were obtained from a universal attenuated total reflectance (UATR) infrared spectrometer Perkin Elmer® infrared spectrometer.

2.6 SELECTIVITY (COMPETITION EXPERIMENTS)

Competition experiments are used to determine the selectivity of a host towards a particular guest in a mixture of guests.

The selectivity of the host compound for a particular guest or isomer will be evaluated using two different steps, the crystals obtained from mother liquor and solid-sorption techniques.

A convenient measure for selectivity is the determination of the selectivity co-efficient. The selectivity co-efficient is defined by:

$$K_{A:B} = (K_{A:B})^{-1} = Z_A/Z_B * X_B/X_A$$

where ($X_A + X_B = 1$), X_A and X_B are mole fractions of the two guests A and B in the mother liquor and Z_A and Z_B are the mole fractions of the guests entrapped in the resultant crystals.

2.7 COMPUTER PACKAGES

ConQuest is the primary program used for searching and retrieving information from the CSD (Bruno et al., 2002). The Cambridge Structural Database (CSD) was used for access and investigation of the published crystal data for the comparison with the inclusion compounds presented in this thesis (Groom et al., 2016), (Allen, 2002). This ensured that the experimentation being done was not a repetition. The program was also accessed to match findings in our crystals with those found in similar documented compounds, for example, bond lengths and bond angles.

SADABS version 2.03 Siemens Area Detector Absorption Corrections is an application in the APEX suite used to scale and correct data for absorption collected on a Bruker AXS area detector (Sheldrick G.M., 2002).

XPREP is a program used to determine the space group, read the raw data file, and write the instruction file, the parameter file written by the diffractometer control program and reflection data file (version 5.1, 1997).

X-SEED is a graphical program interface for crystallography and graphical programs (Barbour, 2001). It was used as graphical program for SHELXS-97, SHELXL-97, SHELXT, POV-RAY, LAZY PULVERIX and SECTION (Yvon et al., 1977).

POV-RAY is a program which generates graphics; it was used to create all molecular packing diagrams.

LAYER is a component of X-seed which displays simulated precision photographs of the reciprocal lattice levels using intensity data (Barbour, 1999). It was used for determining space group symmetry and systematic absences.

LAZY PULVERIX is software which calculates theoretical powder X-ray diffraction patterns from single crystal X-ray diffraction data. It was used for the generation of calculated XRD traces from the crystal structure solution. Input to this programme included atomic fractional coordinates, thermal parameters and space group data (Yvon et al., 1977).

POV-LABEL allows the control of the atom labels on an image rendered using Pov-Ray.

PLATON version 2020.4 was used to calculate molecular structure parameters such as torsion angle, bond lengths, bond angles and parameters defining non-covalent interactions (Spek, 2009).

REFERENCES

Aakeröy, C.B. & Beatty, A.M. 2004. Solid State, Crystal Engineering and Hydrogen Bonds. In *Comprehensive Coordination Chemistry II*. Elsevier Ltd: 679–688.

Allen, F.H. 2002. The Cambridge Structural Database: a quarter of a million crystal structures and rising. *Acta Crystallographica Section B Structural Science*, 58(3): 380–388.

Barbour, L.J. 1999. LAYER - A computer program for the graphic display of intensity data as simulated precession photographs. *Journal of Applied Crystallography*, 32(2): 351–352.

Barbour, L.J. 2001. X-seed - A software tool for supramolecular crystallography. *Journal of Supramolecular Chemistry*, 1(4–6): 189–191.

Brown, M.E. 1989. *Introduction to thermal analysis, techniques and applications*. Kluwer Academic Publishers.

Bruno, I.J., Cole, J.C., Edgington, P.R., Kessler, M., Macrae, C.F., McCabe, P., Pearson, J. & Taylor, R. 2002. New software for searching the Cambridge Structural Database and visualizing crystal structures. *Acta Crystallographica Section B: Structural Science*, 58(3 PART 1): 389–397.

Caira, M. & Nassimbeni, L. 1996. Comprehensive Supramolecular Chemistry, edited by JL Atwood, JED Davies, DD MacNicol and F. Vögtle.

Coats, A.W. & Redfern, J.P. 1963. Thermogravimetric analysis. A review. *The Analyst*, 88(1053): 906.

Groom, C.R., Bruno, I.J., Lightfoot, M.P. & Ward, S.C. 2016. The Cambridge Structural Database. *Acta Crystallographica Section B Structural Science, Crystal Engineering and Materials*, 72(2): 171–179.

Haines, P.J. Peter J.. 1995. *Thermal methods of analysis : principles, applications and problems*. Blackie Academic & Professional.

Lavelle, L. & Nassimbeni, L.R. 1993. Studies on Werner Clathrates . Part 13 . 1 Selective Criteria in Werner Clathrates . Six Crystal Structures with B is (isothiocyanato) tetra (4-vinylpyridine) nicke1 (II) as Host. *Journal of Inclusion Phenomena and Molecular Recognition in Chemistry*, 16: 25–54.

Mimoza, N. 2016. *Seminar I a-1. year, II. cycle FOURIER TRANSFORM INFRARED SPECTROSCOPY.*.

Neumann, T., Jess, I. & Näther, C. 2016. Crystal structure of bis(isonicotinamide-jN1)-bis(thiocyanato-jN)zinc. *Acta Crystallographica Section E: Crystallographic Communications*, 72(7): 922–925.

Rissanen, K. 2014. Advanced X-ray Crystallography. *Encyclopaedia of supramolecular chemistry*, 2: 1586–1591.

Schaeffer, W.D., Dorsey, W.S., Skinner, D.A. & Christian, C.G. 1957. Separation of Xylenes, Cymenes, Methylnaphthalenes and Other Isomers by Clathration with Inorganic Complexes. *Journal of the American Chemical Society*, 79(22): 5870–5876.

Sheldrick, G.M. 2008. A short history of SHELX. *Acta Crystallographica Section A: Foundations of Crystallography*, 64(1): 112–122.

Sheldrick, G.M. 2015a. Crystal structure refinement with SHELXL. *Acta Crystallographica Section C: Structural Chemistry*, 71(1): 3–8.

Sheldrick, G.M. 2015b. SHELXT - Integrated space-group and crystal-structure determination. *Acta Crystallographica Section A: Foundations of Crystallography*, 71(1): 3–8.

Sheldrick, G.M. & Schneider, T.R. 1997. [16] SHELXL: High-resolution refinement. In *Methods in enzymology*. 319–343.

Spek, A.L. 2009. Biological Crystallography Structure validation in chemical crystallography. *Acta Crystallographica Section D: Structural Biology*, 65: 145–155.

Yvon, K., Jeitschko, W. & Parthé, E. 1977. *LAZY PULVERIX* , a computer program, for calculating X-ray and neutron diffraction powder patterns. *Journal of Applied Crystallography*, 10(1): 73–74.

CHAPTER III

TETRAHEDRAL ZINC COMPLEXES

3.1 Introduction

The crystallographic investigation of zinc complexes was based on the design and synthesis of three new complexes with both similar and different ligands linked to a metal centre, to study in detail their behaviour in host-guest chemistry, structure-property relationships and differences observed in the functionalities. The three complexes are of the composition ZnX_2L_2 with X representing a chloride anion and L representing ligands nicotinamide (nic) or isonicotinamide (isonic). Based on the Cambridge Structural Database (CSD) version 5.41, last update 2020, many articles relating to crystal structures were published on similar complexes. Fifty-eight structures were found in the CSD in which the complexes of composition $ZnCl_2X_n$ were investigated, of which 28 hits were for ZnX_nnic_2, 9 hits for $ZnX_nisonic_2$ (with X≠Cl) but none for $ZnX_nnic/isonic$ (where X can be any anion and n = 1 to 5). On narrowing our research on the CSD it was found that only one publication for $ZnCl_2nic_2$ (CSD refcode WUKZAD) was reported by Ide and co-workers (Ide et al., 2002) but no complexes for $ZnCl_2isonic_2$ or $ZnCl_2nic/isonic$ were previously published.

The selection of the metal ion zinc (II) and these ligands were based on their biological activities. Zinc is a building block which plays an important role in liver enzyme function and synthesis (Paşaoğlu et al., 2006). Zinc can inhibit electron transport, by binding to DNA, and interacting with the cell membrane (Sun et al., 2003). Secondly, zinc is the last element in the first row of transition elements. Transition metals have typical metallic properties such as their silvery metal appearance. Compounds of transition metals show coloured inorganic materials. However, zinc is one of the few transition elements which does not exhibit a characteristic colour. For a compound to exhibit colour the central atom of the compound should have at least an unpaired d electron on it. Although zinc is an element of the d-block family, showing two oxidation states that involve (n-1) d^{10} configuration, it has no unpaired electron in the subshell. Therefore, the unpaired electron d-transition is not possible, and no colour is observed. In other words, the colours of transition element compounds are due to d-d transitions which are possible only when the subshell has unpaired electrons. Moreover, the existence of d^{10}-d^{10} interactions between two closed shells of zinc atoms increases the possibility of formation of complicated multi-dimensional systems (Du et al., 2004). Examples are compounds of the ligand pyridylthioacetic acid (pyta) such as $[Zn(pyta)(OH)]_n$ and $[Zn(pyta)_2]_n$ which afford a 2-dimensional homo-chiral helix or 1-dimensional chain patterns of polymeric coordination.

Nicotinamide and isonicotinamide ligand that have meta- or para-amide functional groups are able to give the capacity for hydrogen bonding and the formation of a host framework. These host frameworks are similar to those reported by Wicht et al, although the complexes used the metal nickel and were octahedral (Wicht et al., 2016).

The host complexes are zinc chloride with two neutral ligands which are N-bonded via the nitrogen atom in the pyridine derivative ligands nicotinamide and isonicotinamide as shown in Figure 3.1.
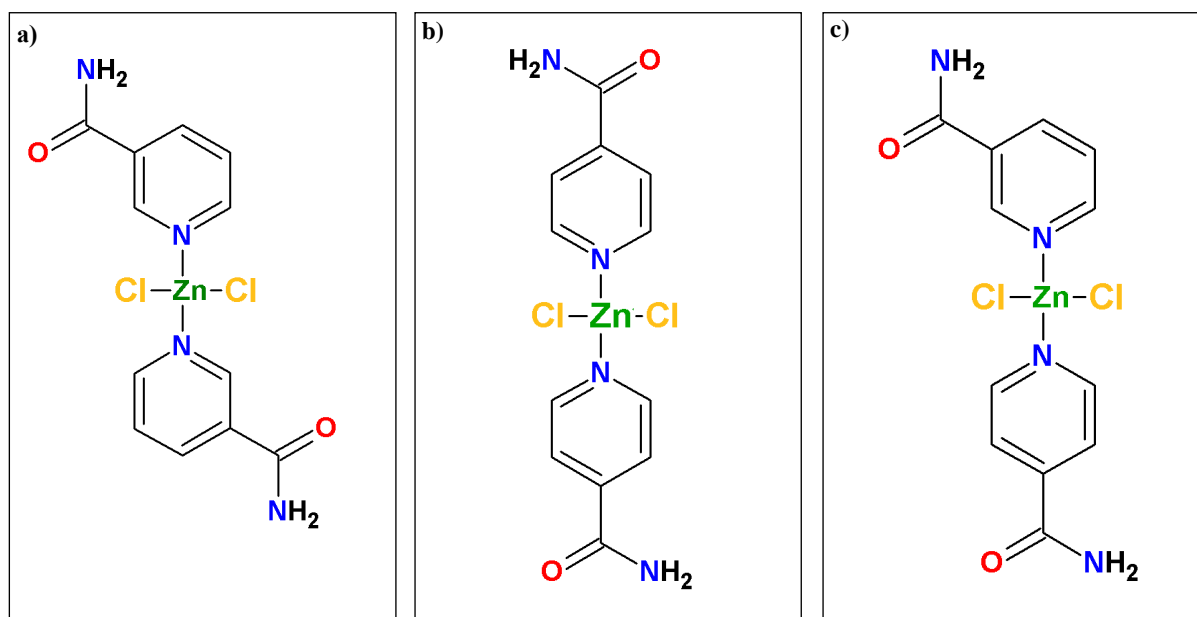
Figure 3.1 Zinc complex structures of a) H1, ZnCl$_2$(nic)$_2$, b) H2, ZnCl$_2$(isonic)$_2$ and c) H3, ZnCl$_2$(nic)(isonic).

The DSC curves show two or three endotherms of each host for the two steps of decomposition of the ligand nicotinamide and isonicotinamide, the first indicating melting and the second showing vaporisation (boiling).

In H1 and H2 the ligands nicotinamide and isonicotinamide were observed to melt at 125 and 140 °C respectively with a boiling point of 329 °C. H3 showed two endotherms for the melting of nicotinamide and isonicotinamide at 97 and 125 °C with one boiling point peak for both at 333 °C.
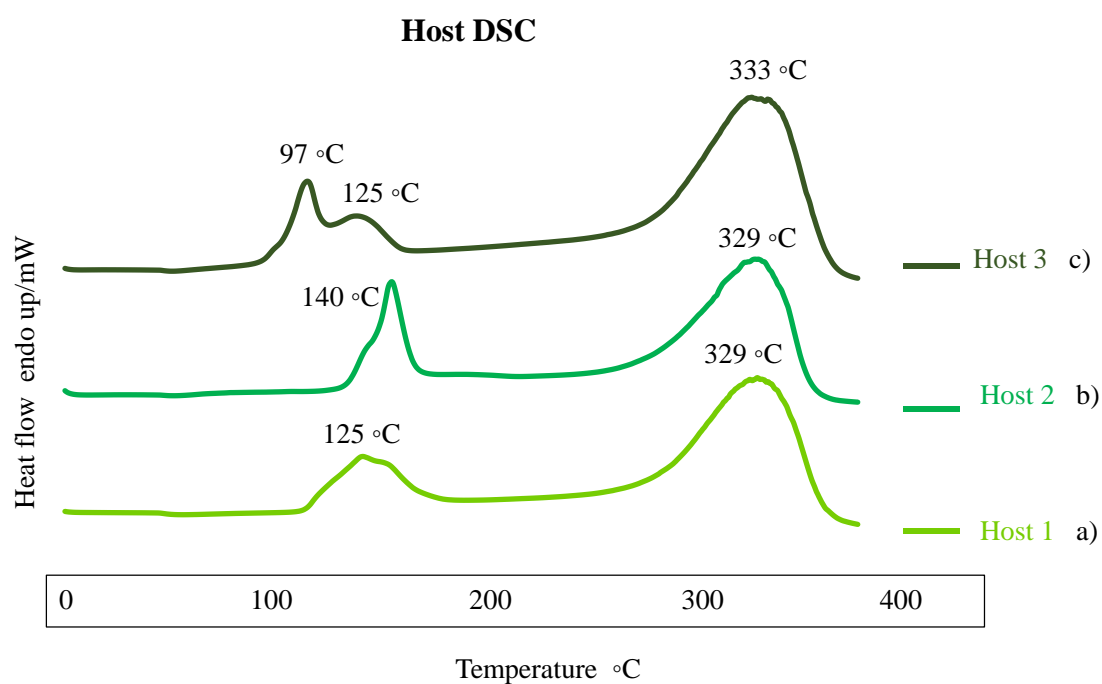
Figure 3.2 DSC curves of zinc complex a) H1, ZnCl$_2$(nic)$_2$, b) H2, ZnCl$_2$(isonic)$_2$ and c) H3, ZnCl$_2$(nic)(isonic).

After synthesis, the hosts formed a white powder with fine granular texture. The three complexes, with zinc (II) cation located in the centre, are $ZnCl_2(nic)_2$ (H1), $ZnCl_2(isonic)_2$ (H2) and $ZnCl_2(nic)(isonic)$ (H3) and are tetrahedral in geometry (Figure 3.1). After crystallisation with several guests only H1 presented inclusion activity and trapped nicotinamide as a guest in its cavities; H2 and H3 did not enclathrate any guests. The complex (H1•nic) presented in Figure 3.3 is the structure of the molecules involved in the clathrate obtained after crystallisation.
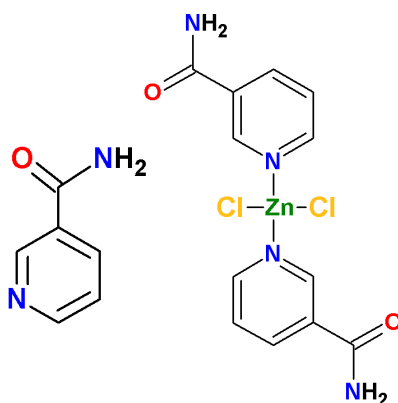
Figure 3.3 Scheme showing the structure of H1•nic.

3.2 Syntheses and geometric structure characterisation of H1•nic, H2$_c$ and H3$_c$ crystals.

Compounds H1, H2 and H3 underwent a process of crystallisation by separately dissolving 50 mg of each host powder in 3 mL of hot hexanol and a few drops of DMSO (solvent) to dissolve the hosts with constant stirring at 50 °C for 30 min. Small colourless crystals were formed within two weeks after slow evaporation at room temperature. After crystallisation, the host did not include hexanol but self-included the ligand nicotinamide as guest in H1 and no inclusion in H2 and H3 was observed. The analysis of the crystals was done using thermal gravimetry (TGA), powder X-ray diffraction (PXRD) and single crystal X-ray diffraction (SCXRD). Crystallographic data and hydrogen bonds for the product complexes of inclusion compound H1•nic, and host crystals H2$_c$ and H3$_c$ are listed in Table 3.1. The same process was applied using other potential guests 1-pentanol, butanol, ethanol and methanol, but no inclusion potential guest occurred.

For all new compounds mentioned in this chapter, the Zn(II) complexes consist of four coordinated atoms around Zn in a near tetrahedral. The zinc atom is surrounded by two chloride atoms and two nitrogen atoms, and the length between Zn-N bond is shorter than the Zn-Cl bond of the anion. For example, in complex H1•nic, the distances between Zn-N are 2.057 Å which are shorter than Zn-Cl

distances of 2.229 Å. The average bond distances of Zn-N and Zn-Cl for all three compounds is 2.049 Å and 2.227 Å respectively. The average for N-Zn-N and Cl-Zn-Cl bond angles is 109.79° and 118.25° respectively.

In H3 specifically, the Zn-N distance for nicotinamide (2.036 Å) was slightly different from the isonicotinamide ligands (2.050 Å). Zn-N distances are in agreement with those where Zn(II) is coordinated to two nicotinamide/isonicotinamide in a tetrahedral geometry in bis(4-ethylbenzoato-κO)bis(nicotinamide-κN1)zinc(II) and (Zn(SCN)$_2$C$_6$H$_6$N$_2$O)$_2$) (Necefoğlu et al., 2011) (Neumann et al., 2016). The Zn-Cl average bond distance (2.227 Å) is comparable for reported Zn-Cl$_2$(X)$_2$ complexes Zn(4-CH$_3$Py)$_2$Cl$_2$ reported in the CSD (version 5.41) latest with the CSD refcode CMPYZN (Lynton & Sears, 1971), and is also coordinated to two chloride and two nicotinamide ligands (ZnCl$_2$(nic)$_2$) in a tetrahedral geometry with the CSD refcode WUKZAD (Ide et al., 2002). In 1971, Baenziger and Schultz summarised the bond lengths in a number of complexes where zinc is in a tetrahedral conformation with the distances falling in a range of 1.99-2.10 Å and 2.18-2.30 Å for Zn-N and Zn-Cl respectively (Baenziger & Schultz, 1971). This work gives the structure of each compound which is discussed individually in more detail with the aid of packing diagrams and orientation of the cavities in which the guest molecules are situated, including shape and size description.

Table 3.1 *Crystallographic data and structure refinement for H1•nic, H2$_c$ and H3$_c$.*

	H1•nic	H2$_c$	H3$_c$
Chemical formula	C$_{24}$ H$_{24}$ Cl$_2$ N$_8$ O$_4$ Zn	C$_{12}$ H$_{12}$ Cl$_2$ N$_4$ O$_2$ Zn	C$_{12}$ H$_{12}$ Cl$_2$ N$_4$ O$_2$ Zn
H:G ratio	½ : 1	-	-
Formula Weight	624.80	380.55	380.55
Temperature/K	173(2)	173(2)	173(2)
Crystal system	orthorhombic	orthorhombic	monoclinic
Space Group (no.)	Pccn (No.56)	Pbcn (No.60)	P2$_1$/c (No.14)
a/Å	27.225(2)	7.3591(12)	8.3948(6)
b/Å	7.5495(6)	10.4514(17)	7.4015(5)
c/Å	12.7553(11)	19.678(8)	24.734(17)
α/°	90	90	90
β/°	90	90	93.1430(13)
γ/°	90	90	90
V/Å^3	2621.7(4)	1513.5(4)	1536.34(3)
Z	4	4	4
D$_{calc}$/g.cm^3	1.583	1.67	1.645
Radiation type	MoKα	MoKα	MoKα
F(000)	1280	768	768
Crystal size/mm^3	0.09 x 0.12 x 0.24	0.05 x 0.08 x 0.12	0.20 x 0.25 x 0.29
Colour, crystal form	colourless	colourless	colourless
No. of total reflections	57058	24140	33207
No. of unique reflections	3277	1884	3833
Θ min-max/°	1.496/28.355	2.07/28.30	1.65/28.37
R [F^2>2σ(F^2)]	0.0376	0.032	0.0251
wR2(F^2)	0.0806	0.076	0.063
S	1.082	1.015	1.040
No. of parameters/ data	177/3277	120/1884	190/3833
Res.peak(max/min)/eÅ^{-3}	0.349/-0.394	0.378/-0.410	0.557/-0.533

3.3 Thermogravimetric analysis of H1•nic, H2$_c$ and H3$_c$ crystals.

The thermal analysis data for the three hosts and crystals H1•nic, H2$_c$ and H3$_c$ are given in Table 3.2 and thermogravimetric and derivative curves are shown in Figure 3.4 with the temperature range between 0 to 400 ˚C. The thermal analysis results show one step in the three complexes, corresponding to the decomposition of the guest and/or ligands for the three hosts (H1, H2 and H3) and three crystal structures. All results from the TG graphs were compared to the host structure and the calculated theoretical weight loss values (Figure 3.4). The H1•nic experimental data showed a similar temperature of decomposition between host and inclusion compound; as the mass loss was lower than the calculated mass loss of the crystal, our explanation for this difference was based on the fact that nicotinamide and isonicotinamide are 'sticky' ligands and therefore the analysis should have been continued to a higher temperature to allow for further decomposition of the crystal. In the case of H2$_c$ and H3$_c$, the release of the ligands occurred at a decomposition point higher in temperature in the crystal complexes compared with those in the host. The TG analyses of all complexes presented some differences from the theoretical values, more than likely due to the ligands' stronger interaction with the zinc metal, therefore requiring a higher temperature of decomposition.

Table 3.2 Thermo-analytical results for the metal complexes H1•nic, H2$_c$ and H3$_c$.

Steps	Temperature of decomposition (˚C)		Crystal mass loss (%)		Host only mass loss (%)		Crystal groups removed
	Crystal	Host	Found	Calc.	Found	Calc.	
H1•nic							
1	261	260	62	73	62	64	3 x nic $_{(2g+1l)}$
H2$_c$							
1	276	234	44	64	66	64	2 x isonic $_{(l)}$
H3$_c$							
1	286	260	49	64	62	64	1 x nic/1 x isonic $_{(l)}$

g=guest; l=ligand.
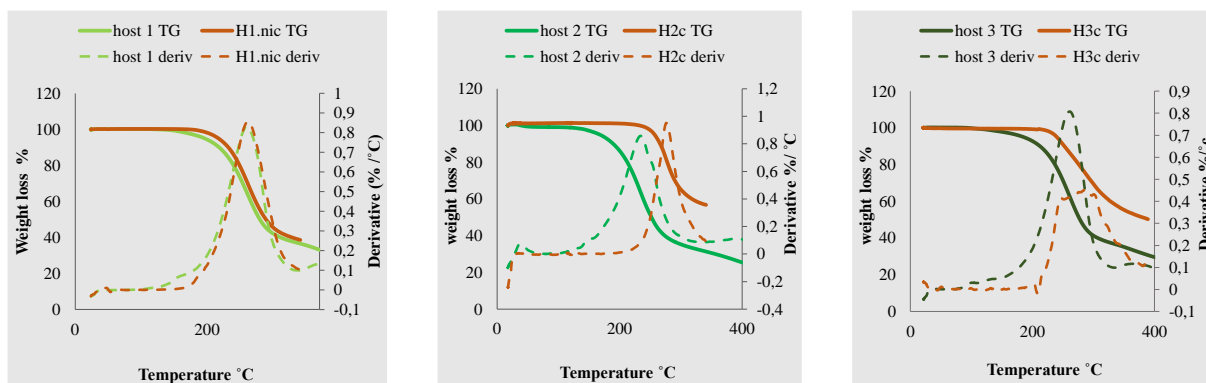
Figure 3.4 TGA and DTG curves for the mass loss (bold curves) and derivative (dotted curves) vs temperature of the crystal (orange curve) and host (green curve) of a) H1•nic crystal and H1 host, b) H2$_c$ crystal and H2 host and c) H3$_c$ crystal and H3 host.

3.4 Crystal structure analysis of H1•nic

H1•nic crystallises in the orthorhombic space group Pccn (No:56) with Z=4. The zinc ion is located on a diad (two-fold rotation) at Wykoff position d. The unit cell of the structure consists of the host ZnCl$_2$(nic)$_2$ and two guest nicotinamides. The Zn(II) atom is bound to the nitrogen atoms of nicotinamide ligands and two chloride ligands in a tetrahedral conformation. The asymmetric unit contains half a host and one guest molecule with molecular formula Zn$_{0.5}$Cl(C$_3$H$_3$N$_2$O)•(C$_6$H$_6$N$_2$O) (Figure 3.5).
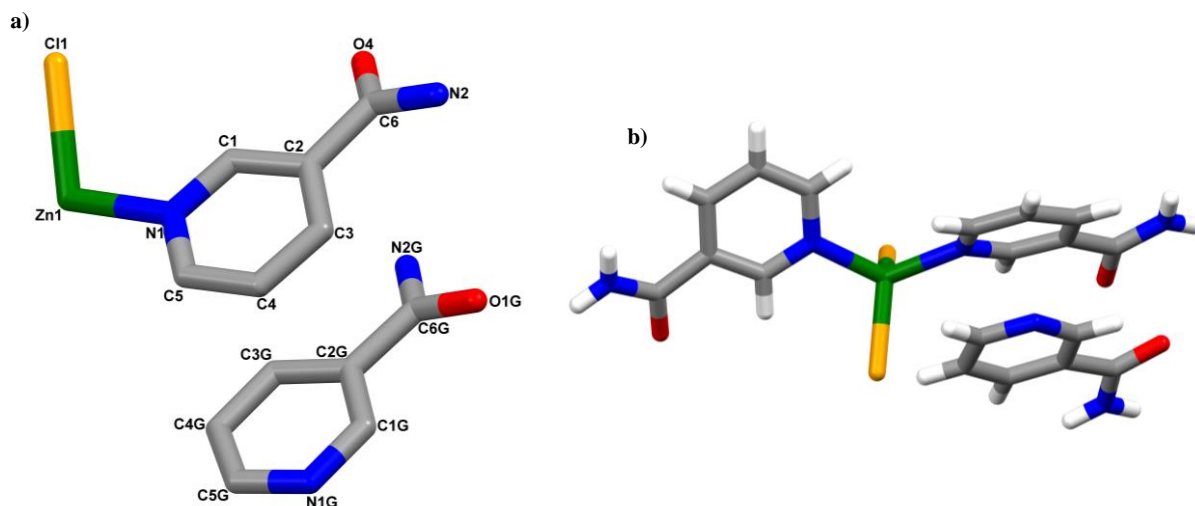
Figure 3.5 a) Numbering scheme for the asymmetric unit of H1•nic (some hydrogen atoms are omitted for clarity) and b) molecular structure of H1•nic.

The H1•nic shows a distorted tetrahedral with the angles around the metal centre falling in the range of 104.18° to 110.31°.

The packing diagram of H1•nic is dominated by supramolecular heterosynthons. Nicotinamide has two acceptor sites, the pyridine ring nitrogen and amide oxygen. As a monodentate ligand, the covalent

bonding takes place through the pyridine ring nitrogen when the molecule coordinates with the metal atom. However, hydrogen bonding interactions of guest nicotinamide may take place through the pyridine ring or through the amide group. Therefore, from the structural analysis, it was observed that the H1•nic structure presented two major hydrogen bonding interactions shown in Figure 3.6 and 3.7.
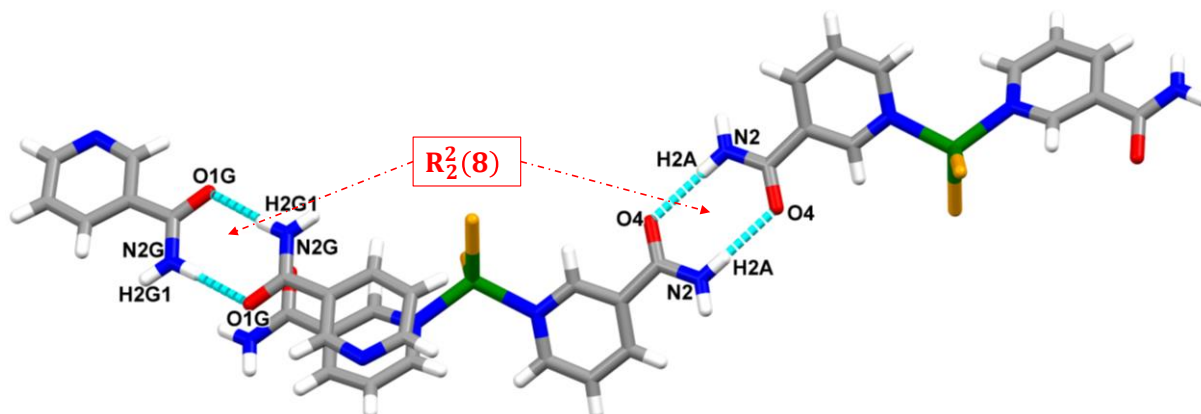
Figure 3.6 Hydrogen bonds numbering schemes showing amide dimers of H1•nic between two hosts and between two guests.

These interactions consist of an intermolecular amide dimer hydrogen bond between guest-guest and host-host described by $R_2^2(8)$ motif of supramolecular synthons. The synthons were observed between two guests via N2G-H2G1•••O1G and between two hosts via N2-H2A•••O4. The N2•••O4 and N2G•••O1G bond distances are 2.067Å and 2.022Å respectively with N2-H2A•••O4 and N2G-H2G1•••O1G angles of 173.70° and 175.50°. As the secondary interaction, Figure 3.7 shows two intermolecular interactions, one through the pyridine ring nitrogen and formed between two guests via N2G-H2G2•••N1G [2.156Å, 148.78°] and the other between host-guest via N2-H2B•••O1G [2.128Å, 159.81°] ($D_1^1(3)$ motif). Table 3.3 summarises the different hydrogen bond metrics for this structure.

Table 3.3 Geometry of the hydrogen bonds and hydrogen bonding interactions for H1•nic.

D-H	d(D-H) (Å)	d(H•••A) (Å)	<DHA (Å)	d(D•••A) A	Symmetry operator
H1•nic					
N2-H2A•••O4	0.880	2.067	173.70	2.943	[-x+1, -y, -z+1]
N2-H2B•••O1G	0.880	2.128	159.81	2.970	[-x+1, y-1/2, -z+3/2]
N2G-H2G1•••O1G	0.880	2.022	175.50	2.901	[-x+1, -y+1, -z+1]
N2G-H2G2•••N1G	0.880	2.156	148.78	2.944	[x, -y+3/2, z-1/2]
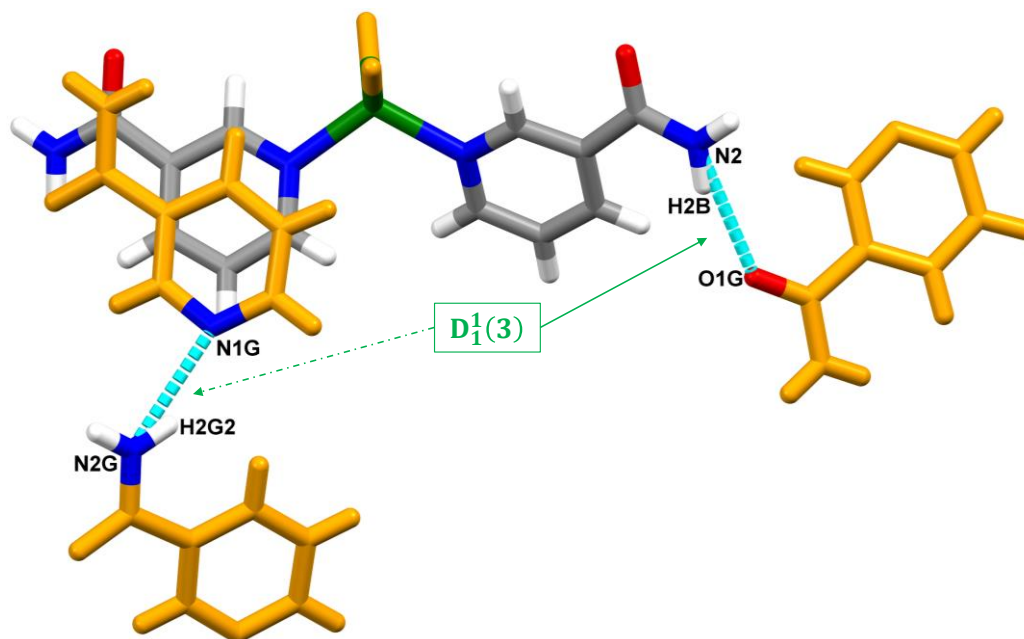
Figure 3.7 *Structure H1•nic showing the secondary hydrogen bonds between host and guest and between two guests, with numbering scheme illustrated.*

The packing diagram along the b-axis is arranged in rows/columns with packing of face-to-face π-π interactions (shown in Figure 3.8) between the aromatic rings of the nicotinamides of the guest and host, with a centroid distance of 3.67Å.

	Centroid	
1	N1GC1GC2GC3GC4GC5G	3.58 Å
2	N1C5C4C3C2C1	3.76 Å
3	Mean value (12 atoms)	**3.67** Å
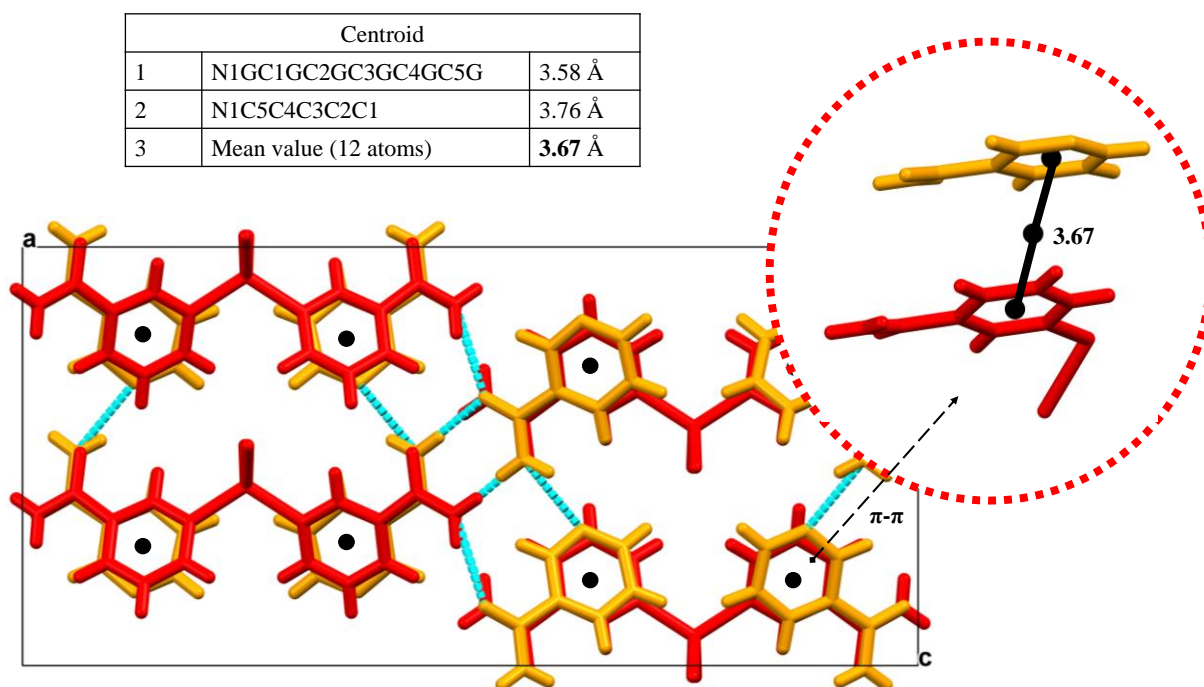
Figure 3.8 *Centroid representation of the unit between host and guest molecules with the packing viewed down the b-axis and table with centroid measurements in Å of the π-π interactions.*

The packing of the structure along the c-axis is arranged in a zig-zag or herringbone pattern of guests (orange space fill) (Figure 3.9a). The void analysis gave a high volume of 1098.40 Å^3 with a percentage unit cell of 41.9% which is also shown in Figure 3.9b and c which shows free space in the packing diagrams in two types of channels along the b and c-axis. The larger channels along the b-axis are occupied by nicotinamide guests as presented in Figure 3.9b, whereas the smaller channels along the b-axis are occupied by chloride atoms (Figure 3.9c).
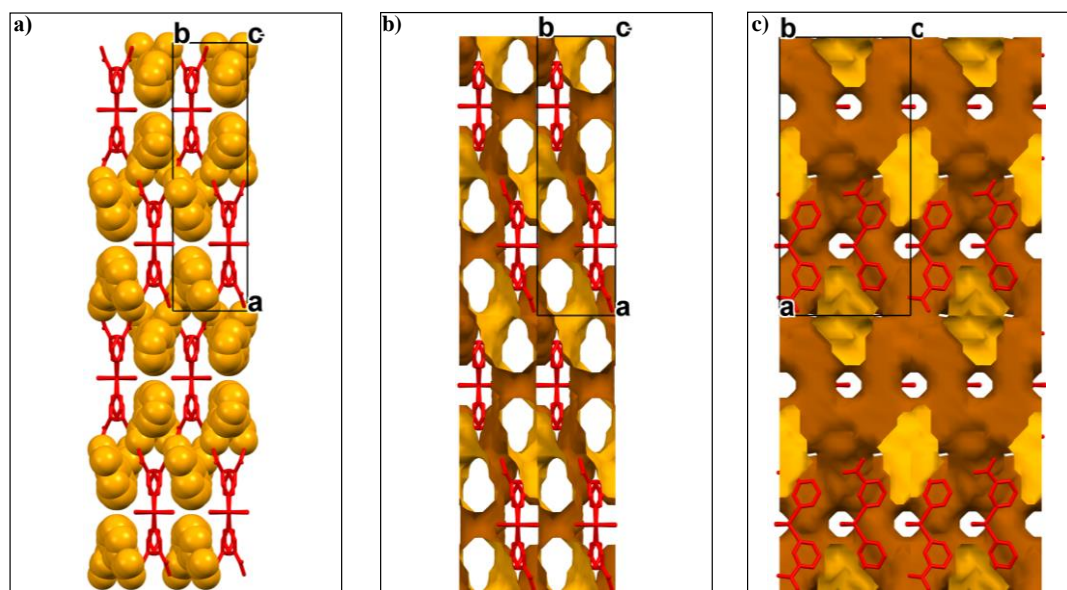
Figure 3.9 *Packing diagram of H1•nic a) viewed along a-axis showing a herringbone pattern of the guest (orange) in space fill configuration and the host (red) in capped stick configuration with alternating guest and host, b) channel view along the a-axis with voids showing guest occupation and c) the void analysis showing channels along the b-axis occupied by chloride atoms.*

3.4.1 Powder X-ray diffraction of H1•nic

The powder X-ray diffraction (PXRD) spectrum of H1•nic was compared to that of the host H1, and these spectra were run between 2θ from 5° to 50°. The analysis was conducted to show the enclathration of nicotinamide as guest and how the two patterns differ from each other. The PXRD pattern of H1 (Figure 3.10, green H1) has a number of peaks which are absent in the crystal H1•nic (Figure 3.10, brown H1•nic) pattern, between 10° and 12° and at 23.5° and 32.5°.
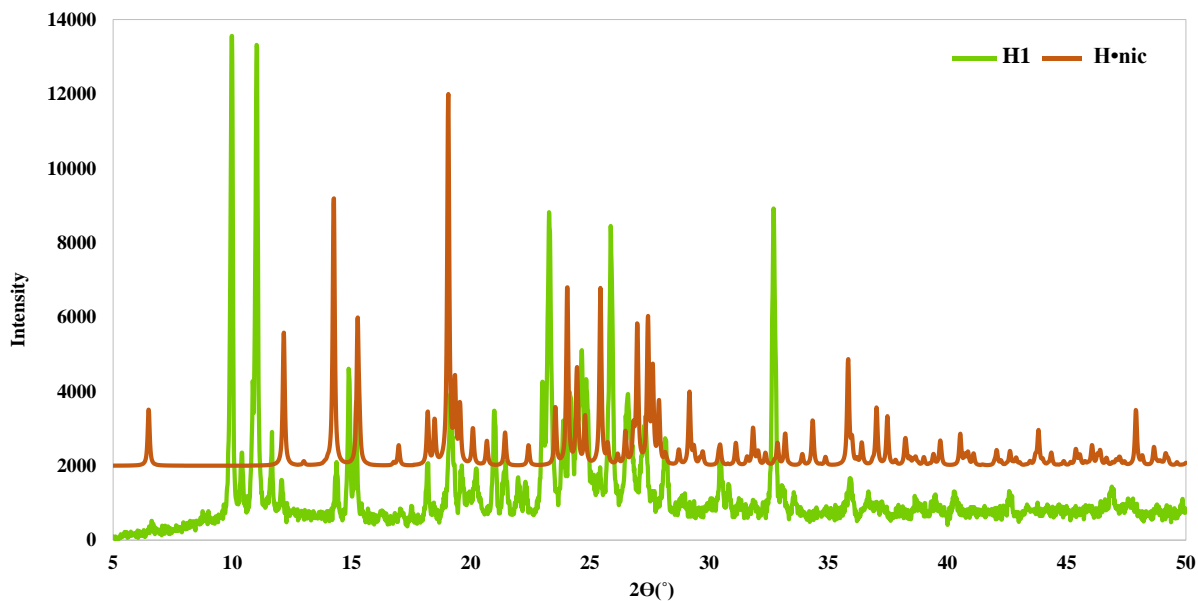
Figure 3.10 PXRD patterns of H1(green) and H1•nic (brown).

3.5 Crystal structure analyses of H2$_c$ and H3$_c$ crystals.

The compounds H2$_c$ and H3$_c$ crystallise in the orthorhombic Pbcn (H2$_c$) and monoclinic P2$_1$/c (H3$_c$) space group respectively with Z=4. The asymmetric structural unit consists of ZnCl$_2$(isonic)$_2$ and ZnCl$_2$(nic)(isonic), with the Zn(II) cation coordinated with two chloride ligand anions and two nitrogen atoms from the isonicotinamide ligands for H2$_c$ and nicotinamide and isonicotinamide ligands for H3$_c$ in a slightly distorted tetrahedral coordination environment. The average bond distance for H2$_c$ and H3$_c$ are Zn-N: 2.053 Å, Zn-Cl: 2.226 Å and Zn-N: 2.043 Å, Zn-Cl: 2.227 Å respectively. The asymmetric unit contains half a host with a molecular formula Zn$_{0.5}$Cl(C$_3$H$_3$N$_2$O) for H2$_c$ and a full molecule with molecular formula of ZnCl$_2$(C$_3$H$_3$N$_2$O)$_2$ for H3$_c$ (Figure 3.11).
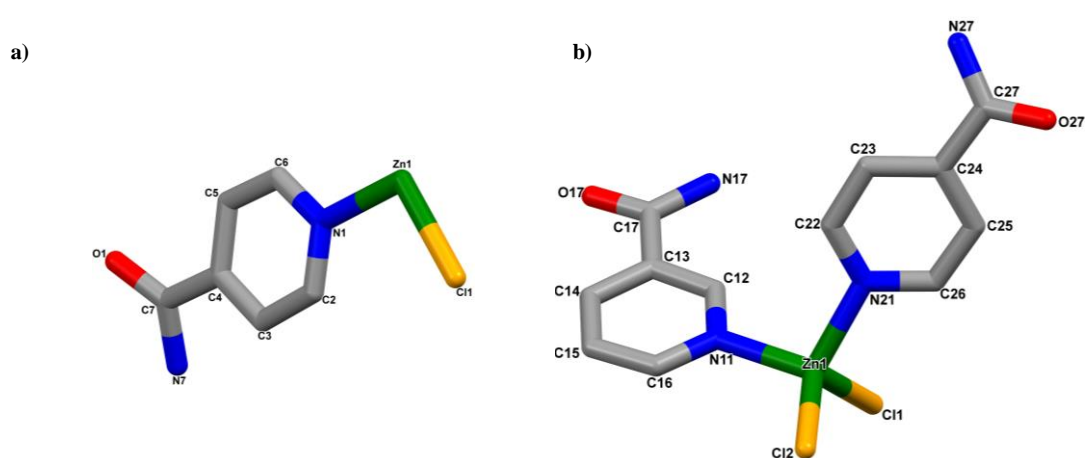
Figure 3.11 Asymmetric unit of a) H2$_c$ and b) H3$_c$ (hydrogens are omitted for clarity).

Isonicotinamide or nicotinamide molecules give three sites for bonding or interactions. These are the pyridine ring nitrogen, the carbonyl oxygen and amide nitrogen. As a monodentate ligand, the isonicotinamide/nicotinamide is covalently bonded to the metal atom via the pyridine ring nitrogen, hence any hydrogen bonding takes place through the amide functional group.

The crystal structure of H2$_c$ is stabilized by two intermolecular interactions N-H•••Cl and N-H•••O. Both hydrogens of the isonicotinamide NH$_2$ group are involved in the intermolecular interactions, the first H forming the N7-H17B•••O1 bond between the amide group and the carbonyl group of the neighbouring complex. The second H atom interacts in a hydrogen bond between the amide group and the chloride atom (N7-H7A•••Cl1) (Figure 3.12). The details of hydrogen bonding geometry are listed in Table 3.4.
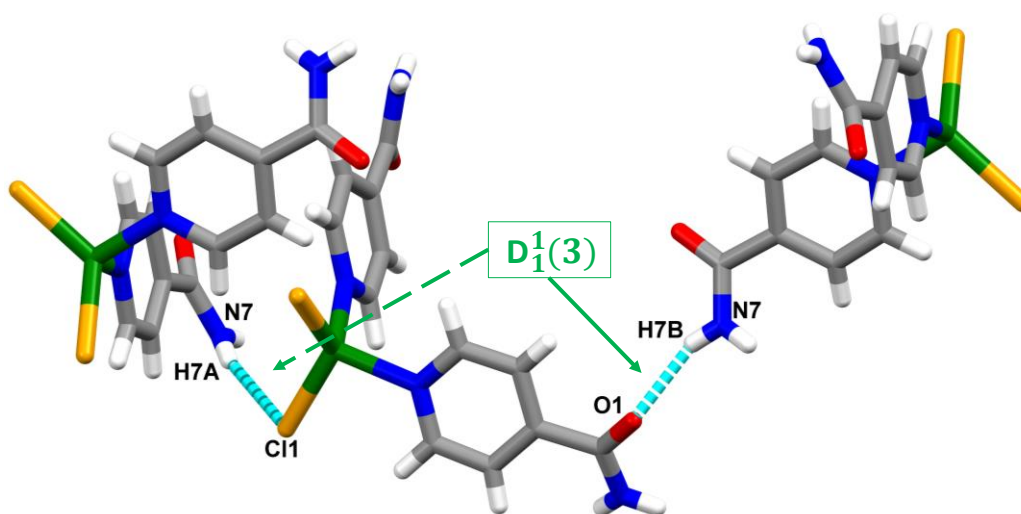
Figure 3.12 *Hydrogen bonding in H2$_c$, described by motif $D_1^1(3)$.*

Table 3.4 *Geometry of the hydrogen bonds and hydrogen bonding interactions of H2$_c$ crystal.*

D-H	d(D-H) (Å)	d(H•••A) (Å)	<DHA (Å)	d(D•••A) A	Symmetry operator
H2$_c$					
N7-H7A•••Cl1	0.820	2.536	165.02	3.334	[x+1/2,y+1/2, -z+1/2]
N7-H7B•••O1	0.816	2.132	153.37	2.884	[x+1/2, -y+3/2, -z]

The two isonicotinamide ligands of H2$_c$ are connected with the two neighbouring molecules through their amides. The isonicotinamide ligands of the adjacent molecule are connected to the neighbouring molecules via N-H•••Cl interactions through the chloride of the adjacent molecule and via N-H•••O interactions through the isonicotinamide NH$_2$ which is not part of the adjacent molecule (red) as illustrated in Figure 3.13 by (1). When the isonicotinamide of the adjacent molecule is linked to the neighbouring molecule via both N-H•••Cl and N-H•••O as illustrated in blue dashed lines in Figure 3.13

(2), the isonicotinamide not in the adjacent molecule (red) links the neighbouring molecule via the N-H···O only as illustrated in Figure 3.13 by the red dashed lines.
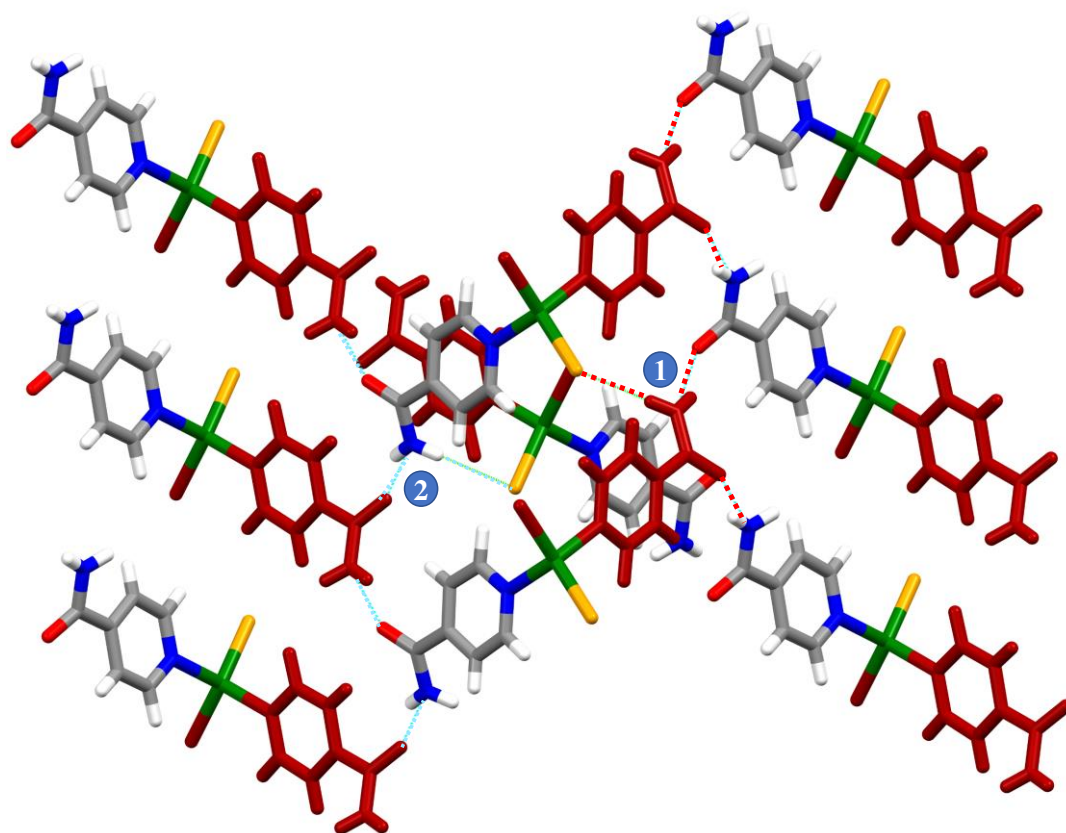
Figure 3.13 *Difference between the hydrogen bonding of the ligands not in the adjacent molecule (red) and ligands in the adjacent molecule of the intermolecular interactions of N-H···Cl and N-H···O represented by blue and red dashed lines.*

N-H···O hydrogen bonding is the main interaction responsible for the packing, as illustrated in Figure 3.14 which views the crystal structure down the a- and b-axis and shows a herringbone pattern when viewed along the a-axis. The interactions shown in the blue dotted circle is a labelled representation of the hydrogen bonding present in the packing diagrams which looks like a dimer linking two molecules when viewed in 2 dimensions. In the packing diagrams, the molecules which appear to be in the same plane are actually one on top of the other hence three molecules are linked as shown in the circle.
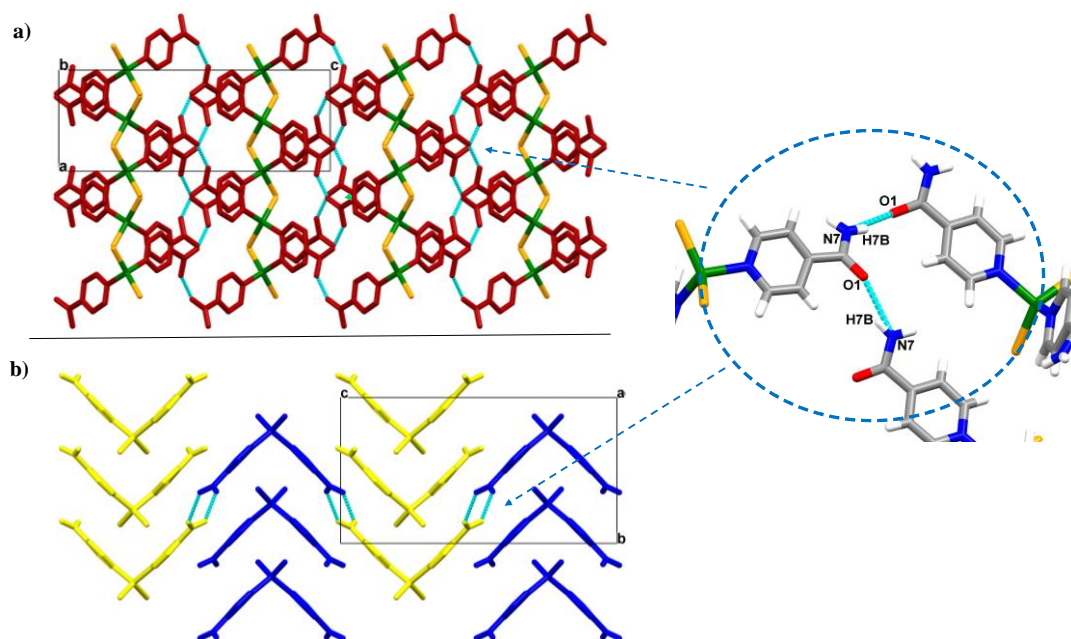
Figure 3.14 *Packing diagram of H2$_c$ showing the hydrogen bonding N-H•••O: a) viewed along the b-axis with zigzag motifs of the zinc chloride (ZnCl$_2$) aligned in columns and b) viewed along the a-axis forming two sets of zigzags coloured accordingly (some hydrogens are omitted for clarity), with a 3 dimensional diagram of the hydrogen bonding shown in the dotted blue circle.*

The crystal structure of H3$_c$ is sustained by N-H•••Cl and N-H•••O main intermolecular interactions. The N-H•••Cl interactions are located between the amide group of the isonicotinamide and the chloride group presented as N27-H27B•••Cl1 with NH•••Cl distance of 2.449 Å. The intermolecular N-H•••O interactions occur between the carbonyl and amide groups of the isonicotinamide and nicotinamide ligands of the neighbouring complex represented as N17-H17B•••O27 with an N-H•••O distance of 2.085 Å (Figure 3.15). These interactions observed can be described as $C_1^1(9)$ and $C_1^1(13)$ graph set motifs respectively (Etter et al., 1990).
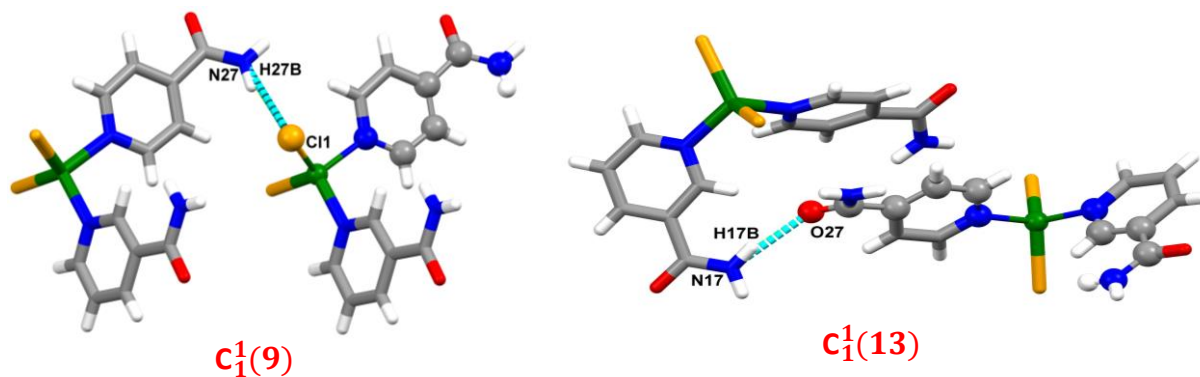
Figure 3.15 *Hydrogen bonding between the host molecules with the capped stick style showing the chains.*

The second chloride Cl2 atom of the ASU is involved in two interactions, one forming a weak hydrogen bond between one aromatic C-H group of the pyridine ring and the chloride of the neighbouring molecule forming C-H•••Cl interactions (C15-H15•••Cl2, 3.615 Å). The second interaction between the amide and the chloride group via N27-H27A•••Cl2 with an N-H•••Cl distance of 3.424 Å is listed in Table 3.5 with the geometries of the other hydrogen bonds.

Discrete assemblies form heterodimer and homodimer synthons, the former constructed via N27-H27•••Cl2 and N17-H17B•••O27 described as a $R_2^2(22)$ graph set as shown in Figure 3.16a. The homodimers are constructed by C15-H15•••Cl2 and N17-H17A•••O17 hydrogen bonds classified as $R_2^2(12)$ (Figure 3.16b) and $R_2^2(8)$ (Figure 3.17) graph sets respectively.
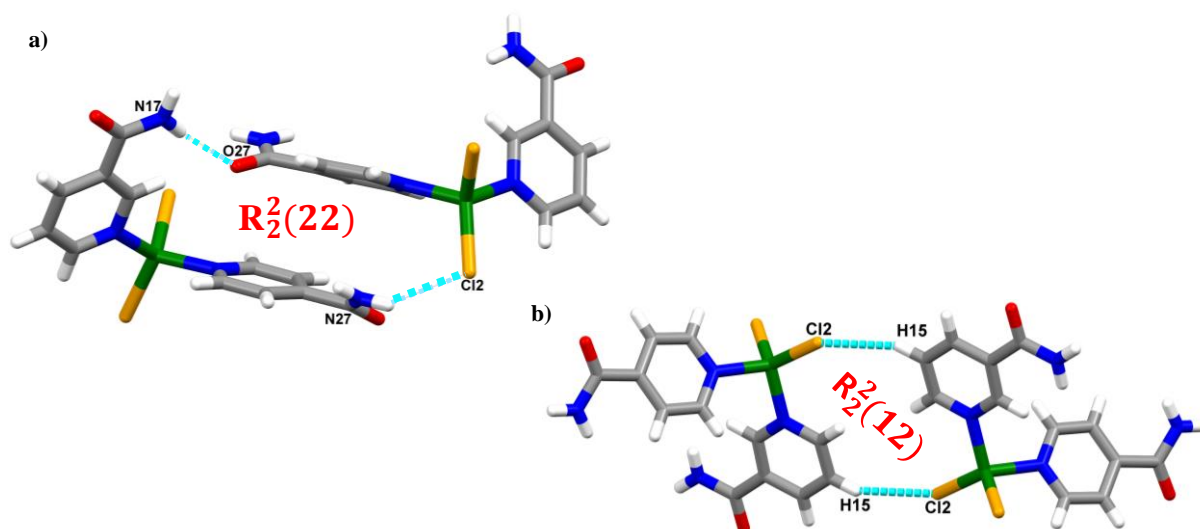
Figure 3.16 *Synthons representation of: a) heterodimer graph set and b) homodimer graph sets between two neighbouring molecules in H3$_c$.*

Table 3.5 *Geometry and interactions of the hydrogen bonds for H3$_c$ crystal.*

D-H	d(D-H) (Å)	d(H•••A) (Å)	<DHA (Å)	d(D•••A) A	Symmetry operator
H3$_c$					
N17-H17A•••O17	0.880	1.997	174.29	2.874	[-x, -y+3, -z]
N17-H17B•••O27	0.880	2.085	153.96	2.901	[-x, y+1/2, -z+1/2]
N27-H27A•••Cl2	0.880	2.659	145.99	3.424	[-x, y+1/2, -z+1/2]
N27-H27B•••Cl1	0.880	2.449	160.88	3.293	[x-1, y, z]
*C15-H15•••Cl2	0.950	2.727	155.88	3.615	

***Weak hydrogen bond

The packing is shown along the b-axis of the $H3_c$ crystal. This is sustained by hydrogen bonds as discussed previously and the homodimer (amide dimer) of the N-H•••O hydrogen bonds is shown in Figure 3.17.
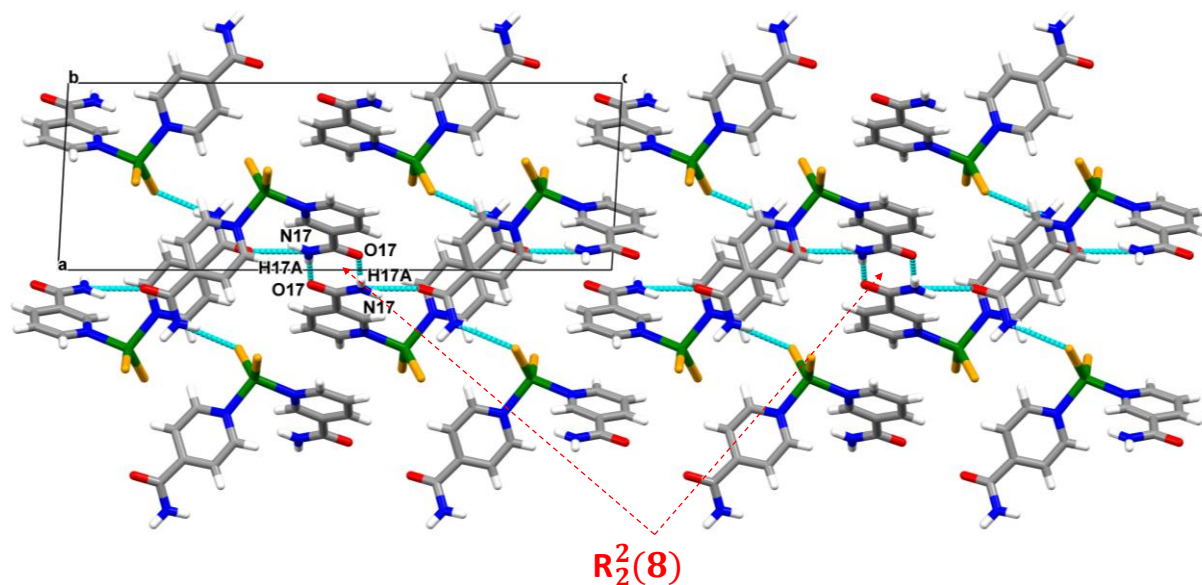
Figure 3.17 *Packing diagram of $H3_c$ viewed along b-axis displaying the amide dimer hydrogen bonding and graph set $R_2^2(8)$).*

3.5.1 Powder X-ray analysis of $H2_c$ and $H3_c$ crystals.

The Powder X-ray diffraction analyses was conducted to show the similarities between the host and the crystal and how they differ from each other. All PXRD analyses were run from 3 to 48 °C two theta and the patterns are illustrated in Figure 3.18. According to SCXRD the host compound and the crystal have the same tetrahedral structure with four ligands, although several peaks have shifted slightly on comparing the crystal patterns with that of the host. Differences are due to the synthetic process of the crystal formation which were different from the hosts. Crystals were made by slow evaporation of the mixture (host and solvent) which differed from the synthesis of the hosts and this modified the PXRD pattern of the crystals.
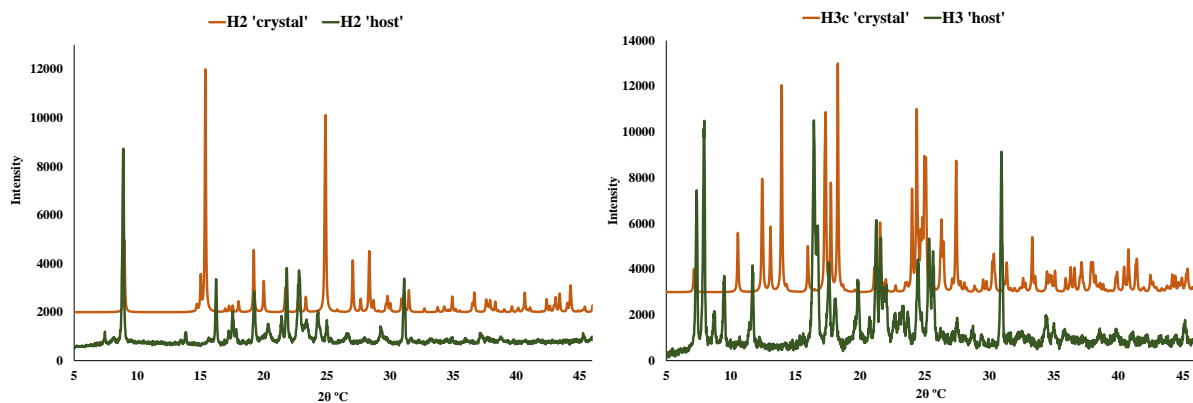
Figure 3.18 *Comparison analysis of PXRD patterns of H2ᶜ crystal (orange) with host 2 (green) and H3ᶜ crystal (orange) with host 3 (green).*

3.6 Analysis of hydrogen bonds N-H•••Cl in zinc Werner complexes published in CSD

The Cambridge Structural Database (CSD, version 5.4, last update November 2019) was searched for N-H•••Cl contacts in the range of $1.6 <$ H•••Cl $(d_1/Å) < 3.0$, $1.7 <$ N•••Cl $(d_2/Å) < 3.4$ and $140° <$ N-H•••Cl $(\theta/°) < 180°$. The research was focused on contacts between amide groups and chloride bonded to the transition metal zinc. This investigation was used to compare the results obtained during this study with published results on the CSD; the mean value of the search on the CSD was compared to the mean value of our research. 703 hits were found for N-H•••Cl with a mean value of 2.373 Å and 3.244 Å for H•••Cl and N•••Cl respectively. All distribution distances are shown in Fig 3.19 with the total number of hits (Thallapally & Nangia, 2001).

Table 3.6 *Hydrogen-bond geometry of H2ᶜ and H3ᶜ, with •••Cl bonds highlighted in yellow.*

D-H	d(D-H) (Å)	d(H•••A) (Å)	<DHA (Å)	d(D•••A) A
H2ᶜ				
N7-H7A•••Cl1$	0.820	2.536	165.02	3.334
N7-H7B•••O1	0.816	2.132	153.37	2.884
H3ᶜ				
N17-H17A•••O17	0.880	1.997	174.29	2.874
N17-H17B•••O27	0.880	2.085	153.96	2.901
N27-H27A•••Cl2$	0.880	2.659	145.99	3.424
N27-H27B•••Cl1$	0.880	2.449	160.88	3.293
Mean value$	**0.860**	**2.548**	**157.30**	**3.350**

$This mean value if for N-H•••Cl interactions found in the crystals.

In our two structures (**H2ᶜ** and **H3ᶜ**) where N-H•••Cl was observed, the mean values were found to be d_1: 2.548 (H•••Cl) Å and d_2: 3.350 (N•••Cl) Å, shown in Table 3.6. In comparison with the mean CSD results for each interaction in Figure 3.19a and b, our interactions fell in the same range.

N-**H**•••Cl

d₁

x-axis
Hit: 703
Min: 1.647
Max: 3.0
Mean: 2.373

N-H•••**Cl**

d₂

x-axis
Hit: 703
Min: 1.803
Max: 3.3
Mean: 3.244

a)

b)
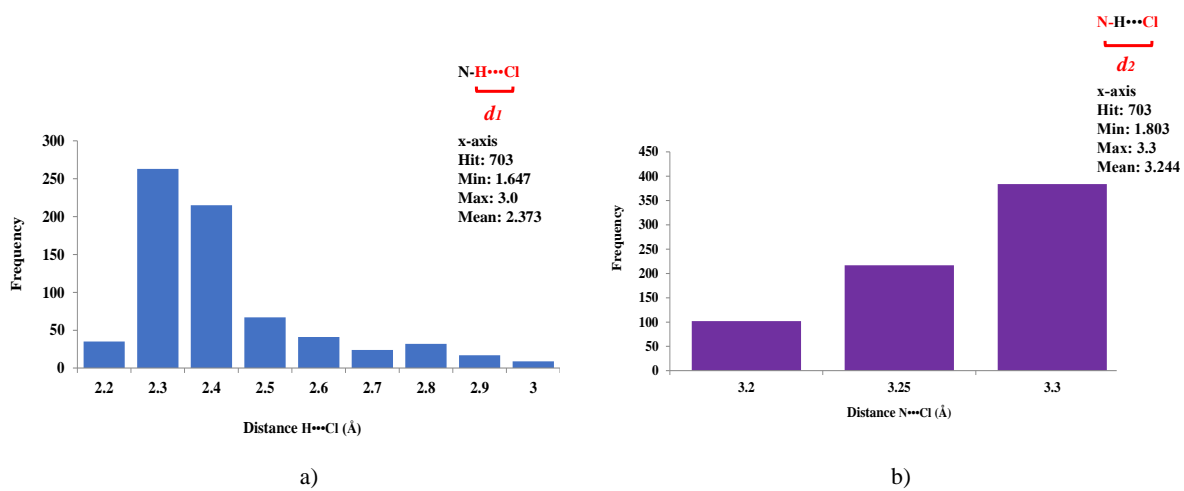
Figure 3.19 *Histogram of the distributions of contact distances of N-H•••Cl hydrogen bonds analysed on the CSD for a)* ***d₁*** *(H•••Cl) and b)* ***d₂*** *(N•••Cl).*

N-H•••Cl

References

Baenziger, C.N. & Schultz, J.R. 1971. Crystal structure of dichlorobis(1-methyltetrazole)zinc(II). *Inorganic Chemistry*, 10(4): 661–667.

Du, M., Zhao, X.J. & Wang, Y. 2004. Crystal engineering of a versatile building block toward the design of novel inorganic-organic coordination architectures. *Dalton Transactions*, (14): 2065–2072.

Etter, M.C., MacDonald, J.C. & Bernstein, J. 1990. Graph-set analysis of hydrogen-bond patterns in organic crystals. *Acta crystallographica. Section B, Structural science*, 46 (Pt 2): 256–62.

Ide, S., Ataç, A. & Yurdakul, Ş. 2002. Spectroscopic and structural studies on dichlorobis(nicotinamide)zinc(II). *Journal of Molecular Structure*, 605(1): 103–107.

Lynton, H. & Sears, M.C. 1971. *Gryskal and Molecular Structure of Diehlorobis(4-methy~pyri(Bine)zine(II), Zn(4-CH,By), C1*. www.nrcresearchpress.com 13 June 2020.

Necefoğlu, H., Özbek, F.E., Aktaş, V., Tercan, B. & Hökelek, T. 2011. Bis(4-ethylbenzoato-κO)bis(nicotinamide-κN1)zinc(II). *Acta Crystallographica Section E: Structure Reports Online*, 67(3).

Neumann, T., Jess, I. & Näther, C. 2016. Crystal structure of bis(isonicotinamide-jN1)-bis(thiocyanato-jN)zinc. *Acta Crystallographica Section E: Crystallographic Communications*, 72(7): 922–925.

Paşaoğlu, H., Güven, S., Heren, Z. & Büyükgüngör, O. 2006. Synthesis, spectroscopic and structural investigation of ZnI2(nicotinamide)2, ZnI2(isonicotinamide)2 and [Zn(H2O)2(picolinamide)2]I2. *Journal of Molecular Structure*, 794(1–3): 270–276.

Sun, D., Cao, R., Sun, Y., Bi, W., Li, Xiaoju, Wang, Y., Shi, Q. & Li, Xing. 2003. Novel Silver-Containing Supramolecular Frameworks Constructed by Combination of Coordination Bonds and Supramolecular Interactions. *Inorganic Chemistry*, 42(23): 7512–7518.

Thallapally, P.K. & Nangia, A. 2001. A Cambridge Structural Database analysis of the C–H···Cl interaction: C–H···Cl− and C–H···Cl–M often behave as hydrogen bonds but C–H···Cl–C is generally a van der Waals interaction. *CrystEngComm*, 3(27): 114–119.

Wicht, M.M., Báthori, N.B. & Nassimbeni, L.R. 2016. Enhanced selectivity towards xylene isomers of a mixed ligand Ni(II) thiocyanato complex. *Polyhedron*, 119.

CHAPTER IV

OCTAHEDRAL COBALT WERNER COMPLEXES WITH HYDROGEN BONDING FUNCTIONALITIES

4.1 Introduction

In this chapter a comprehensive analysis of some metal-organic complexes or Werner complexes containing cobalt as the metal centre with nicotinamide and / or isonicotinamide as main ligands is given. A detailed analysis of each structure demonstrating their properties of enclathration, packing and hydrogen bonding ligands is discussed. The use of ligands with hydrogen bonding functionalities, although not extensively considered in many Werner clathrates, may lead to the production of a framework with versatility in their host structures, offering improved opportunities for inclusion or separation (Aakeröy et al., 1999). The structures in this chapter deal with complexes with cobalt as the central metal. Cobalt metal can exist in different oxidation states which allows variation of two important parameters, spin quantum number and magnetic anisotropy. The main point of oxidation states is that, for every metal, its chemistry in different oxidation states is distinctly different. Cobalt presents two main oxidation states, Co(II) and Co(III). The common oxidation state for simple compounds containing Co^{2+} is slow in its ligand substitution reaction whereas the Co^{3+} is rapid, and each has preferences for ligand types and stereochemistry. Cobalt is attractive for scientists interested in structural chemistry and magnetism (Kurmoo, 2009). It is a critical metal for a variety of technologies and an essential constituent of material used in high technology industries such as the manufacture of rechargeable batteries. Cobalt may be used to create alloys and catalysts and it is also widely used in cancer treatment as a tracer and for radiotherapy (Pourret & Faucon, 2017). One of the interesting structural aspects of cobalt in contrast to some other transition metals is the range of geometries, such as octahedral, square-planar, tetrahedral, square-pyramidal, trigonal-bipyramidal and square-planar, that are stable (Griffith, 1964). Another aspect which makes cobalt a very interesting transition metal is the wide range of colours when in solution. This is useful to identify different phases. The common colours are pink, blue, purple, green and orange depending on the solutions they are in and the type and shape of the complex.

Nicotinamide is an important pharmaceutical molecule, it is the amide form of vitamin B3 (niacin) obtained via synthesis in the body or as a dietary source supplement (DiPalma & Thayer, 1991). Nicotinamide (niacinamide) is a pyridine carboxamide with great properties and uses for the organism. Nicotinamide is found in blood and can easily penetrate the blood-brain barrier (Gulati et al., 2016). It is used to treat arthritis, pellagra and used as a vitamin supplement. A study on health and disease in the central nervous system shows the importance of nicotinamide with neural development. Nicotinamide plays a role in protecting neurons from traumatic injury, ischaemia, stroke and even further it is implicated in neurodegenerative conditions such as Alzheimer's, Huntington's and Parkinson's diseases (Fricker et al., 2018). The ligand isonicotinamide is the isomer of nicotinamide with IUPAC name of 4-pyridine-4-carboxamide and is one of the most effectively used co-crystallizing compounds. This molecule is also used in medicine particularly as an anti-inflammatory and in the treatment of Huntington's disease.

Octahedral Werner complexes are one of the most common coordination shapes for transition metal complexes reported. This results in minimal steric clashing between donors, promotes good metal-ligand orbital overlap and leads to favourable ligand field stabilization energies. Among the great benefit of the six-coordinate complex, it presents a diverse set of ligand combinations around the metal centre depending on the number and type of ligand. For example, MA_6 and MA_5B are common and present only one possible form compared to the others MA_4B_2 or $MA_2B_2C_2$ which present two and five diastereomers respectively (Lawrance, 2010). However, MA_4B_2 and $MA_2B_2C_2$ complexes are well illustrated in this chapter. MA_4B_2 presents two geometric isomers, cis and trans, and $MA_2B_2C_2$ presents five diastereomers. Cobalt hosts H4 ($Co(NCS)_2(nicotinamide)_4$) and H5 ($Co(NCS)_2(isonicotinamide)_4$) are the type MA_4B_2 and host H6 ($Co(NCS)_2(nicotinamide)_2(isonicotinamide)_2$) and complexes $Co(NCS)_2(nicotinamide)_2(MeOH)_2$ (H8), and $Co(NCS)_2(nicotinamide)_2$ $(DMSO)_2$ (H7) are the type $MA_2B_2C_2$. The latter two crystal structures will be dealt with in Chapter 5.

The single crystal structures of the three novel Werner complexes with four guests have been elucidated. The octahedral Werner complexes H4, H5 and H6 with ligands in the trans position, as illustrated in Figure 4.1, were synthesised and used as hosts. They are very soluble in DMF and DMSO, and sparingly soluble in warm methanol and ethanol. Four complexes were obtained from H4 $Co(NCS)_2(nicotinamide)_4$, two from H5 $Co(NCS)_2(isonicotinamide)_4$, and three were synthesised from H6 $Co(NCS)_2(nicotinamide)_2(isonicotinamide)_2$. The study of the nine complexes have been divided in three parts according to the host. The single crystals of four complexes from H4 and H6 yield two types of complexes, Werner clathrates and Werner complexes with the displacement of two ligands. The enclathration results with analysis performed are summarised in Table 4.1.
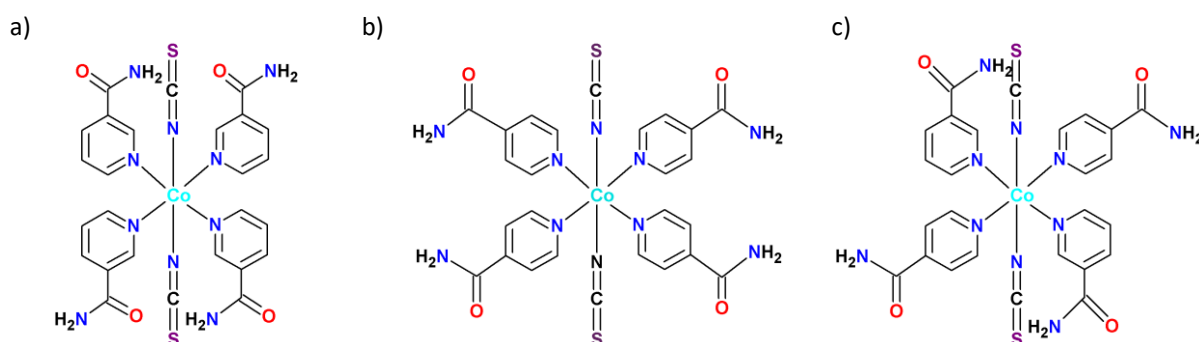
Figure 4.1 *Scheme of three Werner complex hosts, a) H4, b) H5 and c) H6.*

Table 4.1 *Enclathration resulting from H4, H5 and H6 with meOH, propOH, maba (m-aminobenzoic acid), (mx. ox, and px) xylenes and (123, 124 and 135) trimethoxybenzenes.*

Host	Guest	Resulting crystal	Single crystal	PXRD	TG	DSC
H4	meOH	H4meOH (H7)	x	x	-	-
	1-propOH	H4•propOH	x	x	x	x
	123/124/135	H4•nic•H$_2$O	x	x	x	-
	mx/ox/px	-	-	-	-	-
H5	meOH	-	-	-	-	-
	1-propOH	H5•2isonic•propOH	x	x	x	-
	3-pentOH	H5•2isonic	x	x	x	-
	Mx/ox/px	H5•2isonic	x	x	x	-
	123/124/135	H5•2isonic	x	x	x	-
H6	meOH	H6•H$_2$O	x	x	x	-
	1-propOH	-	-	x	x	x
	DMSO	H6DMSO (H8)	x	x	x	-
	ox/px	H6•ox (H9)	x	x	x	x
	123/124/135	-	-	x	x	-

- x: successful analysis
- -: unsuccessful analysis
- DMSO solvent was added to assist with solubility.

4.2 Werner complexes H4 under study

The four structures obtained from host H4 gave rise to two distinct types of complexes, Werner clathrates and Werner complexes with displacement of ligands. The crystallography details and hydrogen bond data for two H4 clathrates are summarized in Table 4.2 and 4.3 respectively, and diagrams of the guests and/or ligand replacers are shown in Figure 4.2. The main difference between H4 and the other hosts H5 and H6 is the four bidentate ligands: in H4 they are nicotinamides.

methanol
(meOH)

Propanol
(propOH)

nicotinamide
(nic)

isonicotinamide
(isonic)
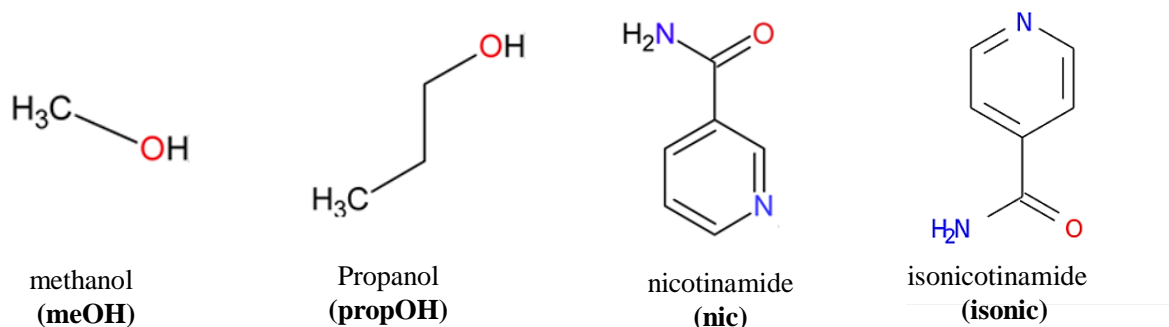
Figure 4.2 *Guest and ligand structures.*

4.2.1 Crystal structure analysis of Werner clathrates H4•nic•H₂O (1) and H4•propOH (2).

The pink block-shaped crystals of (1) and (2) were selected for single crystal X-ray diffraction analysis. These H4•nic•H₂O (1) crystals were obtained after seven days by slow evaporation after dissolving H4 powder in a mixture of the trimethoxybenzene (TMB) isomers plus methanol and heating at 50 ˚C with constant stirring. The purpose of this mixture was to attempt to discriminate between one of the two isomers (1,2,3 or 1,5,3). After crystallisation, it was found that H4 had self-included one nicotinamide ligand as well as water into the clathrate H4•nic•H₂O. The asymmetric unit of the structure comprises half a host and one guest molecule with Co (II) located on a diad at Wyckoff position d. The structure crystallises in the triclinic system, with the space group P$\bar{1}$ (No.2) and Z=1 with a host:guest₁:guest₂ ratio of $\frac{1}{2}$:1:1. Crystal data and refinement details are summarised in Table 4.2. The asymmetric unit consists of half metal Co (II) cation, one thiocyanate ligand, two nicotinamides in the trans position with nicotinamide and water as guests as illustrated in Figure 4.3a. The Co (II) cation is coordinated by two terminal N-bonded thiocyanate anions and four N-coordinating nicotinamide ligands forming a trans octahedral complex.

Table 4.2 Crystal data for H4•nic•H₂O (1) and H4•propOH (2).

	H4•nic•H₂O (1)	H4•propOH (2)
Chemical formula	Co₀.₅(NCS)(C₆H₆N₂O)₂•(C₆H₆N₂O)•(H₂O)	Co₀.₅(NCS)(C₆H₆N₂O)₂•(C₃H₈O)
H:G ratio	½:1:1	½:1
Formula Weight	471.95	391.90
Temperature/K	173(2)	173(2)
Crystal system	Triclinic	Triclinic
Space Group(no.)	P$\bar{1}$ (No.2)	P$\bar{1}$ (No.2)
a/Å	9.3836(10)	8.7135 (17)
b/Å	9.5523(9)	9.2826 (19)
c/Å	13.8210(14)	13.487 (3)
α/°	104.838(2)	70.74 (3)
β/°	95.768(2)	72.74 (3)
γ/°	115.374(2)	62.71 (3)
V/Å³	1050.19(18)	899.2 (3)
Z	1	1
D$_{calc}$/g.cm⁻³	1.492	1.447
Radiation type	MoKα	MoKα
F(000)	489	409
Crystal size/mm³	0.21 x 0.23 x 0.28	0.08 x 0.19 x 0.31
Colour, crystal form	Pink, block	Pink, block
No. of total reflections	26151	30992
No. of unique reflections	5289	4144
Θ min-max$^{/°}$	1.57/28.46	1.67/27.55
R [F²>2σ(F²)]	0.0396	0.0239
wR2(F²)	0.0913	0.0607
S	1.058	1.026

No. of parameters/ data	294/5289	238/4144
Res.peak(max/min)/eA^{-3}	0.313/-0.507	0.460/-0.306

Table 4.3 *Hydrogen-bond geometry (Å, °) with compounds made from H4.*

	d(D-H)(Å)	d(H···A) (Å)	<DHA (Å)	d(D···A) A	Symmetry operator
H4•nic•H₂O					
N2-H2A···O1	0.880	2.051	153.49	2.865	[-x+2, -y+1, -z+1]
N2-H2B···O1G	0.880	2.307	152.12	3.112	
N4-H4A···O1G	0.880	2.172	172.53	3.047	[-x+2, -y+1, -z+1]
N4-H4B···O2G	0.880	2.061	162.18	2.911	[-x+2, -y+1, -z+1]
N1G-H1G1···O2	0.880	2.032	167.33	2.897	[-x+2, -y+1, -z+1]
N1G-H1G2···O1	0.880	2.166	159.11	3.004	[x, y+1, z]
O2G-H2G1···S1	0.795	2.661	170.82	3.448	[-x+2, -y+1, -z+1]
O2G-H2G2···N2G	0.910	1.897	161.05	2.773	[-x+1, -y+1, -z+1]
H4•propOH					
O1G-H1G···S1	0.772	2.536	172.62	3.303	[x-1, y+1, z]
N17-H17A···O27	0.880	2.033	172.10	2.907	[-x+1, -y, -z+1]
N17-H17B···O27	0.880	2.191	141.32	2.930	
N27-H27A···O17	0.880	2.049	166.20	2.911	[-x-1, -y, -z+1]
N27-H27B···O1G	0.880	2.131	159.26	2.970	[x, y-1, z]
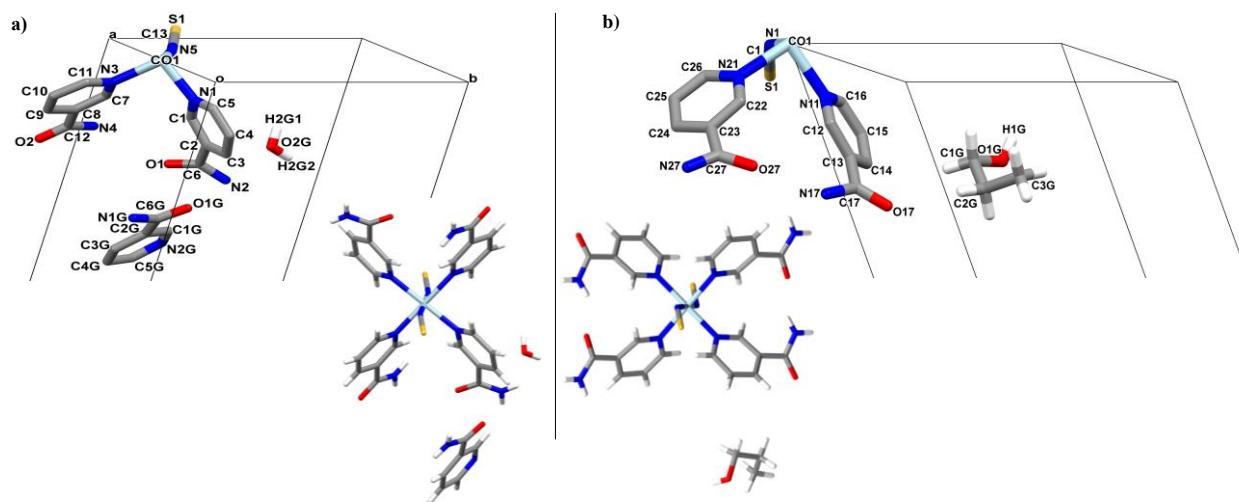
Figure 4.3 *The asymmetric unit and numbering scheme (above) and the full crystal structure for, a) H4•nic•H₂O and b) H4•propOH (some atom labels and hydrogens are omitted for clarity).*

Crystal H4•propOH (2) crystallised after slow evaporation of H4 powder in a solution of methanol:1-propanol (1:2). The triclinic structure in space group P$\bar{1}$ (No.2) has a asymmetric unit comprising half a host with one guest molecule. The Co (II) is located on a diad at Wyckoff position a and host:guest ratio $\frac{1}{2}$:1. The asymmetric unit of this octahedral coordination clathrate is shown in Figure 4.3b.

The Co (II) ion in both complexes is coordinated by six nitrogen atoms, four from the monodentate nicotinamide ligands in the equatorial position and two from the thiocyanate atoms. The coordination

geometry around the metal can be described with Co-N(nicotinamide) distances for (1) and (2) ranging between 2.017 Å - 2.208 Å and 2.052 Å - 2.221 Å with the angles N-Co-N between 88.31° - 90.87° and 89.54° - 105.98° respectively and Co-N(thiocyanate) 2.052 Å for (1) and 2.060 Å for (2) with N-Co-N= 180° respectively, indicating a slightly distorted octahedral. The numbering scheme is written in accordance with the rules for labelling the atoms of the international union of crystallography. The analyses of the crystal packing indicate intermolecular hydrogen bonds in both complexes and intramolecular interactions in the complex (1). The crystal structure of H4•nic•H_2O is characterised by two guests, nicotinamide (guest 1) and water (guest 2). The three molecules are linked together via homosynthon interactions where the molecule of water plays a bridging role connecting guest 2 and the host, N4-H4B···O2G_2 (host-guest 2) and O2G_2-H2G22···N2G1 (guest 2-guest 1). The third interaction, N4-H4A···O1G1 (host-guest 1) allows the molecule to extend to form a $R_6^6(20)$ ring (Fig.4.4), (Etter et al., 1990).
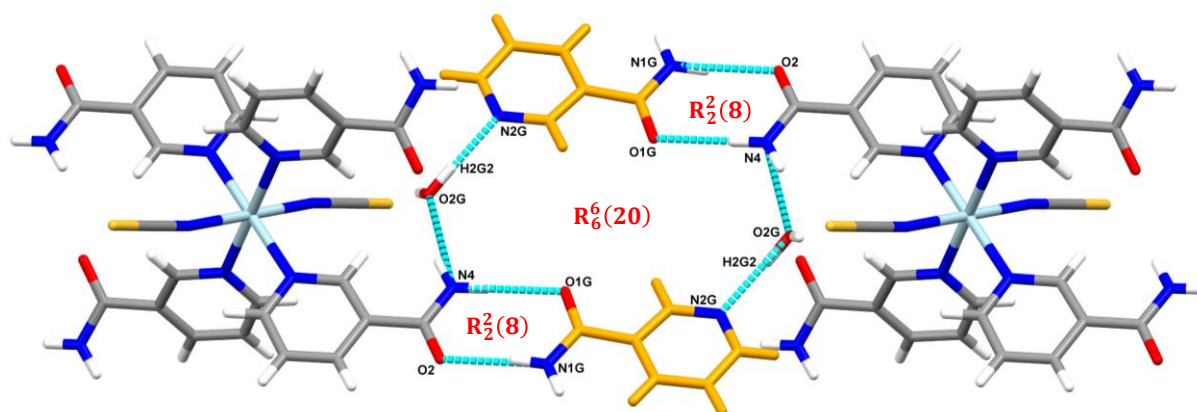
Figure 4.4 Extended 2D structure of H4•nic•H_2O with guests nic in orange showing hydrogen bonding graph sets.

From the structural analysis, three main strong hydrogen interactions were observed. Interactions O-H···N, N-H···O and O-H···S, are observed between guests, within host molecules or between guest and host. Host-host and host-guest were either linked by homosynthons / heterosynthons described by a $R_d^a(r)$ graph set and monocyclic dimer $D_d^a(r)$ graph set only for the host-guest interactions.

Amide dimers coordinated molecule H4 and nicotinamide (guest). As illustrated in Figure 4.5a the host-guest interactions are forming infinite $C_4^4(32)$ chains alternating dimer interactions of $R_2^2(8)$ ring (N4-H4A···O1G and N1G-H1G1···O2) followed by a discrete assembly, $D_1^1(3)$ graph set (N1G-H1G2···O1). Additionally, face to face π···π interactions occur between the aromatic rings of the nicotinamide guest and one of the ligands of H4 with a centroid distance of 3.683 Å.

In this structure, water (guest 2) coordinates with two molecules in three hydrogen bonds, the first (N4-H4B···O2G2) to the host and the second (O2G2-H2G2$_2$···N2G2$_2$) to the guest 1. The third interaction is between the thiocyanate sulfur (O2G-H2G$_1$···S1). These interactions are shown in Figure 4.5b.

The host-host interactions are built by N2-H2···O1 hydrogen bonds in the form of an amide dimer illustrated by homosynthons $R_2^2(8)$ graph set. These host-host interactions form wave like chains alternating via amide dimer interactions to form infinite chains (Fig. 4.5c).
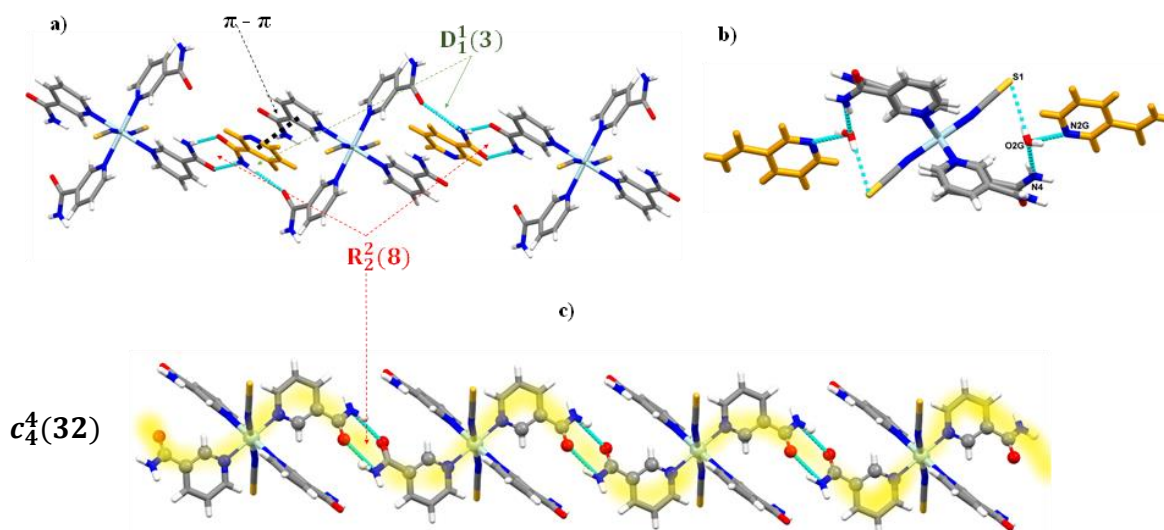
Figure 4.5 *Intermolecular interactions in H4•nic•H$_2$O, a) chains of host-guest interaction and π-π interactions, b) interactions between water, host and nicotinamide and c) wave-like infinite chains (yellow) of homosynthons between host and host.*

Interesting architectures were found in the complex H4•propOH, similar to those researched by Wicht et al. in the thiocyanato nicotinamide nickel clathrates with alcohol guests (Wicht et al., 2019). The structural analysis of H4•propOH (2) presented two major interactions, intermolecular and intramolecular. Hydrogen bonds were observed between the two nicotinamide ligands of neighbouring host molecules forming an amide tetramer (Fig. 4.6). The middle ring has four interactions, two intermolecular bonds (N17-H17B···O27) and (N17-H17A···O27) forming homosynthon $R_4^2(8)$ graph set with the intramolecular bonds completing this structure. The amide tetramer is completed by the two N27-H27A···O17 bonds shown in the synthon $R_2^2(8)$ graph sets (Figure 4.6).
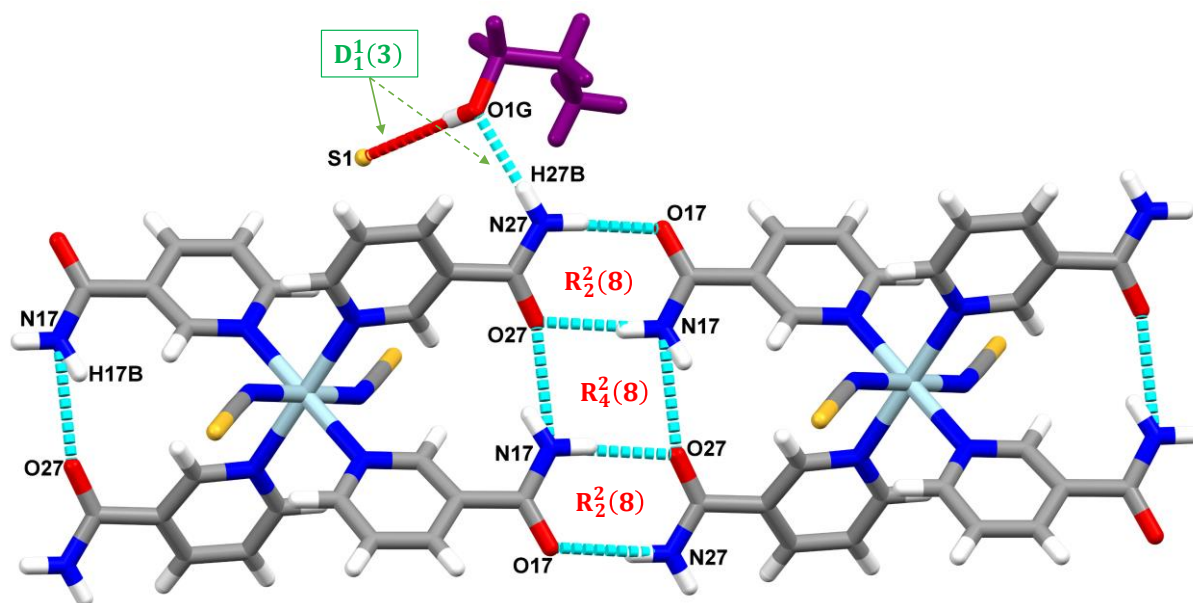
Figure 4.6 *H4•propOH structure, showing all intermolecular and intramolecular interactions occurring in the crystal between host and host and host and guest (in violet).*

Two intermolecular hydrogen bonds, interacting between the guest and host via a hydroxyl group (guest) O1G-H1G•••S1 sulfur (host) and amine group (host) N27-H27B•••O1G oxygen (guest) both forming discrete bonds with motif $D_1^1(3)$ (Fig. 4.6). The weak hydrogen bonds which involve sulfur are discussed later in this chapter.

The crystal packing and voids for both Werner clathrates (1) and (2) which crystallise in the same space group are shown in Figure 4.7 presenting different packing frameworks, shapes and characteristics viewed down the a-axis. Figure 4.7a, b and c display the packing diagrams of clathrate (1) showing the compound in oblique alignment with the host forming a sheet. The packing arrangements were stabilized by π•••π interactions between the guest nicotinamide (light violet) and nicotinamide ligand of the host as shown in Figure 4.7b.
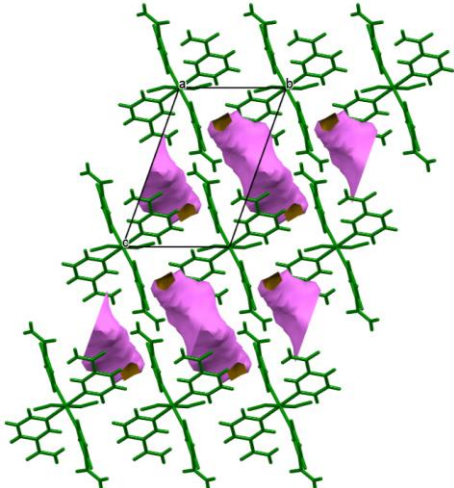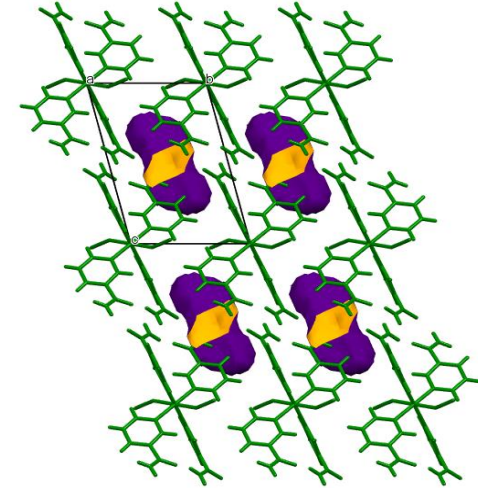
In Figure 4.7d, e and f the host of clathrate (2) is packed in wave like columns with the guest in between them. The packing is stabilized by heterosynthon / homosynthon interactions between the hosts and hydrogen bonding between the host-guest as shown in Figure 4.7e with the guest in violet capped stick model. The packing in Figure 4.7f shows the arrangement of layers of guest in space fill model between the host columns. Once the guests are removed from the structure, channels were observed showing the free space within the crystal architecture as illustrated in Table 4.4. The voids were analysed using the probe size of 1.2 Å and the grid spacing of 0.7 Å in Mercury 4.0. The volume and percentage void space were calculated and are listed in Table 4.4 with the void analysis diagrams presented along the a-axis.
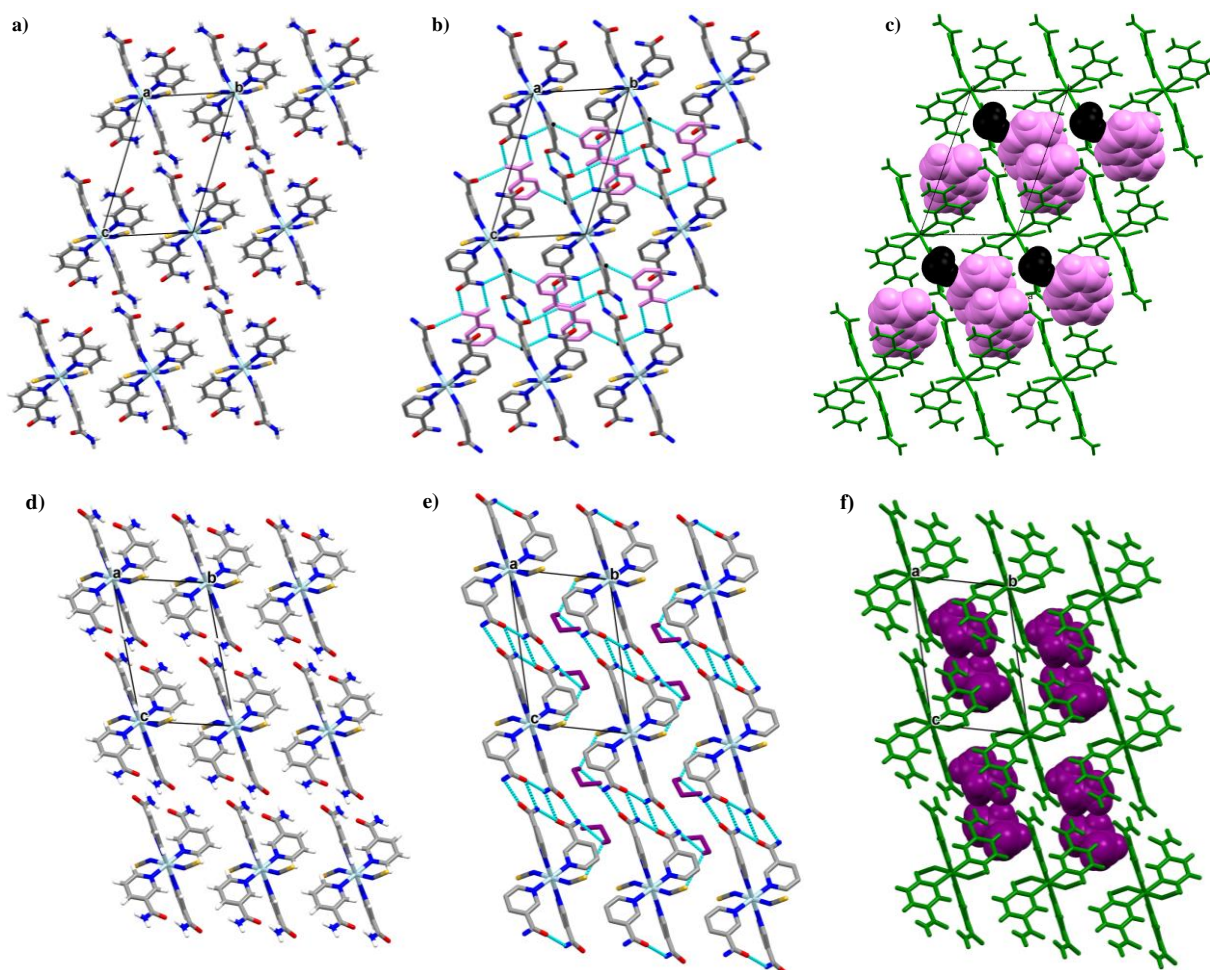
Figure 4.7 *Crystal packing of H4•nic•H₂O viewed down the a-axis, a) packing of the host alone, b) the interactions occurring in the packing diagram with the guest in light violet and black; c) guest in space fill and host in green capped stick model and H4•propOH, d) the wave like column shape of the host alone, e) interactions occurring in the packing diagram with the guest in violet and f) guest and host in violet space fill and green capped stick model, respectively (some hydrogens atoms were removed for clarity).*

Table 4.4 *Void analysis diagrams of H4•nic•H₂O and H4•propOH.*

Crystal	H4•nic•H₂O	H4•propOH
Percentage void%	8.7	5.5
Volume Å	91.62	49.90
No of guest	2	1
H:G ratio	1:1:1	1:1
structure		

4.2.2 Thermal analysis of H4•nic•H₂O (1) and H4•propOH (2)

The thermal analysis experiments were run on the thermogravimetric analyser (TGA) under a nitrogen purge with heating mode of 20 °C/min. The decomposition of the complex (1) and (2) show two steps, firstly the release of the guest/s followed by step 2 the decomposition of the ligands, from the complex.

In the complex (1), whose ASU consists of half the host, one water and one nicotinamide as guests, step 1 corresponds to release of water with the corresponding exothermic DTG peak at 125 °C (exp. 4.9 %) and one mole of nicotinamide with the corresponding DTG at 169.8 °C, followed by the slow loss of the nicotinamide ligands between 170 and 220 °C (Figure 4.8a).

The complex (2) has one propanol guest, which is released with an exothermic DTG peak at 148.9˚C (exp. 15.6%). The next step is attributed to the loss of two ligands as shown in Figure 4.8b.
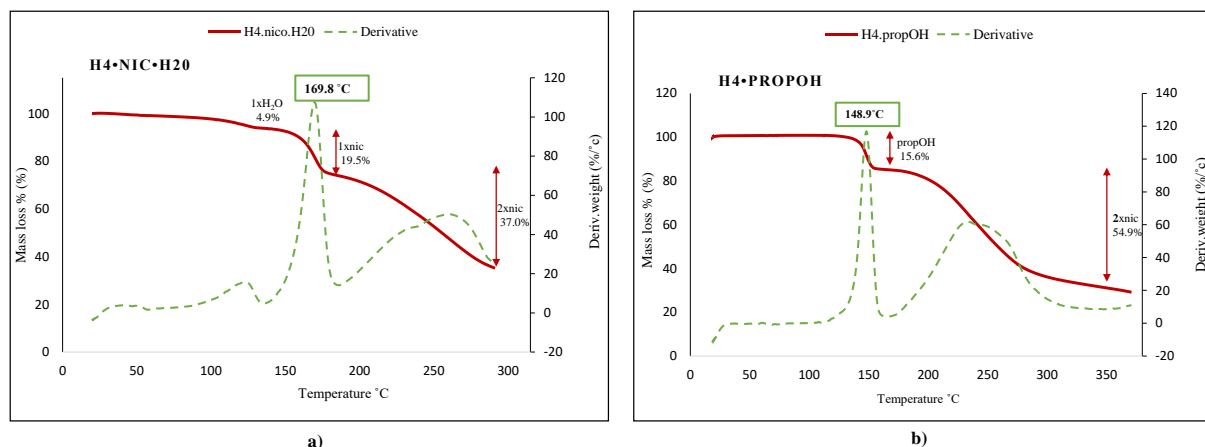
Figure 4.8 *TGA curves of, a) H4•nic•H₂O and b) H4•propOH plotted as mass loss (%) (red curve) and derivative weight (green dot curve) vs temperature (˚C), purge gas: N₂ (40 mL/min), heating rate: 20 ˚C/min.*

Table 4.5 shows the thermal analysis data of (**1**) and (**2**). The temperature range for the compound (1) was from 0 to 300° with the release of the guests water and nicotinamide. The decomposition of the two ligands should be run to a higher temperature to allow for their full release due to the compound's incomplete breakdown, as can be seen from Table 4.5. The experimental and the calculated data for the complex (2) was found to be slightly different. In the complex (2) the mass loss of propanol and the two nicotinamide ligands for the calculated were found to be 15.3 % and 62.3 % and the experimental results of 15.6 % and 54.9 %. Again, longer heating should've enabled more 'sticky' nicotinamide to be released.

Table 4.5 *Thermal analysis data (TG and DTG) of H4•nic•H₂O and H4•propOH.*

Complex	Temp.range (˚C)	DTG (˚C)	Mass loss Δm(%)		Removed group	Crystal colour
			Found	Calc.		
$Co_{0.5}(NCS)(C_6H_6N_2O)_2 \cdot (C_6H_6N_2O) \cdot H_2O$	90-135	123	4.9	3.8	H_2O	
	141-185	170	19.9	25.9	$C_6H_6N_2O$	Pink
	186-285	261	37.0	51.8	$2 \times C_6H_6N_2O$	
$Co_{0.5}(NCS)(C_6H_6N_2O)_2 \cdot C_3H_8O$	90-155	149	15.6	15.3	C_3H_8O	Pink
	156-320	229	54.9	62.3	$2 \times C_6H_6N_2O$	

4.2.3 Powder X-ray Diffraction

The powder X-ray diffraction analysis was carried out on Bruker D8 diffractometer using the Cu K$_\alpha$ radiation. The spectrum was run between 2θ from 6˚ to 40˚. This analysis was used to confirm the enclathration of the guest by using one single crystal and showing how the crystal pattern differs from the host and how the two crystal structures differ from each other (Fig 4.9). The PXRD patterns showed

some acceptable matches between H4•nic•H$_2$O (1) (green), H4•propOH (2) (yellow) and the H4 host (blue) in Figure 4.9. For compound (1) new peaks appear at two theta values of 14° and 27°. In the case of compound (2) new peaks appear at 7°, 29°, 34° and 35°.
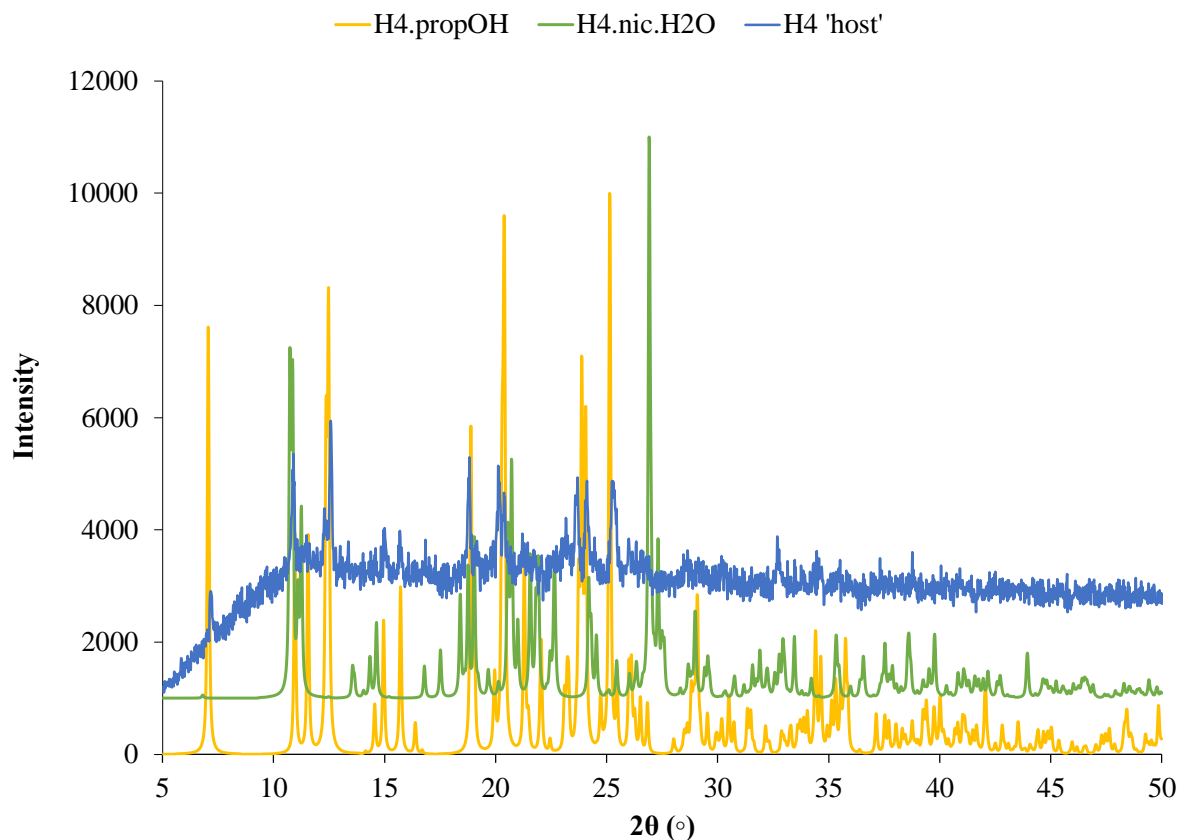
Figure 4.9 PXRD analyses of H4• nic•H$_2$O and H4•propOH and H4.

4.3 Werner complexes H5 under study

Many of the enclathration experiments of H5 with several potential guests (1-propOH, 1-butOH, meOH, 3-pentOH, m/o/p-xylenes, 123/124/135 TBM and m/p-ABA) were not successful: only propanol was included as a guest, while the addition of other prospective guests gave rise to the self-inclusion of the isonicotinamide ligand. H5 was less reactive in comparison to the H4 and H6 hosts in respect of inclusivity, with only two different clathrates being formed. These two Werner clathrates H5•2isonic•propOH (3) and H5•2isonic (4) are reported here. Both (3) and (4) were synthesized by dissolving about 6 mg of H5 in 2 mL of propanol and 3-pentanol respectively with a few drops of methanol (used as a solvent to dissolve the mixture of host and guest). The crystals were obtained three weeks after slow evaporation. The crystallography details for (3) and (4) are summarized in Table 4.6. The complex H5 compared with H4 has four isonicotinamide ligands.

Table 4.6: Crystal data with compound made from H5.

	H5•2isonic•propOH (3)	H5•2isonic (4)
Chemical formula	$Co(NCS)_2(C_6H_6N_2O)_4$ •$2(C_6H_6N_2O)$ •(C_3H_8O)	$Co(NCS)_2$ $(C_6H_6N_2O)_4$ • $2(C_6H_6N_2O)$
H:G ratio	1:2:1	1:2
Formula Weight	967.95	907.86
Temperature/K	173(2)	173(2)
Crystal system	Triclinic	Triclinic
Space Group (no.)	$P\bar{1}$ (No.2)	$P\bar{1}$ (No.2)
a/Å	9.18 (7)	9.1652(7)
b/Å	13.72(10)	13.6148(11)
c/Å	20.33(15)	20.323(16)
α/°	104.20(2)	70.886(2)
β/°	97.44(2)	82.649(2)
γ/°	109.25(2)	70.669(10)
V/A^3	2281.5(3)	2260.37(3)
Z	2	2
D_{calc}/g.cm^{-3}	1.409	1.334
Radiation type	MoKα	MoKα
F(000)	1006	938
Crystal size/mm^3	0.18x0.20x0.25	0.15x0.19x0.23
Colour, crystal form	Pink, block	Pink, block
No. of total reflections	43573	54066
No. of unique reflections	11265	11392
Θ min-max/°	1.06/28.28	1.66/28.43
R [F^2>2σ(F^2)]	0.0538	0.0369
wR2(F^2)	0.1284	0.0857
S	1.070	1.042
No. of parameters/ data	635/11265	550/11392
Res.peak(max/min)/eA^{-3}	0.953/-0.990	0.342/-0.350

For this section of study, the work done by Neumann (Neumann et al., 2016) was used as a reference and comparison for the analysis of structure (3) and (4) as it is the most recent article in the Cambridge Structural Database (Version 5.40 last update 2019). The authors discussed the crystal structure and properties of tetrakis (isonicotinamide)bis (thiocyanato) cobalt (II)•2(isonicotinamide)•ethanol in ratio 1:2:1.

The crystal structure of (3) and (4) were solved in the triclinic $P\bar{1}$ (No.2) space group. The asymmetric units consist of H5, two isonicotinamides and one propanol guests in (3), and in (4) two isonicotinamide guests with molecular formula of $CoC_{41}H_{43}N_{14}O_7S_2$ and $CoC_{38}H_{36}N_{14}O_6S_2$ respectively (Fig. 4.10). The two Werner clathrates present some similarity between each other such as the structure, the crystal size, and others which will be presented later. However, the angles α, β and γ differ somewhat and therefore the two structures are not isostructural.

The structure of (3) presents an incomplete guest, 1-propanol, with a missing hydrogen in the hydroxyl group which could not be found when resolving the structure. The four main atoms of the propanol were about 0.990 Å distant from each other, making it difficult to identify the oxygen atom on the propanol. To assign the oxygen atom the distance between the nitrogen atom of H5 and atom on either side of the 1-propanol was measured to conclude the position of the oxygen atom. The distances were found to be

3.183 Å (O1G-N22) and 3.836 Å (C3G-N15). The position of the oxygen was assigned to the lower distance according to the properties of hydrogen bonds, with the average distance of N-H•••O-H between 2.8-3.1Å (Desiraju et al., 2011). However, due to this finding, the final chemical formula of the Werner clathrate is $Co(NCS)_2(C_6H_6N_2O)_4•2(C_6H_6N_2O)•(C_3H_7O)$, one hydrogen less than expected. This is shown in Figure 4.10a.
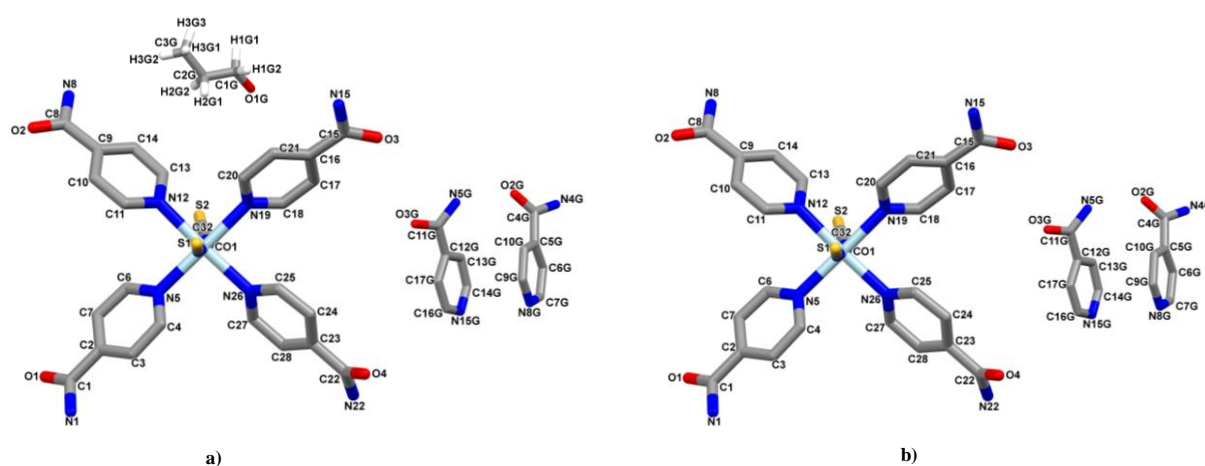
Figures 4.10 *Asymmetric unit of a) H5•2isonic•propOH (3) and b) H5•2isonic (4) (some hydrogens were omitted for clarity, except in the case of propanol).*

The preparation of (4) was made from the mixture of H5 powder (6 mg), 3 mL of 3-pentanol and a few drops of methanol to clarify the solution, as H5 was not soluble in 3-pentanol. The mixture was heated for 30 min at 40 to 50 °C until the solution was clear. After a few days of slow evaporation pink crystals were collected for analysis. The structure of (4) is shown in Figure 4.10b.

The TGA analysis of (4) was performed over a temperature range of 30 – 400 °C at a heating rate of 20 °C min^{-1} under dry nitrogen with a flow rate of 40 mL/min. It revealed the presence of solvents which we could not conclude between methanol or 3-pentanol. The TGA showed loss of weight at two temperatures, around 33.3 °C and 160.2 °C, all with a percentage weight of 7.1% (Fig 4.11) which complicated the determination of the solvent. The calculated percentage weight loss of methanol and 3-pentanol was found to be 4.6 % and 11.7 % respectively which differed from the values obtained from the TGA. So, further analysis was used such as PXRD and SCXRD to determine the solvent observed on the TGA. The PXRD as well shows some differences between the host and the crystal which will be discussed later. The single X-ray analysis presented a disordered solvent which could be attributed to either methanol or 3-pentanol. The structure was solved by direct methods using SHELX-97 and refined using full-matrix least squares methods in SHELX. As we could not model the guest from the structure, we used an alternative method to solve the disorder issue. To address the disorder issue we used a

SQUEEZE method which is a PLATON SQUEEZE tool to calculate the solvent contribution to the structure factors by back-Fourier transformation of the electron density found in the solvent-accessible region of a phase-optimized differences electron-density map (Spek, 2015). According to the SQUEEZE calculation with the guest(s) removed from structure model, the volume of void per unit and the number of electrons per void of solvent recovered from the structure were found to be 210 Å^3 and 45e^- respectively.

The results obtained from the SQUEEZE were used to determine the nature of the disordered guests. The number of electrons from the SQUEEZE CIF file was slightly different from that of the number electrons in 3-pentanol (for one 3-pentanol = 50e$^-$) and equal for methanol (for one 3-pentanol and half methanol = 43e$^-$). After the SQUEEZE calculation the structure was refined by SHELXL refinement and all the disorder peaks disappeared, leaving a structure with only two isonicotinamides as guests and one host.

On reconsidering the total mass percentage loss found in the thermogram, it was concluded that the total percentage loss of six isonicotinamides (guests and ligands) in the compound theoretically is 80.7 %, which matches well with the experimentally determined value of 79.1 %. This is an indication that the isonicotinamides began to decompose at the temperature of 160 °C.
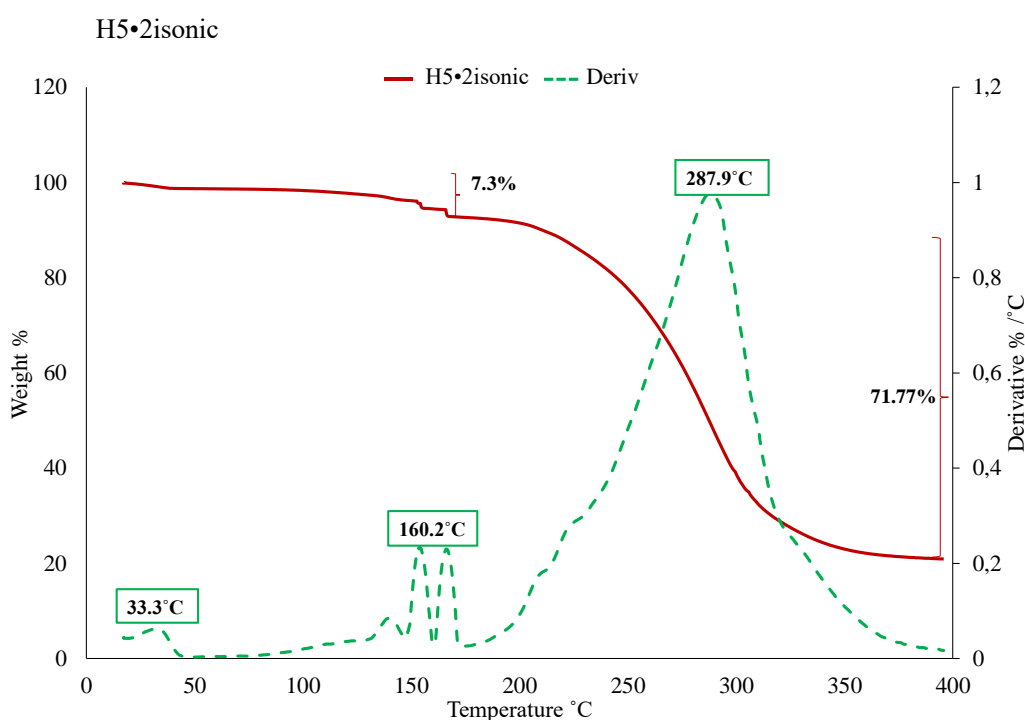
Figure 4.11 *TG (red) and derivative (green) curves of H5•2isonic.*

The interactions between the H5 structure (3) and (4) and the two guest isonicotinamides is similar in both complexes. Both H5 hosts are bonded to isonicotinamide via the carbonyl and the amide through

N4G-H4GA•••O2 and N8-H8A•••O2G interactions classified as a $D_1^1(3)$ graph set (Fig. 4.12). H5 and isonicotinamide are further interacting in discrete assemblies forming heterosynthons described by $R_4^4(16)$ graph sets, with all hydrogen bonds listed in Table 4.7.
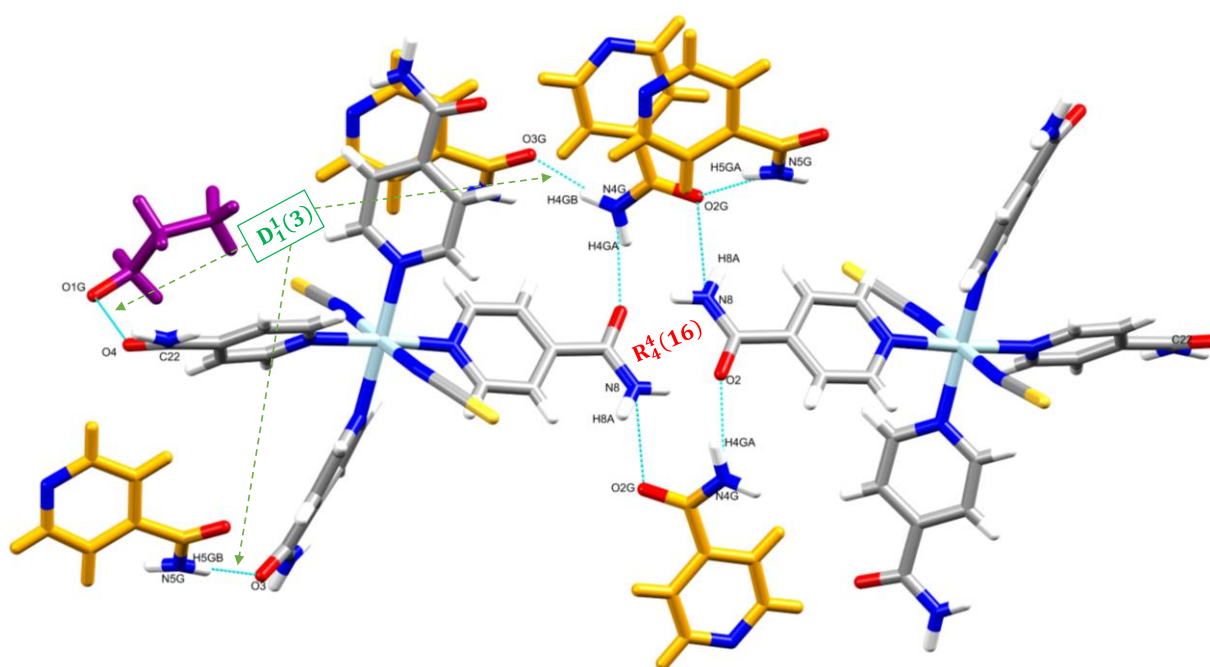
Figures 4.12 *Intermolecular interactions between H5 and guest (isonic in orange and 1-propOH in violet) for complex (3).*

Table 4.7 *Hydrogen-bond geometry (Å, °) of (3).*

	d(D-H) (Å)	d(H•••A) (Å)	<DHA (Å)	d(D•••A) A	Symmetry operator
H5•2isonic•proOH					
N5G-H5GA•••O2G	0.885	2.046	158.17	2.886	
N4G-H4B•••O3G	0.895	1.900	166.14	2.777	[x-1, y, z]
N1-H1A•••N8G	1.012	1.980	161.14	2.959	[-x+2, -y+1, -z+2]
N15-H15A•••O2G	0.730	2.367	169.31	3.087	[-x+1, -y+1, -z+1]
N1-H1B•••O4	0.782	2.206	153.94	2.929	[-x+1, -y+1, -z+1]
N15-H15B•••S2	0.927	2.627	164.67	3.529	[-x+1, -y+2, -z+1]
N4G-H4GA•••O2	0.974	1.937	156.42	2.856	
N8-H8A•••O2G	0.888	2.250	141.85	3.000	[-z+2, -y+1, -z+1]
N8-H8B•••S1	0.800	2.678	160,19	3.441	[-x+1, -y+1, -z+1]
N5G-H5GB•••O3	0.801	2.146	164.74	2.927	[x+1, y-1, z]
N22-H22B•••N15G	0.892	2.062	170.12	2.945	[-x+2, -y+2, -z+2]
N22-H22A•••O1	0.883	2.056	157.04	2.889	[-x+2, -y+2, -z+2]

As well as the above interactions, one of the isonicotinamide guests of H5•2isonic has a four-centre bond via the oxygen atom (O2G). The oxygen atom interacts with two H5 molecules and there is another interaction with isonicotinamide guest 2 via their amide groups as illustrated in Figure 4.13.

a)

Hydrogen bond distances

	D(D…A) Å
O2G•••H-N1	2.882
O2G•••N-H22	3.058
O2G•••H-N1G	2.981

b)
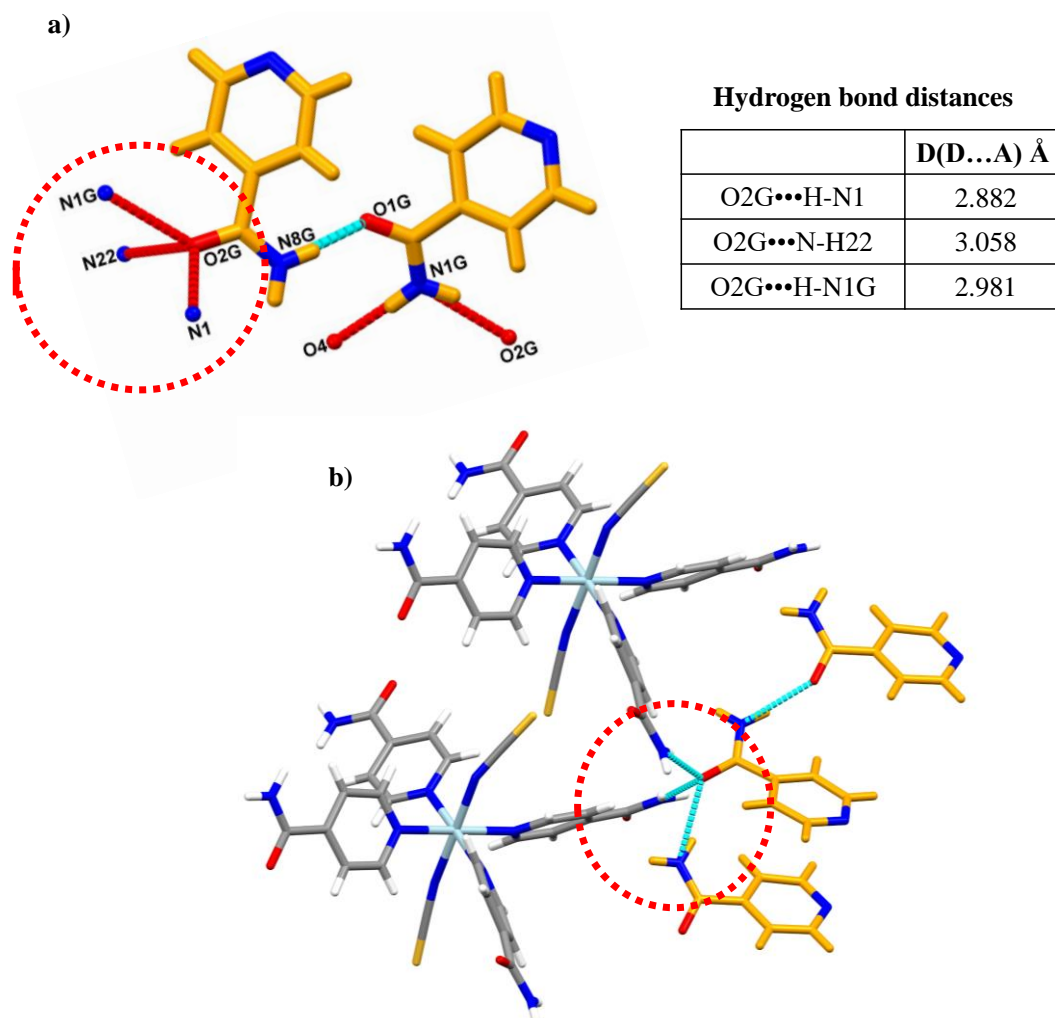
Figures 4.13 *Three intermolecular interactions a) between guest (O2G) with 2 molecules of H5 and the other isonic guest shown in the dotted circle and b) full representation of the interactions in the complex (isonic guests in orange).*

Table 4.8 Hydrogen-bond geometry (Å, °) of (4).

	d(D-H) (Å)	d(H···A) (Å)	<DHA (Å)	d(D···A) A	Symmetryoperator
			H5•2isonic		
N1-H1A···S1	0.880	2.603	160.35	3.444	[-x+1, -y+2, -z+1]
N1-H1B···O2G	0.880	2.237	142.11	2.981	[-x, -y+2, -z+1]
N8-H8A···N12G	0.880	2.100	158.07	2.934	[-x, -y+2, -z+2]
N-8-H8B···O3	0.880	2.096	155.71	2.921	[-x+2, -y+1, -z+2]
N22-H22B···S2	0.880	2.670	161.83	3.517	[-x+2, -y+1, -z+1]
N22-H22A···O2G	0.880	2.218	159.47	3.058	[-x+1, -y+2, -z+1]
N15-H15B···N5G	0.880	2.082	162.55	2.933	[-x+2, -y+1, -z+2]
N8G-H8G1···O2	0.880	2.104	147.29	2.884	[-x+1, -y+1, -z+2]
N8G-H8G2···O1	0.880	2.027	154.95	2.849	
N8G-H8G2···O1G	0.880	1.938	157.82	2.773	
NG-H1G2···O4	0.880	2.082	157.50	2.915	[x-1, y+1, z]
N1G-H1G2···O2G	0.880	2.065	153.88	2.882	[x+1, y. z]

Structure (3) shows bonding of the host to 1-propOH via the carbonyl group through a weak hydrogen bond C22-O4···O1G (note, the hydrogen is not seen in this interaction).

The host molecules in both complexes are linked together in chains by alternating intermolecular N-H···O interactions between the amide and the carbonyl group followed by N-H···S interactions between the thiocyanate anions and the amide H atoms of neighbouring host molecules forming infinite chains (Fig. 4.14).
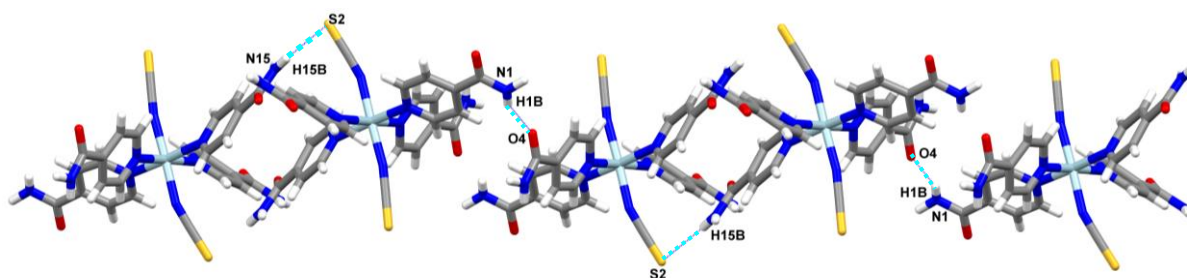
Figure 4.14 Host/host extended hydrogen bonding**.**

The crystal packing in (3) and (4) is stabilized by hydrogen interactions between H5···propOH (C=O···O) and H5···isonic (N-H···O) respectively connecting both guests to the host along the a- and b-axis. Similar to Neumann's article, H5 also has two types of channels along the a-axis in both complexes, with (3) shown in Figure 4.15a and b. In compound (4) (Figure 4.15c and d), a larger channels where the isonicotinamide molecules are located, leaving the small channels empty (Fig. 4.15d) and in (3) the

smaller spaces were occupied by propanol solvent molecules (Fig. 4.15a). Once the guests were removed and the void spaces mapped, the bigger and smaller channels for isonicotinamide and propanol respectively (Fig. 4.15b & Fig. 4.15d) were seen in both complexes. The percentage and volume of void spaces for isonicotinamide and propanol were 13% and 296.65 Å^3 for (3) and 12.16% and 284.16Å^3 for (4) respectively. In (4), the smaller spaces were more than likely filled with solvent molecules not yet determined in our study.

It was noticed that the void percentage obtained from Mercury for H5•2isonic once the guest was removed was 284.16 Å^3 which was different from the voids value from the SQUEEZE of 210 Å^3. The difference observed between the two values was because the value obtained from Mercury was only for one guest isonicotinamide whereas the value obtained from the SQUEEZE included the isonicotinamide and the other solvent(s).

It was noticed that the voids representation in both complexes (3) and (4) are the same (Fig. 4.15b & Fig. 4.15d). It was noted that the small channels which were empty before removing the guest in H5•2isonic are filled with a void on performing the void analysis. The voids present in the small channels in (4) can be one of the two solvents used either methanol or 3-pentanol, or a mixture of both.
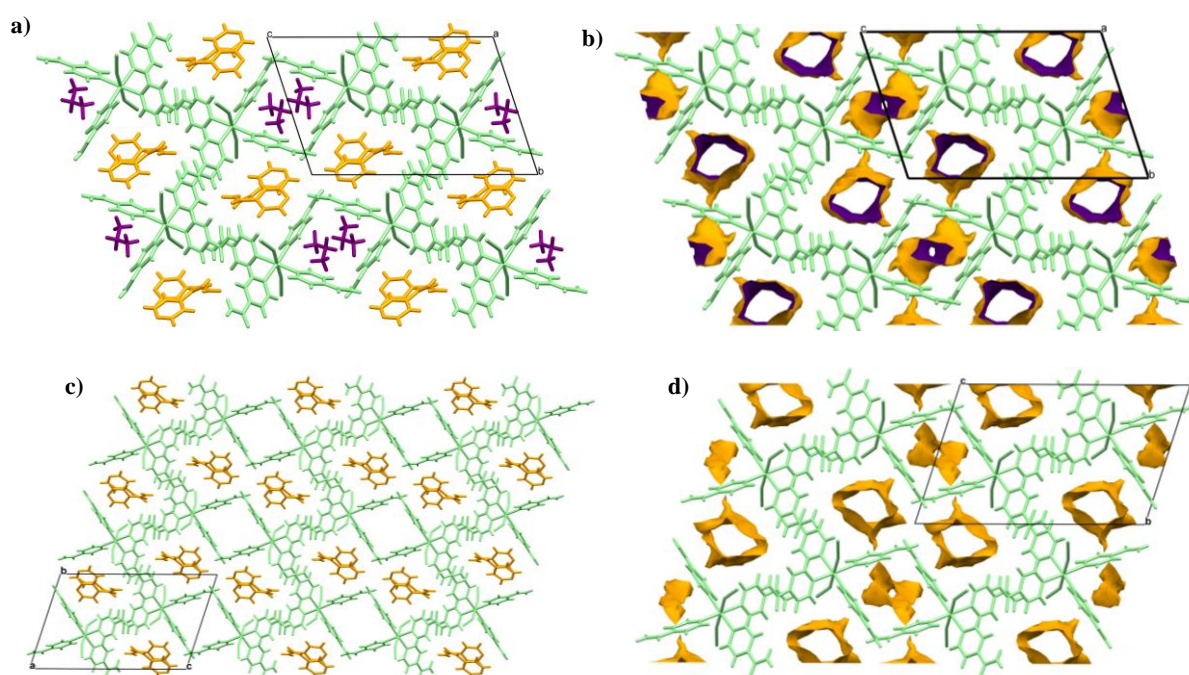
Figure 4.15 *Crystal structure in a viewed along the a-axis, a and c) packing diagram of (3) and (4) respectively; b and d) void channels showing the location of isonicotinamide (orange) and propanol (purple) guests.*

4.3.1 Thermal analysis of H5•2isonic•propOH

The TGA curve of the crystals in Figure 4.16 shows the decomposition of H5 (H5•2isonic•propOH) in two steps. First, the release of propanol (exp.3.42 %; calc.6.5 %) followed by isonicotinamides (exp.74.46 %; calc.77 %). According to the TGA analysis only half of propanol was decomposed during the first step instead of the whole molecule as in the ASU. The DSC was run to confirm the presence of the propanol in the first step. The DSC curve shows one endotherm corresponding to the boiling point of propanol (T_{on}= 63.58 °C, T_{peak}= 95.80 °C) of 97 °C, followed by two endotherms which relate to the decomposition of six molecules of isonicotinamide, two guests (T_{on}= 203.22 °C, T_{peak}= 203.38 °C), and four ligands (T_{on}= 293.75 °C, T_{peak}= 293.98 °C).
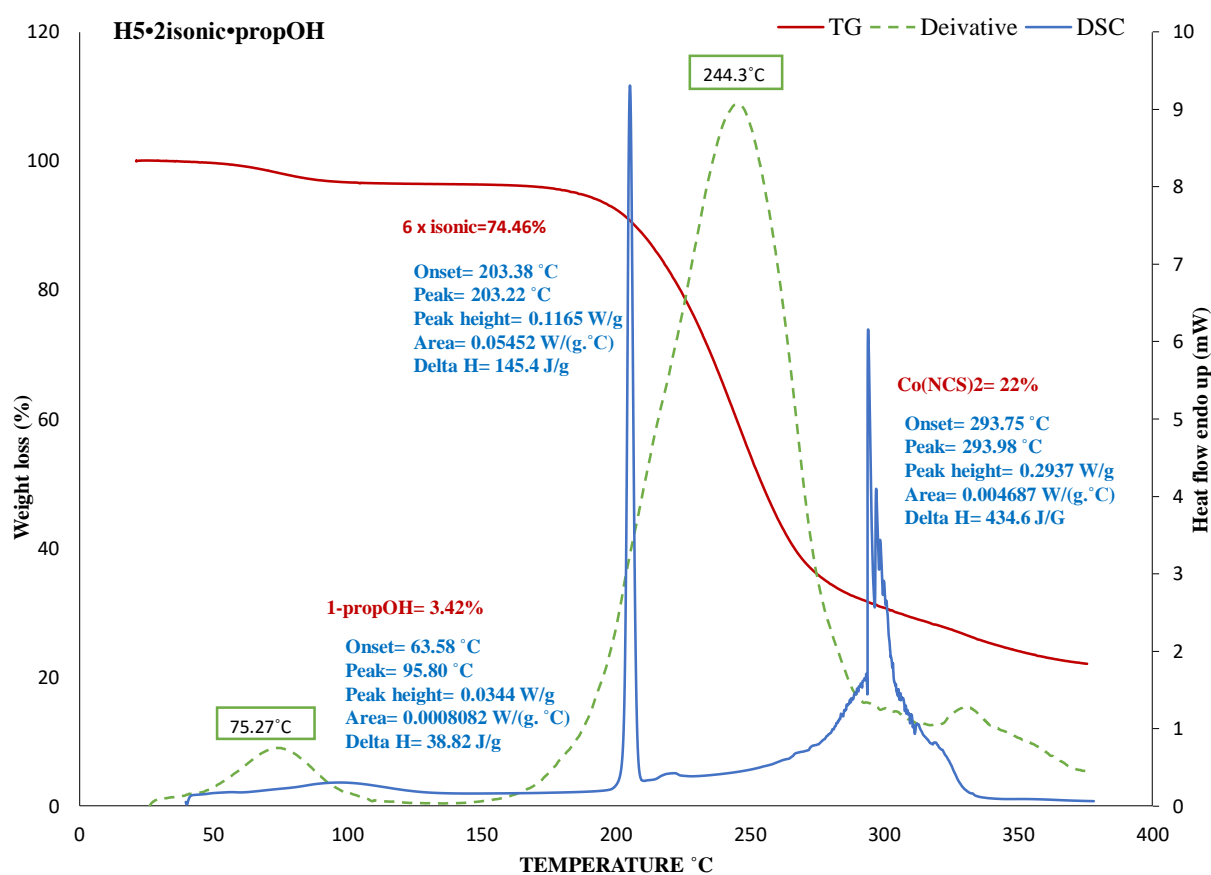
Figure 4.16 DSC (blue), TG (red) and derivative (green) curves of H5•2isonic•propOH.

4.3.2 Powder X-ray diffraction of H5•2isonic•propOH and H5•2isonic

The PXRD pattern of the host (blue, H5) was compared to that of the crystals [(orange (3), green (4)] obtained from LAZYPULVERIX. X-ray powder data were collected in a Bruker D2 PHASER Desktop X-ray diffractometer with copper radiation (CuKα, λ=1.54406 Å) at 30 kV and 10 mA. The spectra for

the crystals and the host were obtained between 2θ values of 6 to 40˚ (Fig. 4.17). The three spectra present many similarities, with the crystals most abundant peaks at 15°, 17°, 18°, 24° and 25° also observed in the host pattern. New peaks were observed at 7° in the crystal patterns, and the peak at 32.5° observed in the host was absent in the crystal patterns.
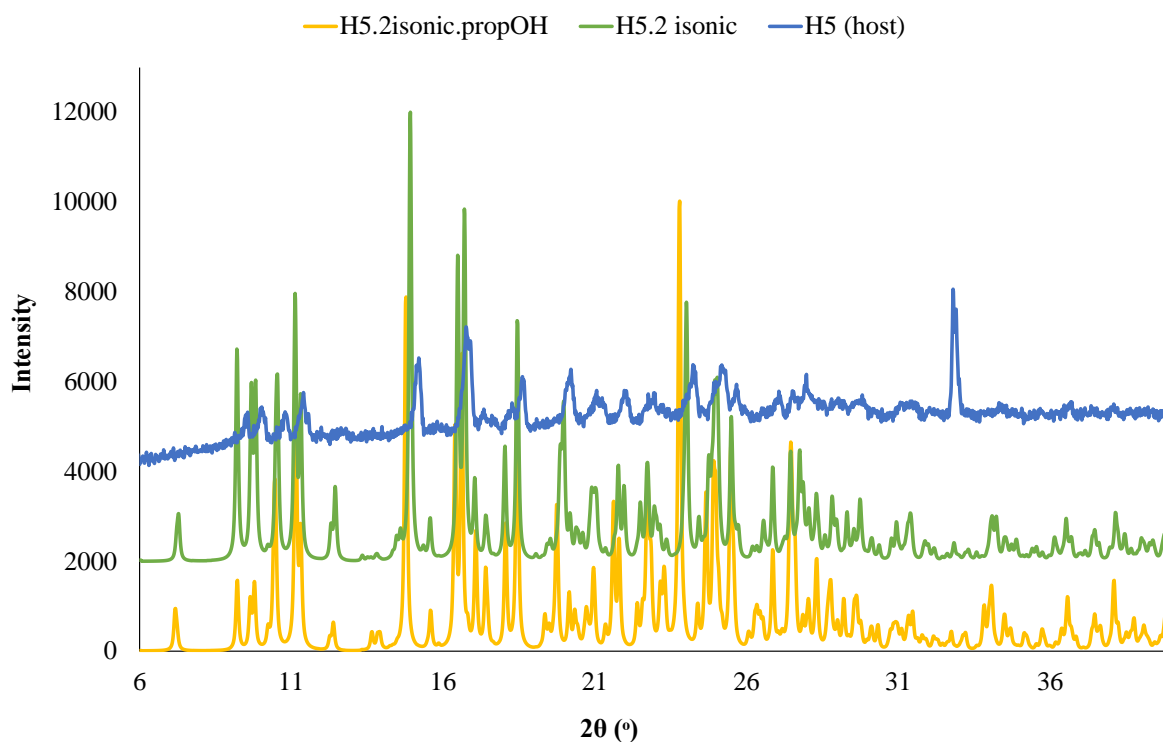
Figure 4.17 *PXRD curve of the crystal H5•2isonic•propOH (3) orange, H5•2isonic (4) green and the host H5 (blue).*

4.4 Werner complexes H6 under study

Host 6 [Co(NCS)$_2$(nicotinamide)$_2$(isonicotinamide)$_2$] formed a Werner clathrate with water as guest in a 1:1 ratio [Co(NCS)$_2$(nicotinamide)$_2$(isonicotinamide)$_2$•H$_2$O] (5). H6 was dissolved in methanol with gentle heating on a hot plate for about 30 min and allowed for slow evaporation at room temperature until the formation of pink block crystals with H6 enclathrating a molecule of water from the methanol solvent were observed. This was a serendipitous inclusion as methanol was not dried. The ASU structure is illustrated in Figure 4.18. The structure of H6 is an octahedral complex with mixed ligands of type MA$_2$B$_2$C$_2$ where M is the metal Co (II) cation with three different ligands A, B and C around the coordination sphere in trans positions. The mixed ligands, two isomers nicotinamide/isonicotinamide and two thiocyanato anions, are N-coordinating to the metal cation. The CoN$_6$ octahedral is slightly distorted with Co-N average distance and angle of 2.138 Å and 178.58° respectively.
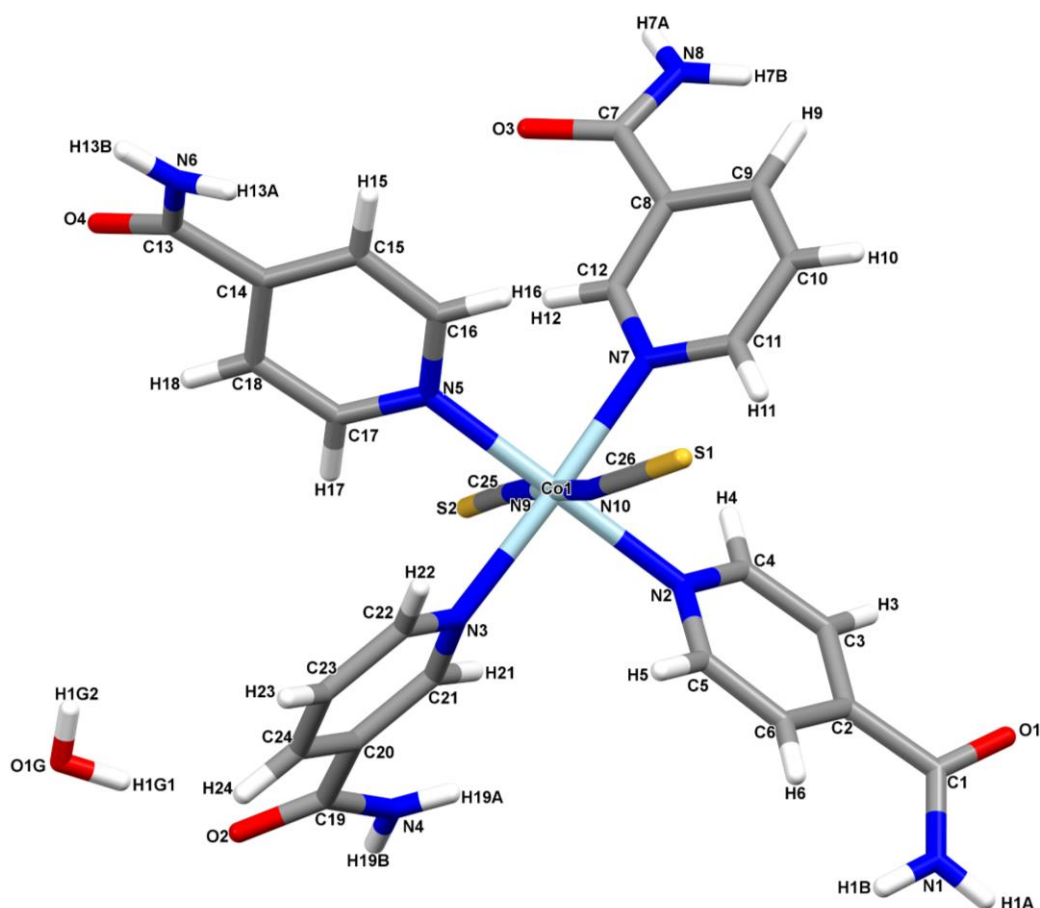
Figure 4.18 *Numbering of the asymmetric unit of H6•H₂O.*

H6•H$_2$O (5) crystallized in the monoclinic space group P2$_1$/n with one molecule of water and one molecule of H6 in the asymmetric unit and molecular formula of CoC$_{28}$H$_{25}$N$_6$O$_5$S$_2$. The crystal with dimensions of 0.06 x 0.13 x 0.22 mm^3 was selected for the single crystal X-ray diffraction analysis. The resulting structure was refined to R$_1$= 0.0333 and wR$_2$= 0.0712 with six formula units in the unit cell. The crystal data and details of the structure refinement are presented in Table 4.9 and hydrogen bond parameters in Table 4.10.

Table 4.9 Crystal data $H6 \cdot H_2O$ (5).

	H6•H₂O (5)
Chemical formula	$Co(NCS)_2$ $(C_6H_6N_2O)_4 \cdot (H_2O)$
H:G ratio	1:1
Formula Weight	681.62
Temperature/K	173(2)
Crystal system	Monoclinic
Space Group (no.)	P21/n (14)
a/Å	11.643(2)
b/Å	20.509(4)
c/Å	13.426(3)
α/°	90.00
β/°	96.21
γ/°	90.00
V/A³	3187.1(11)
Z	4
D_{calc}/g.cm⁻³	1.421
Radiation type	MoKα
F(000)	1404
Crystal size/mm³	0.06x0.13x0.22
Colour, crystal form	Pink, block
No. of total reflections	33440
No. of unique reflections	7329
Θ min-max/°	1.82/27.50
R [F²·>2σ(F²)]	0.033
wR2(F²)	0.072
S	1.038
No. of parameters/ data	437/7329
Res.peak(max/min)/eA⁻³	0.397/-0.291

Table 4.10 Hydrogen-bond geometry (Å, °) with compound made from H6.

D-H	d(D-H) (Å)	d(H···A) (Å)	<DHA (Å)	d(D···A) A	Symmetry operator
			H6•H₂O (5)		
N3-H3B•••O2	0.821	2.071	158.60	2.850	[-x+2, -y+1, -z+1]
N3-H3A•••O3	0.889	1.961	178.02	2.849	[-x+3/2, y+1/2, -z+3/2]
N5-H5A•••S2	0.858	2.744	159.65	3.561	[-x+2, -y+1, -z+1]
N5-H5B•••O1G	0.848	2.013	176.59	2.861	[-x+1, -y+1, -z+1]
N7-H7A•••O1	0.814	2.151	173.69	2.962	[-x+3/2, x+1/2, -z+3/2]
N7-H7B•••O4	0.859	2.037	155.79	2.843	[x+1, y, z]
N10-H10B•••O3	0.865	2.095	161.28	2.927	[-x+1, -y, -z+1]
O1G-H1GB•••S1	0.813	2.521	167.56	3.319	[x-1/2, -y+1/2, z+1/2]
O1G-H1GA•••O1	0.889	1.876	172.83	2.761	

The crystal framework is stabilised by strong and weak hydrogen bonds throughout the complex between water molecule and host. H6 has three donor sites, two from isonicotinamide and nicotinamide isomers and one from the thiocyanato group, all bonded to the water molecule via the amine nitrogen, carbonyl oxygen and sulfur atoms. The water molecule acts as a bridge linking three hosts from three donor sites via three different interactions, N-H•••O, O-H•••O and O-H•••S, connecting the crystal into a 3-D supramolecular network (Fig.4.19a). Additional intermolecular interactions between host-host via amide dimer N4-H19B•••O3 and N8-H7A•••O2 (carbonyl) and N4-H19A•••O1 depicted by $R_2^2(8)$ and $D_1^1(3)$ graph sets are illustrated in Figure 4.19a. A π•••π interaction is observed between

the isonicotinamides of neighbouring hosts. The centroid distance is 5.033Å, with this interaction shown in Figure 4.19a.
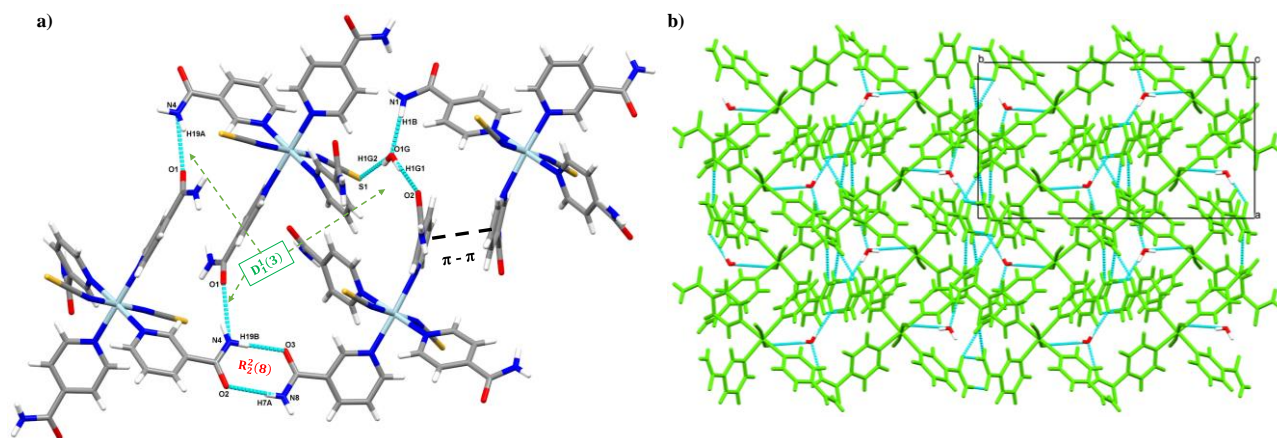
Figure 4.19 *View of H6•H_2O packing diagram a) molecular interactions in H6•H_2O between host and guest and host-host with graph set motif representations and b) hydrogen bond representation between guest and host (light green) packed along the c-axis.*

The crystal structure presents several ring formations of hydrogen bonding between the host-host and between host-guest as illustrated in Figure 4.20. The motifs observed in host-host presented in Figure 4.20 are $R_2^2(14)$, $R_2^2(22)$, $R_2^2(24)$, $R_2^2(26)$ and between host-guest are $R_4^4(30)$ in Figure 4.20e. The ring motifs in host-host interactions involve two hosts via either N-H•••O or N-H•••S or both. The ring motifs are either homo or heterosynthons, involving different hydrogen bonding, N-H•••O and N-H•••S (Fig. 4.20a), or only one type of hydrogen bonding, N-H•••S (Fig. 4.20b) or N-H•••O (Fig.4.20d). Both interactions are found in Figure 4.20c. The ring motif in host-guest is between two waters and two H6 (Fig. 4.20e).
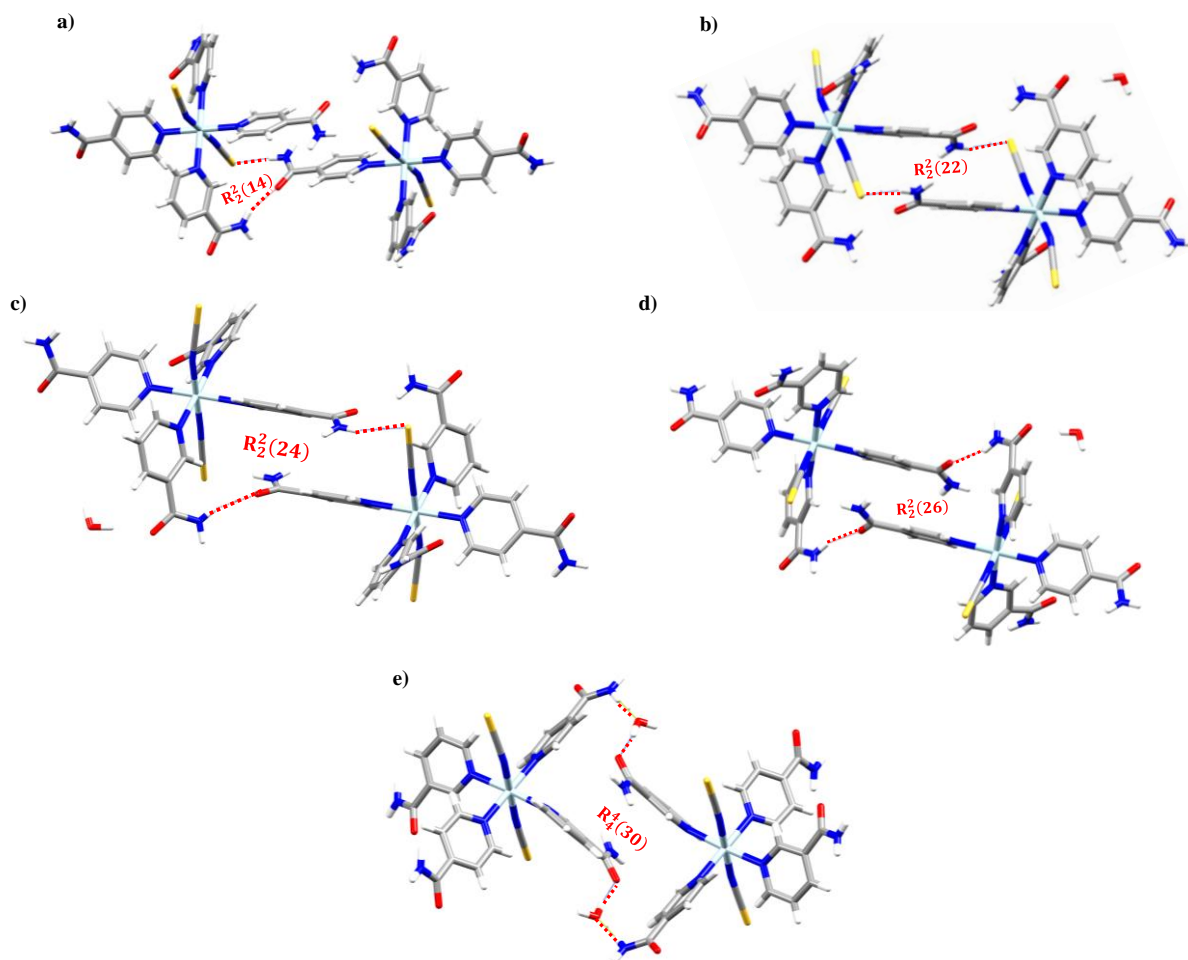
Figure 4.20 *Graph set representations between host-host and host-guest interactions recorded for H6•H$_2$O.*

The hydrogen bonds in the two isomers isonicotinamide (light green) and nicotinamide (green) are very different. The nicotinamide ligand has four donor/acceptor sites whereas isonicotinamide has two (Figure 4.21).

Each nic (green) has four hydrogen bonds, two from the amine group and two from the carbonyl group. One nic is bonded to H6 (nic) via N-H•••O, water via O-H•••O and H6 (nic) via the amide dimer, a homosynthon $R_2^2(8)$ represented with **(A-1)** in Fig. 4.21**.** The second nic is bonded to three H6 molecules via N-H•••O and the graph set $R_2^2(8)$. The oxygens of the carbonyl groups are bifurcated acceptor bonded to two different molecules water/nic and nic/isonic, represented with **(B-1)** in Fig. 4.21.

The two isonic (light green) on the other hand each have two hydrogen bonds from the amide group. One of the isonic is bonded to two H6 (nic) via N-H•••O, represented with **(C-2)** in Fig. 4.21. The second isonic is bonded to H6 (nic) and water molecule, represented with **(D-2)** in Fig. 4.21.
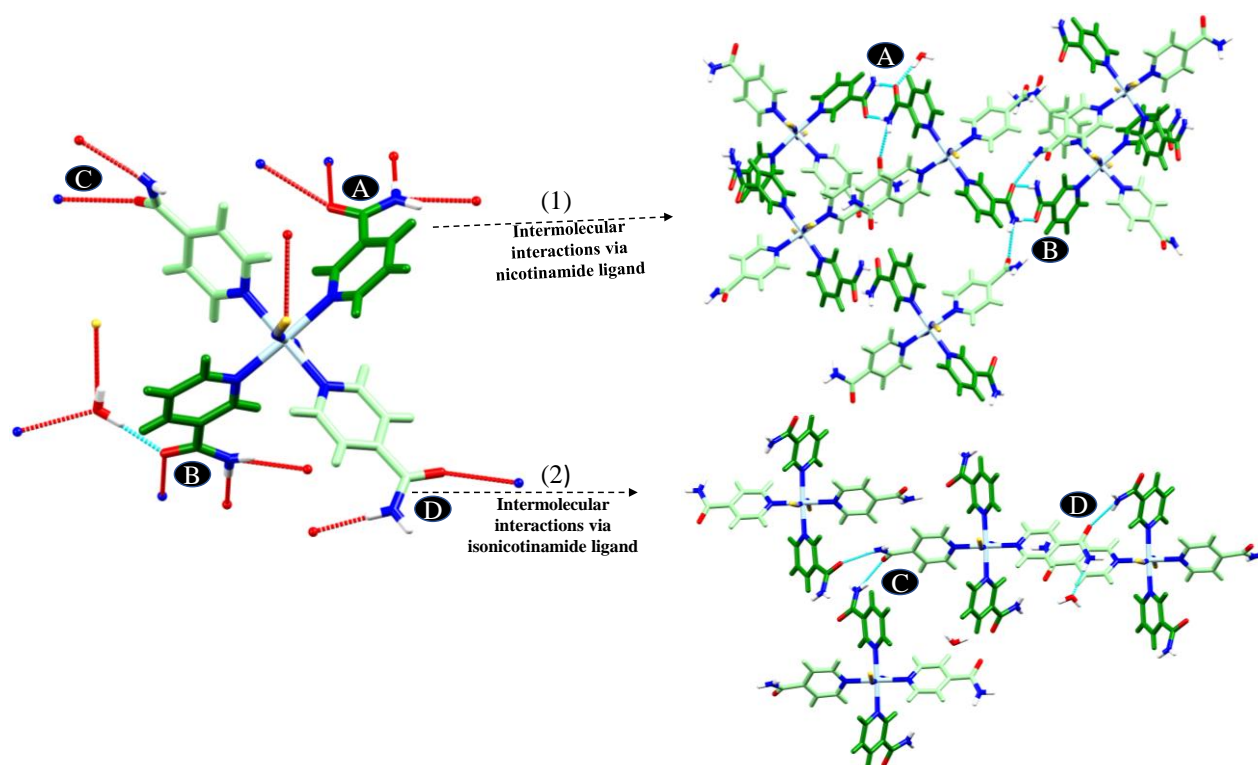
Figure 4.21 *Hydrogen bonding comparison between nicotinamide (green) and isonicotinamide (light green) ligands of H6•H₂O crystal.*

4.4.1 Thermal Analysis of H6•H$_2$O (5)

The TG results for compound H6•H$_2$O is illustrated in Figure 4.22. The decomposition of the crystal is shown in two stages, first the release of one ligand at 159.8 °C followed by the other three ligands between 200 and 300 ℃. The release of water was not observed through the stage. The experimental loss of 76.5 % agrees well with the calculated figure of 73.61 %.
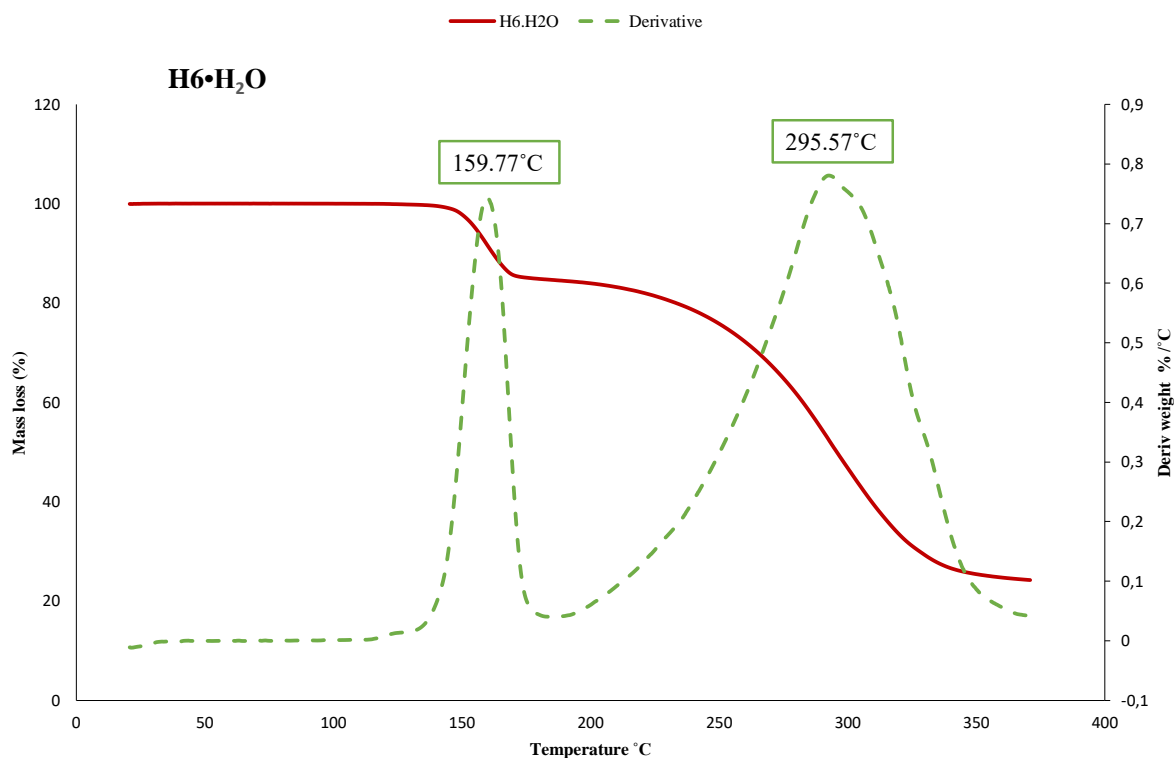
Figure 4.22 *TG and derivative curves of H6•H₂O.*

4.4.2 Powder X-ray Diffraction of H6•H₂O (5)

The PXRD pattern of the host (blue, H6) was compared to that of the crystal (orange, H6•H₂O) obtained from LAZYPULVERIX. The spectra for both the crystal and the host were obtained out between 5 to 50 ° (2 theta) (Fig 4.23). The host 6 pattern shown in Figure 4.23 also appeared noisy as did H4 and H5 in comparison to their crystal patterns. The pattern revealed two new large peaks which were observed around 13 ° and 26 °.
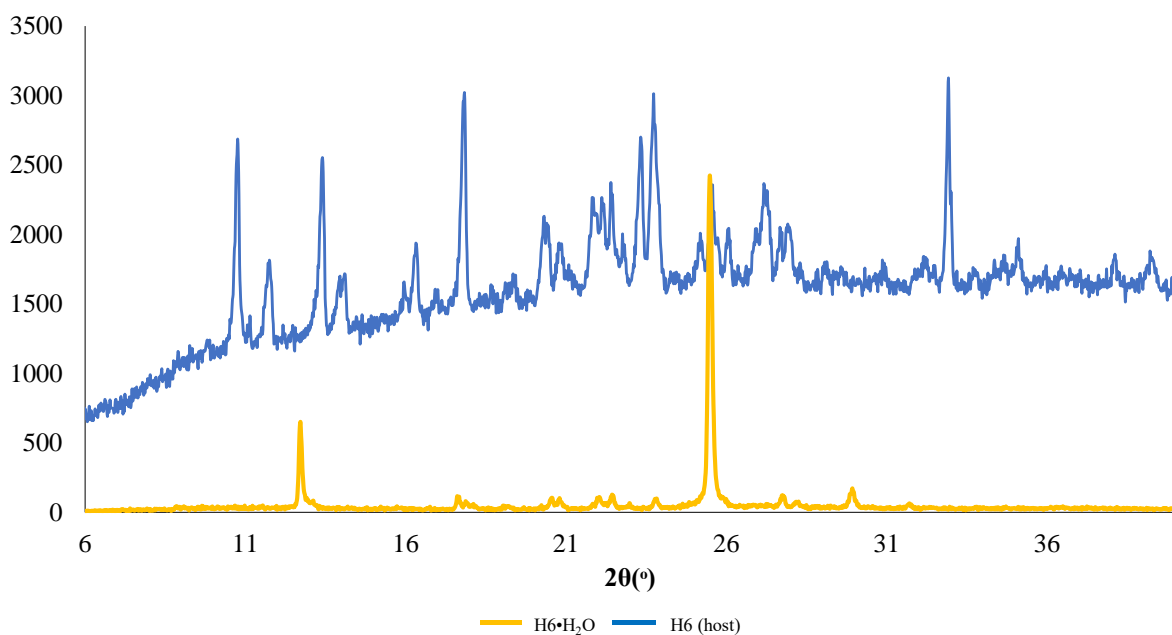
Figure 4.23 *PXRD patterns of H6•H$_2$O in orange and H6 (host) in blue.*

4.5 Bulk analysis of hydrogen bonds N-H···S and O-H···S in cobalt Werner complexes

Both O-H···S and N-H···S are hydrogen interactions occurring in the interaction system between the guest-host, host-host or guest-guest and can be compared to the N-H···O interactions in this research. Even though the hydrogen bond involving sulfur as the acceptor is weaker than one with an oxygen acceptor, the effect of two bonds may lead to a stronger enclathration of the guest or between guest-guest and host-host. O-H···S was observed in H4•H$_2$O, H4•propOH and H6•H$_2$O complexes (see Table 4.11, pink highlight), linking guest H$_2$O and the host and two hosts. N-H···S was observed in H5•2isonic, H5•2isonic•propOH and H6•H$_2$O complexes (see Table 4.11, violet highlight), linking guest-host and host-host. The Cambridge Structural Database (CSD, version 5.4, last update November 2019) was searched for N-H···S and O-H···S contacts in the range of $2.1 < $ H···S $(d_1/Å) < 3.0$, $3.1 < $ N···S/O···S $(d_2/Å) < 3.9$ and $110 < $ N-H···S/O-H···S $(\theta/°) < 180$. The research was focused on contacts between amide or hydroxy groups and thiocyanato bonded to a transition metal. This investigation was used to compare the results obtained during this study from published results residing in the CSD, and the mean value of the search on the CSD was compared to the mean value of our research. 208 hits were found for N-H···S with a mean value of 2.592 Å and 3.504 Å for H···S and N···S respectively, and 181 hits for O-H···S with a mean value of 2.423 Å and 3.329 Å for H···S and O···S respectively. All distribution distances are shown in Figure 4.25 and Figure 4.26, and all refcodes were counted (including duplicates) (Thallapally & Nangia, 2001).

In our three structures (3, 4 and 5) where N-H···S was present the mean values were found to be d_1: (H···S) 2.664 Å and d_2: (N···S) 3.498 Å (Table 4.11), which were consistent with CSD mean values in Figure 4.24a and b.

In the three structures (1, 2 and 5) where O-H···S was observed the mean values were found to be d_1: (H···S) 2.548 Å and d_2: (O···S) 3.355 Å (Table 4.11) and the histogram of the CSD values for the two distances are shown in Figure 4.25a and b.

Table 4.11 Hydrogen-bond geometry of H4, H5 and H6.

D-H	d(D-H)(Å)	d(H···A) (Å)	<DHA (Å)	d(D···A) A
(1)				
O2G-H2G1···S1$	0.795	2.661	170.82	3.448
(2)				
O3-H19···S1$	0.840	2.461	174.35	3.298
(3)				
N15-H15B···S2#	0.927	2.627	164.67	3.529
N8-H8B···S1#	0.800	2.678	160.19	3.441
(4)				
N1-H1A···S1#	0.880	2.603	160.35	3.444
N22-H22B···S2#	0.880	2.670	161.83	3.517
(5)				
N5-H5A···S2#	0.858	2.744	159.65	3.561
O1G-H1GB···S1$	0.813	2.521	167.56	3.319
Mean values				
Mean value of N-H···S#	0.869	2.664	161.34	3.498
Mean value of O-H···S$	0.816	2.548	170.91	3.355

#: N···S bonds $: O···S bonds
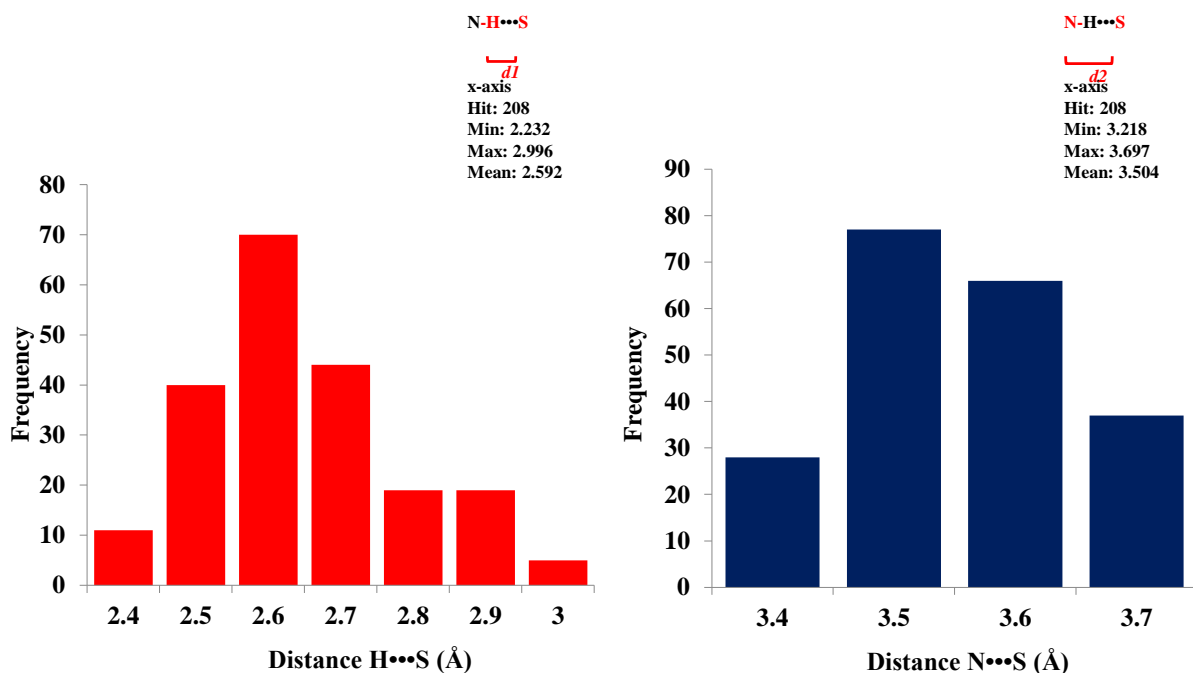
Figure 4.24 Histogram of the distributions of contact distances of N-H···S hydrogen bonds analysed on the CSD for a) d_1 (H···S) and b) d_2 (N···S).
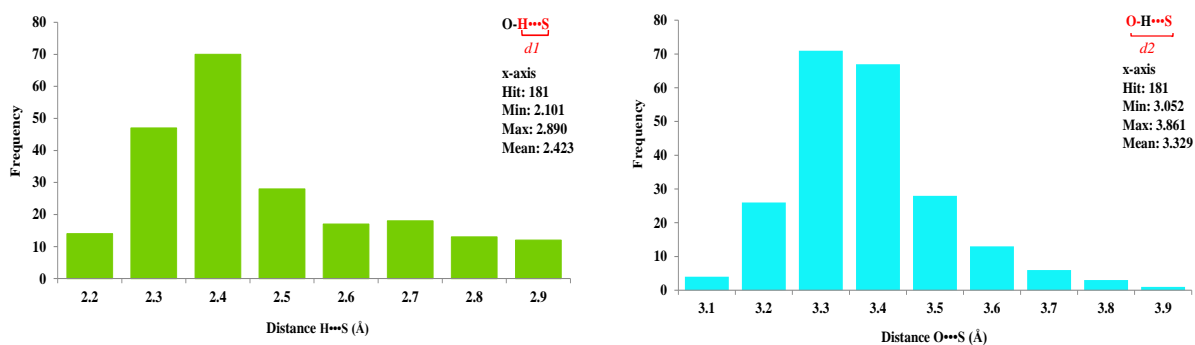
Figure 4.25 Histogram of the distributions of contact distances of O-H•••S hydrogen bonds analysed from the CSD for a) d_1 (H•••S) and b) d_2 (O•••S).

4.6 Torsion angles

Co(II) is surrounded by six nitrogen atoms in each host, with two thiocyanate anions are in the trans position and four coordinated ligands either nicotinamide in H4, isonicotinamide in H5 and both isonicotinamide and nicotinamide in H6 in an equatorial fashion. The bond distances between $Co-N_{NCS}$ were found to be shorter than $Co-N_{ligands}$ with a mean value of 2.076 Å and 2.175 Å respectively, which allowed considerable torsional flexibility of the ligands toward the thiocyanato groups. It is clearly indicating a four-blade propeller conformation of host H5 and H6. The conformation of the nicotinamide of H6 demonstrates some deviation from the true propeller arrangement and the behaviour of host H4 is different from the other two. Host H4 was found to adopt a different conformation between the nicotinamide and the thiocyanato ligands after crystallisation, representing a linear conformation as illustrated in Figure 4.27 (H4). This behaviour shows the considerable torsional flexibility in the ligands, which is based on the four main atoms (N-Co-N-C) in the torsion. The position of the amide group on nic (meta) is different from isonic (para). To describe the conformations of the hosts, the following torsion angles were considered, τ_1, τ_2, τ_3 and τ_4 as represented in Figure 4.26. The four torsion angles were carried out cyclically to yield the minimum in the sum of the square of their differences (Table 4.12). It should be noted that the negative and the positive signs observed with the angle measurement were not considered during the analysis.

When considering H4 versus H5 and H6, it can be seen that the torsion angles for H4 are less than those for H5 and H6. This confirms the difference in the positioning of the nicotinamide ligands (H4) compared with the ligands in H5 and H6.
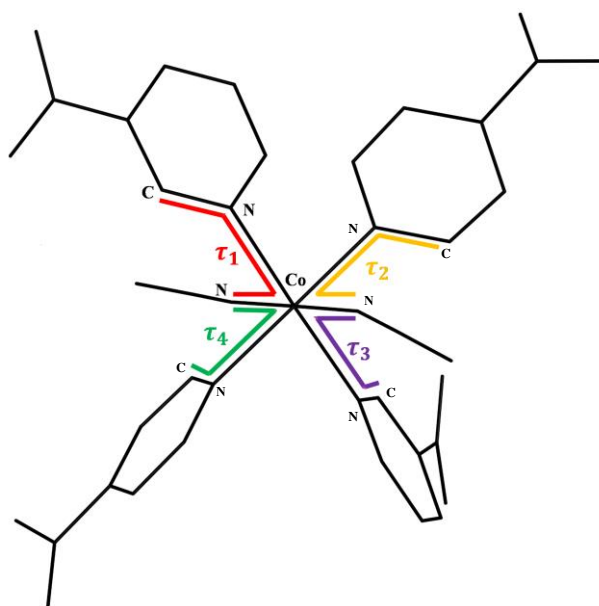
Figure 4.26 *Schematic representation of torsion angles of H6.*

Table 4.12 *Torsions angles between the five structures and between same host and different guests.*

Host	$\tau_1\,^\circ$	$\tau_2\,^\circ$	$\tau_3\,^\circ$	$\tau_4\,^\circ$
H4•propOH	-35.54	32.67	35.54	-32.67
H4•nic•H$_2$O	-28.50	43.29	28.50	-43.29
H4 Mean	32.02	37.98	32.02	37.98
H5•2isonic•propOH	-37.07	-47.70	-44.24	-48.16
H5•2isonic	-34.84	-46.82	-43.53	-45.07
H5 Mean	35.96	47.26	43.89	46.62
H6•H$_2$O	35.37	51.00	39.98	41.28

The most common shape of a Werner complex is presented as a propeller conformation as shown in H5 and H6, but it can swap to a linear conformation (as presented in H4) due to certain conditions. The "pedal" conformation (with aromatic ligand rings aligned at 180 ℃ to each other) on the H4 structure can be explained by the presence of intramolecular interactions N-H•••O between nitrogen and oxygen of two opposite nicotinamide molecules (Fig 4.6). This causes the two nicotinamides to twist in an opposite direction to each other as shown in H5 and H6. The two nicotinamides present an attractive interaction between the amide group on one side and carbonyl group on the other side with a distance of 2.923 Å between the nitrogen and the oxygen (N-H•••O). In H5 and H6, the ligands are further from each other with a repulsive interaction between two amide groups which allow more flexibility of the ligands around the metal centre (Figure 4.27). This is of interest when considering the molecules from the side and leads to the observation that there is also flexibility in the bond between the carbon atom at the centre of the amide functional group and the aromatic carbon on the pyridine ring of the ligand.
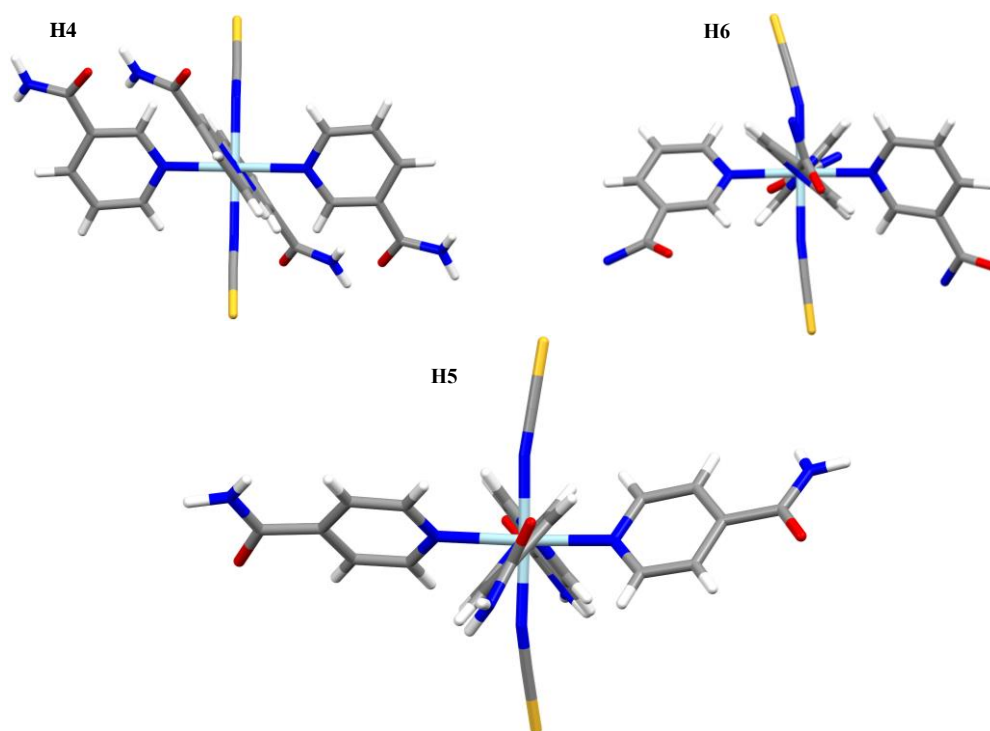
Figure 4.27 Conformation behaviour of H4, H5 and H6, showing "pedal" in H4, but "propeller" conformation in H5 and H6.

Based on the values obtained from the torsion angle calculations and the overlay of H4 structures and H5 structures using Mercury (version, 4.0, 2019) with the RMSD values of 0.4963 and 0.0894 respectively, it was concluded that H5 has more freedom of rotation when combined with a guest than H4. The overlay of H4 structures show a difference between the two hosts compared to the similarity of the H5 overlay structures shown in Figure 4.28 (H5).

H4   **H5**
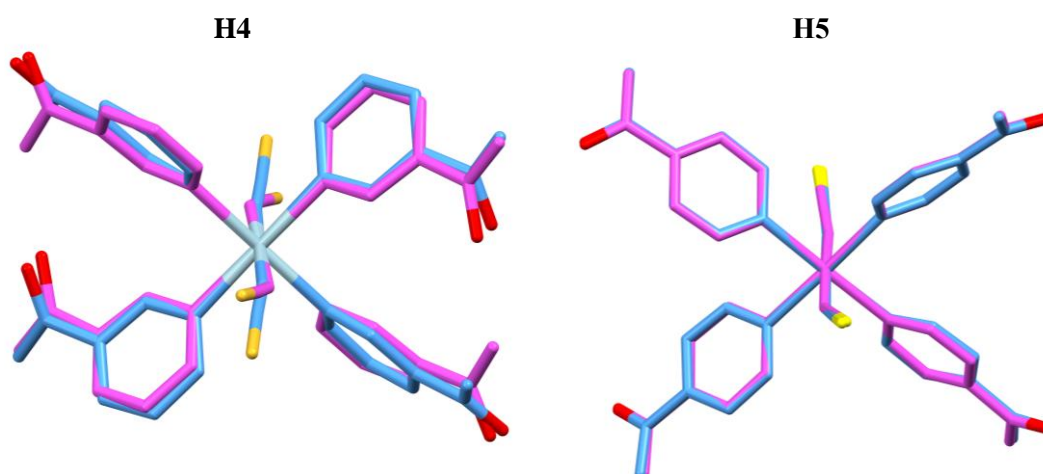
Figure 4.28 Overlay of H4 (blue H4•propOH and pink H4•nic•H₂O) and H5 (blue H5•2isonic•propOH and pink H5•2isonic).

References

Aakeröy, C.B., Beatty, A.M. & Leinen, D.S. 1999. A versatile route to porous solids: Organic-inorganic hybrid materials assembled through hydrogen bonds. *Angewandte Chemie - International Edition*, 38(12): 1815–1819.

Desiraju, G.R., Vittal, J.J. & Ramanan, A. 2011. *Crystal Engineering*. Co-Published with Indian Institute of Science (IISc), Bangalore, India.

DiPalma, J.R. & Thayer, W.S. 1991. Use of Niacin as a Drug. *Annual Review of Nutrition*, 11(1): 169–187.

Etter, M.C., MacDonald, J.C. & Bernstein, J. 1990. Graph-set analysis of hydrogen-bond patterns in organic crystals. *Acta crystallographica. Section B, Structural science*, 46 (Pt 2): 256–62.

Fricker, R.A., Green, E.L., Jenkins, S.I. & Griffin, S.M. 2018. The Influence of Nicotinamide on Health and Disease in the Central Nervous System. *International Journal of Tryptophan Research*, 11.

Griffith, J.S. (John S. 1964. *The theory of transition-metal ions.* Print book. Cambridge University Press.

Gulati, K., Anand, R. & Ray, A. 2016. Nutraceuticals as adaptogens: Their role in health and disease. In *Nutraceuticals: Efficacy, Safety and Toxicity*. Elsevier Inc.: 193–205.

Kurmoo, M. 2009. Magnetic metal-organic frameworks. *Chemical Society Reviews*, 38(5): 1353–1379.

Lawrance, geoffrey A. 2010. *introduction to coordination chemistry*. Callaghan Australia.

Neumann, T., Jess, I. & Näther, C. 2016. Crystal structure of tetrakis(isonicotinamide-κN)bis(thiocyanato-κN)cobalt(II)-isonicotinamide-ethanol (1/2/1). *Acta Crystallographica Section E: Crystallographic Communications*, 72(Ii): 1077–1080.

Pourret, O. & Faucon, M.-P. 2017. Cobalt. In *Encyclopaedia of Geochemistry*. 1–4.

Spek, A.L. 2015. PLATON SQUEEZE : a tool for the calculation of the disordered solvent contribution to the calculated structure factors PLATON SQUEEZE : a tool for the calculation of the disordered solvent contribution to the calculated structure factors.

Thallapally, P.K. & Nangia, A. 2001. A Cambridge Structural Database analysis of the C–H···Cl interaction: C–H···Cl− and C–H···Cl–M often behave as hydrogen bonds but C–H···Cl–C is generally a van der Waals interaction. *CrystEngComm*, 3(27): 114–119.

Wicht, M.M., Nassimbeni, L.R. & Báthori, N.B. 2019. Werner clathrates with enhanced hydrogen bonding functionality. *Polyhedron*, 163: 7–19.

CHAPTER V

SUBSTITUTION OF LIGANDS IN WERNER COMPLEXES

5.1 Introduction

In this chapter, the impact of substitution reactions, replacement of ligands and mixed ligands are examined, for a full detailed analysis of the two new complexes H7 [Co(NCS)$_2$(isonicotinamide)$_2$ (DMSO)$_2$] and H8 [Co(NCS)$_2$(nicotinamide)$_2$ (MeOH)$_2$] (Figure 5.1). The new complex structures are constructed of a central metal ion and mixed organic ligands (methanol, nicotinamide, isonicotinamide, dimethyl sulfoxide, and thiocyanate) all connected to the metal centre via coordination interactions with a general formula of MX$_2$A$_2$B$_2$, where M is a divalent metal ion Co (II), X is an anionic ligand NCS$^-$, A is a neutral base (isonicotinamide or nicotinamide) and B a solvent or (guest) liquid used for the crystallisation process.
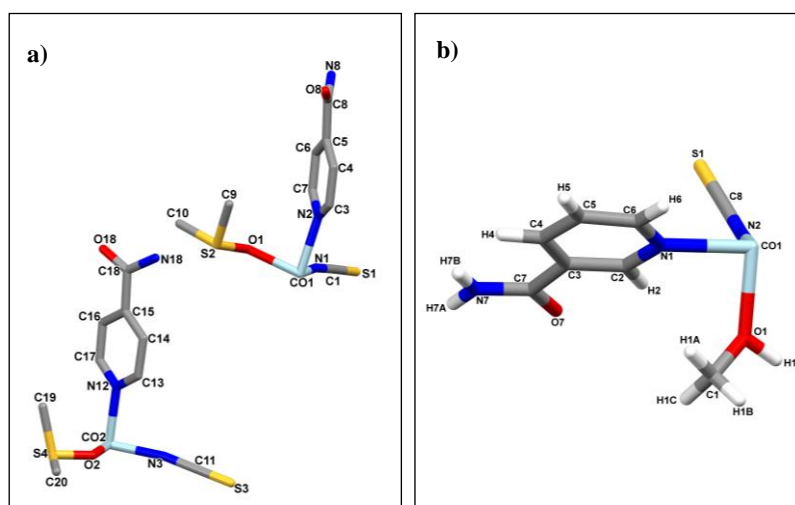
Figure 5.1 *Numbering scheme of the asymmetric unit structure of, a) H7, b) H8 (some hydrogens are omitted for clarity).*

The organic ligands are connected to the metal centre via O-donor atoms, which act as bridging linkers and play an essential role. Organic mixed ligands give the opportunity to construct new structures with higher complexity due to the distinct donor which can coordinate with metal centres through different coordination modes (Zhao & Sun, 2014). Many factors such as pH values, temperatures, ligands and reactant ratios can affect the structural function of the analysis. The nature of the organic ligands and the metal dominate the final structures as well as physical properties (Lin et al., 2014). Thus, increasing the number of ligands (mixed ligands) required more studies into the nature of the final structure as each ligand has different physical properties and applications.

Nevertheless, studies showed that mixed ligand MOFs (metal organic frameworks) compared to single ligand MOFs have reached a new level of rational design and construction, which involves the synergetic coordination of different ligands with metal and subsequent networking (Yin et al., 2015). The Zhao article reported that the use of organic mixed ligand MOFs possess great advantages of tuneable structure and pores, large surface areas and high stabilities (Zhao & Sun, 2014).

The new complexes were obtained upon crystallisation of Werner complexes H4 [Co(NCS)$_2$(nicotinamide)$_4$] and H6 [Co(NCS)$_2$(nicotinamide)$_2$(isonicotinamide)$_2$] with guests which were to be enclathrated within the host cavities. The host-guest products obtained after crystallisation presented complexes where the guest or the solvent used in the process substituted two of the ligands in the host structure. This substitution was only observed with some of the H4 and H6 crystallisations, however, the H5 structure remained unchanged upon crystallisation. The synthesis of the hosts were made using the Schaeffer and co-workers method (Schaeffer et al., 1957), which is based on the direct reaction of host in a specific solvent system. The new complex structures were synthesised from the host powders (H4, H5 or H6). Thus, the substitution of ligands should be due to other factors such as the solvent used, reaction temperature in the crystallisation process, reactant concentration and others, in order to produce the new outcome complexes. The availability of the oxygen lone pair, in the hydroxide of the methanol or sulfoxide in DMSO, on these ligands is not reduced by steric hindrance. The basicity of each "guest" relative to the ligands already covalently bonded to the metal need to be considered. In the formation of the new complex H7, nicotinamide (pKa 3.54) in H6 was displaced by DMSO (pKa 35.15) and methanol (pKa 15.5) substituted two of the nicotinamides (pKa 3.54) in H4 to form complex H8 (Figures 5.2).
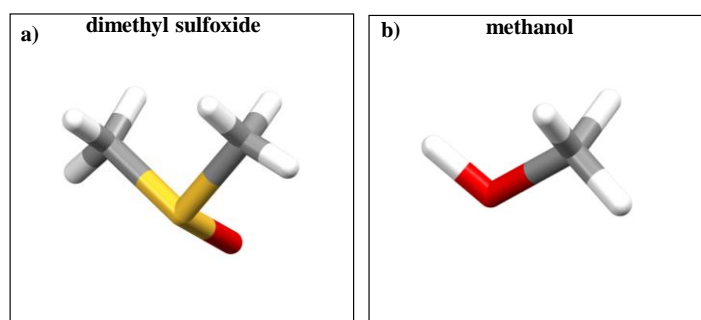
Figure 5.2 *Structural schematic of exchange ligands, a) DMSO and b) methanol.*

It is difficult to find a suitable procedure and condition to control the outcome of some crystallisation processes (Han et al., 2014). So, the process of crystallisation can be subject to many factors which may alter the final product. A substitution reaction, in which any atom or group in a molecule is replaced or exchanged by another atom or group, is usually used to improve the function of the complex (Han et al., 2014). This type of substitution is also known as solvent assister linker exchange (SALE) (Son et al., 2020) or post synthetic ligand exchange (ligand-based PSE) (Jeong et al., 2013). The overall substitution reaction is represented as:

$$R\text{-}X + S \rightarrow R\text{-}S + X$$
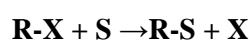
where R-X is the reactant, substrate S the attacking reagent and R-S and X the substituted product and the leaving product respectively (Langford, Cooper H., Gray, 1966).

The substitution can be divided in three types 1) solid-solid substitution, where two types of solid are mixed together and suspended in a specific solvent for a given period to achieve the reaction; 2) solid-liquid substitution, one solid is soaked in a solution containing the attacking metal complex or guest molecule to get substituted and 3) liquid-liquid substitution, a soluble guest is reacted with metal complex in given solvents to get a new complex, which is exactly the process our Werner complexes underwent.

The substitution reaction can be partial or complete; in partial substitution the framework is often maintained, while in a complete substitution, structural transformation such as structural interpenetration, framework dimensionality and changes in the coordination environment can be caused. The substitution of the organic ligand can tune pore size for example. Recent research has shown that the substitution reaction can be used as a new strategy in the synthesis and modification of MOFs (molecular organic frameworks) and MOPs (molecular organic polyhedra), particularly for pre-designed structures and functions. Manos and co-workers reported a successful substitution of organic ligands in order to create a new structure, with the substitution of the ligand DMF by a series of guest solvent molecules methanol, ethanol, THF, pyridine and acetone in the MOF structure $[Nd_2(CIP)_2(DMF)_{2.8}(H_2O)_{1.2}]_n$ via single-crystal to single-crystal transformation (SC-SC) (Manos et al., 2012).

Nevertheless, substitution in some highly stable crystals is quite difficult due to the strong bonds between metal ions and organic ligands. For example, MIL-101 (Cr)[52] is a chemically stable MOF whose attempts to exchange the metal ion or the organic ligand failed (Kim et al., 2012).

The first of the new complexes H7 is the result of crystallisation of host H6 with hexanol plus 4 drops of DMSO solvent to increase the solubility of H6. The ligands nicotinamide ligands were substituted with the solvent DMSO, in the H6 Werner complex (Fig. 5.2a).

H8 was straight forward, it resulted after crystallisation of the host H4 with methanol, Fig. 5.2b. Two nicotinamide ligands were substituted with methanol molecules.

SUBSTITUTION REACTIONS
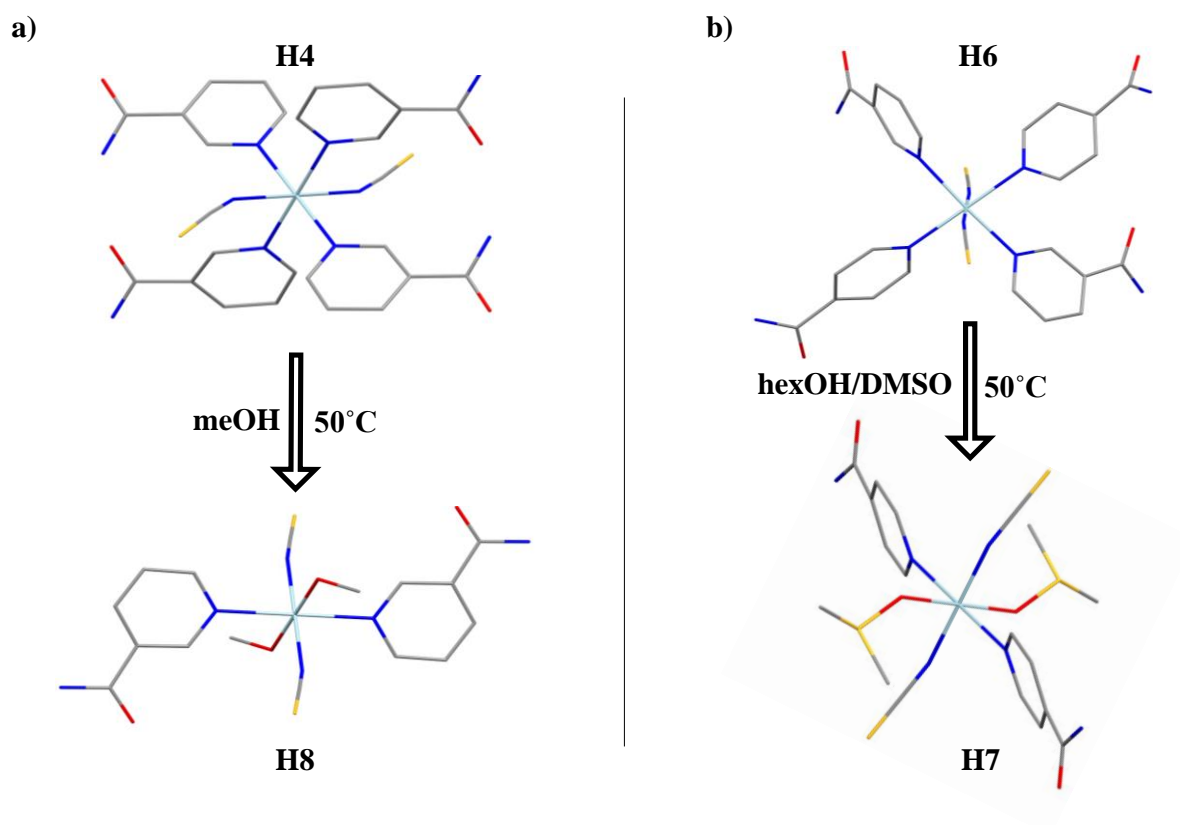
Figure 5.3 Summary of the substitution reactions between the host and guest resulting in the exchange of nicotinamide ligands by, a) meOH within H4 complex and b) DMSO within H6 complex (hydrogens were omitted for clarity).

These results were confirmed by TGA, DSC, PXRD and SXCRD, presenting two new complexes with mixed ligands coordinated to metal centre Co^{2+}. The complexes after crystallisation were H7 $Co(NCS)_2(isonicotinamide)_2(DMSO)_2$ and H8: $Co(NCS)_2(nicotinamide)_2(meOH)_2$, and all crystal data are summarised in Table 5.1. The structural properties and a comparison of their behaviour with the original host complexes and other similar Wener complexes/ clathrates with the same central metal ion will be discussed here.

Table 5.1 *Crystal data of H7 and H8.*

	$Co(NCS)_2(isonic)_2$ $(DMSO)_2$ (H7)	$Co_{0.5}(NCS)(nic)$ $(meOH)$ (H8)
Chemical formula	$Co(NCS)_2$ $(C_6H_6N_2O)_2(C_2H_6OS)_2$	$Co_{0.5}(NCS)$ $(C_6H_6N_2O)(CH_4O)$
Host in ASU	1	½
Formula Weight	575.60	483.43
Temperature/K	173(2)	173(2)
Crystal system	Triclinic	Triclinic
Space Group (no.)	$P\bar{1}$ (No.2)	$P\bar{1}$ (No.2)
a/Å	7.2767(2)	6.9209(5)
b/Å	13.6020(15)	8.3007(6)
c/Å	14.0390(15)	10.1794(8)
α/°	75.986(2)	84.802(2)
β/°	75.386(2)	72.708(2)
γ/°	75.631(2)	71.030(2)
V/A³	1278.4(2)	528.02(7)
Z	2	2
D_{calc}/g.cm^{-3}	1.495	1.520
Radiation type	MoKα	MoKα
F(000)	594	249
Crystal size/mm³	0.09x0.11x0.16	0.15x0.29x0.39
Colour, crystal form	Pink, block	Pink, block
No. of total reflections	27518	12142
No. of unique reflections	6402	2618
Θ min-max/°	1.527/25.42	2.10/28.30
R [F²>2σ(F²)]	0.0395	0.0278
wR2(F²)	0.0841	0.0743
S	1.022	1.096
No. of parameters/ data	397/6402	138/2618
Res.peak(max/min)/eA^{-3}	0.354/-0.438	0.295/-0.458

5.2 Structure analysis of H7

5.2.1 Thermogravimetric analysis

The crystal of the complex H7 was first analysed by TG, showing the decomposition of H7 in steps of the crystal structure stoichiometry (Figure 5.4). The release of 2 mol of DMSO ligand followed by 2 mol of isonic ligands is shown in the combination of the TGA, DTA and DSC data. According to the DSC, the first two peaks can be attributed to the endothermic phase change of 2 mol of DMSO (131.76 and 143.93 °C) (literature value of 189˚C), followed by the last peak for 2 mol isonic (315.23 °C) (literature, 334 °C). The decomposition of these ligands can also be seen in the derivative curve, showing losses in mass at 139.72 °C and a combination of peaks later at 248.58 °C. Theoretical calculation suggests a loss of 27.25 % for DMSO and 42.43 % for isonicotinamide.

H7
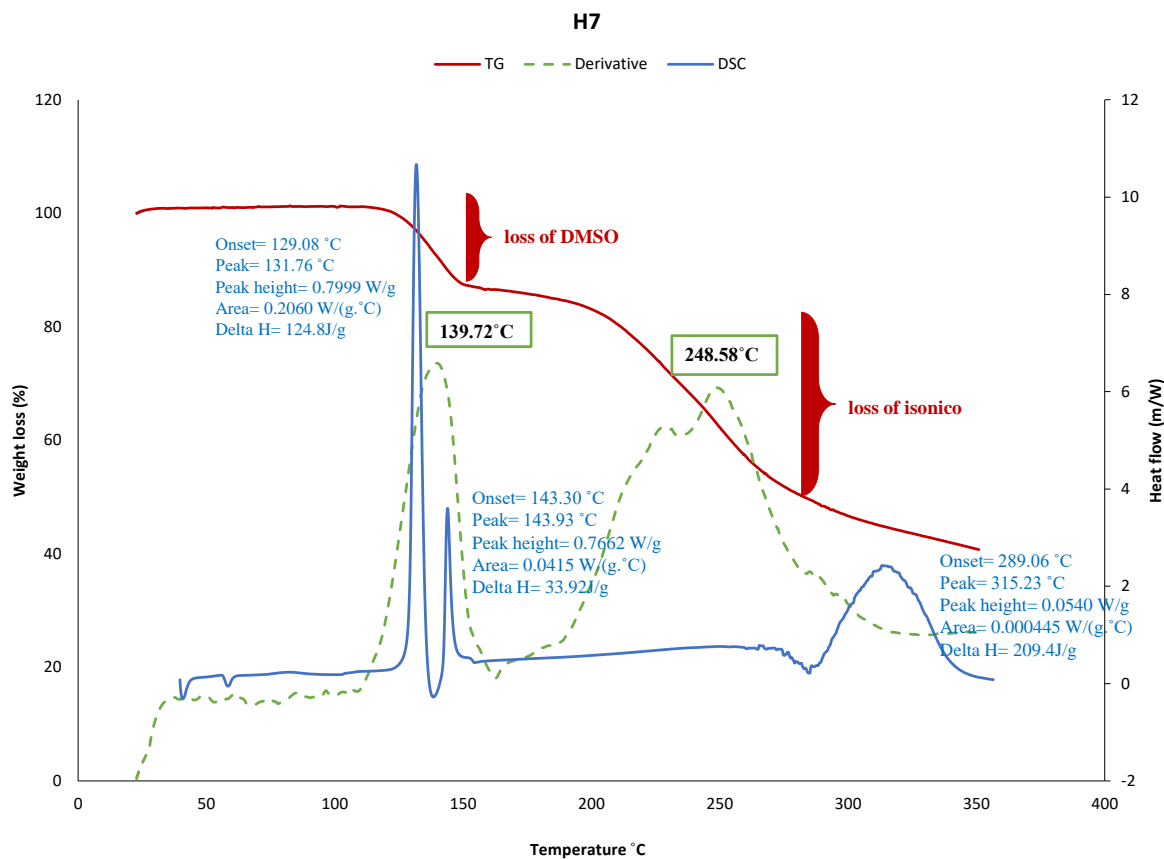
Figure 5.4 Thermal analysis curves of complexes H7 as mass loss percentage (red curve), the derivative weight (green curve) and heat flow (blue curve) vs temperature (°C), purge gas: N_2 (40 mL/min) heating rate: 20 °C/min.

5.2.2 Single crystal analysis of H7

A suitable crystal of H7 complex with dimensions 0.09 x 0.11 x 0.16 mm^3 was selected for data collection for the single crystal analysis using a Bruker AEX II DUO diffractometer. H7 crystallizes in a triclinic system in the space group P$^-$1 with two identical half molecules in the asymmetric unit as illustrated in Figure 5.1a. The asymmetric unit contains two half metal ions Co^{2+} located on a centre of symmetry and coordinated by four nitrogen atoms of thiocyanate and isonicotinamide ligands and two oxygen atoms from DMSO ligands. The coordination geometry around the metal can be described as octahedral. The two complexes of the ASU present two identical structures I and II (Figure 5.5) with the Co-O bond distances falling in the range of 2.107 Å and 2.108 Å [light blue (I) and dark blue (II) structure respectively] and Co-N bond distances are 2.147 Å and 2.127 Å (I and II, respectively) and the Co•••Co distance is 9.222 Å. In comparison to H6, H7 adopts a pedal-type conformation where the H6 is a propeller-type conformation as illustrated in Chapter 4. This behaviour can be due to the intermolecular interactions N-H•••S (between the nitrogen of the isonicotinamide and nitrogen

thiocyanato sulfur and weak hydrogen bonds such as C-H•••N, and C-H•••O, stopping the isonicotinamides from twisting in an opposite direction to each other.

Table 5.2 *Distance measurement in H7*

DISTANCES (Å)		
Co(NCS)2(isonic)2(dmso)2	Dark blue **II**	Light blue **I**
Co-O(dmso)	2.107	2.108
Co-N(NCS)	2.105	2.097
Co-N(isonic)	2.189	2.157
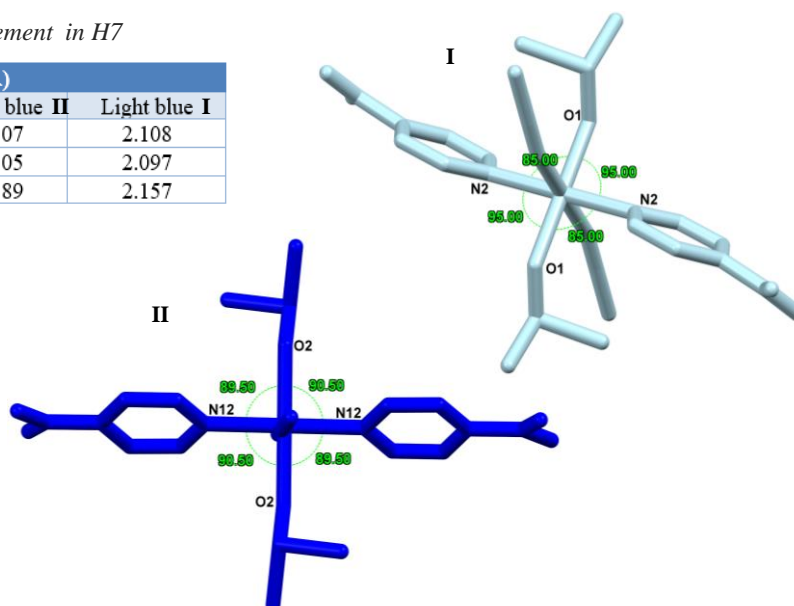
Figure 5.5 *Bond distances and angle measurements in H7*

When investigating the two hosts I and II, differences are seen in the angles and distances between ligands and thiocyanato as shown in Table 5.2 (Figure 5.5). The two structures differed in the direction of the thiocyanato and the ligands. The overlay of the two structures in Figure 5.6a illustrates these differences and in Figure 5.6b planes between DMSO and thiocyanate are illustrated. From this diagram it can be seen that the planes are not parallel (mean: N3 O2 N3 / N12 O13 N12) and angles between the green plane (N12 O13 N12) and the pink plane (N1 O1 N1) are perpendicular (differing by less than 1° from 90°).

a)   b)
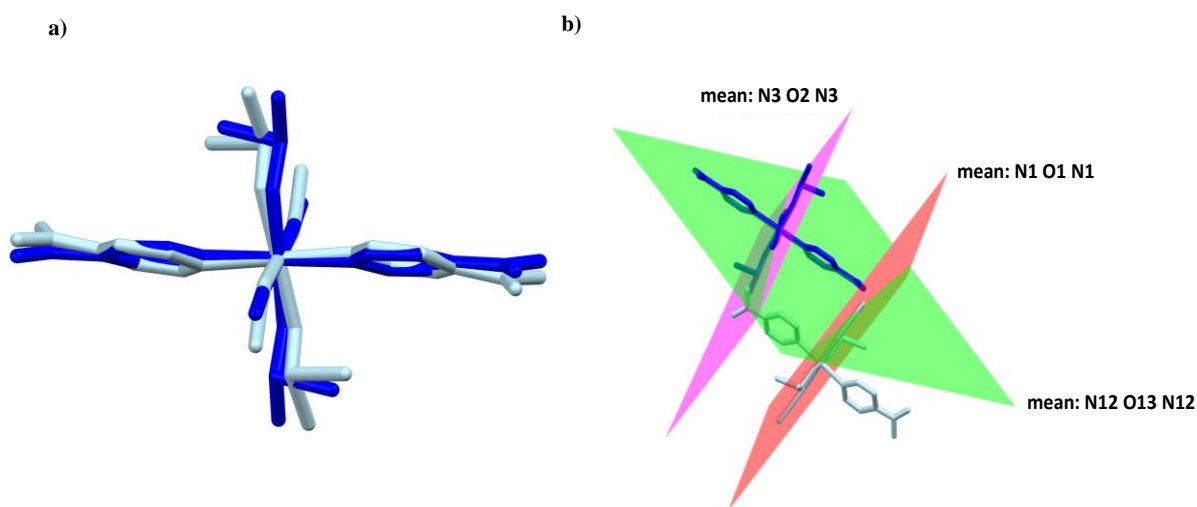
Figure 5.6 *Structure of H7, a) overlay of structures I and II and b) dihedral angle between the planar grouping of structure I in red and structure II in green (some hydrogen atoms were omitted for clarity).*

The two compound assemblies in H8 are linked together into a sheet by a combination of the two major hydrogen bonds N-H•••S and N-H•••O. N-H•••O hydrogen bonds are formed between the isonicotinamides (amide group) and N8-H8A•••O8 (carbonyl group) forming amide dimer synthons, classified as $R_2^2(8)$ graph set (Figure 5.7). N-H•••S on the other hand links the two complexes of the ASU via (amine group) N8-H8B•••S3 (thiocyanato group) hydrogen bonds forming $C_2^2(22)$ chains as illustrated in Figure 5.7 in ball stick style.

Table 5.3 Hydrogen-bond geometry (Å, °) of H7

| D-H	d(D-H) (Å)	d(H..A) (Å)	<DHA (Å)	d(D..A) A	Symmetry operator
Co(NCS)2(isonic)₂(DMSO)₂ (H7)					
N8-H8A•••O8	0.876	2.093	170.10	2.960	[-x, -y-1, -z+1]
N8-H8B•••S3	0.787	2.621	151.52	3.332	[-x+1, -y, -z+1]
C20-H20A•••O8	0.999	2.363	147.33	3.249	[-x+2, -y, -z]
C16-H16•••O2	0.960	2.444	145.61	3.281	[x-1, -y, z]
C9-H9A•••O18	0.975	2.508	167.57	3.466	[-x+1, -y, -z]
C6-H6•••O1	0.901	2.603	137.80	3.326	[-x, -y, -z+1]
N18-H18A•••O18	0.825	2.035	170.79	2.852	[-x+1, -y, -z]
N18-H18B•••S1	0.866	2.699	147.79	3.462	[-x+1, -y, -z+1]
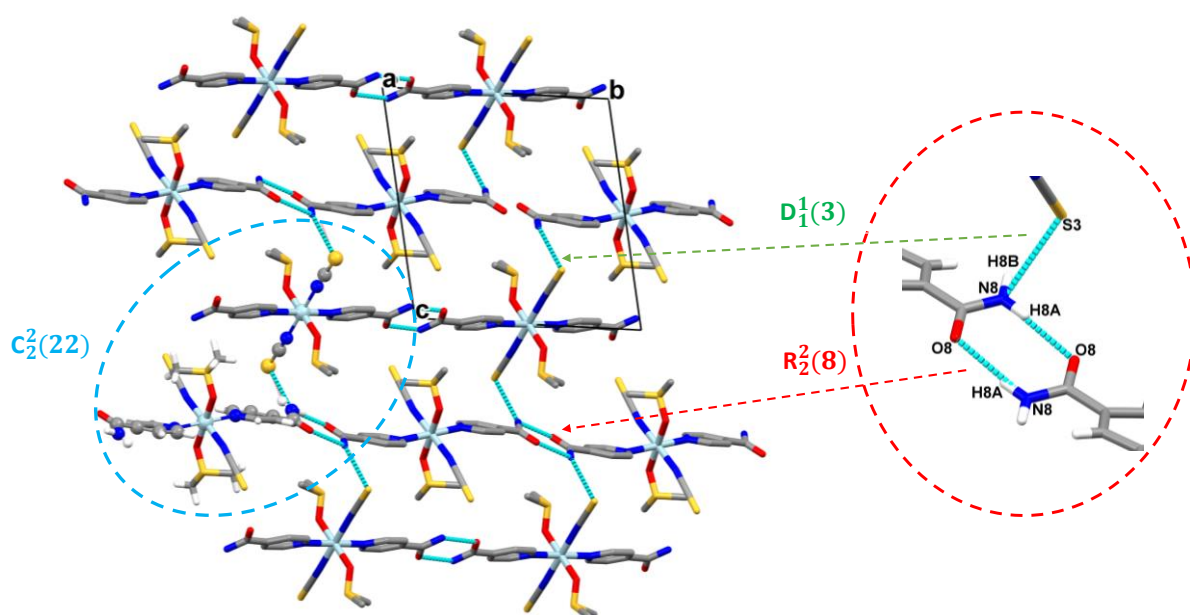
Figure 5.7 Packing diagram viewed along the a-axis showing the molecular hydrogen bonds forming a sheet with labelled contact atoms of the graph sets and chains within the complex (some hydrogen atoms are omitted for clarity).

Weak interactions were observed between the DMSO and isonic ligands linking the two molecules and are characterised by CH•••O hydrogen bonds. Four weak main interactions were formed, two in each complex. Two weak interactions shown in I (light blue) in Figure 5.8b, one linking the two different

complexes [I (light) and II (dark blue) molecules] via (DMSO methyl group) C20-H20A•••O8 (carbonyl group) with a distance of 3.249 Å and angle of 147.33 °C and the other linking the same complexes (complex I) via (isonicotinamide aromatic) C16-H16•••O2 (sulfoxide group) with a distance 3.281 Å and angle of 145.61 °C (Figure 5.8b). The interactions and assemblies were observed with the second complex in H7 (complex II) by C9-H9A•••O18 and C6-H6•••O1 as illustrated in Figured 5.8c. Table 5.3 provides the different hydrogen bond data for H7.

Furthermore, the two complexes of H7 are packed along the a-axis into sheets with alternating horizontal chains of complex with the molecules linked by $R_2^2(8)$ graph sets (Figure 5.7 and 5.8a). These chains are inter-linked by the synthons indicated by the $D_1^1(3)$ graph set (shown in Figure 5.7).
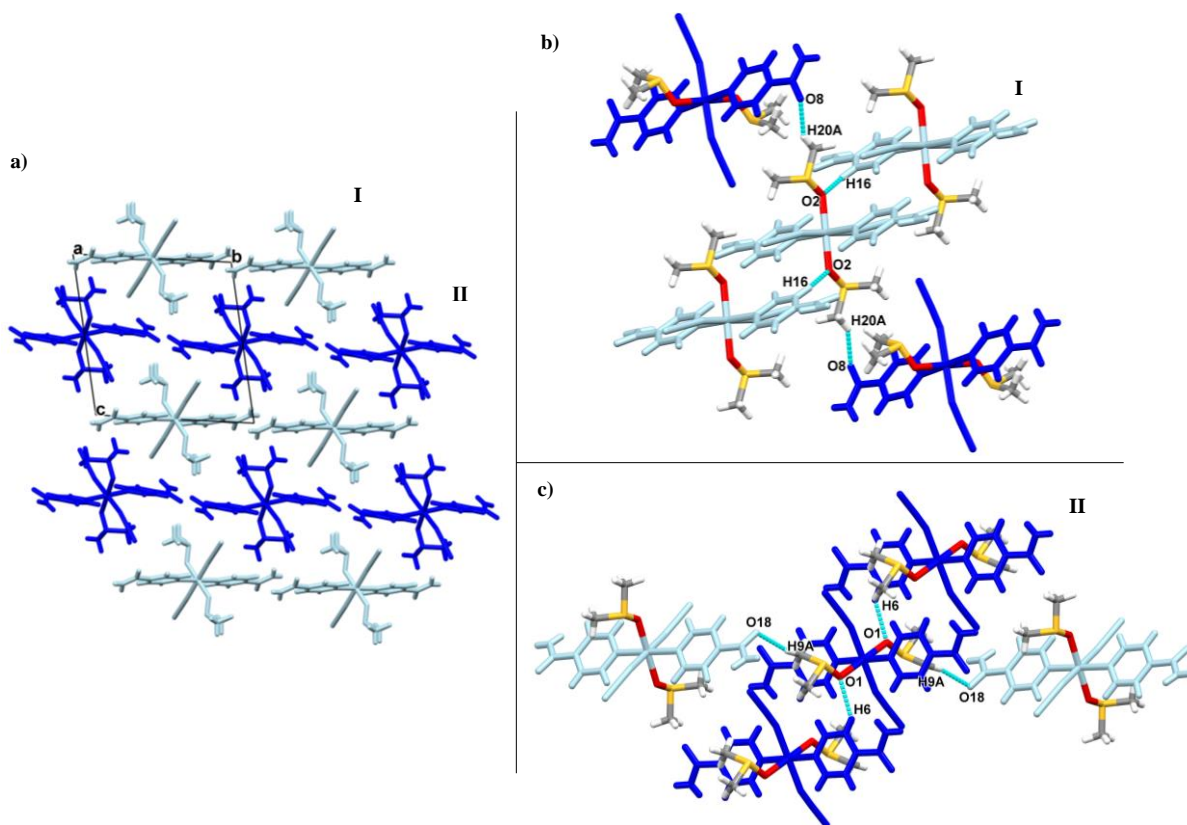
Figure 5.8 *Packing diagram, a) viewed along the a-axis with the two complexes of H7 in light (I) and dark blue (II) showing their diverse positions in the crystal structure, b) weak intra- and intermolecular hydrogen bonding in H7 in complex I (light blue) and c) weak intra- and intermolecular hydrogen bonding in H7 for the complex II (coloured in dark blue), (some hydrogen atoms were omitted for clarity).*

5.3 Structure analysis of H8

The analysis of H8 was done using SCXRD and PXRD, while TGA and DSC were not carried out due to the lack of sufficient crystals and unsuccessful recrystallization experiments. After crystallisation, a few pink crystals formed after two weeks of slow evaporation. A crystal with dimensions 0.15 x 0.29 x 0.39 mm³ was selected for single crystal analysis. H8 crystallizes in the triclinic system in space group P$\bar{1}$ (No. 2) with the asymmetric unit containing half a molecule (Figure 5.1b). The structure of H8 is constituted of a metal centre Co (II) coordinated to six ligand nitrogen and oxygen atoms, two coordinated by O of the methanol ligands and four N-coordinated by two thiocyanato and two nicotinamide ligands forming an octahedral complex as illustrated in Figure 5.9a.

In this complex, hydrogen bonding scaffolds the framework. The nicotinamide ligands are hydrogen bonded to other ligands methanol and thiocyanate via O-H•••O or N-H•••S interactions. The O-H•••O hydrogen bonds involve methanol and nicotinamide ligands interacting via the (methanol hydroxy) O1-H1•••O7 (amide). N-H•••S forms between the thiocyanate and nicotinamide characterised by (amide) N7-H7B•••S1 (thiocyanate). The N-H•••O interactions involve the two nicotinamides connecting via amide dimers N7-H7A•••O7 forming a $R_2^2(8)$ graph set. All hydrogen bond data of H8 are summarised in Table 5.4.

Table 5.4 Hydrogen-bond geometry (Å, °) of H8

D-H	d(D-H) (Å)	d(H..A) (Å)	<DHA (Å)	d(D..A) A	Symmetry operator
Co(NCS)2(nic)₂(meOH)₂ (H8)					
O1-H1•••O7	0.980	1.786	163.42	2.739	[-x, -y+1, -z+1]
N7-H7A•••O7	0.880	2.096	166.20	2.958	[-x-1, -y+1, -z+2]
N7-H7B•••S1	0.880	2.673	164.26	3.528	[-x, -y+1, -z+2]

The oxygen (O7) of the nicotinamide ligands is acting as a bifurcated acceptor as it is bonded to the amine group and at the same time to the methanol hydroxy group.

The crystal structure is stabilized by this combination of two hydrogen bonds N-H•••O and O-H•••O between nicotinamide and methanol represented in the packing diagram in Figure 5.9b showing the arrangement in columns. The structure arrangement was also stabilized by π•••π interactions between the six membered rings of the nicotinamides with centroid distance of 3.460Å (Fig. 5.9c).

a)

b)

c)

$D_1^1(3)$

$R_2^2(8)$

$R_2^2(16)$

π-π
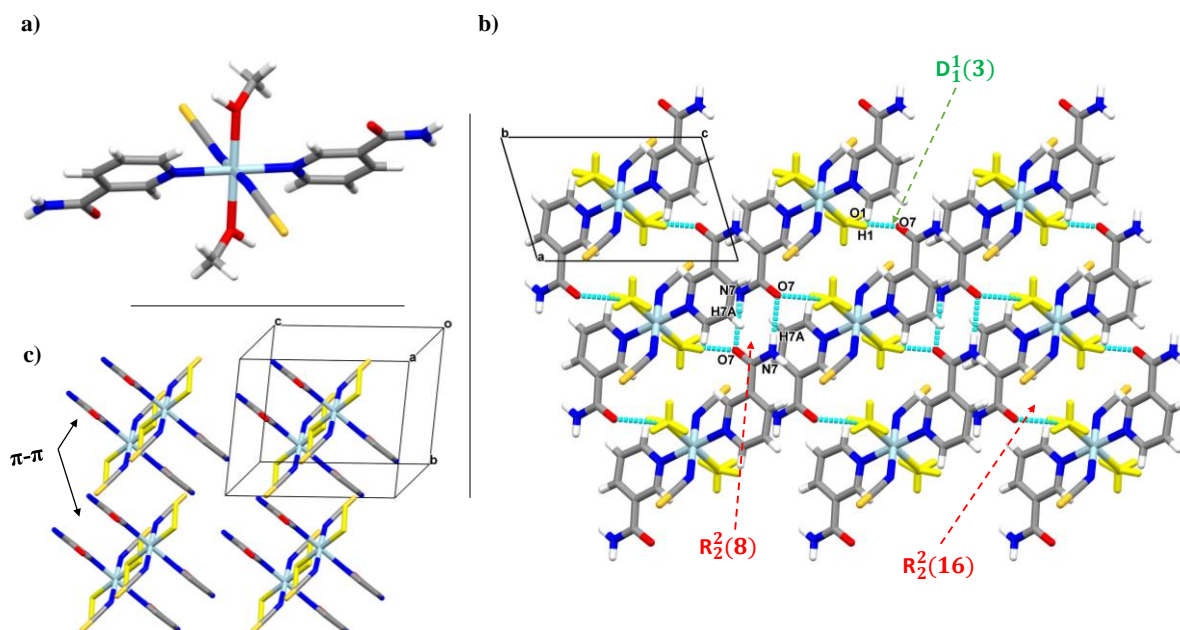
Figure 5.9 Crystal structure of complex H8, a) molecular octahedral structure, b) sheet arrangement in the projection along the b-axis showing the hydrogen bonds in network lattice with labelled contact atoms of the graph sets and c) π•••π interactions between aromatic rings of nicotinamide in crystal packing in the projection along the a-axis (some hydrogen atoms were omitted for clarity).

There is a ring formation of hydrogen bonding interactions between the nicotinamide and the methanol described by the $R_2^2(16)$ ring motif (Figure 5.9b) and between the nicotinamide and the thiocyanate described by $R_2^2(20)$ ring motifs (Figure 5.10).

$R_2^2(20)$
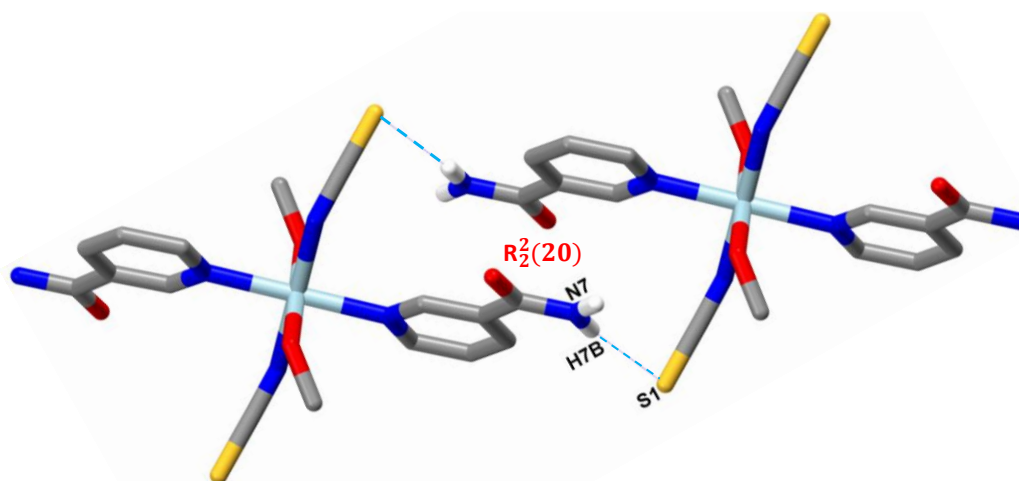
Figure 5.10 Representation of the ring graph set between two nicotinamides linked by N-H•••S interactions (some hydrogen atoms were omitted for clarity).

5.4 Powder X-ray diffraction analysis of H7 and H8.

The PXRD analyses were used to compare the host starting materials and the new complexes obtained after crystallisation. The spectra of all materials were carried out between 2θ of 5° to 50° (Fig. 5.11). After crystallisation new complexes were obtained where the guest or the solvent used replaced the nicotinamide ligands in host 4 (Fig.5.11b, blue curve) and host 6 (Fig.5.11a, blue curve). So, the PXRD was used to confirm the absence of nicotinamide in H7 and its presence in H8. As the host 4 and host 6 patterns appeared noisy in comparison to the new complexes, we used the PXRD patterns of the starting materials directly to make the comparison.

The H7 spectrum (Fig.5.11a, orange curve) in comparison to the isonicotinamide spectrum showed the presence of isonicotinamide ligands (brown curve) with relevant peaks 17.68˚ and 23.40˚ in the new complex. The nicotinamide spectrum (green curve) most relevant peaks 11.39˚, 14.93˚ and 19.94˚ are absent in the H7 spectrum but present in the H8 spectrum (Fig. 5.11b, orange curve).
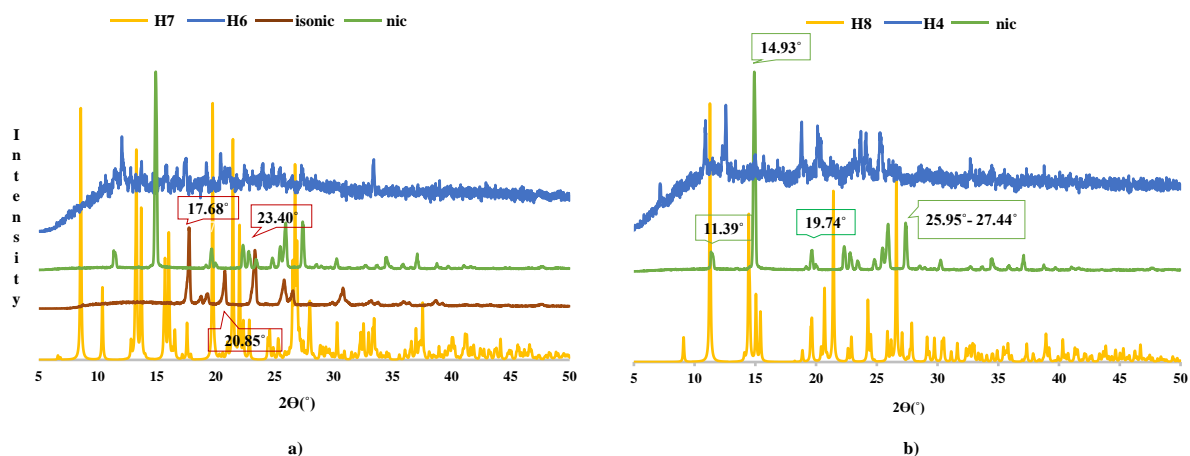
Figure 5.11 *PXRD patterns of a) H7 and the starting materials nic, isonic and host 6 and b) H8 and the starting materials nic and host 4. Note that Label nic = nicotinamide and isonic = isonicotinamide.*

5.5 Elucidation of ligand substitution

It was noticed that in each host only nicotinamide ligands were substituted and replaced by a guest or a solvent. As explained previously, the substitution reaction is one of the frequently exhibited reactions by metal ion complexes. The substitution may be the same ligands or a different ligand, the ligands which may be chemically similar or different. In our cases it was the replacement of two nicotinamides from the four present in H4 and two in H6, which also contained two isonicotinamides. According to Carrel and co-worker a coordination position is considered free if it is occupied by a water molecule, which is a weak ligand that can be easily replaced (J. Carrell et al., 2002). So, the substituted ligand may be considered as a weak ligand or at least it is weaker than the ligand which replaces it.

As both nicotinamide and isonicotinamide are derivatives of pyridine, which is a strong ligand, they may be considered as strong ligands. Therefore, their pKa values were used to see which one is weaker and easy to replace. The higher the pKa value the stronger the bond strength between the ligand and the metal ion with all pKa values are listed in Table 5.5. As nicotinamide had a lower pKa value than the isonicotinamide and the guest methanol and dimethyl sulfoxide, the nicotinamide was acting as a weak ligand in comparison to its isomer isonicotinamide and the guests.

Table 5.5 pKa and dipole moment values of all ligands

pKa and dipole moment values				
Ligand	Nicotinamide	Isonicotinamide	Methanol	DMSO
pKa	3.30	3.61	15.5	35.1
Dipole moment (Daltons)	2.19*	2.19*	1.70	3.96

* Dipole moment of pyridine

*In this discussion, the dipole moment of pyridine [2.19D, (Ralph D. N., et al., 1967)] was used as reference as the nicotinamide and isonicotinamide are derivatives of the pyridine.

The substitution reaction affected the bond strength between the metal and the ligands in the complexes leading to a stronger bond via a new ligand. In solution the metal complexes were subject to chemical factors which affect the stability of the complex such as the presence of guest or solvent having high affinity toward the metal ion than some of its ligands. According to Kettle, a stable metal complex exists under favourable conditions without undergoing decomposition and has a considerable shelf life period (Kettle & Kettle, 1996). Once the metal complex is in solution, there are many factors that can influence the stability such as the nature of the guest or solvent, nature of the ligand, resonance effect, bonding between metal ions and ligands and hindrance effect, as well as others (Muthaiah et al., 2020). So, the metal complex will become unstable in a new mixture due to the presence of guest and/or solvent with high affinity toward the metal ion. To give a completely stable structure after the evaporation process, the ligands must be substituted and in our case two trans ligands were removed. All the guest, solvent and ligands are shown in Figure 5.12.
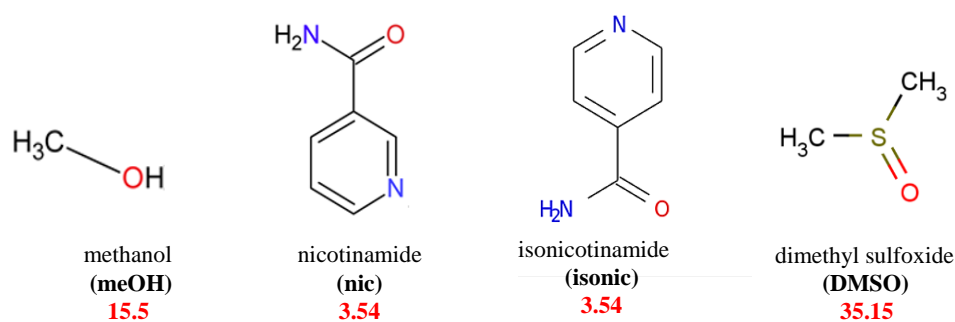

Figure 5.12 Ligand, guest and solvent structures with their pKa values.

The bond strength between the metal ion and a ligand depends, in addition to the electronic characteristics of the cation itself such as size, ion potential and polarizability, on the permanent dipole moment and polarizability of the neutral ligand (Tsintsadze et al., 1986). This mean that the affinity depends on the polarity, the bond strength and/or the dipole moment of the neutral ligand or guest in the mixture affecting its attraction toward the metal cation. The substitution occurs because the guest or solvent has a higher dipole moment [for example DMSO: 3.96 D and methanol: 1.70 D, (Ralph D. N., et al, 1967)] or the guest is more polar than the ligand substituted.

The dipole moment gives extremely valuable information on the geometry of the compound, spatial arrangement of ligands and nature of the chemical bond produced on complex formation (Osipov et al., 1967). The larger dipole moment, the greater the polarity and the greater the bond strength. The solvent DMSO (3.96 D) has a greater dipole moment than nicotinamide (2.19 D), therefore it is more polar and the bond strength Co-O is stronger than Co-N for nicotinamide. So, the metal ion has a better stability and affinity toward the DMSO as a ligand than nicotinamide.

Methanol (1.70D) has a lower dipole moment than nicotinamide but greater polarity and bond strength, so the metal complex has better stability bonded to methanol than nicotinamide.

Table 5.6 Electronegativity values of bonding atoms

Electronegativity values				
Hydrogen	Carbon	Sulphur	Nitrogen	Oxygen
2.2	2.55	2.58	3.04	3.44

References

Han, Y., Li, J.R., Xie, Y. & Guo, G. 2014. Substitution reactions in metal-organic frameworks and metal-organic polyhedra. *Chemical Society Reviews*, 43(16): 5952–5981.

Carrell, J.C., Carrell, H.L., Erlebacher, J. & Glusker, J.P. 2002. Structural aspects of metal ion carboxylate interactions. *Journal of the American Chemical Society*, 110(26): 8651–8656.

Jeong, S., Kim, D., Song, X., Choi, M., Park, N. & Soo Lah, M. 2013. Postsynthetic Exchanges of the Pillaring Ligand in Three-Dimensional Metal–Organic Frameworks. *Chemistry of Materials*, 25(7): 1047–1054.

Kettle, S.F.A. & Kettle, S.F.A. 1996. Typical ligands, typical complexes. In *Physical Inorganic Chemistry*. Springer Berlin Heidelberg: 7–23.

Kim, M., F. Cahill, J., Fei, H., A. Prather, K. & M. Cohen, S. 2012. Postsynthetic Ligand and Cation Exchange in Robust Metal–Organic Frameworks. *Journal of the American Chemical Society*, 134(43): 18082–18088.

Langford, Cooper H., Gray, H.B. 1966. Ligand substitution processes. *Journal of the Franklin Institute*, 282(4): 262–263.

Lin, H.Y., Luan, J., Wang, X.L., Zhang, J.W., Liu, G.C. & Tian, A.X. 2014. Construction and properties of cobalt(ii)/copper(ii) coordination polymers based on N-donor ligands and polycarboxylates mixed ligands. *RSC Advances*, 4(107): 62430–62445.

Manos, M.J., Kyprianidou, E.J., Papaefstathiou, G.S. & Tasiopoulos, A.J. 2012. Insertion of functional groups into a Nd 3+ metal-organic framework via single-crystal-to-single-crystal coordinating solvent exchange. *Inorganic Chemistry*, 51(11): 6308–6314.

Muthaiah, S., Bhatia, A. & Kannan, M. 2020. Stability of Metal Complexes. In *Stability of Coordination Compounds*. IntechOpen.

Osipov, O.A., Garnovskii, A.D. & Minkin, V.I. 1967. Dipole moments and the structure of coordination compounds, *Journal of structural Chemistry,* 8: 817-828.

Ralph D. N., Ranaa R. L., Arthur. A.M. 1967. Selected Values of Electric Dipole Moments for Molecules in the Gas Phase. *U.S. Departement of commerce National Bureau of Standard*.

Schaeffer, W.D., Dorsey, W.S., Skinner, D.A. & Christian, C.G. 1957. Separation of Xylenes, Cymenes, Methylnaphthalenes and Other Isomers by Clathration with Inorganic Complexes. *Journal of the American Chemical Society*, 79(22): 5870–5876.

Son, F.A., Atilgan, A., Idrees, K.B., Islamoglu, T. & Farha, O.K. 2020. Solvent-assisted linker exchange enabled preparation of cerium-based metal-organic frameworks constructed from redox active linkers. *Inorganic Chemistry Frontiers*, 7(4): 984–990.

Tsintsadze, G. V, Kiguradze, R.A., Shnulin, A.N., Mamedov, K.S., Tsion, E.A. & Gverdtsiteli, M. V. 1986. Structure of diaquacupric bis(formato)bis(nicotinamide) dihydrate, [Cu(H20)2(CsH4NC(O)NH2)2(HCO2)2].2H20. *Journal of structural chemistry*.

Yin, Z., Zhou, Y.L., Zeng, M.H. & Kurmoo, M. 2015. The concept of mixed organic ligands in metal-organic frameworks: Design, tuning and functions. *Dalton Transactions*, 44(12): 5258–5275.

Zhao, X.L. & Sun, W.Y. 2014. The organic ligands with mixed N-/O-donors used in construction of functional metal-organic frameworks. *CrystEngComm*, 16(16): 3247–3258.

CHAPTER VI

SEPARATION OF ISOMERS BY ENCLATHRATION

6.1 Introduction

Should structural isomers have similar physical properties, the separation of a mixture of these isomers into their individual components using traditional methods is often not feasible. para-Xylene, an important commodity of the petrochemical industry, is one of the three xylene isomers, ortho (**ox**), meta (**mx**) and para (**px**) xylenes. They have respective boiling points of 144.4 °C, 139.1 °C and 138.4 °C, hence distillation is an ineffective undertaking for differentiation, especially in terms of the latter two aromatics. para-Xylene is one of the most valuable products obtained from crude oil and is used as raw material for the production of polyethylene terephthalate (PET), fibres, and polyester films (Silva et al., 2012). Inclusion within a host material has been broadly studied and significant success has been achieved. Metal-organic hosts (Zaworotko, 2001 and Braga, 2000) demonstrate the ability for selective inclusion and prediction of crystal structures and their properties. If one of the guest isomers is preferentially selected from a mixture of the isomers, the crystalline material can be filtered and retrieved from the solution. This procedure will promote the extraction of the isomer and allow for the recycling of the host material. Alterations in the 'tunability' of Werner hosts arise on transformation of the nature and size of the inclusion cavities formed by the packing in square-planar or octahedral geometries (Aakeröy et al., 1999). The Werner compounds under study, and specifically complexes with cobalt as the central transition metal, demonstrate 'sticky' or attractive (such as hydrogen bonding) functionality, and rely on different architectures of the host suitable for the set of guest isomers (Pivovar et al., 2001a). Two new three-dimensional porous structures of cadmium and cobalt demonstrated selective gas adsorption of CO_2 rather than N_2 and H_2 (Shi et al., 2014).

The main objective of this chapter is to demonstrate that cobalt thiocyanate Werner complexes with nicotinamide and/or isonicotinamide ligands may be used to differentiate between molecules of substantially identical physical properties via host-guest chemistry as a tool of separation, where the method relied on the recognition by inclusion cavities of the host.

This chapter shows the selectivity ability of the Werner complex H6, $Co(NSC)_2(nicotinamide)_2(isonicotinamide)_2$, toward the three xylene isomers with similar boiling points, ortho-, meta- and para-xylene (ox, mx and px: Figure 6.1).
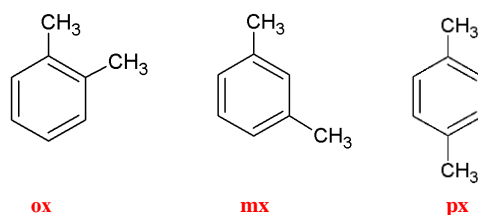
Figure 6.1 Skeletal structures of the xylene isomers.

The world demand for xylene is fast increasing, therefore their separation is a fundamental requirement. Some compounds are difficult to separate with conventional methods, such as distillation, when they have similar boiling points and molecular structures. The physical properties of xylene compounds differ slightly from isomer to isomer, with similar boiling points and densities but different melting points, as shown with orange highlights in Table 6.1. The separation of isomer mixtures into their individual components involves exploiting the differences specific to physical properties. ortho-Xylene is more readily separated from meta- and para-xylene because of a 5 °C difference in boiling points. Should a method involving melting point be used, the difference between the melting points of para-xylene (13.263 °C) from the other two isomers, makes it more easily separable from the other isomers with values of -25.182 (ox) and -47.872 °C (mx). These differences are large enough should a suitable method be found (Daramola, 2013).

Table 6.1 *Some useful physical properties of xylene compounds, (adapted from* Daramola, 2013).

Property	o-xylene	m-xylene	p-xylene
Molecular formula	C_8H_{10}	C_8H_{10}	C_8H_{10}
Molecular weight	*106.167*	*106.167*	*106.167*
Colour	*Colourless*	*Colourless*	*Colourless*
Physical state	*Liquid*	*Liquid*	*Liquid*
Density (g/cm^3)	*0.8802*	*0.8642*	*0.8610*
Boiling point (°C)	*144.41*	*139.12*	*138.37*
melting point (°C)	*-25.182*	*-47.872*	*13.263*
Refractive index @ 25°C	*1.5054*	*1.4971*	*1.4958*

Previously, the use of Werner complexes has demonstrated enhancement of the selectivity of the host towards one guest from a mixture of physically similar guests, such as structural isomers. The process of enclathration with a suitable host complex is one of the usual methods. This type of separation of xylenes has been reported by Nath, who discusses the separation of xylene isomers through selective inclusion using coordination polymers of Cu(II) bis (pyridylcarboxamide) (Nath & Biradha, 2016). The selective enclathration of methyl-and dimethylpiperidines by fluorenol hosts has been shown by Sykes et al., (Sykes et al., 2017) and the enhanced selectivity towards xylene isomers of a mixed ligand Ni(II) thiocyanato complex was recently discussed by Wicht and co-workers (Wicht et al., 2016). The separation protocols were based upon selective inclusion and require that the host exhibits some preference for inclusion of one particular guest over another (Pivovar et al., 2001b). This separation technique was attempted with H4 and H5 but only H6 presented positive results. Unfortunately, H4 and H5 did not enclathrate any isomers through the crystallisation of xylene isomer mixtures.

6.2 Structural analysis of H9•ox

Experiments to determine the selectivity profile of a host were carried out using the method of dissolving the host in liquid mixtures of the guests with known proportions. Crystals of inclusion compounds formed were harvested, dried and lightly crushed for analysis. These competition experiments between pairs of xylene isomers (ox/px, ox/mx and mx/px) were performed at molar ratios of 50:50 in solvent dimethylsulphoxide (DMSO). Due to extremely low solubility of the hosts in the xylene guests, solubility was increased using DMSO as solvent. The outcome of the experiment was successful in the case of $Co(NCS)_2(nicotinamide)_2(isonicotinamide)_2$, H6, although replacement of the nicotinamide ligands with DMSO occurred.

The selectivity of H6 for one of the xylene isomers showed a preference towards ortho-xylene from a 50:50 mixture of om-xylene, but no enclathration occurred for a mixture of mp-xylene, op-xylene (50:50) and omp-xylene (33:33:33). As single crystal X-ray diffraction was the only method of selectivity determination in our case, refinement of the crystal structure did not show methyl electron density in any other position of the xylene isomer.

The crystallisation of H6 with a mixture of om-xylene guest was done by first combining a 50:50 mixture of ortho- and meta-xylenes in a vial. 60 mg of H6 was dissolved in a few drops of DMSO prior to the addition of the mixture of om-xylene. The mixture was heated to 45 °C for 30 min with constant stirring then cooled and sealed with pierced para-film. After slow evaporation at room temperature for a few days, pink crystals appeared at the bottom of the vial. The analysis of the crystals was done using thermal gravimetry (TGA), powder X-ray diffraction (PXRD) and single crystal X-ray diffraction (SCXRD). The same procedure was followed with op-xylene, mp-xylene and omp-xylene mixtures, all equivalent mixtures of the isomers, in all cases, the crystallisation were successful but no enclathration resulted.

As presented in Chapter 5, on crystallisation the two ligands nicotinamide were replaced by the two DMSO ligands, forming Co-O bonds trans to each other in the new host which enclathrated ortho-xylene as guest. Although this host is the same as H7, as reported in Chapter 5, we have named it H9•ox because the starting material was not host H7. The Werner clathrate obtained after crystallisation was $Co(NCS)_2(isonic)_2(dmso)_2$•ox, (H9•ox), where H9 is the new host with mixed ligands, two isonicotinamides and two dimethylsulfoxides.

6.2.1   Thermogravimetric analysis

The TG trace of H9•ox is presented in Figure 6.2, showing three distinct decomposition steps which confirmed the crystal structure stoichiometry. Step 1 indicates the loss of the guest, ox, with a loss of

26.4 %, followed by Step 2 representing the decomposition of the host by a loss of one DMSO ligand with a mass loss of 17.3 %. Step 3 corresponds to the decomposition of one isonic ligand with a mass loss of 27 %. The observed and calculated TG results are summarised in Table 6.2. As isonicotinamide is a sticky ligand, the full mass loss is slightly lower than the calculated values and a TGA to a higher temperature may have allowed all the ligands to be fully released.
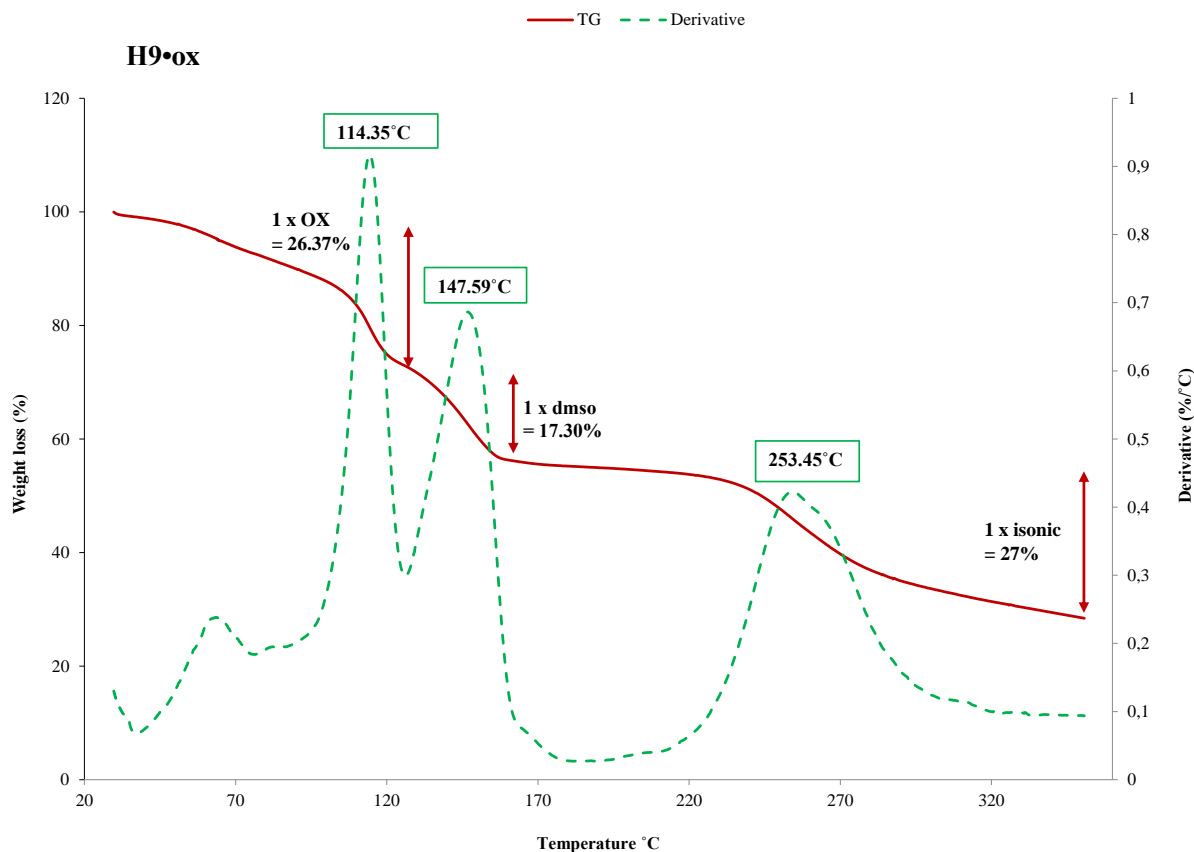

Figure 6.2 *TGA curve of H9•ox plotted as mass loss percentage (red curve) and the derivative weight (green curve) vs temperature (˚C), purge gas: N₂ (40mol/min) heating rate: 20˚C/min.*

Table 6.2 *Thermal analysis results for H9•ox.*

Compound / Mass loss	H9•ox		
	Experimental data %	Calculated data %	Co $_{0.5}$(NCS)(isonic)(dmso)•ox
Step 1	26.37	26.97	Co$_{0.5}$(NCS)(isonic)(dmso)
Step 2	17.30	19.80	Co$_{0.5}$(NCS)(isonic)
Step 3	27.00	31.00	Co$_{0.5}$(NCS)

6.2.2 Single crystal analysis of H9•ox

A pink H9•ox crystal with a dimension of 0.15 x 0.19 x 0.19 mm^3 was selected for single crystal X-ray diffraction analysis using a Bruker APEX II DUO diffractometer. The structure was solved in a triclinic space group P$\bar{1}$ (No.2) and refined to R$_1$= 0.0688 and wR$_2$= 0.0486. The asymmetric unit contains one half host and one guest with the molecular formula of C$_{17}$H$_{22}$N$_3$O$_2$S$_2$Co$_{0.5}$ (Fig. 6.3a) with a $\frac{1}{2}$: 1 host:guest ratio. As explained previously, two of the ligands of H6 (H9 was obtained by the crystallisation of H6 and ox) particularly nicotinamide ligands were replaced by the solvent DMSO during crystallisation. The presence of the new ligands did not affect the distance of Co-N (average distance is 2.138 Å, H6 Chapter 4). However, the angle N-Co-N was altered from 178.5° (H6 Chapter 4) to 90°. The average distance and angle of the DMSO ligands were determined to be 2.122 Å and 90° for Co-O and O-Co-O respectively. The structure of H9 host comprises one Co (II) cation, two thiocyanate anions and four coordinating ligands two isonicotinamides (isonic) and two dimethyl sulfoxides (DMSO) forming an octahedral complex. The crystal data are listed in Table 6.3.
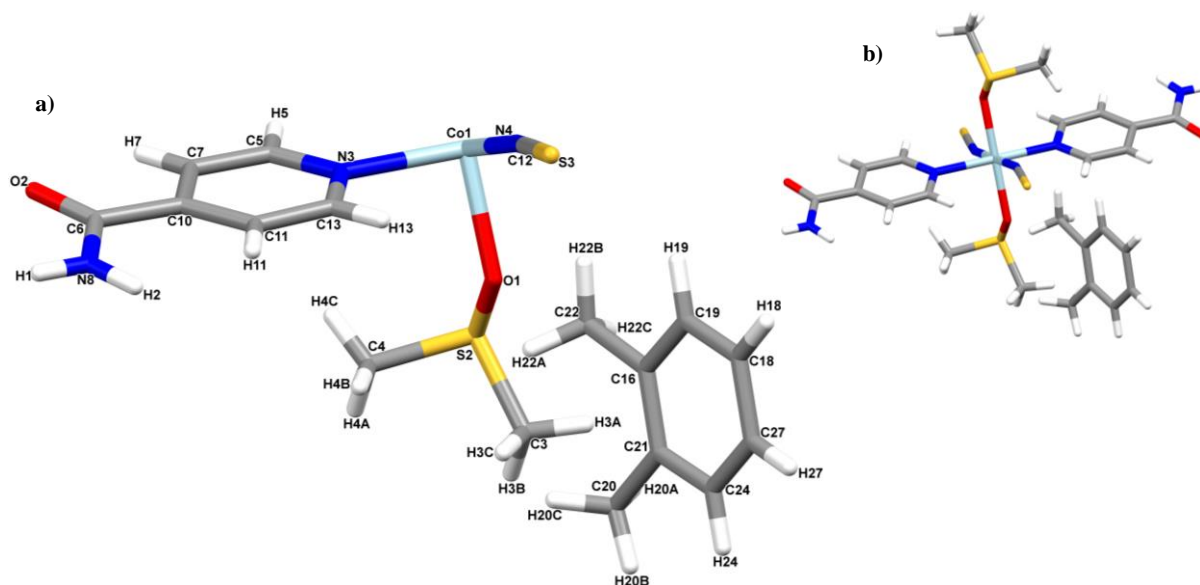
Figure 6.3 *a) Numbering scheme of the asymmetric unit of H9•ox, b) schematic representation of the full host and guest.*

Table 6.3 Crystal data of H9•ox.

	H9•ox
Chemical formula	$Co_{0.5}(NCS)(C_6H_6N_2O)(C_2H_6OS)•(C_8H_{10})$
H:G ratio	½:1
Formula Weight	393.96
Temperature/K	173(2)
Crystal system	Triclinic
Space Group (no.)	P$\bar{1}$ (No 2)
a/Å	8.0066(10)
b/Å	10.5155(14)
c/Å	12.1839(16)
α/°	81.505(3)
β/°	73.186(3)
γ/°	88.227(3)
V/A^3	971.1(2)
Z	1
D$_{calc}$/g.cm^{-3}	1.347
Radiation type	MoKα
F(000)	413
Crystal size/mm^3	0.15x0.19x0.19
Colour, crystal form	Pink block
No. of total reflections	23218
No. of unique reflections	4857
Θ min-max/°	1.96/28.35
R [F^2>2σ(F^2)]	0.0486
wR2(F^2)	0.1105
S	1.083
No. of parameters/ data	235/485
Res.peak(max/min)/eA^{-3}	0.616/-0.472

The crystal structure presented two main interactions identified as C-H•••π interactions and intermolecular hydrogen bonds. The structure displays a lot of C-H•••π interactions (edge-to-face) between H9 and ox between the aromatic pyridine rings of the isonicotinamide and the xylene (Figure 6.4 a). The intermolecular hydrogen bonds were observed in the extended 2D structure of H9 between two isonicotinamides (N-H•••O) showing an amide dimer, and between one isonicotinamide and dimethyl sulfoxide (N-H•••O). The intermolecular hydrogen bond N-H•••O is described by the $R_2^2(8)$ graph set as an amide N8-H1···O2 (carbonyl) as illustrated in Figure 6.4b. The DMSO interaction is described by the $D_1^1(3)$ graph set and the hydrogen bonds is N8-H2•••O1 (sulfoxide) (Figure 6.4b). The hydrogen bonds are listed in Table 6.4.

Table 6.4 Hydrogen-bond geometry (Å, °) for H9•ox.

D-H	d(D-H) (Å)	d(H..A) (Å)	<DHA (°)	d(D..A) (Å)	Symmetry operator
H9•ox					
N8-H1•••O2	0.859	2.055	171.76	2.907	[-x-1, -y, -z+2]
N8-H2•••O1	0.911	2.278	166.02	3.170	[-x, -y, -z+1]
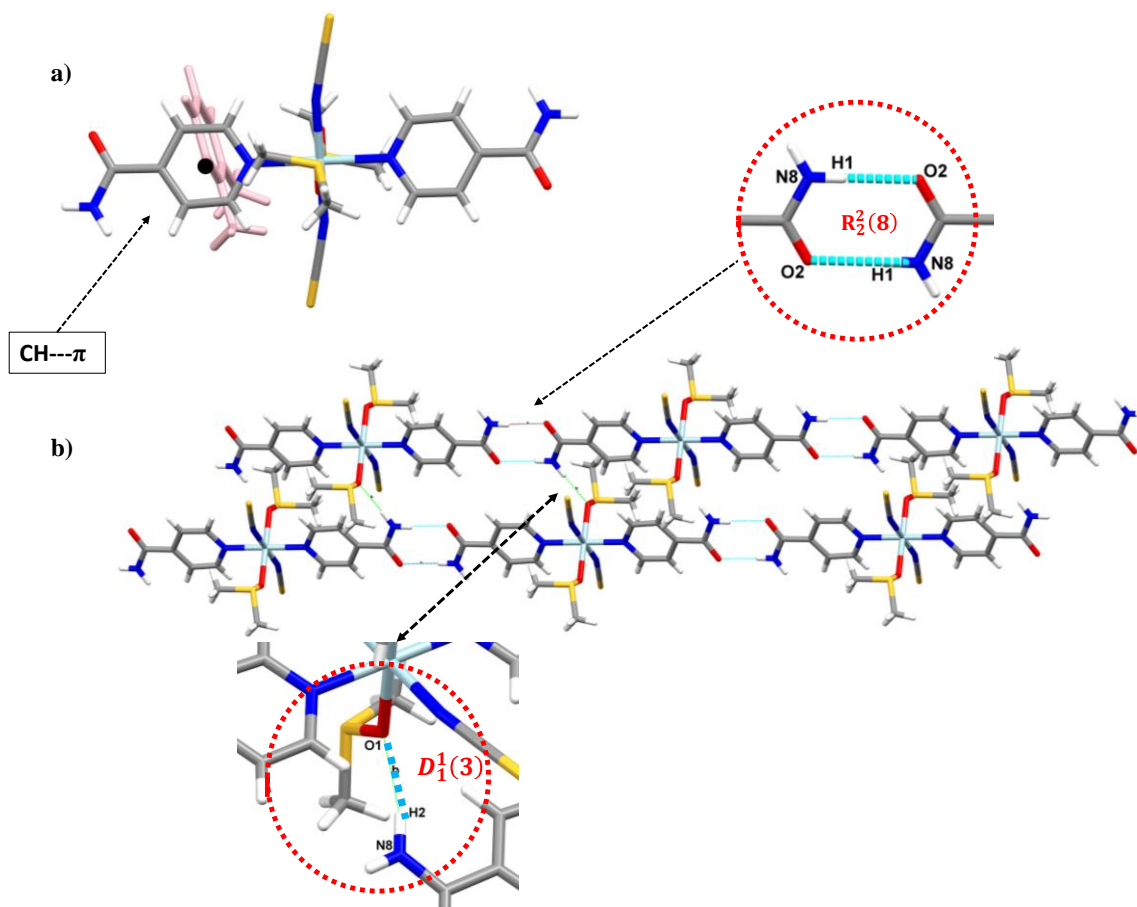
***Figure 6.4** Intermolecular interactions, a)* C-H•••π *interactions between ox (pink) and H9, b) extended 2D structure of host molecules showing hydrogen bond interactions and graph sets.*

The packing diagrams of the crystal in Figure 6.5a show how the xylene molecules (spacefill model) are aligned in beween the host vertically and horizontally, looking down the a-axis. In Figure 6.5b, both the amide dimers and the C-H•••π interactions can be seen. Furthermore, the void of the xylene forms channels when the packing is viewed along the a-axis with a volume of 373.14 $Å^3$ and percentage void of 38.4 % (Figure 6.5c).
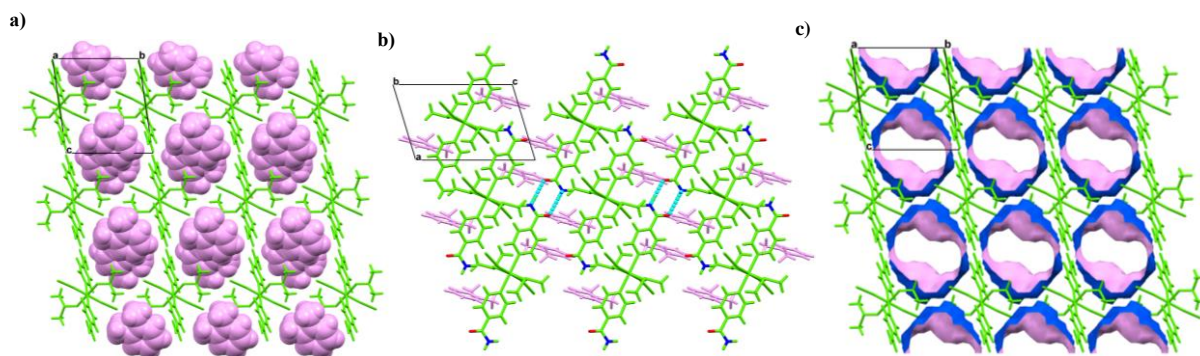
Figure 6.5 *Packing diagrams, a) view along the a-axis with ox presented in spacefill model, violet b) view along the b-axis showing the C-H•••π interactions between the host and guest and amide dimers in blue; c) channels along the a-axis showing the voids in location of ox guests.*

The selectivity preference of H6 between xylene isomers was toward the ortho-xylene in a mixture of ox/mx. After crystallisation from both mixtures, ortho-xylene was chosen above the other two isomers para- or meta-xylene. This outcome was confirmed by single X-ray crystal diffraction SXCRD. The mixture ox/px, mx/px and ox/mx/px were not successful in terms of differentiating one of the isomers, in fact during crystallisation no enclathration was observed.

6.3   Hirshfeld Surface and Fingerprint analysis

Intermolecular interactions between the ortho-xylene (ox) guest and the host framework were analysed using the program Crystal Explorer (Turner et al., 2017) which calculates the Hirshfeld surface of a target molecule in a crystal structure and depicts all its interactions with the neighbouring molecules. The property mapped onto the surface is the distance from the surface to the nearest external nucleus and is called d_e. The nature of intermolecular contacts in the crystal are described by this property. d_i is defined as the distance from the surface to the nearest nucleus inside the surface as shown in Fig. 6.6b and, when used in conjunction with d_e, the normalised contact value d_{norm} represents the sum of d_i and d_e.

Fig. 6.6a shows the ox guest surrounded by its Hirshfeld surface when enclosed by host molecules and the generated fingerprint plot, the 2D representation of the 3D surface. The red areas on the surface indicate close contacts which are shorter than the van der Waals contact, and it represents the C-H⋯O contacts between the ox and the host sulfoxide ligand. The distance of this contact shown by lobe ① on the fingerprint plot Fig. 6.6c is 2.35 Å and comprises ca. 5% of the interactions. The outer lobes,

labelled ②, represent C-H···π contacts between the ox hydrogens to the aromatic system of the host, and the reverse interaction between the hydrogens of the ligands and the aromatic region of the ox, and this accounts for 22% of the interactions. On the Hirshfeld surface in Fig 6.6a, these interactions are shown by the white colouration on the left surface of the ox molecule indicating that the distance is the same as the sum of the van der Waals radii. Interestingly, the observed hydrogen bonding (ox) C-H···S (host thiocyanate) with (d_i+d_e) of 4.1 Å has previously been identified by Đaković et al. in Ni(II) complexes (Đaković et al., 2011).
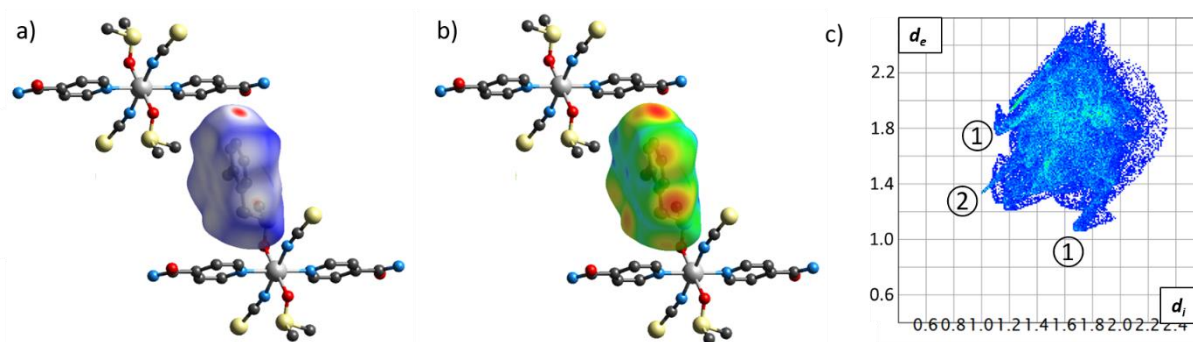
Figure 6.6 *Hirshfeld surfaces of H9•ox showing (a) the **d_{norm}** surface and (b) the **d_i** surface of the guest towards the host. The fingerprint plot (c) indicates close C-H···O contacts between **ox** and the host sulfoxide ligand ①, and between hydrogens and the aromatic system ②, both internally and externally*

As no clathrate was formed with the other xylene isomers no comparative Hirshfeld surfaces could be discussed. This Hirshfeld surface study, however, illustrates the contacts achieved between ortho-xylene and the host, H9.

References

Aakeröy, C.B., Beatty, A.M. & Leinen, D.S. 1999. A Versatile Route to Porous Solids: Organic-Inorganic Hybrid Materials Assembled through Hydrogen Bonds. *Angewandte Chemie (International ed. in English)*, 38(12): 1815–1819.

Braga, D. 2000. Inorganic crystal engineering: A personal perspective. *Journal of the Chemical Society, Dalton Transactions*, (21): 3705–3713.

Đaković, M., Vila-Viosa, D., Calhorda, M.J. & Popović, Z. 2011. Coordination-driven self-assembly of thiocyanate complexes of Co(ii), Ni(ii) and Cu(ii) with picolinamide: A structural and DFT study. *CrystEngComm*, 13(19): 5863–5871.

Daramola, M.O. 2013. *Xylenes : synthesis, characterization and physicochemical properties*. Nova Science Publishers, Inc.

Nath, K. & Biradha, K. 2016. Separation of Xylene Isomers through Selective Inclusion: 1D → 2D, 1D → 3D, and 2D → 3D Assembled Coordination Polymers via β-Sheets. *Crystal Growth and Design*, 16(10): 5606–5611.

Pivovar, A.M., Holman, K.T. & Ward, M.D. 2001a. Shape-selective separation of molecular isomers with tunable hydrogen-bonded host frameworks. *Chemistry of Materials*, 13(9): 3018–3031.

Pivovar, A.M., Holman, K.T. & Ward, M.D. 2001b. Shape-selective separation of molecular isomers with tunable hydrogen-bonded host frameworks. *Chemistry of Materials*, 13(9): 3018–3031.

Shi, J.T., Yue, K.F., Liu, B., Zhou, C.S., Liu, Y.L., Fang, Z.G. & Wang, Y.Y. 2014. Two porous metal-organic frameworks (MOFs) based on mixed ligands: Synthesis, structure and selective gas adsorption. *CrystEngComm*, 16(15): 3097–3102.

Silva, M.S.P., Mota, J.P.B. & Rodrigues, A.E. 2012. Fixed-bed adsorption of aromatic C 8 isomers: Breakthrough experiments, modeling and simulation. *Separation and Purification Technology*, 90: 246–256.

Sykes, N.M., Su, H., Weber, E., Bourne, S.A. & Nassimbeni, L.R. 2017. Selective Enclathration of Methyl- and Dimethylpiperidines by Fluorenol Hosts. *Cryst Growth & Design*, 17(2) 819-826.

Turner, M.J., McKinnon, J.J., Wolff, S.K., Grimwood, D.J., Spackman, P.R., Jayatilaka, D. and Spackman, M.A. 2017. CrystalExplorer17, University of Western Australia.

Wicht, M.M., Báthori, N.B. & Nassimbeni, L.R. 2016. Enhanced selectivity towards xylene isomers of a mixed ligand Ni(II) thiocyanato complex. *Polyhedron*, 119.

Zaworotko, M.J. 2001. Superstructural diversity in two dimensions: Crystal engineering of laminated solids. *Chemical Communications*, (1): 1–9.

CHAPTER VII

CONCLUSION

Two families, zinc (II) chloride and cobalt (II) thiocyanato, Werner complexes with nicotinamide and isonicotinamide have been successfully designed and used as a starting material or host for the synthesis and characterisation of new compounds to understand their properties, architecture of the structure and the mechanism of selectivity of Werner complexes toward a given isomer. The latter process was one of the main goals of this research and one of the difficult procedures in the chemical industry. During this study new assignments were added to the research focus with the formation of new families of mixed ligand complexes via the crystallisation process. The crystal complexes made were characterised using analytical techniques such as powder X-ray diffraction (PXRD), differential scanning calorimetry (DSC), thermogravimetry (TGA) and infrared spectroscopy (IR). The structure elucidation and refinement were done using single crystal X-ray diffractometry. The two families were subject to the same crystallisation process with solvent used as guest.

The crystallisation of the cobalt and zinc host complexes with guest presented eight and three new complexes respectively. Although the two host complexes are different in geometry (tetrahedral and octahedral) and composition [$Zn(Cl)_2$ and $Co(NSC)_2$] no similarity was observed; they reacted totally differently. In comparison to the cobalt host and their crystal complexes, the zinc complex study presented few crystal complexes, long slow evaporation (two to three weeks) for the formation of a crystal with very tiny colourless crystals in needle shape. However, the experimental results of the cobalt complexes were successful. All the TG, PXRD and DSC graphical analyses were clear and close to the expected results compared to the cobalt structures. In the three crystalline products, careful elucidation of the interactivity between the functional groups in the form of hydrogen bonding and $\pi\cdots\pi$ interactions was taken.
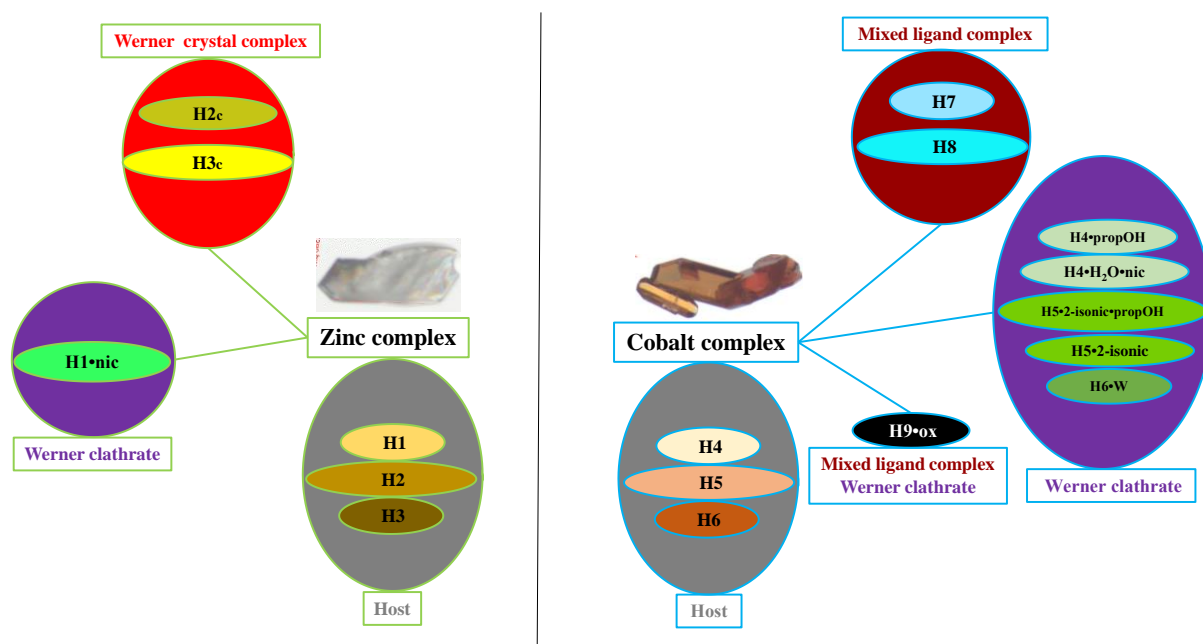

Figure 7.1 Schematic comparison of cobalt and zinc crystal structures

On the other hand, cobalt host complexes achieved better expectations from the primary objectives of this work than zinc host complexes, i.e. the enclathration of a guest to form a Werner clathrate, analysis and characterisation of new complexes and selectivity toward a xylene isomer were all achieved and presented in Chapter 4 and 6. Furthermore, the formation of mixed ligand complexes by crystallisation and by substitution of two nicotinamide ligands were well presented in Chapter 5.

The crystallisation of the six hosts with different guests gave rise to four types of complexes, all summarised in Table 7.1, Werner crystal complex (wcc), Werner clathrate complex (wc), mixed ligand complex (mlc) and mixed ligand Werner clathrate (mlwc).

In the Werner crystal complex (wcc), the crystal structure was obtained after the host-guest crystallisation process. This was identical to their host starting material of general formula and structure (MX_2L_n) from which it was made. These are $H2_c$ and $H3_c$. This type of crystal was only observed in zinc complexes with H2 and H3 host. The packing was sustained by N-H•••Cl and N-H•••O interactions. Chloride forms the acceptor in a number of hydrogen bonding interactions. The importance of halide interactions is demonstrated in these molecular structures and the importance of the formation of frameworks to stabilise the structure is an important quality of the crystal structures.

Table 7.1 Crystal complex characteristics summary

Num	Complex	Host	Guest	Complex ratio	Space group	Family
Zinc						
1	**H1•nic**	**H1**	nic	1 : 1	Pccn	wc
2	**H2$_c$**	**H2**	-	1	Pccn	wcc
3	**H3$_c$**	**H3**	-	1	P2(1)/C	wcc
Cobalt						
4	**H4•propOH**	**H4**	propOH	1 : 1	P$\bar{1}$	wc
5	**H4•nic•H$_2$O**	**H4**	water - nic	1 : 1 : 1	P$\bar{1}$	wc
6	**H8**	**H4**	-	1	P$\bar{1}$	mlc
7	**H5•2-isonic**	**H5**	isonic	1 : 2	P$\bar{1}$	wc
8	**H5•2-isonic•propOH**	**H5**	propOH - isonic	1 : 2 : 1	P$\bar{1}$	wc
9	**H6•H$_2$O**	**H6**	water	1	P21/n	wc
10	**H7**	**H6**	-	2	P$\bar{1}$	mlc
11	**H9•ox**	**H6**	ox	1 : 1	P-1	mlwc

wc = Werner clathrate; wcc = Werner crystal complex; mlc = mixed ligand complex; mlwc = mixed ligand Werner clathrate

In the Werner clathrate (wc) crystal structures, the guest is enclathrated in their metal host cavities to form the following inclusion compounds H1•nic, H4•propOH (1), H4•nic•H$_2$O (2), H5•2isonic (3), H5•2isonic•propOH (4) and H6•H$_2$O (5). In overall, six inclusion compounds were obtained with either a new guest or a self-inclusion of the ligand nicotinamide / isonicotinamide as guest were observed, one crystal structure with zinc complex (H1) and five with cobalt complexes (H4, H5 and H6). The zinc family did not enclathrate a new guest but preferred to self-include the ligand nicotinamide with Host

1. The two structures guest and host were sustained by face-to-face π···π interactions and the void analysis once the nicotinamide guest was removed from the structure resulted in large channels with a volume of 1098.40 $Å^3$. All cobalt crystal complexes were stabilised by O-H···N, N-H···O and O-H···S, linking either between guest-guest, host-host or host-guest. The behaviour of H4 and H5 toward the presence of the guest was analysed by giving the torsion flexibility and behaviour conformation of the host. This was achieved by overlaying the two same hosts from the complexes, each with a different guest. Thus, the presence of the intramolecular interactions in one of the H4 crystal structure affected the conformation by twisting two thiocyanato molecules which shows their flexibility. H5 crystal structures kept their propeller conformation to a perfect overlay of the host of the two structures. The packing arrangement in the two H5 crystal structures are almost identical, although not isostructural. In both, H5 presented a small and a large channel for the position of two guests. The same observation occurred in H4, where the same column arrangement was presented in H4•propOH (1) and H4•nic•H_2O (2) complexes with voids between the columns. The presence of a mixed ligand nicotinamide and isonicotinamide in H6 demonstrated high ring formation of hydrogen interactions. In both complexes where water was included H4•nic•H_2O (2) and H6•H_2O (5), water acts as a bridge between the guest and the host in (2) and in (5) linking three hosts or a mixture of host and guest in the same interactions O-H···N, O-H···O and O-H···S. The importance of chalcogen bonding was highlighted in a number of the H5 complexes illustrating the strength of a sulfur bond in the stabilisation of these complexes. The bond lengths of these interactions were compared with a selection of similar bonds published in the CSD.

Mixed ligand complex (mlc) crystal structures were presented in Chapter 5, whereby two ligands were substituted from the mother host and replaced by two guests to form a new structure with a chemical formula of $MX_2A_2B_2$ are named H7 and H8. As the overall packing structure of these complexes was too dense to allow enclathration to occur, the guest was substituted in a replacement of two nicotinamide ligands in H4 and H6 host complexes. In H8, two methanols replaced the nicotinamides and H7 had two DMSO molecules also replacing the nicotinamides. The crystal H7 displayed strong intermolecular interactions of N-H···S forming a dimer of $R_2^2(8)$ and N-H···O forming $C_2^2(22)$ described as a chain. H7 also presented weak interactions of C-H···O linking the two ASU's of H7. The crystal H8 displayed strong interactions O-H···O, N-H···S and N-H···O. The packing is stabilised by π···π interactions between the six membered rings of the nicotinamides. The formation of mixed ligand complexes required an understanding of the strength of interaction between the ligand and the metal ion. The investigation of pKa and dipole moment values for these components enabled clarification on this process.

A mixed ligand Werner clathrate (mlwc) crystal with both characteristics of a mixed ligand and Werner clathrate included in the same structure was H9•ox. In this study, only H6 produced selectivity activity compared to all the other hosts, either zinc or cobalt centred. This host's selectivity showed a preference

towards ortho-xylene from a 50:50 mixture of om-xylene. The single crystal structures and detailed thermal behaviour as well as a discussion on the Hirshfeld surfaces for this confirmation were discussed.

This thesis has provided detail in the comparison of zinc and cobalt complexes and has given an understanding of the mixed ligand complexes and their properties. The halide and chalcogen interactions have verified the strength and stabilising effect these have on the complexes with chloride or thiocyanate as ligands.

As a recommendation, further comparative studies between different transition metals and a range of ligands will provide knowledge on the geometry and architecture of these metal complexes, specifically Werner complexes. Whilst this thesis dealt only with ligands containing amide functional groups which resulted in a combination of hydrogen bonding, other pyridine derivative ligands which rely on $\pi \bullet \bullet \pi$ interactions would be an interesting exercise to continue with this research.

APPENDIX

TG AND DSC THERMOGRAMS

ZINC COMPLEXES TG AND DSC GRAPHS

CHAPTER 3

Host 1
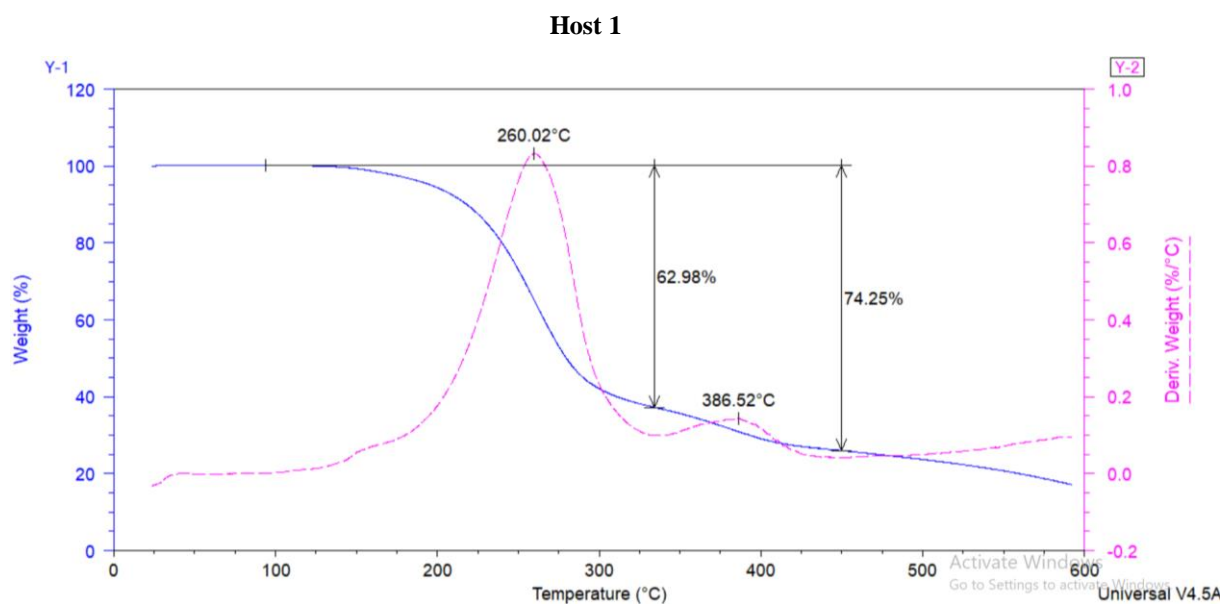
Figure 2.2 *TGA and DTG curves for the mass loss and derivative vs temperature of H1 host.*

Host 1
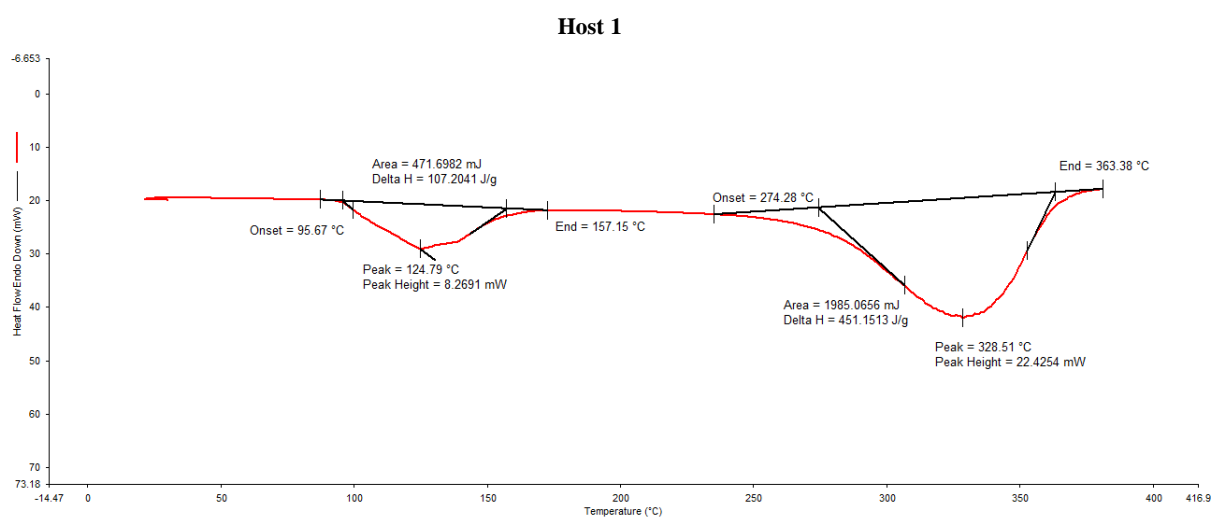
Figure 3.2 *DSC curves of H1 host.*
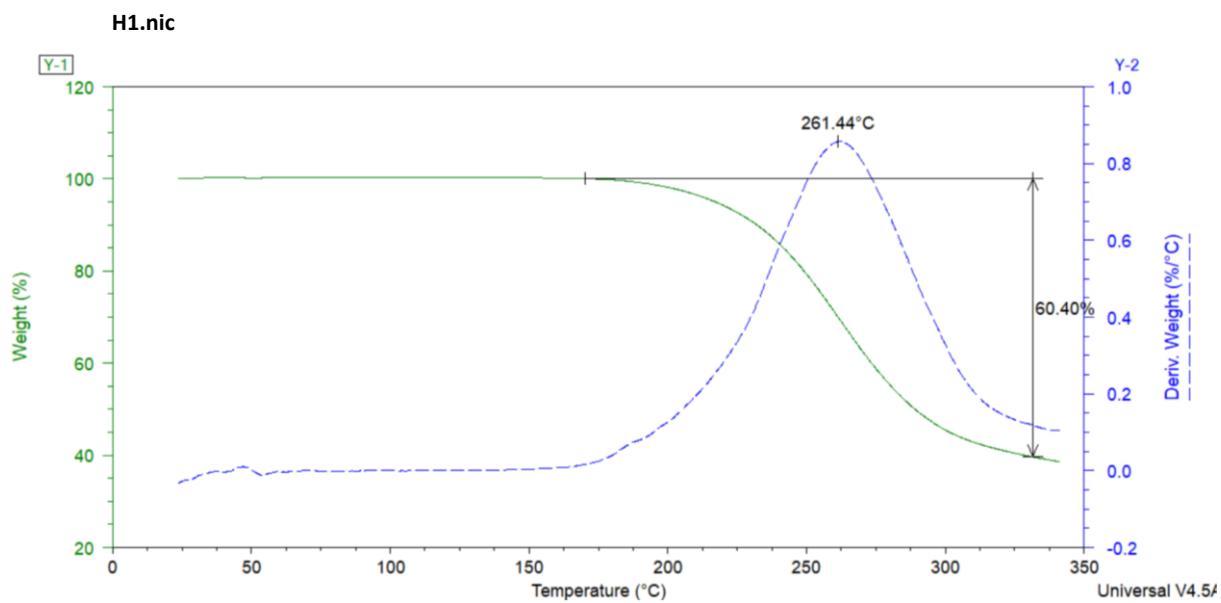
H1.nic

Figure 3.3 *TGA and DTG curves for the mass loss and derivative vs temperature of H1•nic crystal.*
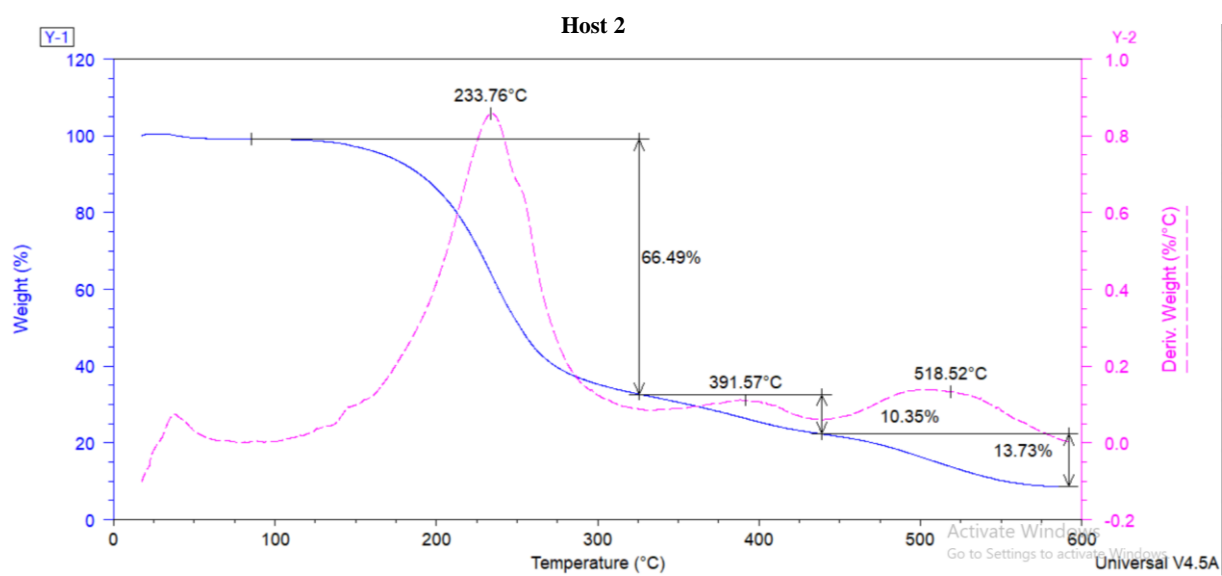
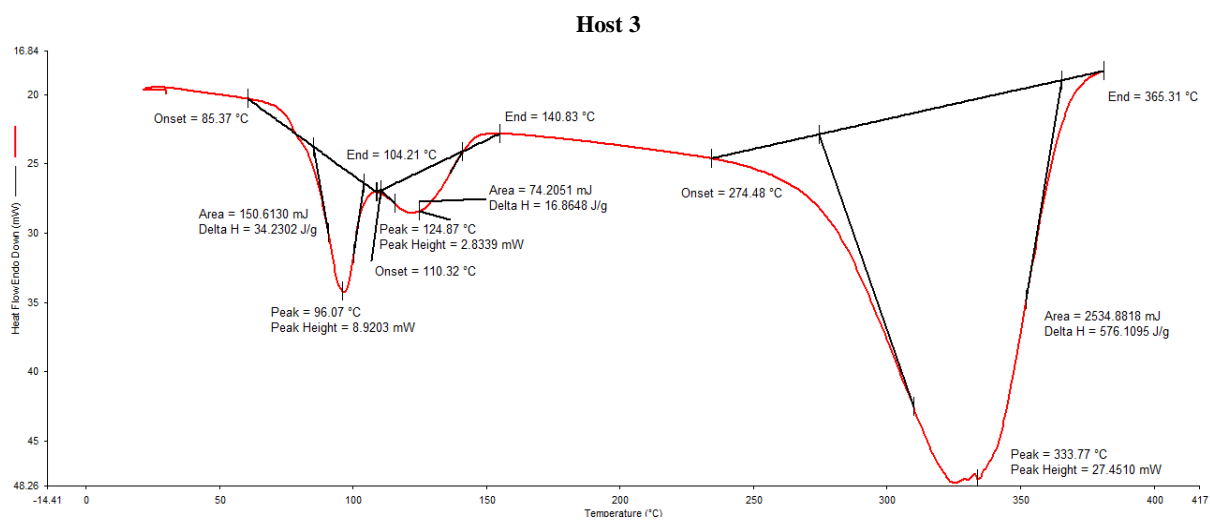***Figure 2.2*** *TGA and DTG curves for the mass loss and derivative vs temperature of H2 host.*

Host 2
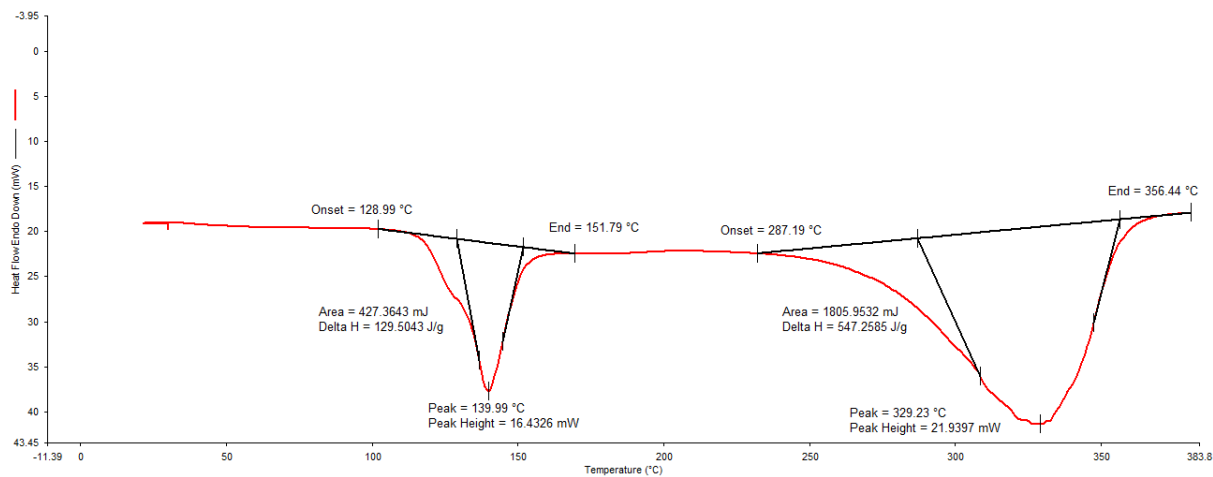
Figure 3.2 DSC curves for H2 host.

H2 crystal
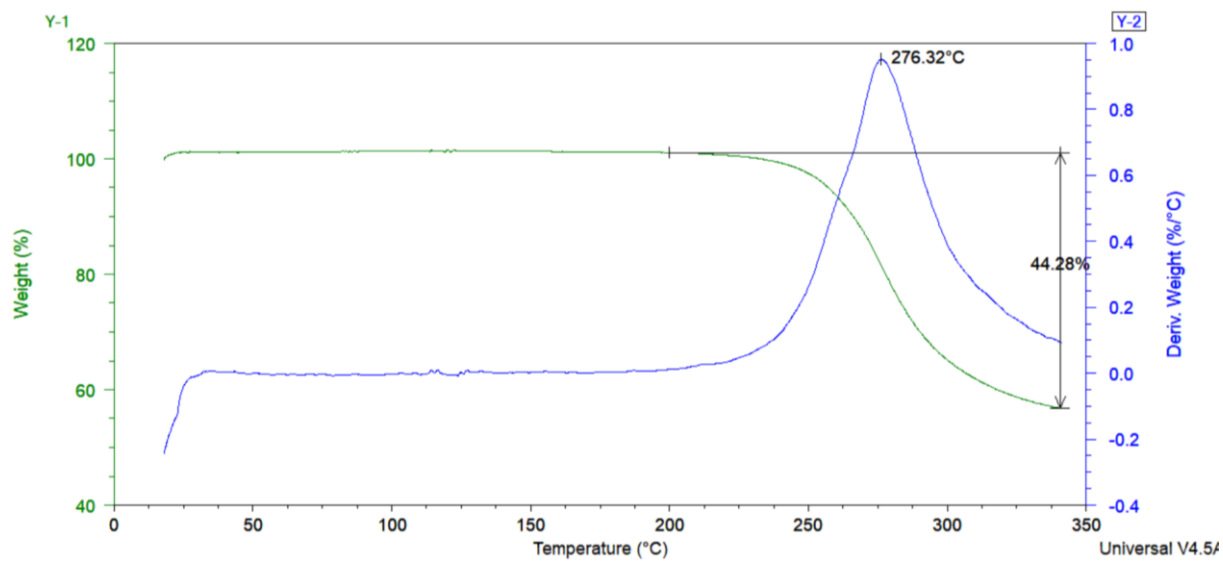
Figure 3.3 TGA and DTG curves for the mass loss and derivative vs temperature of H2 crystal and H2 host.
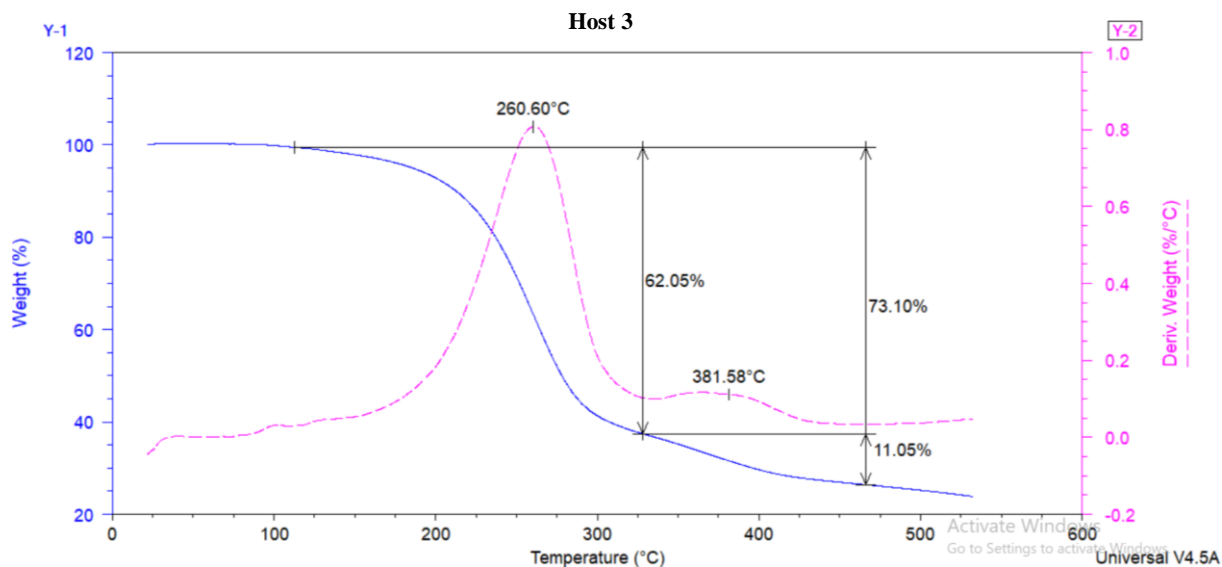
Figure 2.2 *TGA and DTG curves for the mass loss and derivative vs temperature of H3 host.*

Figure 3.2 *DSC curves temperature of H3 host.*
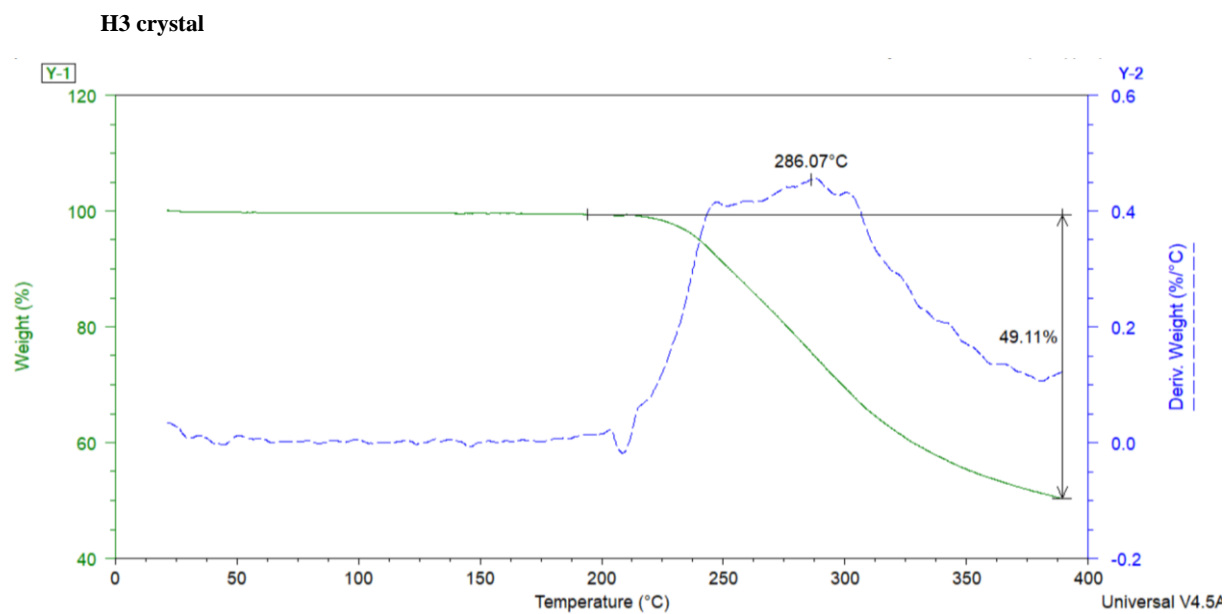
H3 crystal

Figure 3.3 *TGA and DTG curves for the mass loss and derivative vs temperature of the crystal and host of H3 crystal and H3 host.*

COBALT COMPLEXES TG AND DSC GRAPHS

CHAPTER 4
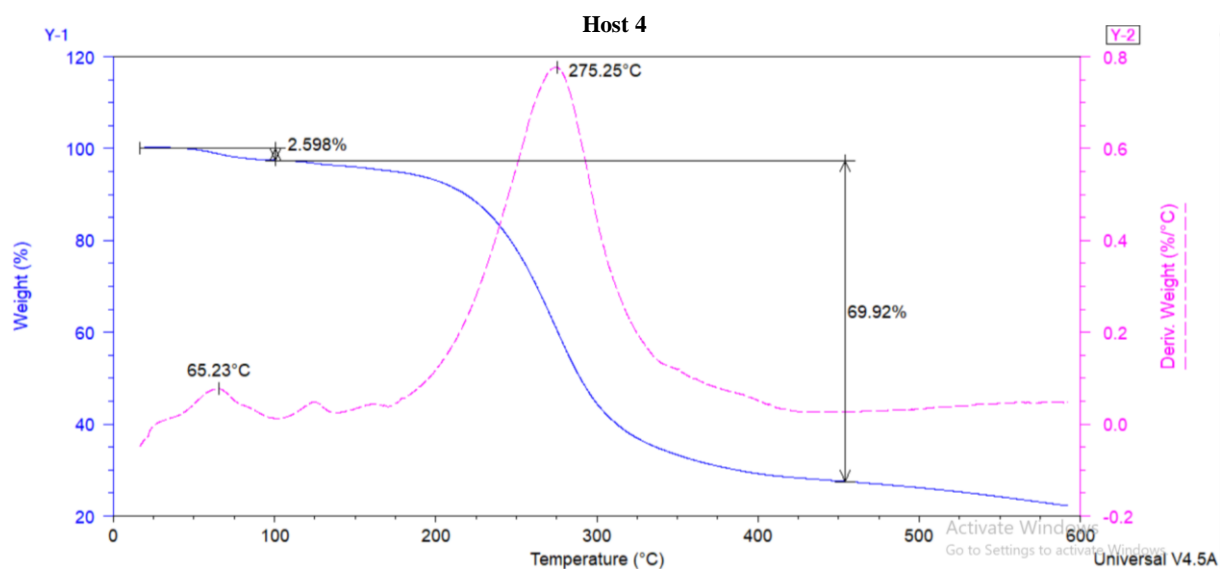
Figure 2.2 *TGA curves of **H4** plotted as mass-loss (%) and derivative weight vs temperature (˚C), purge gas: N₂ (40 mol/min) heating rate: 20˚C/min*
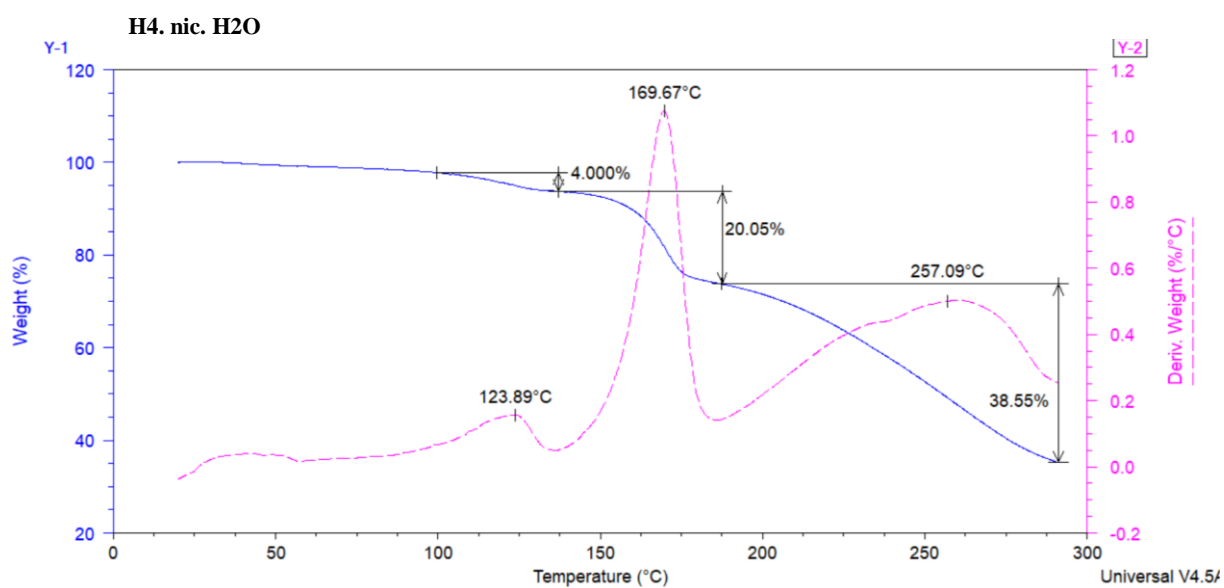
Figure 4.8 *TGA curves of **H4• Nic•H₂O** plotted as mass-loss (%) and derivative weight vs temperature (˚C), purge gas: N₂ (40 mol/min) heating rate: 20˚C/min*
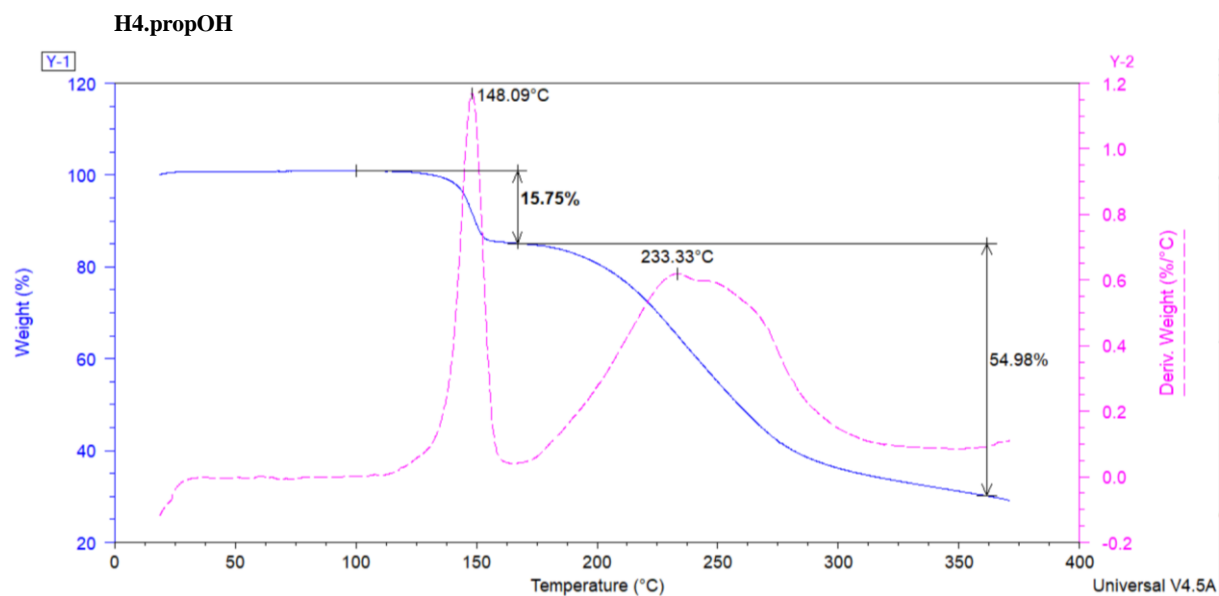
H4.propOH

Figure 4.8 TGA curves of **H4•1-propOH** plotted as mass-loss (%) and derivative weight vs temperature (˚C), purge gas: N₂ (40 mol/min) heating rate: 20˚C/min

Host 5

Figure 2.2 TG and derivative curves of H5.

138

H5.2isonic
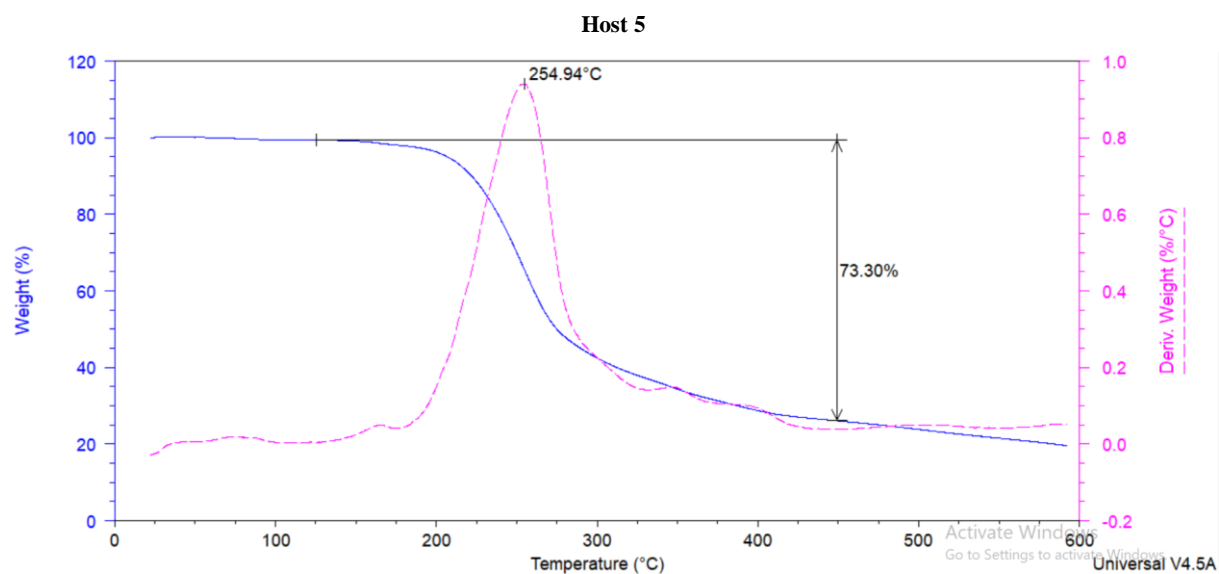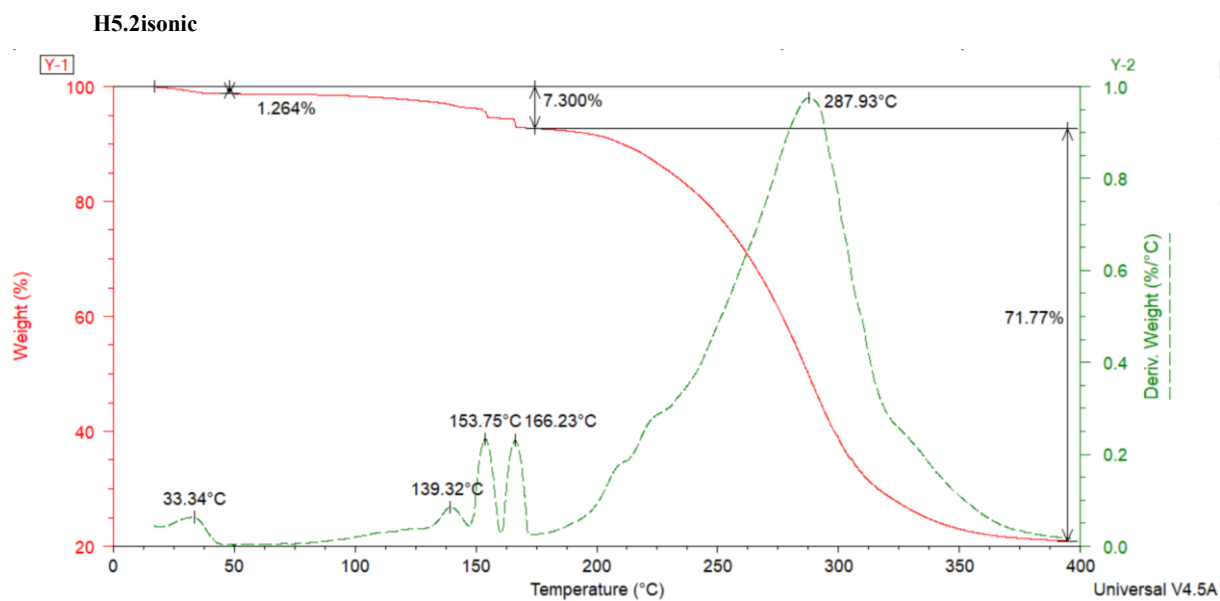
Figure 4.11 *TG and derivative curves of H5•isonic.*

H5.2-isonic.2-propOH
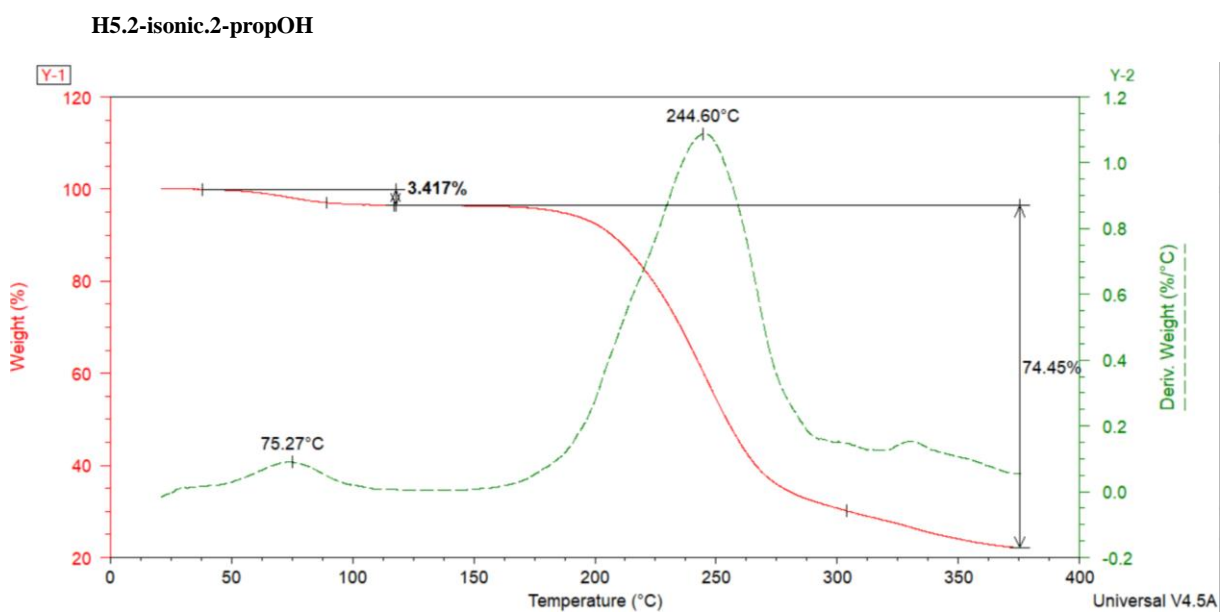
Figure 4.16 *TG and derivative curves of H5•1-propOH*

H5.2-isonic.2-propOH
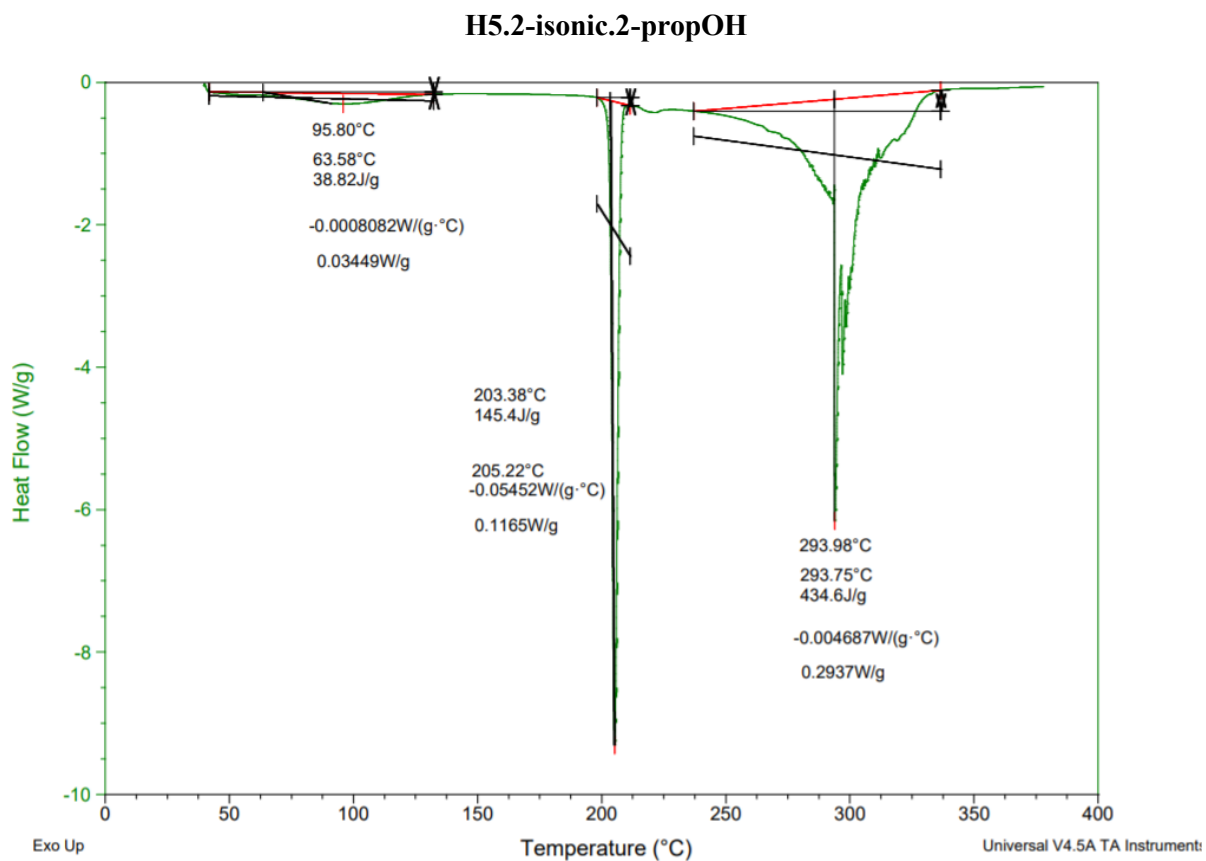
Figure 4.16 DSC curve of H5•1-propOH

Host 6
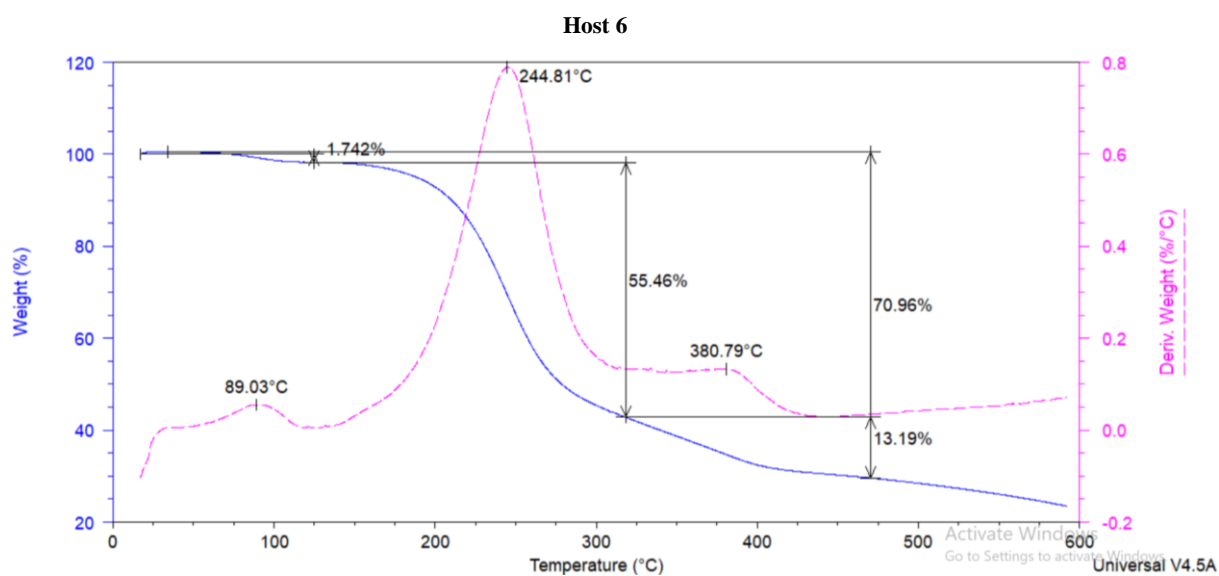
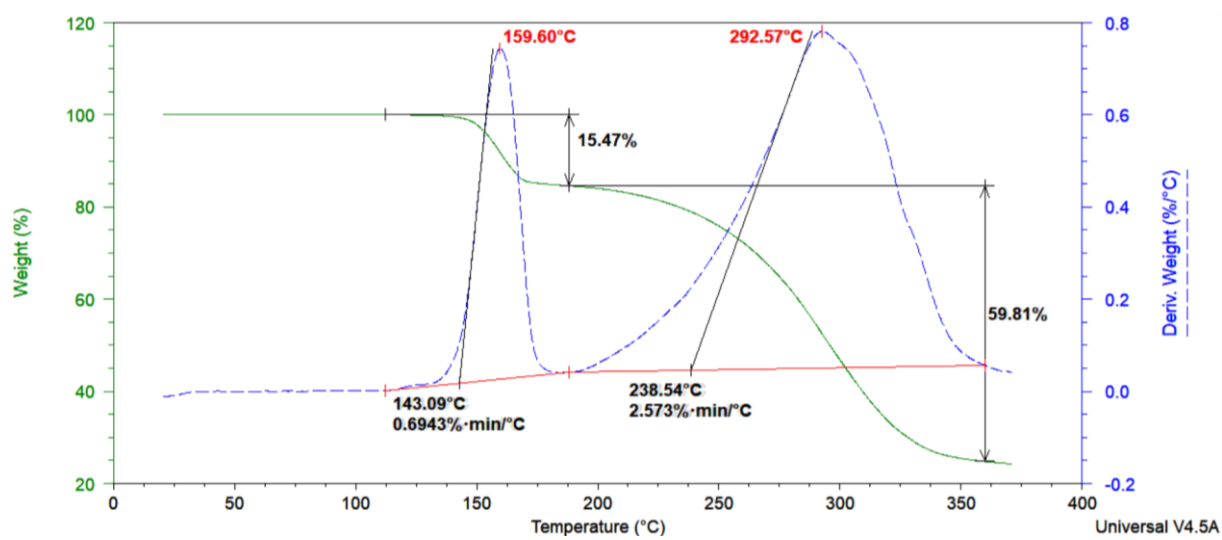*Figure 2.2* TG and derivative curves of H6

H6.H$_2$O

Figure 4.22 TG and derivative curves of H6•W
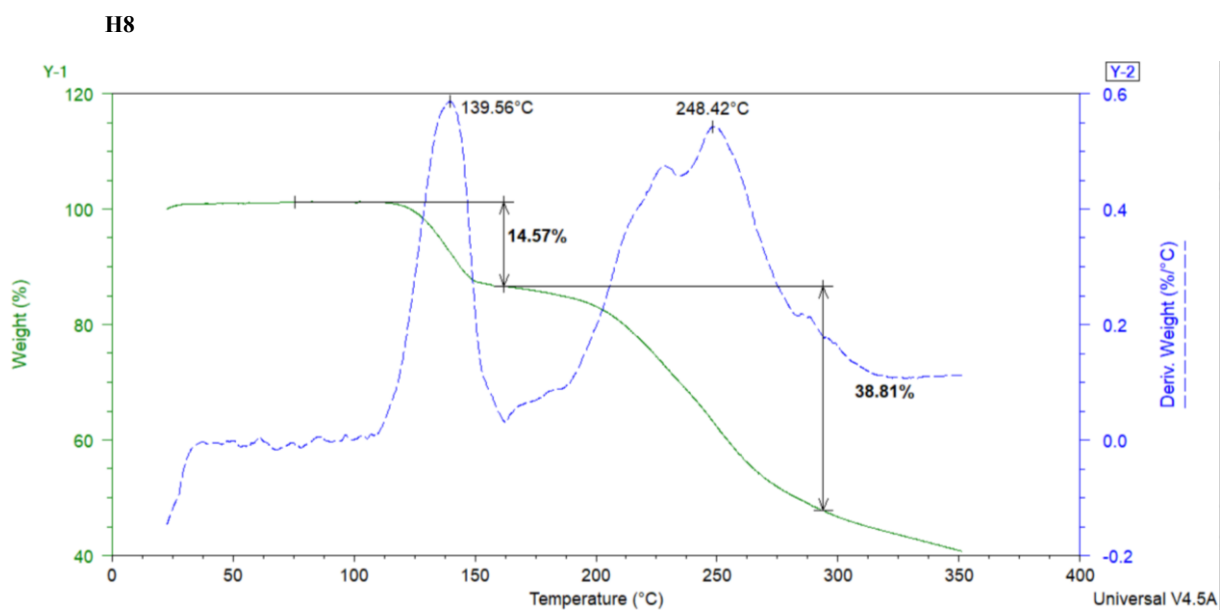
CHAPTER 5

H8

Figure 5.4 *Thermal analysis curves of complexes H8 as mass loss percentage and the derivative weight curves, purge gas: N_2 (40mol/min) heating rate: 20˚C/min*
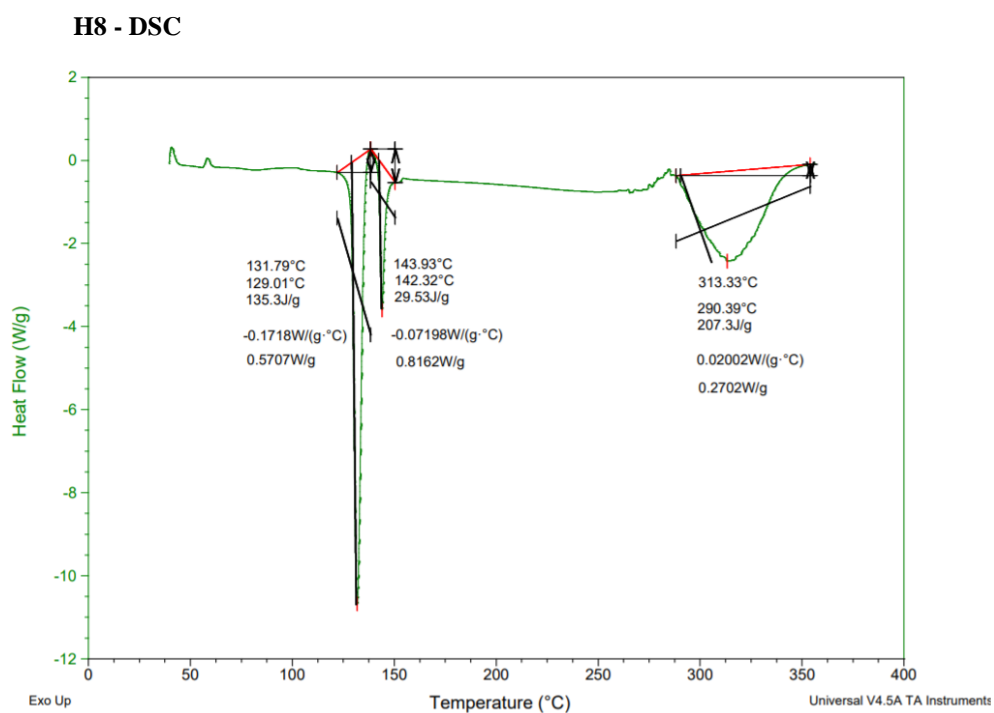
H8 - DSC
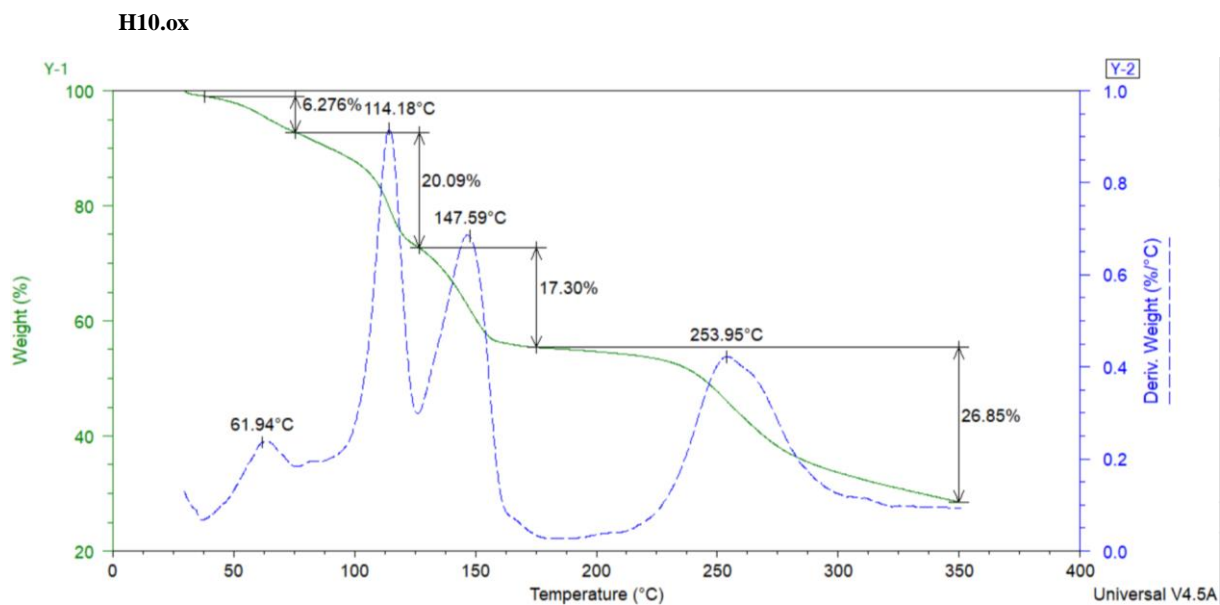

Figure 5.4 *Thermal analysis curves of complexes H8 heat flow vs temperature (˚C), purge gas: N_2 (40mol/min) heating rate: 20˚C/min.*

CHAPTER 6

H10.ox

Figure 6.2 *TGA curve of H10•ox plotted as mass loss percentage and the derivative weight vs temperature (˚C), purge gas: N₂ (40mol/min) heating rate: 20˚C/min.*